

TECHNISCHE UNIVERSITÄT MÜNCHEN
Lehrstuhl für Proteomik und Bioanalytik

Quantitative Studies of Tau Protein and Tauopathy

Waltraud Mair

Vollständiger Abdruck der von der Fakultät Wissenschaftszentrum Weihenstephan für Ernährung, Landnutzung und Umwelt der Technischen Universität München zur Erlangung des akademischen Grades eines

Doktors der Naturwissenschaften

genehmigten Dissertation.

Vorsitzender:

Prof. Dr. Wolfgang Wurst

Prüfer der Dissertation:

1. Prof. Dr. Bernhard Küster
2. Prof. Dr. Judith Steen

Die Dissertation wurde am 22.03.2016 bei der Technischen Universität München eingereicht und durch die Fakultät Wissenschaftszentrum Weihenstephan für Ernährung, Landnutzung und Umwelt am 19.04.2016 angenommen.

*"You can't connect the dots looking forward;
you can only connect them looking backward.
So you have to trust that the dots
will somehow connect in your future."*

STEVE JOBS, 2005
Stanford Commencement Speech

Acknowledgments

Without the help of many others this dissertation would not have been possible. Thus, at this point I would like to thank all the people that have made a big or small contribution to the realization of this work.

First of all, I would like to express my deepest gratitude to Prof. Judith Steen for giving me the opportunity to work on this exciting project, and for her constant guidance and support. Throughout the years of working together, she has taught me many things - not only about neuroscience, mass spectrometry and life in academia, but also about myself. Furthermore, I am extremely grateful to Prof. Bernhard Kuster for formal supervision and examination. Finally, my thanks go to Prof. Hanno Steen for valuable advice and many good ideas over the course of this work.

I am thankful to Sasha Singh, who trained me in the first few months and introduced me to the world of tau. To my many collaborators: Eva-Maria and Eckhardt Mandelkow, Katharina Tepper, Kenneth Kosik, William W. Seeley, and John Hedreen

I am grateful to the following tissue banks for providing human tissue resources: NIH NeuroBioBank at the University of Maryland, Baltimore; Harvard Brain Resource Tissue Center, McLean Hospital; the Neurodegenerative Disease Brain Bank (NDBB), Memory and Aging Center, University of California, San Francisco (UCSF); the University of Miami (UM) Brain Endowment Bank, University of Miami Miller School of Medicine, Miami; the Human Brain and Spinal Fluid Resource Center (HBSFRC), University of California, Los Angeles (UCLA).

I would like to thank all members of the Steen&Steen laboratory, former and present ones. My special thanks goes to Jan Muntel, for being a patient and knowledgeable supervisor in the early years of this work, and for providing mental and technical support. I am thankful to Shaojun Tang for help with informatics and statistical analysis, Sebastian Berger for his readiness to help in instrument related issues, and the whole lab for constant help and discussions during weekly meetings and journal clubs. Then I am thankful to Ruchi Chauhan, Ertrugul Cansizoglu, Hui Chen, and Hendrik Wesseling for many fruitful discussions and for providing a productive and cheerful working atmosphere in CLS, involving countless bags of cookie and sweets, hot chocolates and fun coffee/tea times. My thanks also go to the technical staff of the Steen&Steen Lab: Ceren Uncu, Saima Ahmed and John Sauld, who, each in a special way, were key to the unique and fresh lab atmosphere.

Finally, I thank my family and friends for their unconditional support and encouragement. I am grateful to my many dragon boat team mates that supported me both on and off the water; to my parents Lore and Gunther who taught me the pursuit of knowledge and to maintain a critical mind, and who gave precious input in the final stages of this work; and to my sisters Julia and Iris for their encouraging words in good and bad times. Special thanks go to my dear friends Kalli and Gemma, for always believing in me. We share an incredible bond full with food, wine, laughter, and tears. And finally, I thank Thanos, for his wisdom and love, for giving me strength, and for relentlessly and invigoratingly putting things into perspective.

Summary

Tauopathies, such as Alzheimer's Disease (AD), are a heterogeneous class of neurodegenerative disorders that exhibit a common pathological hallmark: the abnormal aggregation of aberrantly phosphorylated, misfolded tau protein inside neuronal and/or glial cells in the brain. Tau aggregation has been associated with tau gene missense mutations, changes in tau spliceform homeostasis, and many different post-translational modifications (PTMs). In particular, the pathological state of tau is often referred to as "hyperphosphorylated", as phosphorylation is increased and present on several non-physiological sites in pathological conditions. Deciphering the role of tau phosphorylation and other PTMs has been a major goal in the field of neurodegeneration, as it may help in defining targets for prognostic and diagnostic approaches as well as clinically effective therapeutic strategies. Although current technologies, in particular mass spectrometry (MS)-based proteomics, have allowed for detailed mapping of tau phosphorylation and other PTMs, the disease-relevant sites remain elusive, as these qualitative studies yield limited information about functionality. Besides, only easily detectable modifications can be observed. In order to identify functionally relevant sites, the acquisition of comprehensive, quantitative data is indispensable.

The aim of this thesis is the development of an analytical method to quantify tau and its PTMs in a precise manner. This assay, termed FLEXITau, is a sensitive MS-based targeted assay that measures unmodified tau peptide species relative to peptides from a heavy isotope-labeled standard, thus providing an indirect but precise measure of the amount of modification present. In combination with traditional PTM mapping, site occupancy of individual sites can be calculated. The power of this assay was demonstrated by measuring the state of hyperphosphorylation of tau expressed in a cellular model for AD pathology, the Sf9 insect cells, mapping and calculating site occupancies for over 20 phosphorylations. In addition, FLEXITau was employed to define the tau PTM landscape present in AD post-mortem brain. The data confirms that regions containing epitopes recognized by AD-specific antibodies are similarly modified in AD-tau and Sf9-tau. However other regions show large discrepancies in their PTM pattern, revealing limitations of Sf9-tau as a model system for tau pathology.

Diagnosis of tauopathies *in vivo* as well as post-mortem is hampered by the clinicopathological heterogeneity of the diseases, the overlap of many pathological features, and the lack of accurate diagnostic tools. Thus, in the second part of this thesis, FLEXITau was applied to identify differences and similarities in the modification landscape of tau in human tissue from multiple tauopathies, namely AD, progressive supranuclear palsy (PSP), Pick's disease

(PiD), corticobasal degeneration (CBD), as well as non-demented individuals as a control group. The FLEXITau data show that each condition presents with a unique molecular composition - a signature - determined by the tau PTM state and isoform distribution. Supervised machine learning approaches were then used to extract distinct peptide features from the FLEXITau data and train a computational classifier to distinguish each disease category. The diagnostic potential of the developed tool was corroborated by validation with an independent sample test set, where it achieved accuracies of 80% for PSP, 92% for PiD, 94% for CBD and controls, and 96% for AD.

Altogether these findings show that FLEXITau is a versatile assay to analyze tau PTMs with unprecedented precision, with application to a wide range of biological and clinical questions. Thus in the future it may have a significant impact on the characterization, diagnosis and prognosis of tauopathies and could lay the ground for novel disease-modifying and preventative therapeutics.

Zusammenfassung

Tauopathien, wie z.B. die Alzheimer-Krankheit (AK), sind eine heterogene Klasse von neurodegenerativen Erkrankungen, die ein gemeinsames pathologisches Merkmal aufweisen: die Ablagerung von abnormal phosphoryliertem Tau-Protein in Neuronen oder Gliazellen im Gehirn. Die Aggregation von Tau ist mit Punktmutationen des Tau-Gens, Veränderungen in der Tau-Isoform-Homöostase und vielen verschiedenen post-translationalen Modifikationen (PTMs) assoziiert. Insbesondere wird der pathologische Zustand des Tau-Proteins oft als "hyperphosphoryliert" bezeichnet, da Phosphorylierung im pathologischen Zustand im erhöhten Maße und an unphysiologischen Stellen auftritt. Die Entschlüsselung der Rolle von Tau-Phosphorylierung und anderen PTMs ist ein wichtiges Ziel im Forschungsbereich der Neurodegeneration, da diese zur Bestimmung von molekularen Targets für prognostische und diagnostische Ansätze sowie für therapeutische Strategien benutzt werden könnte. Obwohl derzeitige Technologien, insbesondere die massenspektrometrie-basierte (MS-basierte) Proteomik, eine detaillierte Kartierung von Phosphorylierungsstellen und anderen Tau-PTMs ermöglicht haben, ist es derzeit nicht eindeutig, welche PTMs krankheitsrelevant sind, da diese qualitativen Studien nur begrenzt Informationen über die Funktionalität der einzelnen Modifikationen liefern. Zudem können nur leicht nachweisbare Veränderungen mit diesen Techniken beobachtet werden. Um funktionsrelevante PTMs zu identifizieren, ist es unentbehrlich, umfassende und quantitative Daten zu gewinnen.

Das Ziel dieser Arbeit war die Entwicklung eines Analyseverfahrens, das Tau und seine PTMs in einer präzisen Art und Weise quantifizieren kann. Der entwickelte Assay, FLEXI-Tau genannt, ist ein empfindlicher MS-basierter Test, der unveränderte Peptide von Tau (also ohne PTMs) im quantitativen Vergleich zu schweren Tau-Peptiden misst. Diese stammen von einem Protein-Standard, der mit schweren Isotopen markiert ist. Hierdurch kann indirekt, aber präzise, der Bruchteil der modifizierten Peptide abgeleitet werden. In Kombination mit traditionellen PTM-Analysen kann die Stelle der Modifikation teilweise mit aminosäure-genauer Auflösung bestimmt werden. Um die Verwendbarkeit des Assays zu testen, wurde hyperphosphoryliertes Tau in Sf-9-Insektenzellen, einem Zellmodell für AK, exprimiert und dessen Tau-PTM-Muster analysiert. Hierbei wurden über 20 Sf-9-Tau Phosphorylierungsstellen lokalisiert und deren Besetzung berechnet. Zudem wurde FLEXI-Tau dazu benutzt, das Tau-PTM-Muster zum Vergleich in AK-post-mortem Gehirnproben zu bestimmen. Die Ergebnisse bestätigen, dass Regionen, die Erkennungssequenzen für AK-spezifische Antikörper enthalten, im Sf-9-Tau tatsächlich ähnlich stark modifiziert sind wie im AK-Tau. Allerdings zeigen andere Regionen große Unterschiede in ihrem PTM-Muster,

was offenbart, dass das Sf-9-Tau nur beschränkt als Modellsystem für AK-Tau geeignet ist. Die differentielle Diagnose von Tauopathien, sowohl klinisch als auch post-mortem, wird erschwert durch Uneindeutigkeit der Symptome, durch Überlappung vieler pathologischer Merkmale, aber auch durch mangelnde Zuverlässigkeit der aktuellen Diagnose-Methoden. Daher wurde im zweiten Teil dieser Arbeit FLEXITau angewandt, um Unterschiede und Ähnlichkeiten im Modifikationsmuster von Tau in menschlichem post-mortem-Gehirngewebe aus mehreren Tauopathien zu identifizieren, und zwar von Patienten mit AK, progressiver supranukleärer Blickparese (PSP), Pick-Krankheit (PiK), corticobasaler Degeneration (CBD) sowie von Personen ohne Demenzerkrankung (Kontrolle). Die FLEXITau-Daten zeigen, dass jede Krankheit eine eindeutige molekulare Zusammensetzung von Tau aufweist, eine Art Signatur, bestimmt durch die Verteilung von Tau-PTMs und Isoformen. Durch "überwachtes maschinelles Lernen" (engl. supervised machine learning) wurden bestimmte Peptidmerkmale aus den FLEXITau-Daten herausgefiltert und dazu verwendet, einen Klassifizierungs-Algorithmus zu erstellen, der in der Lage ist, jede Krankheitskategorie von den anderen zu unterscheiden. Die Leistungsfähigkeit der entwickelten Methode zur Diagnose von Tauopathien wurde mit einem unabhängigen post-mortem-Datensatz validiert, wobei Genauigkeiten von 80% für PSP, 92% für PiK, 94% für CBD und Kontrollen, sowie 96% für AK erreicht wurden.

Insgesamt zeigen diese Ergebnisse, dass FLEXITau ein vielseitiger Test ist, der Tau-PTMs mit neuartiger Präzision misst und so auf eine Vielzahl biologischer und klinischer Fragen angewendet werden kann. Damit könnte er in Zukunft die Charakterisierung, Diagnose sowie Prognose von Tauopathien vorantreiben und sogar neue Strategien für krankheitsverändernde und präventive Therapien ermöglichen.

Contents

Summary	v
Zusammenfassung	vii
1 Introduction	1
1.1 Neurodegenerative diseases	1
1.2 Tau protein	3
1.2.1 Tau gene, mRNA and splicing	3
1.2.2 Physiological functions of tau	5
1.2.3 Tau PTMs in physiology	6
1.2.4 Genetics of tau	6
1.3 Tau pathology	7
1.3.1 Tau aggregation	9
1.3.2 Tau aggregation and toxicity	10
1.3.3 Propagation of tau pathology	11
1.3.4 The role of tau PTMs in disease	11
1.4 Tauopathies	15
1.4.1 AD	16
1.4.2 FTLD-tau	17
1.4.3 Other tauopathies	19
1.4.4 Age-related changes in tau	20
1.4.5 Diagnosing tauopathies	20
1.4.6 Therapeutic approaches for tauopathies	24
1.5 Mass spectrometry (MS)-based proteomics	27
1.5.1 Key principles and instrumentation	28
1.5.2 Shotgun proteomics: Protein identification and quantification	28
1.5.3 Targeted proteomics	31
1.5.4 Data-independent acquisition approaches	33
1.5.5 Identification and quantification of PTMs by MS	34
1.6 Approaches to analyze tau and tau PTMs	35
1.6.1 Antibody-based approaches	35
1.6.2 MS-based approaches	36
1.7 Aim of this work	38

2	FLEXITau: A Novel MS-based Tau PTM Assay	39
2.1	Summary	39
2.2	Introduction	39
2.3	Experimental procedures	41
2.4	Results	48
2.4.1	Development of the quantitative SRM FLEXITau assay	48
2.4.2	Sensitivity of the FLEXITau assay	50
2.4.3	Analytical precision of the FLEXITau assay	51
2.4.4	Quantitative PTM profiling of "hyperphosphorylated" tau	52
2.4.5	Creating a quantitative PTM map	54
2.4.6	Calculation of site occupancy using FLEXITau	58
2.4.7	Determining the average number of phosphorylations per tau molecule	61
2.4.8	Using FLEXITau to examine the PTM landscape of human AD-tau	62
2.5	Conclusion	65
3	Quantitative Profiling of Tau PTM Signatures of Tauopathies	67
3.1	Summary	67
3.2	Introduction	67
3.3	Experimental procedures	69
3.4	Results	77
3.4.1	Profiling of tau peptides identifies molecular signature of tauopathies	77
3.4.2	Mapping of PTMs in human insoluble brain-derived tau	78
3.4.3	Development of a computational classifier for tauopathies	80
3.4.4	Detection of co-pathologies and misdiagnoses	84
3.4.5	Performance of the computational classifier on the testing set	86
3.5	Discussion	87
3.6	Supplementary Tables	91
4	Discussion	97
4.1	Development of FLEXITau and proof of principle	97
4.2	Identification of tau PTM signatures of tauopathies	101
4.3	Future perspective	105
4.4	Closing remarks	108
	Bibliography	115
	Appendix	155
	List of publications	
	Curriculum Vitae	

1 Introduction

1.1 Neurodegenerative diseases

Neurodegenerative disease is an umbrella term for a range of heterogeneous conditions that primarily affect the neurons in the human brain. Neurodegeneration usually causes dementia, i.e. the deterioration of cognitive function beyond what might be expected from normal aging. Individuals with neurodegenerative diseases usually suffer from impairment in abstract thinking, emotions, cognition, and memory. Furthermore, degeneration of the brain can affect many of the body's activities, such as balance, movement, talking, breathing, and heart function. Neurodegenerative diseases are a major cause of disability and premature death among older people worldwide.

Protein aggregation as common mechanism in neurodegeneration

Although neurodegenerative disorders manifest with diverse clinical phenotypes, a growing body of evidence suggests that they have in common one pathological hallmark: the atypical accumulation and deposition of specific proteins into large insoluble aggregates (also called lesions) inside or among specific neurons and glial cells. These diseases are therefore also encompassed by the umbrella term "proteinopathies". Different types of lesions have been demonstrated at the beginning of the 20th century using histological staining techniques, such as the silver staining [473], which was an excellent tool to reveal the so-called "tangles", the markers of neurofibrillary degeneration. Using these techniques, neuropathologists have been able to detect tangles in many clinical conditions that are now well defined, such as Alzheimer's disease (AD), frontotemporal dementia (FTD) with parkinsonism linked to chromosome 17 (FTDP-17) [405], Pick's disease (PiD), corticobasal degeneration (CBD) [123], progressive supranuclear palsy (PSP) [228], post-encephalic parkinsonism [305], argyrophilic grain disease (AGD) [425], Huntington's disease (HD) [81, 298] and amyotrophic lateral sclerosis (ALS) [393], amongst others.

Because tangles were found in a variety of very different diseases, initially it was thought that their formation was a response to different types of insult, and therefore a consequence, not a cause [420]. However, electron microscope observations and X-ray diffraction analyses revealed that tangles have distinct structural conformations and are not the same in all diseases. Today it is well known that pathological lesions, apart from presenting distinct structures, can be composed of different proteins. For example, sporadic AD is characterized by aggregates composed of microtubule (MT) associated protein tau within bundles of

paired-helical filaments (PHF), together with extracellular deposits of amyloid β ($A\beta$). The pathogenesis of HD, on the other hand, is associated with neuronal accumulation of aggregated forms of huntingtin. Characteristic for sporadic Parkinson's disease (PD) and PD with dementia is the intra-neuronal accumulation of α -synuclein in Lewy bodies and Lewy neurites [405]. Furthermore, almost all cases of ALS, as well as a subgroup of cases of frontotemporal lobar degeneration (FTLD; the pathological cause for FTD), are characterized by aggregates of TAR DNA-binding protein 43 (TDP-43) (FTLD-TDP-43) [324]. The second subgroup of FTLD is associated with aggregation of fused in sarcoma protein (FUS) (FTLD-FUS) [118] (Fig. 1.1).

Notably, the deposition of tau fibrils is observed not only in AD. In the absence of $A\beta$ plaques, tau inclusions are the pathological hallmark of a diverse group of neurodegenerative diseases that are collectively called tauopathies. These disorders comprise the third subgroup of FTLD pathology, which is designated as FTLD-tau; examples include the above-mentioned PiD, CBD, PSP and AGD. The following sections give a brief overview of tau protein with a focus on tau pathology and tauopathies (sections 1.3 and 1.4), as well as current diagnostic and therapeutic approaches for tau-mediated neurodegeneration (sections 1.4.5 and 1.4.6).

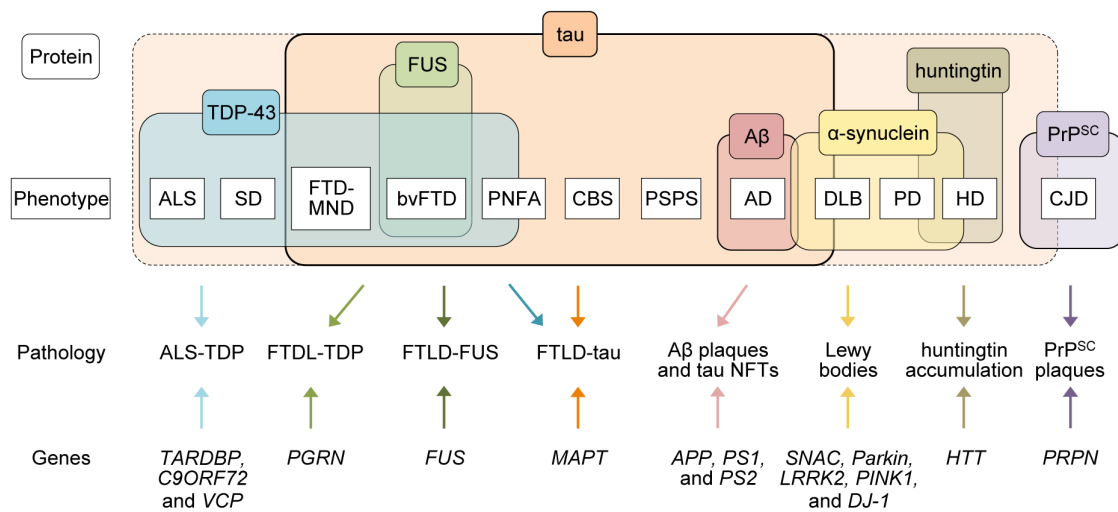


Figure 1.1: Scheme for the clinical, pathological and genetic spectrum of proteinopathies. Several neurodegenerative diseases, collectively termed proteinopathies, are characterized by abnormal assembly and deposition of specific proteins in the brain. The same protein can be found in different clinical presentations (phenotype), reversely the same phenotype can be the result of different genes and/or misfolded proteins. Tau protein (orange) is a key player in the majority of these disorders. The dotted box encompasses phenotypes where altered tau has been observed, with less established evidence. Importantly, this scheme is not complete; for instance rare variants of the APP genes can contribute to PD [384], and FUS mutations have been associated with ALS and PD [265]. Adapted from [441]. bvFTD, behavioral variant FTD; CBS, corticobasal syndrome; CJD, Creutzfeldt-Jakob Disease; DLB, dementia with Lewy bodies; FTD-MND, frontotemporal dementia with motor neuron disease; PNFA, progressive nonfluent aphasia; PrP^{Sc}, cellular and scrapie form of prion protein; PSPS, PSP syndrome; SD, semantic dementia.

1.2 Tau protein

1.2.1 Tau gene, mRNA and splicing

Tau is a highly conserved protein belonging to the family of MT-associated proteins (MAPs). It is exclusively found in higher eukaryotes, including *Caenorhabditis elegans* [161, 297], *Drosophila* [87, 221], rodents [257, 268], monkeys [322], and human [165, 166]. In human, tau protein is primarily expressed throughout the central nervous system (CNS), and particularly abundant in neuronal axons (reviewed in [382, 434]). It can also be expressed in non-neuronal cells such as glial cells, mainly in pathological conditions [92]. Furthermore, trace amounts of tau mRNA and proteins have been detected in several peripheral tissues such as heart, kidney, lung, muscle, pancreas, testis, as well as in fibroblasts [183, 218, 437]. In human, *tau* is encoded by a single gene located on the long arm of chromosome 17 in locus 17q21.3, occupying over 100 kb [325]. Among the 16 exons of the *tau* gene, exons 1, 4, 5, 7, 9, 11, 12, and 13 are constitutive exons. In contrast, exons 4A, 6 and 8 are never present in any mRNA in human brain. Of these, exon 4A is only transcribed in the peripheral nervous system, whereas exons 6 and 8, to date, have not been found to be transcribed in human [19, 82]. Finally, exons 2, 3 and 10 are alternatively spliced and are adult brain-specific, whereby exon 3 never appears independently of exon 2 [18, 19]. As summarized in Fig. 1.2, alternative splicing of these three exons allows for six possible combinations corresponding to the six tau isoforms expressed in human brain.

The six tau variants range from 352 to 441 amino acids (AAs), and their molecular weight (MW) is between 45 to 65 kDa when run with polyacrylamide gel electrophoresis in presence of sodium dodecyl sulfate (SDS-PAGE). Under normal physiological conditions (i.e. in soluble forms), tau has little secondary structure; it is mostly disordered and flexible, predominantly acquiring random coil structure [46]. In respect to primary structure, tau protein is divided into four regions: 1) a negatively charged acidic region in the N-terminal part (exons 1-5), where exon 2 and 3 encode for N-terminal inserts (N1 and N2); 2) a positively charged proline-rich region encoded by exon 7 and a part of exon 9; 3) a region responsible for binding of tau to MTs encoded by exons 9-12, each containing one of the four repeat domains (R1, R2, R3, and R4), whereby exon 10 contains R2; and 4) a carboxy-terminal (C-terminal) region encoded by exon 13 (Fig. 1.2) [165, 166, 204]. Thus the six tau isoforms that arise from alternative splicing differ from each other by the number of tubulin-binding repeats (either three (3R-tau) or four (4R-tau) repeats, depending on the absence or presence of exon 10), and the presence of zero, one, or two N-terminal acidic inserts (referred to as 0N, 1N or 2N, depending on the absence or presence of exons 2 and 3). The six isoforms are thus usually denoted as 0N3R, 1N3R, 2N3R, 0N4R, 1N4R and 2N4R tau.

Although the tau isoforms appear to be broadly functionally similar, each one is likely to have a precise, and to some extent distinctive, physiological role. In human fetal brain, only

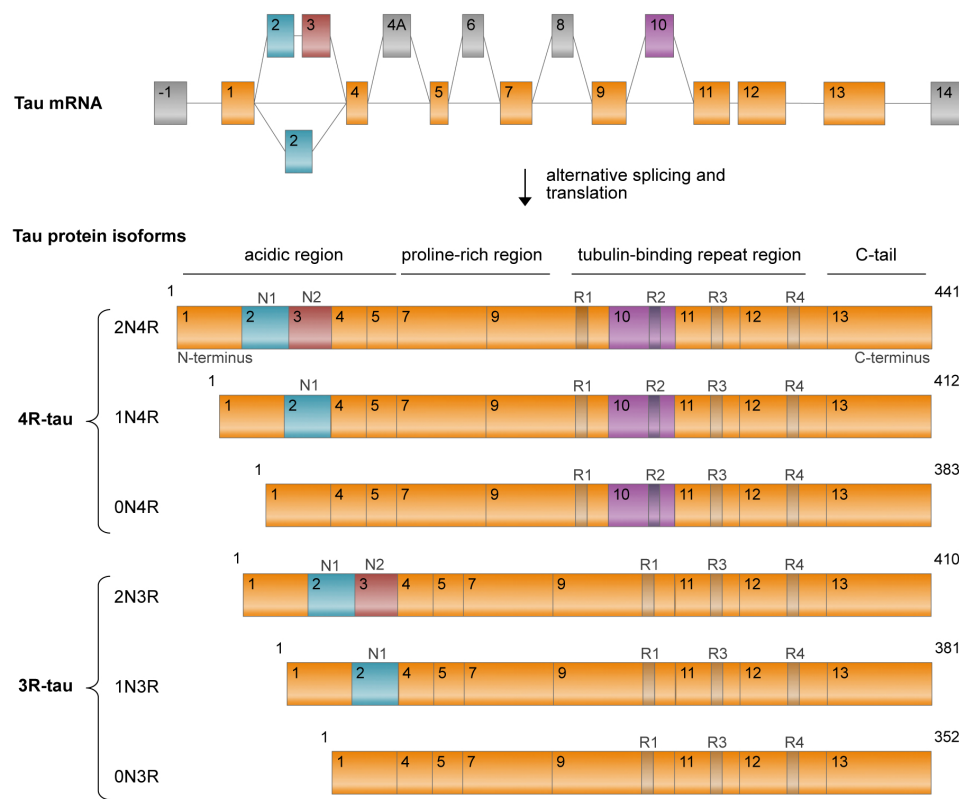


Figure 1.2: Schematic representation of the human *tau* gene and the six human tau protein isoforms. Tau mRNA contains 16 exons (top panel). Of these, exons 1, 4, 5, 7, 9, 11, 12, and 13 are constitutive (orange), whereas exons 4A, 6 and 8 (gray) are not transcribed in human. Exons 2 (blue), 3 (red), and 10 (purple) are alternatively spliced, with exon 3 only being transcribed in presence of exon 2. The combination of splicing of exons 2/3 and 10 gives rise to six different transcripts, translated into six different tau isoforms (bottom panel). Exon 2 and 3 encode for 29 AA long inserts in the amino-terminal (N-terminal) acidic region, while exon 10 is located in the MT-binding domain and encodes for one (R2) of the four repeat regions (R1-R4, dark shaded boxes). Thus, the six tau isoforms differ by the absence or presence of N-terminal inserts (0N, 1N, or 2N), in combination with either 3 (R1, R3 and R4) or four (R1-R4) MT-binding repeats. The latter are termed 3R-tau and 4R-tau isoforms, respectively. Adapted from [79] and [452].

0N3R, the shortest isoform (lacking the two N-terminal repeats and the extra MT-binding repeat) is expressed. In contrast, in human adult brain, balanced splicing of exon 10 results in approximately equal amounts of both 3R-tau and 4R-tau [166]. Deviations from this ratio are characteristic for several tauopathies (see section 1.4). Although the functional differences between 3R and 4R-tau remains unclear, *in vitro* studies suggest that 4R-tau binds MTs three times more strongly than 3R-tau, owing to the presence of the additional MT-binding repeat [83, 162, 281, 339].

1.2.2 Physiological functions of tau

Since its discovery approximately 40 years ago, a number of well-defined functions of tau have been revealed and extensively characterized (reviewed in [82]). One of its main functions is the stabilization of axonal MTs. Tau interacts with tubulin via its binding repeat regions R1-R4 in the MT-binding domain. These repetitive regions are composed of a highly conserved 18 AA long binding elements, and are separated from each other by flexible, less conserved 13 or 14 AA inter-repeat domains [166, 204, 268, 269]. In addition, tau binding to MTs has been shown to promote tubulin polymerization *in vitro* [64, 75, 95, 96, 429]. Importantly, under normal conditions, tau is in a constant dynamic equilibrium of attachment and detachment (on and off the MTs). The MT-tau interaction is thought to be regulated primarily by the phosphorylation state of tau, which in turn is determined by the balanced action of kinases and phosphatases (Fig. 1.3, see also section 1.2.3). Abnormal phosphorylation of tau leads to detachment of tau from MTs and is associated with pathological conditions.

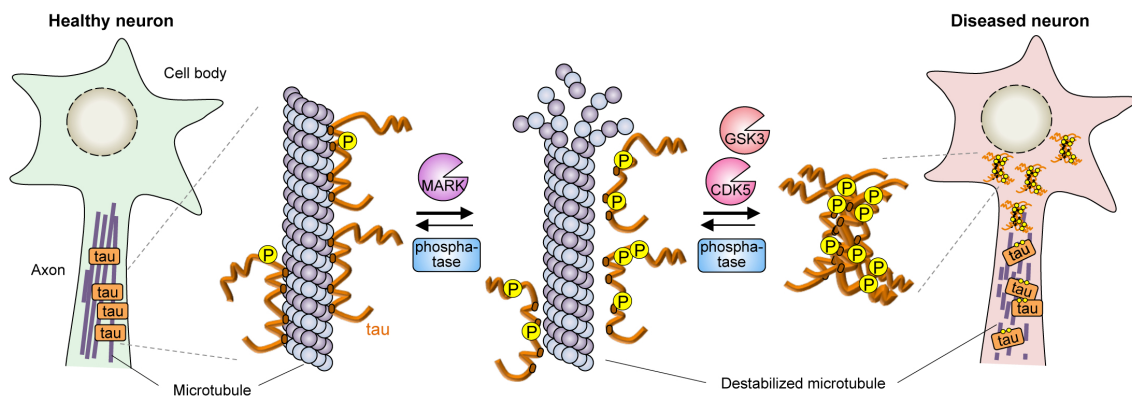


Figure 1.3: The role of tau phosphorylation in physiology and disease. Under normal physiological conditions, tau binding and detachment to MTs is coordinated by phosphorylation and dephosphorylation, requiring the precise interplay of multiple kinases (such as MARK) and phosphatases. Aberrant phosphorylation by specific kinases (such as GSK3 and CDK5) is associated with increased detachment of tau from MT and loss of its MT-stabilizing function, and can lead to tau misfolding and self-aggregation inside the neuron.

With its ability to modulate MT dynamics, tau contributes directly or indirectly to structural and regulatory cellular functions, such as the maintenance of neuron morphology. Furthermore, the interaction of tau with the MT network is key to the axonal transport machinery that allows signaling molecules and other essential cellular constituents, including organelles (e.g. mitochondria and vesicles), to travel along the axons. Thus, tau has profound effects on the function and viability of neurons and their axonal extensions [85, 103, 135, 171, 289]. Notably, because other MAPs perform similar functions, it is possible that they can compensate for a tau deficiency or loss, which may account for the report that tau knockout mice did not show any overt phenotype [197].

1.2.3 Post-translational modifications (PTMs) of tau in physiological conditions

Phosphorylation is the most common and most studied tau PTM. Multiple kinases are able to phosphorylate tau, many of which are proline-directed protein kinases, such as glycogen synthase kinase 3 (GSK3), cyclin-dependent kinase-5 (CDK5), mitogen-activated protein kinase (MAPK) and stress-activated protein (SAP) kinases. On the longest tau isoforms, there are 85 putative serine (S), threonine (T) and tyrosine (Y) phosphorylation residues in total, and phosphorylation at 75 of these sites has been reported. However, only half of these have been found phosphorylated in physiological conditions [57, 82, 293]. As indicated above, phosphorylation on specific sites can effectively decrease the binding affinity of tau for MTs and/or increase its propensity to assemble into fibrils [53, 74, 130, 295, 476] (Fig. 1.3, see also section 1.3.4).

Although in the course of tau-mediated neurodegeneration, aberrant tau phosphorylation is always observed, the importance of individual phosphorylation sites in regulating tau function has been debated for some time. For example, phosphorylation of S262, which lies in the first MT-binding repeat and is phosphorylated by MAP/microtubule affinity-regulating kinase (MARK), is thought to strongly reduce tau binding to MTs, but has been shown to prevent tau fibrillization [53].

Apart from phosphorylation, several other modifications have been described, including ubiquitination, acetylation, and glycosylation, among others (see [292] and [91] for comprehensive reviews). These modifications have been studied mostly in pathological conditions. Their exact role in physiological conditions is unclear, and little is known about their baseline state. Probably physiological tau exists as a mixture of differentially modified molecules. The role of PTMs in tau pathology and aggregation is described in more detail in section 1.3.4.

1.2.4 Genetics of tau

The cause-effect relationship between tau dysfunction and neurodegeneration remained under debate until the early 90s, when genetic studies established an unequivocal connection. First, an autosomal dominantly inherited form of FTD and parkinsonism was linked to chromosome 17, a region containing *tau*, which led to the introduction of the term FTDP-17 [458]. In 1998 multiple *tau* gene mutations were discovered in the majority of patients with FTDP-17, providing evidence that tau abnormalities alone are sufficient to cause neurodegenerative disease. Today, 51 pathogenic *tau* mutations have been identified and account for 5% of cases of FTD [167].

The majority of mutations are located in exons 9-12 (encoding the repeat regions) and the intronic regions between exons 10 and 11 (Fig. 1.4). Some mutations have a primary effect at the protein level and result in AA changes that reduce the ability of tau to interact with MT [114, 201, 208] and/or increase the susceptibility of tau to form fibrils [37, 152, 319]. However, a substantial proportion of the known *tau* mutations in FTDP-17 affect the

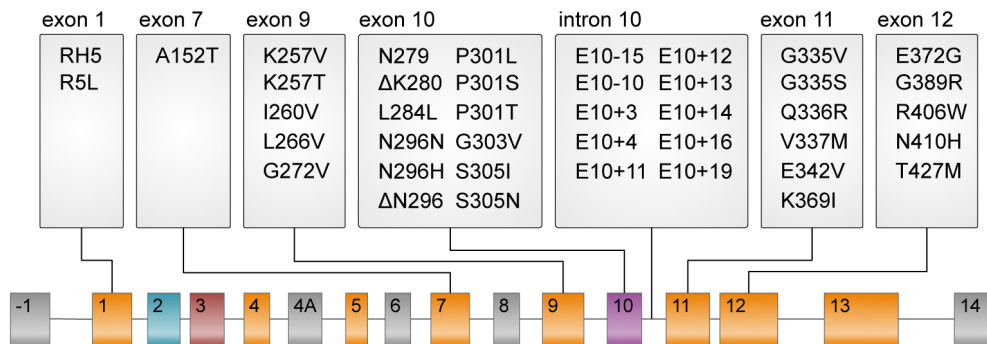


Figure 1.4: The *tau* gene mutations associated with FTDP-17. *Tau* mutations that cause FTDP-17 are primarily located in exons 9-12 or in the intronic region between exons 10 and 11. Exon 10 and intronic mutations affect the splicing of exon 10 and generally result in an increase of exon 10-containing 4R-tau. Adapted from [79] and [406].

alternative splicing of tau mRNA, in particular exon 10, which perturbs the normal ratio of 3R-tau to 4R-tau isoforms. Most of these mutations result in an increased prevalence of exon 10-containing 4R-tau.

Clinically, FTDP-17 has very similar phenotypes to the clinical presentation of non-familial FTLD-tau, such as PiD, PSP, and CBD. Patients present with behavioral changes followed by cognitive decline, eventually leading to dementia, the onset being highly variable [309, 370]. The main pathological hallmark is the invariable presence of neuronal AD-like tau deposits. Due to the symptomatic and molecular similarities to non-familial tauopathies, many of these FTDP-17-causing *tau* mutations have been used to develop animal models for tau aggregation and neurofibrillary degeneration [134, 174, 175]. The most widely used mouse models contain the P301L and P301S missense mutation located on exon 10. While not affecting the relative ratio of 3R to 4R-tau, they appear to promote the self-assembly of mutant tau into filaments and tangles [480].

Notably, there are no reported *tau* gene mutations in AD. Instead, familial AD is caused by mutations in the amyloid precursor protein (APP) (from which A β is derived by proteolytic cleavage) and in the presenilin-1 (PS1) and presenilin-2 (PS2) genes, both of which encode proteins involved in A β formation (see also Fig. 1.1, bottom). These pathogenic mutations account for less than 1% of AD cases [116].

1.3 Tau pathology

As mentioned above, the defining common neuropathological hallmark of all tauopathies is the neuronal (or neuronal and glial) accumulation of tau protein. Although natively unfolded, during disease progression, tau assembles into various filamentous forms. Possible causes for the formation of tau aggregates include an imbalance of tau kinases and/or phosphatases, other PTMs, truncation, mutations in the *tau* gene, and possibly others (Fig. 1.5).

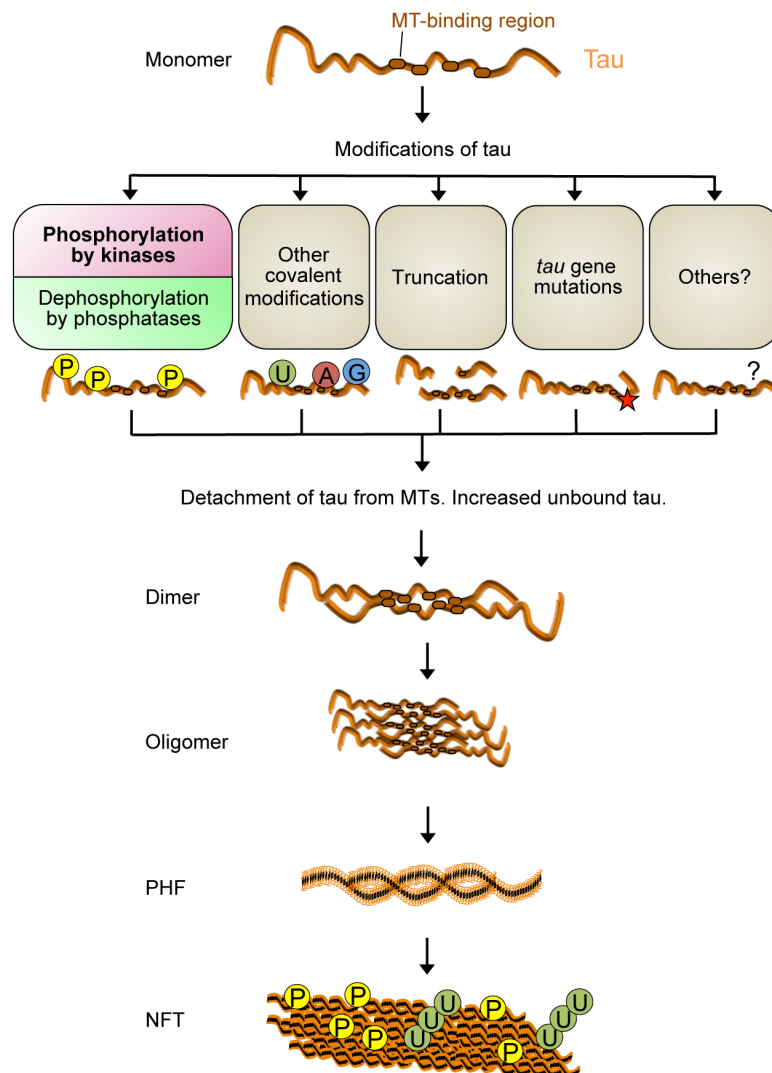


Figure 1.5: A putative sequence of events in the formation of pathological tau aggregates. Detachment of tau from the MTs and an increase in cytosolic concentration of tau are likely the first events that lead to aggregation. Possible causes for abnormal disengagement of tau from MTs are an imbalance of kinases and/or phosphatases, other covalent PTMs, truncation, mutations in the *tau* gene, and possibly others. Larger tau aggregates like PHFs and NFTs evolve from the successive aggregation of smaller tau species such as monomers, dimers, and oligomers. Adapted from [33] and [104]. P, phosphorylation; U, ubiquitination; A, acetylation, G, glycosylation.

The precise role of these aggregates and their precursors in the different stages of neurodegenerative disease pathology is not yet fully understood. It is generally known that the cortical density of tau tangles in post-mortem brain from tauopathy patients correlates with pre-morbid cognitive dysfunction and neuronal loss. Moreover, it is clear that tau by itself can be the disease-causing agent. However, several lines of research have suggested different, at times even contradictory, cause-and-effect relationships. Especially for the non-familial tauopathies, up to today, it remains controversial whether tau aggregation is a primary causative factor, plays a peripheral role in the disease, or may even be a protective response. To add to the complexity, recent reports indicate that oligomeric pre-fibrillar forms of misfolded tau may be the disease-causing agent. All these aspects are discussed in more detail in the following sections.

1.3.1 Tau aggregation

As mentioned above, under pathological conditions, tau affinity for MTs is aberrantly decreased, likely due to an increased rate of phosphorylation (see also 1.3). Abnormal detachment of tau from MTs results not only in the destabilization of MTs, but also in an increase in the levels of free soluble tau (in the monomeric form). The latter causes a perturbation of the equilibrium of bound and unbound tau to MT. Cytosolic unbound tau monomers can undergo conformational changes and be targeted by other PTMs that attenuate the MT-binding affinity of tau further, and/or increase its propensity to aggregate into filaments [47, 146, 256] (see also section 1.3.4). It is possible that the higher concentration of cytosolic tau by itself increases the chances of pathogenic conformational changes that then favor misfolding and may, as a result, make it more prone to aggregate. The morphology of tau filaments can vary. In AD, the predominant filaments are straight or paired helical filaments (SFs and PHFs, respectively). While these can also occur in other tauopathies, different shapes such as twisted ribbons or rope-like conformations exist [109]. Tau filaments can self-aggregate to highly ordered bigger structures (lesions), and also here different types exist. They include neurofibrillary tangles (NFTs), the classic fibrillary tangles first described by Alzheimer in 1907. In AD brains, NFTs consist of large bundles of fibers made mostly of PHFs and rare SFs (see Fig. 1.5). They are often described as having "flame-shaped" form, and may fill the entire neuronal cytoplasm. NFTs can also be found in PSP, although with a different anatomical distribution compared to AD [271]. Another type of neuronal fibril that occurs in AD and several other tauopathies are neuropil threads, which are bundles of SFs and PHFs that occupy dendrites and largely displace the cytoskeleton [347]. Glial lesions include the so-called astrocytic plaques which are typical for CBD, and tufted astrocytes that are exclusively found in PSP.

There are other forms of pathological insoluble tau found in human brains that may be filamentous, yet are non-fibrillar in structure. Such aggregates include Hirano bodies and Pick bodies. Hirano bodies have been described in AD and PiD, amongst others. They are intraneuronal filament arrays made of tau, actin, cofilin, and other actin-binding proteins [205, 284]. Pick bodies are argyrophilic grains that are made of disorganized bundles of filaments which form spherical cytoplasmic inclusions. They have been described in AD, PiD, and AGD.

Importantly, tau lesions are not always composed of all isoforms of tau. While PHFs and SFs formed in AD are equally made of all six splice variants, the tau lesions in PSP and CBD comprise mostly the 4R-tau isoforms [478]. In contrast, Pick bodies are comprised only of the 3R isoforms of tau [115]. More details about these tauopathies and their histopathology can be found in section 1.4 (see also Table 1.2).

Structurally, the path from normal soluble tau to large aggregates is thought to be a multi-step phenomenon, and has been best studied for the PHFs in AD (reviewed in [301], see also Fig. 1.5): First, newly formed soluble monomers dimerize in an anti-parallel manner

linked by disulfide bonds. Next, small non-fibrillary oligomeric tau deposits are formed (normally referred to as "pretangles"). The assembly of these pretangles into PHFs involves the formation of the characteristic pleated β -sheets. More precisely, the conformation of two hexapeptide motifs in the MT-binding region of tau (VQIINK and VQIVYK) changes from random coil to a β -sheet structure [47, 331, 459]. Because of the cross- β structure in their core, PHFs are considered amyloid filaments [49]. The structure of the remainder of the protein, including the N-terminal half and the C-terminal tail, has been difficult to study and has been dubbed "fuzzy coat" [110, 456, 466].

1.3.2 Tau aggregation and toxicity

Determining which forms of tau are actually toxic remains one of the largest questions in the field. NFTs were a vital historical clue to the involvement of tau in neurodegenerative disease, and initially, tangles themselves were considered the species most likely to be neurotoxic. However, although theories about direct physical disruption of cellular function remain intuitive, several lines of evidence weigh against tangles as a form of tau toxicity, at least they suggest that they are neither necessary nor sufficient.

The evidence that supports the notion that tau aggregates are associated with neurotoxicity are largely of correlative nature. For example, studies of human post-mortem brains show a strong spatial and temporal correlation between NFTs and severity of dementia, and between NFTs and neurodegeneration or neuronal death [28, 70, 122, 170, 180, 320, 426]. Furthermore, some tau transgenic mouse models, such as tau P301L, show neuronal apoptosis at the same ages as filaments and NFTs are formed, and there is a correlation between reduction of NFT and improvement in cognition [173, 330]. More direct evidence comes from mice conditionally expressing human tau variants harboring pro-aggregation or anti-aggregation mutations. Pro-aggregation mice develop pretangles, PHFs and NFTs, followed by synaptic and neuronal loss, whereas mice expressing the same tau with the anti-aggregation mutation do not develop this neuronal pathology [136, 306]. Finally, after suppression of the expression of the human tau, these mice recover from toxicity, both in terms of cell death and cognition [230, 413].

Although all these studies represent very strong data in favor of PHFs and/or NFTs as the toxic species, there is evidence from a number of models that NFTs are not required for tau-induced neuronal dysfunction and toxicity, and/or that cell death occurs prior to NFT formation. For example, in some mouse models, cognitive/behavioral impairments and cell death can be demonstrated prior to NFT formation [17]. In most *Drosophila* models of tauopathy, despite clear neurodegeneration and functional phenotypes, neuronal NFTs are not formed at all [259, 302, 313, 462, 468]. This indicates that filaments are not necessary for tau-induced toxicity. Other evidence suggests that filaments are also not sufficient, since they continue to form in the conditional mice mentioned above, even when the transgenic tau expression is suppressed and memory function as well as neuronal loss are recovered

[379]. This is corroborated by another study in which successful treatment reduced motor deficits despite failing to reduce NFTs [101].

In summary, while these studies do not exclude the possibility that tangles are ultimately toxic, they do suggest that NFTs themselves might not be solely responsible for the initial tau-induced neurodegeneration and dysfunction. Possibly tangles are a late-stage manifestation contributing to the disease progression by physically interfering with normal cellular functions.

1.3.3 Propagation of tau pathology

In AD and other tauopathies, it is well documented that the NFT pathology propagates in a defined manner, and that its progression throughout the brain correlates well with decline in cognitive function [323]. First, NFTs accumulate in the entorhinal cortex (EC), from where the pathology spreads to other brain regions such as hippocampus, and ultimately the neocortex, crossing limbic and association cortices in a predictable pattern [27, 70].

Until recently, it was unclear how exactly tau pathology spreads in the human brain. Recent findings point to the presence of multimeric tau species which are intermediates between tau monomers and filaments, and are referred to as tau oligomers [48, 287, 377]. They have recently received considerable attention because *in vitro* and *in vivo* studies suggested that these oligomeric species initiate toxicity, and can induce synaptic dysfunction and cell death in neurodegenerative tauopathies [48, 105, 255, 287, 377, 407]. Furthermore, several data now support the possibility that these soluble tau oligomers can be released from affected neurons, followed by their uptake into neighboring neurons. However the exact mechanism by which these oligomeric species propagate from one neuron to the next remains to be fully determined.

Furthermore, several groups report that tau propagation is a self-perpetuating process similar to that observed in prion diseases, suggesting that tau propagates in a "prion-like" manner - prion-like since they lack the infectious properties that characterize true prion diseases (reviewed in [239]). In the first step, this involves a misfolded tau protein forming a template that progressively induces other native tau proteins to adopt the same pathological conformation (also called "seeding"). In a second step, aggregates of misfolded tau species are thought to propagate from affected brain regions to unaffected regions (reviewed in [157, 448]). A recent study even provided evidence for the existence of distinct conformational states of misfolded tau, referred to as tau "strains" [378]. However, the exact association between these oligomeric species and tau seeding, propagation and neurotoxicity remains debated.

1.3.4 The role of tau PTMs in disease

In all diseases in which tau filaments are implicated, tau is found to be excessively modified, and modifications that occur prior to oligomerization or filament formation may promote

toxicity. By far, the most common and best studied PTM is phosphorylation. Several other PTMs exist, including glycosylation, ubiquitination, sumoylation, acetylation, methylation, oxidation, nitration, truncation by proteases, deamidation, prolyl isomerization, and non-enzymatic cleavage. Generally these PTMs have been associated in some way with the aggregation of tau into tangles, or the enhancement of other events such as phosphorylation or modification of tau function and structure which might in turn facilitate the formation of pathological tau species. However their study is still in its infancy. In the following section, the implication of each PTM in tau aggregation and pathogenesis is briefly summarized according to current knowledge.

Phosphorylation: Excessive tau phosphorylation is thought to play a crucial role in mediating toxicity and aggregation. In pathological conditions, both extent and number of sites of phosphorylation are increased. For example, in healthy brains, tau contains on average 2-3 phosphates per molecule, whereas tau from PHFs of patients with AD carries 6-8 phosphates [240, 263]. From the 85 potential sites, 75 have been found to be phosphorylatable [196]. 45 of these - more than half of all phosphorylatable residues - have been found in AD brain [21, 194, 196, 391, 470]. While some sites are exclusively found to be phosphorylated in diseased brain and do not occur in physiological conditions at all, others occur both in physiological and pathological conditions, although phosphorylated to different extent (Fig. 1.6). A subset of sites have received significant attention since they are recognized by antibodies raised against AD tau in a phosphorylation-dependent manner and thus are useful for diagnostic means. These include AT8 (pS202/pT205), AT100 (pT212/pS214), AT180 (pT231/pS235), 12E8 (pS262/pS356) and PHF1 (pS396/pS404) [55, 163, 178] (Fig. 1.6, top).

Since in AD brain, increased signal of these antibodies is detected compared to normal brain, historically pathological tau is referred to as being "hyperphosphorylated". Although widely used to describe the increased phosphorylation state of pathological tau, a clear definition of this term is missing (e.g. number of sites and/or the extent of phosphorylation of each site) (see also chapter 2). Over decades of extensive studies, it has become clear that tau phosphorylation and its consequences on tau aggregation and pathology is bewilderingly complex. Even though it is well accepted that aberrant tau phosphorylation is a major early characteristic of tau aggregation, it is not clear whether this process is necessary or sufficient for filament assembly. Elevated tau phosphorylation is not necessarily detrimental, as it occurs also naturally. For example, during development of fetal mammalian brain, the phosphorylation state of tau is substantially higher compared to adult brain under physiological conditions [164, 483]. Moreover, transient increased tau phosphorylation is observed in hibernating animals [22, 200, 411] and during hypothermia [354]. Furthermore, tau expressed during division of neuronal cells acquires a phosphorylation state similar to that found in AD [217, 358, 442]. Finally, phosphorylation at certain sites even protects against aggregation [381]. In conclusion, hyperphosphorylation is not an absolute indicator

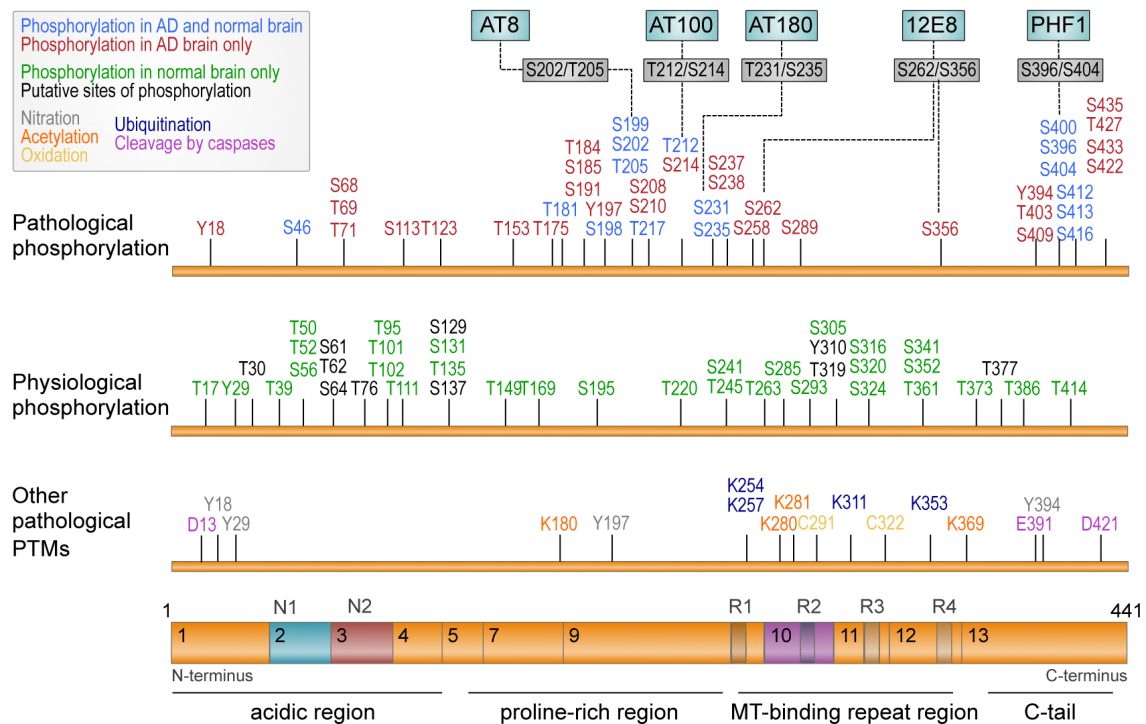


Figure 1.6: Human tau PTM sites in physiology and disease. Of the 85 tau phosphorylation sites, 45 have been described in PHF-tau derived from AD brain (top panel); of these, 29 are found in AD brain only (red) and 16 are found in both AD and normal brain (light blue). Epitopes of the AD-diagnostic antibodies are indicated. 30 phosphorylation sites are only described in normal brain (green), and the remaining 10 sites are putative (mid panel). Sites for various other PTMs have been described in AD brains (bottom panel). These include nitration (gray), acetylation (orange), ubiquitination (dark blue), and oxidation (brown). Sites of cleavage by caspases are also shown (pink). Adapted from [292], [210] and [451].

of the disease state but rather appears to reflect a state of the cell where the balance of kinases and phosphatases is perturbed in favor of phosphorylation. Despite its ambiguity, for the sake of simplicity the term "hyperphosphorylation" is used in the remaining work when referring to the state of increased phosphorylation in respect to tau pathology.

Glycosylation: Protein glycosylation is the covalent attachment of oligosaccharides to a functional group on a protein. Two types of glycosylation exist: N-linked and O-linked glycosylation. N-linked glycans are produced by the attachment of a sugar to an amine radical in the side-chains of asparagines or arginines. O-linked glycans result from the attachment of the sugar to hydroxyl radicals of serines and threonines, respectively. Tau from the brain of AD patients was found to be abnormally glycosylated [415, 450], and *in vitro* deglycosylation leads to the conversion of tau tangles into filaments, restoring their accessibility to MTs [450]. On the other hand, the O-linked attachment of N-acetylglucosamine (O-GlcNAc) on several serines and threonines decreases tau phosphorylation by the kinases

protein kinase A (PKA), CDK5 and GSK3 [276]. It is believed that O-GlcNAc counteracts phosphorylation by competition for the same sites. As such it has been proposed to prevent tau phosphorylation, thereby decreasing dissociation of tau from MT and tau aggregation [26, 275, 484].

Ubiquitination and sumoylation: Ubiquitination is the binding of one or more ubiquitin molecules (a small protein) onto proteins, and serves as a signal for their degradation by the proteasome. Tau in physiological conditions has been shown to be ubiquitinated and proteolytically processed by the ubiquitin-proteasome-system (UPS) [25, 113, 279]. In disease, excessive tau ubiquitination was proposed to occur in PHFs as a late event, after its hyperphosphorylation. Polyubiquitination in PHFs from AD was reported on several lysine (K) residues (K254, 257, 311, 317 and perhaps others) that are all in the MT-binding repeat domain [108, 308, 423]. Tau protein can also be sumoylated at K340 *in vitro* by SUMO1 (small ubiquitin-like modifier protein-1) and to lesser extent by SUMO2 and SUMO3 [128, 129, 414]. In AD, sumoylation probably counteracts ubiquitination [414], warranting further studies.

Acetylation: Another modification targeting lysine residues is acetylation, a reversible reaction that refers to the process of covalently transferring or removing an acetyl group onto or from an AA. This reaction relies on acetyl-coenzyme A and catalyzing enzymes such as histone acetyltransferases (HATs) and histone deacetylases (HDAC). Tau acetylation has been found to be increased in AD brains, and acetylation on K280 has been suggested to impair MT-binding of tau and promote aggregation [98]. Potentially acetylation interferes with ubiquitination and thus degradation of tau [303], but may also serve alternate regulatory functions.

Methylation: Methylation of tau on lysine and arginine residues has been described very recently [150, 186, 423], and the functional effects are mostly unknown.

Oxidation: Oxidation, which is prominent in aging neurons, affects two cysteines (C) in the repeat regions of tau, C291 (in R2) and C322 (in R3). The formation of dimers formed by cross-linking via two oxidized cysteines greatly enhances the rate of aggregation [386].

Nitration: Nitration is the addition of nitrogen dioxide on tyrosine (Y) on an organic molecule. Nitration has been found on both soluble tau and insoluble tau on four out of the five tyrosine residues. [89, 367]. Nitration on Y29 was found to be increased in AD [367] and was proposed to decrease tau ability to promote tubulin assembly, leading to tau oligomerization [488].

Truncation: Another major modification of tau associated to neurodegeneration and neurotoxicity is proteolytic cleavage. Tau contains several cleavage sites accessible to multiple proteases, yielding breakdown products that could be toxic in various ways. So far, proteases

found to cleave tau include calpain, caspases, and PSA (puromycin-sensitive aminopeptidase). Cleavage in AD brain patients has been shown to occur at D13, E391 and D421 [41, 209]. Truncation at these sites enhances the capacity of tau to aggregate and contributes to neuronal apoptosis [94, 141, 154].

Non-enzymatic tau PTMs: Finally, because tau and its aggregates are long-lived, they are subject to various non-enzymatic modifications, such as glycation by AGEs (advanced glycation end products), deamidation, prolyl-isomerization, cross-linking and non-enzymatic cleavage around aspartic acid (D) residues. These may be the cause of the "high MW smear" typical of AD tau preparations run on SDS gels [455].

From the evidence above, it is difficult to define which of the tau PTMs are preferentially implicated in tau pathology. Although tau phosphorylation can be considered as the major tau PTM due to the large number of sites involved, this should not preclude the qualitative importance of each of the other PTMs during the pathological process. It can be concluded that tau undergoes a wide range of biochemical and conformational changes that may occur simultaneously, and cooperation between several tau PTMs may be required for aggregation of tau into toxic species. However, the timing and significance of all these modifications in tau pathogenesis remains to be further investigated.

1.4 Tauopathies

As mentioned above, many neurodegenerative diseases are associated with tau inclusions, and they are collectively referred to as tauopathies. An extensive list of tauopathies can be found in Table 1.1. Based on their predominance, tauopathies are recognized as the most common proteinopathy (see also Fig. 1.1).

Apart from AD, other common non-familial tauopathies are PSP, CBD, and PiD, which all fit into the spectrum of FTLD-tau (the other subtypes of FTLD presenting with ubiquitin-positive and TDP-43-positive, but tau-negative inclusions (FTLD-TDP-43), or FUS aggregates (FTLD-FUS) [285]). FTLD-tau disorders are characterized by selective atrophy of the frontal and temporal cortex with neuronal loss, gliosis, as well as tau-positive inclusions. Despite the tau accumulation as common pathological hallmark, clinical presentations and selective vulnerability of anatomic systems vary across these disorders (see also Fig. 1.7). Furthermore, each of these tauopathies is characterized by characteristic inclusions and lesional distributions. Finally, the preferential accumulation of alternative splice forms (3R-tau or 4R-tau) contributes to heterogeneity of tau neuropathology [117, 477]. The latter led to the differentiation of 4R tauopathies (4R>3R) and 3R tauopathies (4R<3R). In the following section, a summary for each of the above mentioned tauopathies is provided, including a description of the biochemical and ultrastructural characteristics of the tau lesion that are found in neurons and glia in these patient brains (for a summary see Table 1.2).

Table 1.1: Diseases with tau inclusions. Tauopathies examined over the course of this work are marked in bold.

Pathological diagnosis
Alzheimer’s Disease (AD)
Amyotrophic lateral sclerosis of Guam
Argyrophilic grain disease (AGD)
Chronic traumatic encephalopathy
Corticobasal degeneration (CBD)
Diffuse neurofibrillary tangles with calcification
Down’s syndrome
Familial British dementia
Familial Danish dementia
Frontotemporal dementia and parkinsonism linked to chromosome 17 (FTDP-17)
Frontotemporal lobar degeneration (some cases caused by C9ORF72 mutations)
Gerstmann-Sträussler-Scheinker disease
Guadeloupean parkinsonism
Myotonic dystrophy
Neurodegeneration with brain iron accumulation
Niemann-Pick disease, type C
Non-Guamanian motor neuron disease with neurofibrillary tangles
Parkinsonism-dementia complex of Guam
Pick’s disease (PiD)
Postencephalitic parkinsonism
Prion protein cerebral amyloid angiopathy
Progressive subcortical gliosis
Progressive supranuclear palsy (PSP)
SLC9A6-related mental retardation
Subacute sclerosing panencephalitis
Tangle predominant dementia
White matter tauopathy with globular glial inclusions

Further below, current approaches for their differential diagnosis and therapy are described (sections 1.4.5 and 1.4.6).

1.4.1 AD

AD is the best-studied tauopathy and the most common form of dementia in the aging population. Contributing to 60-70% of cases, it is estimated to affect more than 30 million people worldwide, a number that is expected to triple by the year 2050 [359]. Characteristic features are the flame-shaped NFTs in cell bodies and apical dendrites of neurons, and neuropil threads in distal dendrites. In a strict sense, AD is not a primary tauopathy since tau pathology is evident in conjunction with extracellular $A\beta$ deposition into neuritic plaques. Glial inclusions are not prominent in AD, but PHF as well as SF have been found in astrocytes and coiled bodies in AD brains of patients with long duration [23, 216, 321, 328, 474]. Furthermore, AD brains contain higher quantities of tau than unaffected subjects [246, 247] (see also section 3.4, Fig 3.2).

AD patients typically present initially with memory impairment, correlating with tau

Table 1.2: Biochemical characteristics of sporadic tauopathies. AD and several disorders from the spectrum of FTLD-tau present with distinct tau isoform distributions and characteristic tau inclusions in neurons and glia cells.

	Isoforms	Filaments	Neuronal inclusion	Glial lesion
AD	3R \approx 4R	PHF » SF	NFT, neuropil threads	rare SF/PHF in astrocytes and coiled bodies
PSP	4R>3R	SF; rare twisted filaments	globose NFT, pretangles, ballooned neurons	tufted astrocytes, coiled bodies
CBD	4R>3R	SF; rare twisted filaments	pretangles, ballooned neurons	astrocytic plaques, coiled bodies
AGD	4R>3R	SF; rare twisted filaments	pretangles, ballooned neurons	coiled bodies
PiD	3R>4R	SF; loose twisted filaments	Pick bodies, Pick cells	rare ramified astrocytes

NFT load in medial temporal lobe structures, including the entorhinal cortex, amygdala, and hippocampus early in the disease process [28, 70]. The stereotypic progression from temporal lobe to association cortices and eventually the involvement of primary cortex was originally described by Braak and Braak [70]. Dementia associated with AD pathology has an insidious onset with progressive deterioration of cognitive functions. The recently updated clinical diagnostic criterion for dementia associated with AD pathology incorporates imaging and cerebrospinal fluid (CSF) biomarkers in efforts to improve early detection and tracking of disease progression, which are further described below (section 1.4.5) [13, 300]. Atypical AD cases have been reported that don't fit the Braak staging scheme and show a different distribution and density of NFTs. They also show defined clinical characteristics and thus have been considered as distinct subtypes of AD [227, 316].

1.4.2 FTLD-tau

PSP: PSP was first described in 1964 by Steele, Richardson and Olszewski [408]. Like other disorders from the type FTLD-tau, PSP is a sporadic neurodegenerative disorder that is characterized with prominent hyperphosphorylated tau aggregates in the brain accompanied by neuronal loss and gliosis. Because of the preferential accumulation of 4R-tau isoform, PSP is considered a 4R tauopathy. The core neuroanatomical regions affected in all cases of PSP include the basal ganglia, subthalamic nucleus and the substantia nigra [202]. Cortical involvement is minimal but if present it is greatest in motor and premotor cortices [235]. Often, PSP can be diagnosed on macroscopic examination by severe midbrain atrophy with dilation of the superior cerebellar peduncle [430], but in atypical cortical presentations of PSP this atrophy may be mild or absent.

Microscopically, PSP neuropathology is characterized by neuronal inclusions called globose NFTs. The hallmark glial lesion is the tuft-shaped astrocyte or tufted astrocyte, apart from tau immunoreactive inclusions in oligodendrocytes, termed coiled bodies. Tufted astrocytes are abundant in the motor cortex and the corpus striatum. Neuronal loss and gliosis is

most marked in the substantia nigra and subthalamic nucleus, where thread-like processes and coiled bodies are often found. Ultrastructural analysis of PSP pathology reveals that most inclusions are 4R-tau isoforms that aggregate into SFs, while rare twisted filaments have been observed (Table 1.2).

Patients with PSP usually present with a late-onset atypical parkinsonism. Most cases suffer from axial rigidity, postural instability and unexplained falls, and personality changes, with most patients also developing progressive vertical gaze palsy (for which the disorder is named). Although these symptoms describe the typical PSP cases, there is a great deal of pathological heterogeneity that causes patients to present with various clinical syndromes. Typically, the particular clinical phenotype is determined by the distribution of tau pathology. Variants of PSP include behavioral variant FTD (bvFTD) [56], progressive nonfluent aphasia (PNFA) or apraxia of speech [232], corticobasal syndrome (CBS), the clinical presentation of CBD [234, 431], and pure akinesia with gait freezing (PAGF) [9, 463]. The cause of this extensive variability associated with PSP is currently unknown but underlying genetic variance is expected to play a role.

CBD: CBD was first described in 1967 by Rebeiz and colleagues and referred to as corticodentatonigral degeneration with neuronal achromasia [363]. Like PSP, CBD is a neurodegenerative disorder classified as 4R tauopathy due to neuronal and glial aggregates of hyperphosphorylated 4R-tau isoforms. Tau lesions in the brains of CBD patients are found in both gray and white matter of the neocortex, basal ganglia, thalamus, and to a lesser extent, the brain stem [121]. Gross examination of the brain varies from patient to patient. Most cases are asymmetric, with only one hemisphere affected.

The hallmark glial lesion in CBD is the astrocytic plaque, which is not observed in other disorders [142, 253]. Microscopic analysis of affected cortices often shows cortical thinning with neuronal loss, gliosis, and many ballooned neurons. These achromatic neurons appear enlarged, with a pale, glassy cytoplasm, are often vacuolated and with swollen dendrites. They can be immunostained with phosphorylated neurofilament, tau, and beta-crystallin antibodies. Ultrastructural characterization of tau pathology in CBD reveals mostly SFs with some wide twisted filaments, similar to PSP (Table 1.2).

The classic clinical presentation of CBD is atypical parkinsonism and is specifically referred to as CBS. It is associated with asymmetrical rigidity and apraxia, often with dystonia and the classic symptom of "alien limb" [274]. Moderate dementia emerges sometimes late in the course of disease [369]. CBD is associated with focal cortical atrophy and because of this patients can present with a wide range of clinical syndromes depending on the location of the highest tau burden pathology and marked cortical atrophy. Because of the heterogeneity of symptoms and clinical phenotypes, defining clinical diagnostic criteria for CBD has been extremely challenging. Common atypical cases include presentations with bvFTD or PNFA with focal degeneration in peri-Sylvian areas. Furthermore, it is increasingly recognized that CBD has substantial overlapping pathological and clinical features with PSP and other

disorders such as PD and dementia with Lewy bodies (DLB) which often make a differential diagnosis difficult, both on clinical and pathological level.

PiD: Pick's disease is a less common cause of FTLD-tau, accounting for less than 5% in autopsy series of dementia [38]. It is classically associated with severe circumscribed cortical atrophy of the frontal and temporal lobes. Also here, the clinical presentation is determined by the distribution of the most affected cortical degeneration.

Neuropathologically, apart from the frontotemporal lobar and limbic atrophy, PiD is defined by marked neuronal loss, spongiosis, and gliosis. The characteristic histopathological inclusions observed in PiD, termed Pick bodies, are round intraneuronal inclusions composed of hyperphosphorylated 3R-tau [360, 398]. Pick bodies are argyrophilic on some silver stains, e.g. Bielschowsky, but consistently negative with the Gallyas Braak silver stain method. Another less specific feature of PiD are ballooned achromatic neurons (also called Pick cells), similar to those observed in CBD. Tau-immunoreactive glial inclusions, including small, round inclusions in oligodendrocytes and ramified astrocytes are sometimes present in PiD but not as frequent as seen in the 4R tauopathies (see above). Interestingly, glial lesions contain predominantly 4R-tau [207] which may contribute to the variability in the ratio between 3R and 4R-tau isoforms observed in different biochemical studies. There is overlap between subcortical nuclei affected in PiD compared to both CBD and PSP [143]. Ultrastructural analysis of tau pathology in PiD reveals mostly SF, with some wide twisted filaments that aggregated in close proximity and can be associated with dense granular material.

PiD patients with frontotemporal atrophy often present with bvFTD [100], while frontoparietal atrophy presents with apraxia [267], and peri-Sylvian atrophy with PNFA [176]. When amnesic symptoms prevail, clinical diagnosis is often initially AD. PiD is a disorder that is usually associated with "presenile dementia" with age of onset younger than 65 years. Familial forms of PiD are rare and are due to mutations in the *tau* gene [77, 207, 318].

1.4.3 Other tauopathies

Another disorder of the FTLD-tau group is AGD, a highly frequent but atypical 4R tauopathy that is not always associated with clinical progression. Although it will not be part of the presented work, it is described here for the sake of completeness. AGD is characterized by the presence of abundant spindle-shaped argyrophilic grains in the neuronal processes, pre-neurofibrillary tangles, and coiled bodies in oligodendrocytes, all positive for 4R-tau. Because clinicopathological studies failed to show a distinctive clinical or imaging phenotype associated with AGD, recent studies raise the hypothesis that AGD may be a defense mechanism against the spread of other neuropathological entities, in particular AD [371]. Recent evidence links the lack of tau acetylation in AGD to its protective role against the spread of AD [179], a hypothesis that remains to be investigated.

Other tauopathies include Down's syndrome, parkinsonism with dementia, myotonic dys-

trophy, prion diseases with tangles, Blunt disease (an ophthalmologic disorder), dementia pugilistica, dementia with tangles only, ALS, and parkinsonism-dementia complex of Guam. For a complete list of tauopathies see Table 1.1 (reviewed in [82] and [219]).

1.4.4 Age-related changes in tau

While extensive neuronal loss and the formation of NFT is generally associated with neurodegenerative disorders, these changes have also been observed in normal aging brain. For example, evidence of neuronal loss has been shown in the brain of patients with very mild cognitive dysfunction [311], and other studies indicate that age-related events lead to the formation of NFTs that are indistinguishable from those of AD, with the difference that no $A\beta$ plaques are found. Recently, this NFT pathology has been considered to represent a distinct disease, termed primary age-related tauopathy (PART) [106]. Moreover, FTLD-tau-like pathology was reported in non-demented elderly individuals exhibiting argyrophilic grains and oligodendroglial coiled bodies in a pattern similar to AGD. It is not clear whether these cases represent preclinical stages of AD or specific FTLD-tau subtypes, or whether such lesions are age-related as suggested for PART [71, 421, 425].

1.4.5 Diagnosing tauopathies

Pre-mortem clinical diagnosis

As discussed above for each individual disorder, FTLD-tau may present as several clinical syndromes: behavioral/dysexecutive syndrome (bvFTD), language disorder (primary progressive aphasia variants such as semantic dementia (SD) and PNFA), and motor disorders (ALS, CBS, PSP syndrome). Although specified diagnostic criteria have been established for the typical clinical symptoms associated with each disease [13, 24, 202, 300], there is a substantial overlap and a vast heterogeneity in clinical presentations of underlying neuropathologies, including AD (Fig. 1.7A). For example, some patients with confirmed CBD pathology at autopsy have a clinical presentation indistinguishable from that of PSP. Reversely, it has also become clear that CBS, the classical syndrome of CBD, is not specific to CBD [63, 273, 443]; to the contrary, evidence suggests that CBS is more likely to be caused by a pathology other than CBD, e.g. PSP, AD, PiD, or a pathology unrelated to tau [63, 273, 443], such as FTLD-TDP-43 (Fig. 1.7B). Other clinical phenotypes with profound neuropathological heterogeneity are bvFTD and PNFA. In summary, due to the absence of reliable diagnostic criteria or biomarkers, current clinical criteria do not reliably predict underlying proteinopathies, and an unequivocal differential diagnosis can often only be confirmed by histopathological examination of the brain post-mortem. Although it is the most common form of dementia, this is currently also the case for AD.

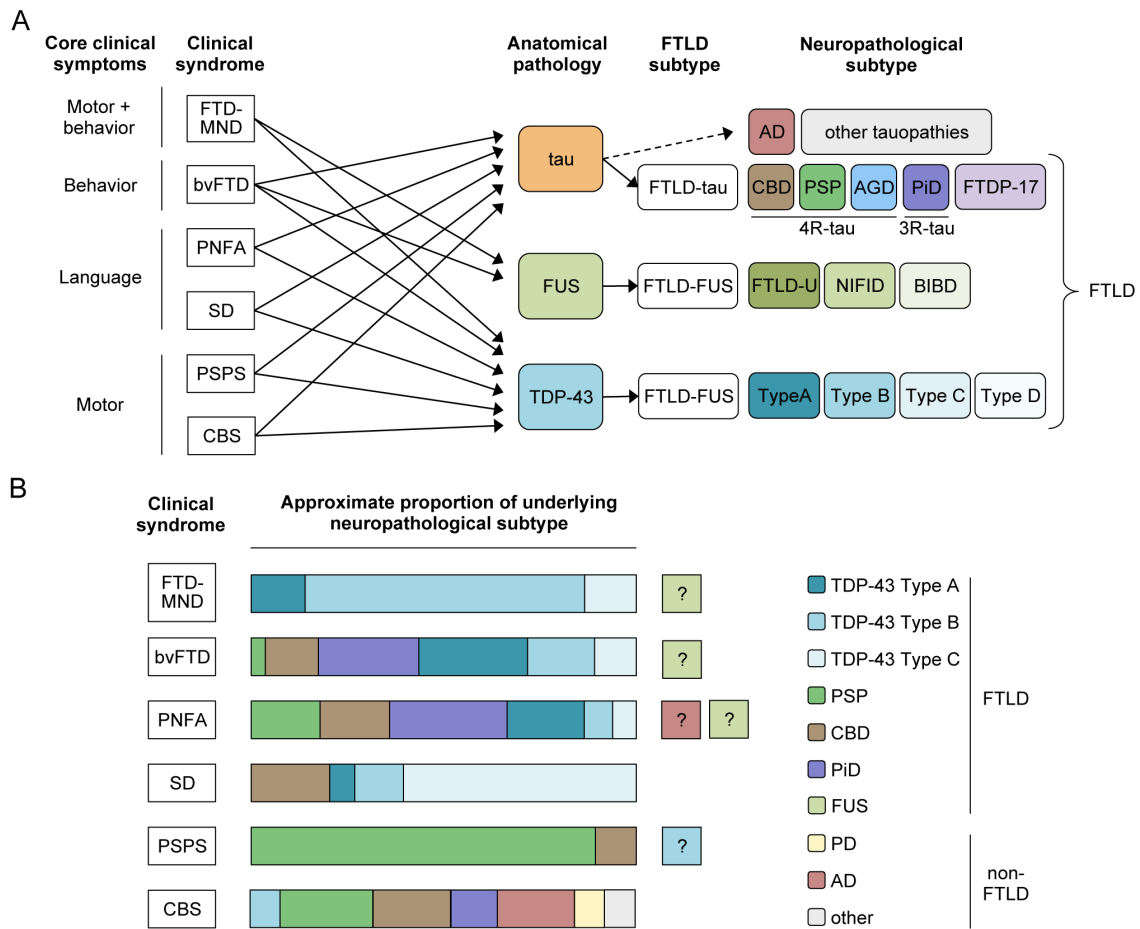


Figure 1.7: Relationship between clinical FTD phenotypes and underlying disease pathologies. **A.** Patients with FTD usually present with deficits in behavior, language and/or motor function. Each clinical subtype can be caused by several underlying molecular pathologies: tau, FUS, or TDP-43. The associated disease neuropathology is denominated FTLD-tau, FTLD-FUS, and FTLD-TDP-43. **B.** For each clinical subtype, the estimated proportion of underlying pathology is depicted. Question marks indicate that the proportion of the respective pathology is unknown. Adapted from [111] and [167].

Biomarker development

A biomarker is defined as "a characteristic that is objectively measured and evaluated as an indicator of normal biologic processes, pathogenic processes, or pharmacologic responses to a therapeutic intervention" [182]. A biomarker can thus predict and diagnose disease, monitor disease progression and response to therapy, as well as help in drug discovery. In view of current difficulties in reliably diagnose tauopathies prior to autopsy, extensive efforts have been put into biomarker research including 1) body fluid analysis and 2) neuroimaging. They were initially developed for AD and are being expanded to other tauopathies.

1) **Body fluid biomarkers:** Unlike in other disease such as cancer, biochemical changes in the diseased brain cannot be directly visualized by *in vivo* tissue sampling. Thus, numerous

investigations have focused on peripheral biomarkers. One approach is the identification of changes (increases or decreases) of protein levels in CSF and plasma from patients compared to controls and MCI patients. In the mid 90s, three protein biomarkers have been established for AD: 1) total tau levels, believed to reflect the axonal degeneration of neurons; 2) phosphorylated tau levels (pT181), thought to reflect NFT pathology; and 3) $A\beta$ levels, correlating to amyloid plaques [61, 312]. Since they represent the key elements of AD pathology, these biomarkers are considered the "core" AD biomarkers, and they were incorporated into the clinical diagnostic criteria for dementia associated with AD pathology [13, 300]. However, the vast majority of studies investigating these biomarkers have not followed a standardized protocol for recruitment of patients, sample size, sample collection, or reporting, and have been criticized for lack of consistency. Furthermore, although they can distinguish between AD and control patients, they do not reflect the clinical course of the disease over time [68], and they cannot distinguish AD from other neurodegenerative disorders, including FTLT-tau [383]. In order to discriminate AD from other primary dementia disorders, more accurate and specific markers are needed. Preliminary evidence suggests that quantification of tau which is phosphorylated at other sites than pT181 could improve early detection and differential diagnosis [60]. When combined with the established AD biomarkers, the level of α -synuclein and neurofilament light chain may improve differential diagnosis of AD from parkinsonian disorders such as PSP, CBD, DLB and PD [188]. Several other novel biomarker candidates that are currently being investigated are β -site APP cleaving enzyme 1 (BACE), soluble APP proteins α and β , and soluble $A\beta$ oligomers [190, 471].

2) **Tau imaging:** Another method to detect and monitor tauopathies are neuroimaging approaches that determine distinct patterns in the brain using different brain-scanning techniques. Due to the death of specific neuronal populations, disease-specific atrophy distribution and/or distinct changes in brain function may occur in each tauopathy. Two noninvasive imaging technologies are currently used to measure tau pathology in the brain: positron emission tomography (PET) [151], and magnetic resonance imaging (MRI) [314]. PET imaging is used for measuring tau-mediated neuronal injury. It involves intravenous injection of a radioactive tracer into the patient. The tracer binds to a biologically active molecule of interest, here tau, and decays to produce gamma radiation that can be measured using PET cameras. Especially after the invention of the excellent $A\beta$ plaque binding tracers, such as radio-labeled Pittsburgh compound B and florbetapir, the search for a tau binding tracer has intensified [250, 294]. However, owing to the vast molecular heterogeneity of tau, development and validation of selective tau PET tracers is not straightforward [317]. This quest has seen recent advances with the development of several classes of tau-specific PET ligands [6, 332, 395, 487] but their potential in differentially diagnosing tauopathies needs to be further validated.

MRI is based on the principle of nuclear magnetic resonance of the atomic nuclei. It captures

structural changes that occur on a microscopic level, such as gray and white matter atrophy. Significant advances have been made in identifying neuroanatomical patterns underlying different FTLD clinical syndromes [248, 317, 364]. Although phenotypic heterogeneity has been linked to distinct atrophic patterns, studies are usually inconclusive in respect to whether atrophy can predict the subtypes of FTD-tau [181, 248, 346]. Furthermore, the extent of brain atrophy and neuronal injury does not always correlate with the amount of cognitive decline, further complicating the identification of specific diagnostic patterns.

Post-mortem diagnosis

Due to the challenges associated with pre-mortem diagnosis, to date an accurate diagnosis of tauopathies is often only possible post-mortem by investigation of form and location of inclusions among the diseases using several neuropathological techniques. Post-mortem classification and differential diagnosis is a tedious and time-consuming endeavor as it involves gross and microscopic assessment of anatomical distributions and abnormalities in a stepwise manner. Diagnosis is based on the identification of characteristic morphological changes, as well as distribution and type of lesions in several brain sections, using various staining techniques that visualize all suspect pathologies.

The most accurate method existing today is immunohistochemistry, as it can be used to detect aberrantly phosphorylated tau and distinguish tau isoforms [73]. The phospho-specific tau antibody most widely used in diagnostic practice is AT8 (pS202/pT205), but several other well-characterized commercially available diagnostic antibodies exist. Importantly, different phospho-specific antibodies can detect pathological structures differently in the same brain depending on the anatomical region and their binding specificity. This means that not all phospho-specific tau antibodies will result in the visualization of the same structures, which may have implications in diagnostic practices. In addition to phospho-specific antibodies, tau isoform-specific antibodies (RD3 and RD4) are available that stain 3R-tau and 4R-tau isoforms, respectively [397]. Furthermore, immunodetection of ubiquitin or p62-containing aggregates is becoming more common in diagnostic practice [264].

Traditionally, labeling of aggregates is performed using silver stains (such as Bielschowsky, Bodia, Gallyas, Campbell-Switzer) [435]. β -sheet structure-specific fluorescent labels have been proposed as a quicker and easier alternative, for example Thioflavin S, which has been shown to label NFTs in AD comparably to the Gallyas silver staining method [412].

Although the silver stainings in combination with immunohistochemistry are widely used for the differential pathological diagnosis of tauopathy brains at autopsy, their application is hindered by the difficulties of the techniques, variability of staining qualities, and the lack of standardized protocols [12]. Neuropathological evaluation requires the careful interpretation of silver stained and immunoreactive structures that are visible using these techniques. In neurons, tau immunoreactivity applies to (i) pretangles, (ii) NFTs, (iii) Pick bodies and other spherical cytoplasmic inclusions, (iv) dystrophic neurites, (v) neuropil threads and

(vi) grains. In astrocytes, the most relevant tau immunoreactive morphological features are tufted astrocytes (PSP) and astrocytic plaques (CBD) (see also Table 1.2). Further complicating interpretation, these structures all show variable silver staining or ubiquitin/p62 immunoreactivity. This is because it is thought that aggregates develop in a particular sequence, following a hierarchical pathway and spreading across the brain sequentially. Thus, aberrantly phosphorylated pretangles (detectable by phospho-tau immunostaining) are an early stage of ubiquitinated, fibrillar NFTs (detectable by silver stains and ubiquitin/p62 immunostaining). In summary, tau-immunoreactivity 1) can vary between regions of the same brain, and 2) may not overlap with the silver stain and ubiquitin/p62 staining pattern, hindering unequivocal diagnosis. Furthermore it has to be kept in mind that co-morbidities can occur, e.g. AD-related pathologies can be observed in patients with PiD, PSP, CBD, and non-demented elderly individuals.

1.4.6 Therapeutic approaches for tauopathies

To date, no effective disease modifying or preventive therapy exists for tauopathies. This is partially due to the absence of accurate early differential diagnosis and the lack of specific biomarkers and selective PET tracers to measure effectiveness of treatment (see section 1.4.5). Thus, current therapy does not address cause, but provides symptomatic relief either by temporarily improving symptoms above baseline or by delaying cognitive decline.

Most therapeutic efforts have focused on AD, the most common and best characterized form of dementia, while the treatment of FTLD disorders has received much less attention [111]. Based on the amyloid cascade hypothesis of AD [198], wherein abnormal accumulation of $A\beta$ is speculated to be the most important and first disease specific mechanism, the majority of drug trials initially targeted $A\beta$ removal or reduction in the brain. However, more than 100 candidate treatment compounds have failed in Phase III latest (where the drug is tested in symptomatic patients) [43–45]. Recognition of the central role of tau in AD disease pathogenesis and many other disorders, as well as the correlation of tau aggregates with cognition and memory deficits have led to a paradigm shift. Increasing efforts are now going towards the development of tau-targeted treatments, and many clinical trials for AD are ongoing, and a handful for FTLD-tau. While initially the major focus was the reduction of NFTs, to date many different approaches are being pursued that aim to reduce in some way the consequences of tau pathogenesis in AD and related tauopathies. These strategies are described below, with a focus on PTM-related targets (also summarized in Fig. 1.8).

MT-stabilization: Because tau sequestration into NFTs or other fibrillar structures results in a loss of normal tau stabilization of MTs, MT-stabilizing agents might compensate for a reduction of the tau-MT interaction, and thus sustain axonal transport and cellular morphology. Programs for such drugs are at various stages of development, ranging from preclinical investigations to Phase II studies. Examples for MT stabilizing drugs are Epoposin D and davunetide (also referred to as NAP and AL-108) [39, 80, 485]. The

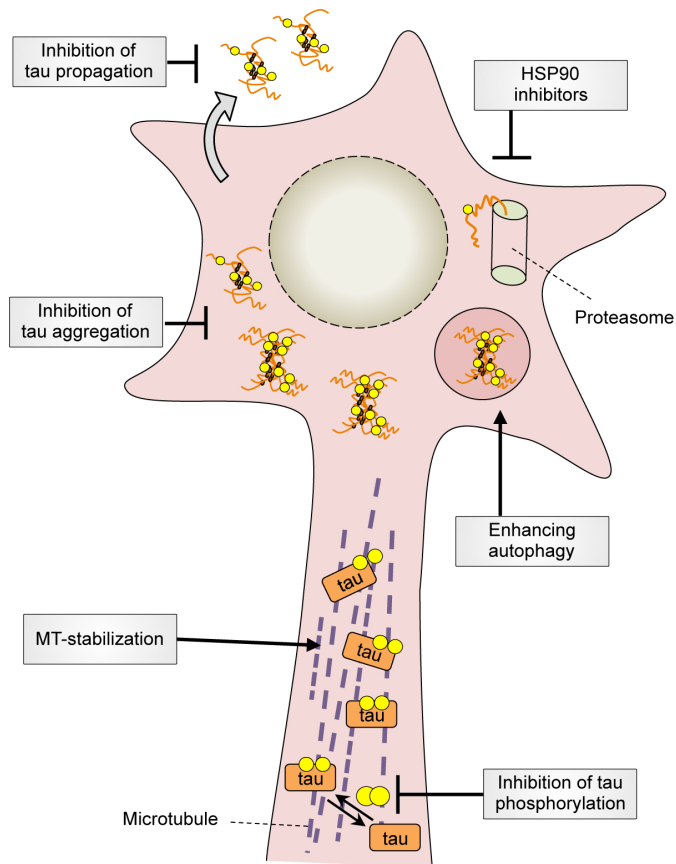


Figure 1.8: Therapeutic approaches to reduce tau-mediated neuropathology and toxicity. Several strategies are being pursued to decrease the consequences of pathological tau in AD and related tauopathies. In these diseases, hyperphosphorylated tau detaches from MT, leading to destabilization of MTs and aggregation of tau. MT-stabilizing agents might compensate for the loss of normal tau stabilization. Inhibitors of kinases and/or activators of tau phosphatases might improve both MT function and reduce the formation of tau multimers. Another approach is the upregulation of tau degradation; HSP90 inhibitors might increase proteasome-mediated clearance and remove misfolded and/or phosphorylated tau monomers, whereas autophagy enhancers might increase the removal of tau fibrils. Last but not least, clearance of extracellular tau might decrease the propagation of toxic oligomeric tau species.

latter is undergoing Phase II clinical trials for the treatment of PSP [168], FTDP-17, CBD and PNFA (NCT01056965). However, a recently published trial (Phase II/III) reported davunetide to be ineffective for treatment of PSP [69].

Inhibition of tau assembly into oligomerization and fibrils: Although it is still debated whether fibrillar tau aggregates are toxic or result from an effort of the cell to sequester these toxic species (see also section 1.3.2), in either case inhibiting the process of aggregation should be a promising target. Inhibition of novel tau fibril formation or dissolution of pre-existing aggregates may prevent toxic gain of functions and/or increase the levels of monomeric tau, which could contribute to MT stabilization (compensating loss of function). Several programs have conducted high-throughput screening studies to identify aggregation inhibitors that are now in early stages of clinical Phases. An advanced example is the dye methylene blue, which has shown positive therapeutic effects in a Phase II clinical trial and is now undergoing Phase III clinical trials for AD [465] (NCT01689233, NCT01689246).

Upregulating intracellular tau degradation: Another strategy to reduce harmful levels of pathological tau species is to enhance its degradation, either via the ubiquitin-proteasome pathway or the autophagy (lysosomal) system (reviewed in [270]). Inhibitors of Heat shock protein 90 (HSP90), a molecular chaperone that assists in the folding of many proteins, have shown to decrease the amount of hyperphosphorylated tau in mouse models [119, 283].

There is also growing evidence that upregulation of the autophagy mediated degradation system with drugs like rapamycin might be a potential strategy for the treatment of tauopathies [189].

Inhibition of tau pathology propagation by immunotherapy: Evidence suggests that extracellular abnormal tau can enter cells and induce a templated seeding process, thus leading to propagation of misfolded tau and tau pathology (see also section 1.3.3). Thus, removal or degradation of extracellular tau should be a promising therapeutic approach. Several studies using tau antibodies to clear the misfolded propagating tau species (with either active or passive immunization strategies) have shown beneficial effects in preclinical studies [30, 52, 65, 67].

Attenuation of inflammation: Inflammatory response plays an important role in AD [10, 418] and other tauopathies [156, 225]. Moreover, a chronic inflammatory state, including diabetes mellitus and hypertension, was reported to be a risk factor for AD [361]. A relationship between microglial activation and NFT burden has also been demonstrated [88, 107, 394]. Several clinical trials targeting inflammation have been conducted and are at various stages of development [249, 343, 428].

Targeting tau PTMs: Tau PTMs, including phosphorylation, glycosylation, ubiquitination, and acetylation, are thought to be an important regulatory mechanism both in physiological and pathological processes. Several PTMs have been suggested to contribute to the propensity of tau to aggregate in AD and/or related tauopathies (see section 1.3.4). Targeting PTMs represents promising therapeutic avenues as it may restore physiological tau function as well as decrease its aggregation (reverting loss of function and decreasing gain of toxic function).

Reducing pathological tau phosphorylation, either by inhibition of kinases or activation of phosphatases has been a major focus in the development of tau-targeting therapeutics (reviewed in [195]). However, reducing tau phosphorylation levels is associated with several challenges. Many kinases have been shown to phosphorylate tau *in vitro*, but the identity of the true physiological and pathological kinases *in vivo* remains unclear. This process also requires detailed knowledge of all phosphorylation sites in both physiological and pathological states. Although extensively investigated, of the 45 AD-specific sites known to date [195], only a small number of sites have been well characterized. It remains uncertain which of these sites are the most important for tau hyperphosphorylation in human disease. Thus, the identification of relevant tau kinases and phosphatases as therapeutic targets is not straightforward. Another challenge is the high risk of off-target effects, as most kinases regulate multiple cellular processes. Finally, achieving selectivity of kinase inhibitors has been difficult [158].

GSK3 and CDK5 are among the best studied tau kinases and are thought to be good targets for treatment: Both are known to phosphorylate tau at a large number of sites,

and their expression levels in the brain are high. Furthermore, both kinases have been shown to be associated with all stages of NFT pathology in AD [261, 345]. Various compounds targeting GSK3 and CDK5 kinase inhibition are currently at different stages of preclinical investigation [479]. Only GSK3 inhibitors have entered clinical trials to date, with tideglusib being the most advanced (Phase II), for treatment of mild-to-moderate AD (<http://clinicaltrials.gov/ct2/show/NCT01350362>).

In addition to phosphorylation, several other PTMs are thought to alter tau function directly or indirectly during disease (see also section 1.3.4). Because tau O-GlcNAc and phosphorylation seem to be reciprocally regulated, inhibition of β -N-acetylglucosaminidase (O-GlcNAcase) might be another approach for decreasing pathological tau phosphorylation. PHF-tau from AD brain is highly glycosylated and forms advanced glycation end products that generate oxygen free radicals, which might contribute to AD pathogenesis [475]. Recent studies have indicated that tau acetylation may contribute to tau mediated neurodegeneration by driving tau aggregation and inhibiting its degradation [98, 223, 303]. Furthermore, nitration has been observed on four residues in the tau protein, and each nitration site has a different pathological significance. For example, nitration at Y29 or Y197 increases, but that at Y18 or Y394 decreases the propensity of tau to form filaments *in vitro* [367]. Antibodies selectively recognizing nitration at Y29 or Y197 are able to stain NFTs in AD brain, furthermore an antibody to nitration at Y29 was shown to stain neuronal tau inclusions in the brains of CBD and PSP patients [367]. Last but not least, the involvement of the ubiquitin-dependent clearance pathway that requires the action of ubiquitin-ligases and molecular chaperones offers multiple targets for treatment. For example, manipulation of HSP70/CHIP or inhibition of HSP90 has been shown to induce proteasome-mediated tau degradation and a decrease in tau steady-state levels, as well as a selective clearance of phosphorylated tau [119, 349]. In summary, modulation of non-phospho PTMs of tau holds promise for many potential therapeutic targets, but much more research is needed to advance them into preclinical studies.

1.5 Mass spectrometry (MS)-based proteomics

MS-based proteomics enables the identification and quantification of thousands of peptides or proteins in complex biological samples (tissue, cell culture, organelles, body fluids). Apart from the analysis of primary sequence, proteomics allows for the analysis of PTMs and protein-protein interactions. To date, MS-based proteomics has reached high-throughput capabilities due to routine sample preparation and analysis workflows, as well as the availability of large protein sequence databases for many organisms. Still, due to the rapid development of more sensitive, faster technologies and improved workflows, its sensitivity, reliability and versatility is constantly improving.

1.5.1 Key principles and instrumentation

Mass spectrometry is an analytical technique for the determination of the elemental composition of a sample or a molecule. It can also be used for structural analyses of molecules such as peptides or chemical compounds. The principle of MS consists of ionizing the components of a sample and measuring their mass-to-charge (m/z) ratios. A typical MS experiment consists of two steps: First the analyte is transferred to gas phase and ionized, resulting in the formation of charged particles. The two techniques most commonly used for volatilization and ionization are electrospray ionization (ESI) and matrix-assisted laser desorption/ionization (MALDI) [144, 238]. In the second step, the ions are accelerated by an electric field, the m/z of the ionized particles is measured by a mass analyzer, and a detector registers the number of ions for each m/z value. The analyzer is, literally and figuratively, central to the technology, determining the sensitivity, resolution and mass accuracy of the instrument. Several analyzers can be combined to perform tandem (MS/MS) spectrometry to generate information-rich ion mass spectra from peptide fragments (called tandem mass, MS/MS, or MS2 spectra) [4, 290, 340]. The most common analyzers include quadrupole, time-of-flight and ion trap mass analyzers [8].

1.5.2 Shotgun proteomics: Protein identification and quantification

Traditionally an MS-based proteomics experiment aims for the identification and often quantification of ideally all proteins present in a complex peptide mixture. This approach is also referred to as shotgun proteomics, or discovery proteomics.

Protein identification

A typical shotgun proteomics experiment consists of the following steps (for a schematic of the workflow, see Fig. 1.9, left panel): first, proteins to be analyzed are extracted from their biological source (cell lysate or tissue) and optionally fractionated biochemically or by affinity selection. Proteins are then enzymatically cleaved into peptides, usually by trypsin. The resulting peptide sample is further fractionated by liquid chromatography (LC) and eluted into an ESI ion source. The volatilized, multiply charged droplets give rise to ionized peptides that are subjected to a first round of mass spectrometric analysis where the mass spectrum of peptides eluting at a certain time point is analyzed (MS1 spectrum). Specific ions, typically the most abundant, are then selected and subjected to further fragmentation through collision, resulting in a MS2 spectrum which can be used to deduce the corresponding AA sequence. This acquisition mode is also known as data-dependent acquisition (DDA) mode. MS2 spectra are then assigned to their corresponding peptide sequences by database searching which in turn allows for the identification of the proteins in the original sample [5, 409]. The combination of LC separation and MS/MS analysis is commonly referred to as LC-MS/MS.

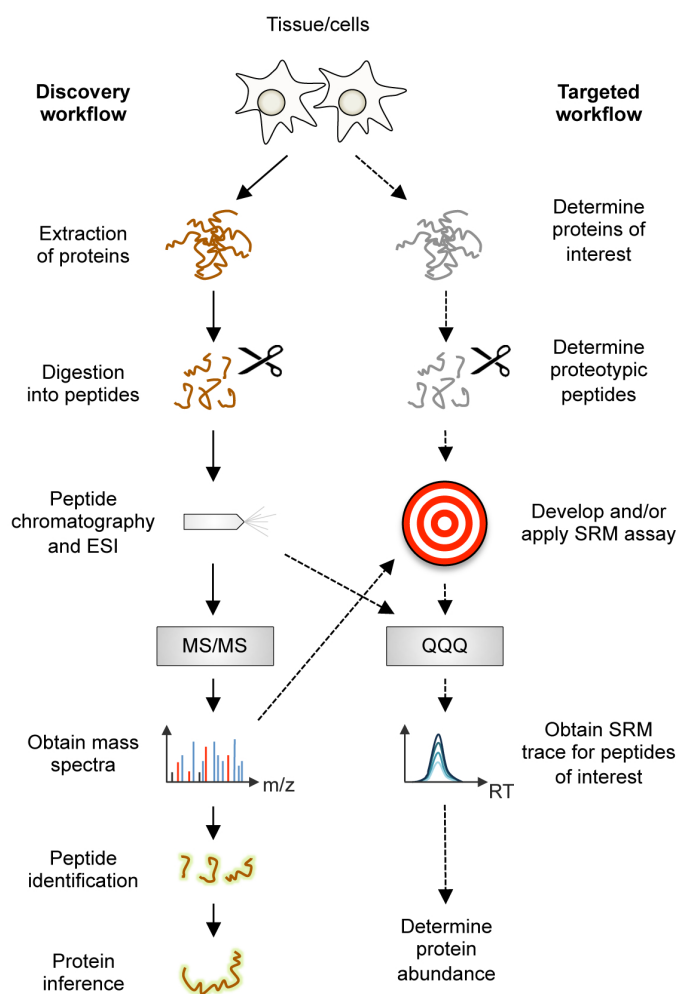


Figure 1.9: Generic discovery and targeted workflow in MS-based proteomics. In a typical shotgun experiment (left panel), the proteins to be analyzed are extracted from cell or tissue lysate and cleaved into peptides, which are then separated by LC and eluted into an ESI source. MS1 spectra (and in LC-MS/MS, MS2 spectra) are obtained. Comparison of acquired spectra against a database enables the identification of peptides, which allows for the inference of protein identity. In a targeted workflow (right panel), proteins and proteotypic peptides have to be determined prior to analysis. Once the targeted assay (e.g. an SRM assay) is developed, the sample workflow prior to MS is the same as for the discovery experiment. In SRM, traces for each peptide are obtained and quantities can be inferred (for details see section 1.5.3).

Protein quantification

In addition to the identification of the proteins in the sample of interest, quantitative information can be obtained through a variety of techniques (depicted in Fig. 1.10). These can be generally divided into label-free and label-based methods. A basic label-free technique involves quantification based on measurements of spectral counts (from MS/MS data), where protein abundance is estimated from the number of MS2 spectra identified for a certain protein (also called spectral counting) [224, 333]. This strategy, however, is not very precise and has difficulties in quantifying proteins of low abundance [137, 277]. Another label-free strategy determines the relative protein abundance across samples based on the intensity of the MS1 features of the corresponding peptides. Here, the step of feature quantification is independent from the LC-MS/MS peptide identification, enabling the unbiased identification of high and low abundant peptides across samples [490]. Because samples are analyzed separately, label-free methods allow for the analysis of a limitless number of samples. However, a key drawback herein is the introduction of variability due to experimental and instrumental variation [385, 385].

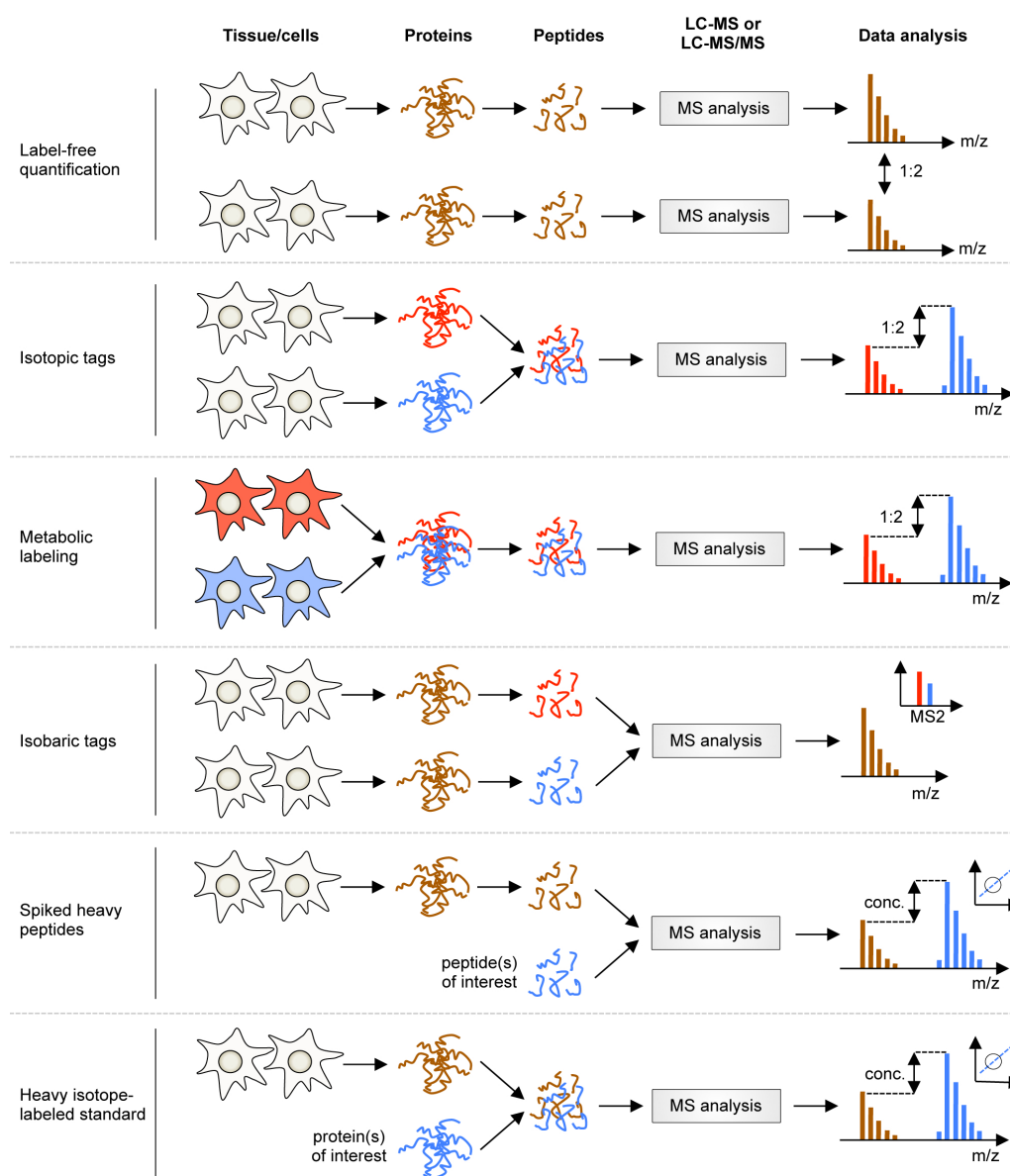


Figure 1.10: Quantification approaches in LC-MS and LC-MS/MS-based proteomics. Label-free strategies involve the analysis of samples separately, and peptide intensities from each MS run are compared. A variant is spectral counting, where the number of acquired MS2 spectra for each protein are compared between samples. Labeling strategies involve the labeling of one or more samples, such that samples can be mixed prior to MS analysis. Depending on when the labeling occurs in the experimental workflow, mixing occurs prior to lysis, after lysis, or after digestion. Labeling methods include metabolic labeling of cells (SILAC), or isotope labeling of proteins with chemical isotopic tags. Samples can also be labeled on peptide level via isobaric tags (e.g. TMT or iTRAQ). In targeted workflows (see also section 1.5.3), heavy isotope-labeled peptides or proteins of interest are added to the endogenous sample allowing absolute quantification (bottom two panels). Adapted from Thermo Fisher.

In contrast, label-based methods allow for the combined analysis of samples of interest, thus not only improving precision, but also reducing instrument time. One commonly used labeling technique is the stable isotope labeling of proteins. This is achieved either chemically, such as with isotope coded affinity tags (ICAT) [187], or metabolically, for example stable isotope labeling with amino acids in cell culture (SILAC) [336]. In both techniques, proteins in the samples to be compared are either labeled with a light or a heavy mass tag, which allows for the mixing of samples prior to digestion (in the case of SILAC, even prior to cell lysis). The mass shift that is introduced allows for the quantification of MS1 features corresponding to the same peptides, the ratio representing their relative abundance in different samples. Another approach involves labeling peptides with isobaric tags (that are the same in mass), which fragment during MS/MS to yield reporter ions of different mass. To date two types of isobaric tags are commercially available: tandem mass tags (TMT) [424] and isobaric tags for relative and absolute quantification (iTRAQ) [372]. Peptide mixtures labeled with different isobaric tags are mixed at equal ratios and during the LC-MS/MS analysis, peptides are fragmented to produce product ions, which help to determine the peptide sequence, as well as reporter tags, whose abundance reflects the relative ratio of the peptide in the samples that were combined.

1.5.3 Targeted proteomics

Apart from shotgun proteomics, a second main strategy has emerged over the past decade, referred to as targeted proteomics. While shotgun proteomics aims for discovering the maximal number of proteins from the sample(s) of interest, in targeted proteomics the goal is the reproducible detection and accurate quantification of sets of specific peptides and proteins, such as those constituting particular cellular networks or candidate biomarkers. Targeted proteomics thus requires the identification of proteins and proteotypic peptides of interest prior to analysis. Once the targeted assay is developed, the sample workflow prior to MS is the same as for the discovery experiment (Fig. 1.9, right panel).

Selected reaction monitoring (SRM)

A widely used targeted MS approach is SRM [160, 177, 352]. Unlike discovery proteomics experiments in which full-scan MS2 spectra are collected, in SRM only a small number of predetermined fragment ions per precursor ion are monitored. Typically, SRM is coupled to LC-MS and exploits triple quadrupole mass spectrometry (QQQ), where three quadrupoles act as mass filter and monitor the fragment ions generated from the precursor analyte by collisional dissociation [254, 481, 482] (Fig. 1.11). The pair of precursor ion mass and fragment ion mass is termed SRM transition.

In proteomics applications of SRM, the experimental workflow prior to MS analysis is identical to shotgun proteomics (see also Fig. 1.9, right panel). Peptides are produced from protein samples by enzymatic digestion and loaded on the the LC-MS system. In the first

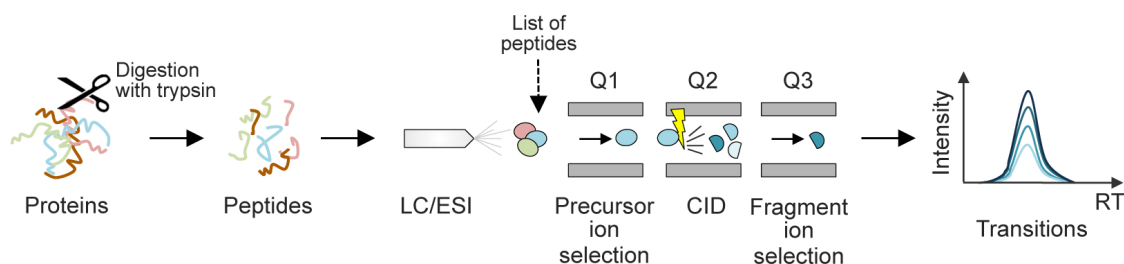


Figure 1.11: A typical SRM workflow. Proteins are digested into peptides and separated using chromatography, followed by injection into the mass spectrometer. In Q1, precursor ions are selected according to the transition list. In Q2, precursors are fragmented and the resulting fragment ions are filtered in Q3 for predetermined product ions. Signal intensities of several transitions for one peptide over time result in a chromatographic trace that can be quantified.

mass analyzer (Q1), ions are selected within the mass range centered around the mass of the targeted peptide (the precursor mass). In Q2, the selected precursor ions are fragmented at the peptide bonds. One or several of the resulting fragment ions are then measured by a second mass analyzer (Q3). The number of these fragment ions that reach the detector is counted over time, resulting in a chromatographic trace with retention time and signal intensities as coordinates (Fig. 1.11). The integration of the chromatographic traces of several transitions for the same precursor ion allows for the reliable quantification of the targeted peptide initially released from the protein. Transitions can be sequentially and repeatedly measured at a periodicity that is fast compared to the analyte's chromatographic elution. In other words, for each transition, chromatographic peaks are generated and quantified quasi concurrently, allowing for the quantification of multiple analytes in parallel. This multiplexing ability has led to the term multiple reaction monitoring (MRM), which is frequently used as a synonym for SRM [352].

SRM-based experiments can yield quantitative information by either relative (differential) or absolute protein quantification strategies. Relative quantification aims to measure the amount of a protein or peptide in one state or sample relative to that of a second state or sample. Similar to shotgun proteomics, relative quantification can be achieved either label-free by direct evaluation of MS signal intensities of the chromatographic peaks, or through labeling approaches to improve precision of quantification (see Fig. 1.10). Because a limited, predetermined number of analytes is targeted, SRM also allows for absolute quantification. The most commonly used approach relies on the addition of known quantities of isotopically labeled reference peptides that are chemically identical to the light native peptides (AQUA peptides) [155]. As the synthetic peptides are added to the endogenous sample late in the sample processing workflow, quantification may be inaccurate because of partial loss of the endogenous target peptide (for instance due to incomplete digestion of the protein or artifactual modifications of the target peptide). Another disadvantage of AQUA peptides is that they are expensive and, depending on the number and sequence

of analytes monitored, laborious to prepare. An alternative is the heterologous expression and metabolic labeling of concatenated tryptic peptides (QconCATs) [50]. The QconCAT protein is added to the sample prior to the enzymatic digestion step. The drawback of this approach, in turn, is that tryptic digestion efficiency can vary due to different sequence context, thus affecting the accuracy of quantification. Finally, to circumvent these issues one can add full-length isotope-labeled proteins into the sample, each an analog to the target protein [132] (see Fig. 1.10, bottom). This approach is limited by the capability of expression, purification and quantification of protein standards. The performance of these different strategies has been extensively reviewed [304, 388, 486].

The key advantage of the SRM approach over discovery-based methods is its sensitivity. Because the mass spectrometer only looks at the fragments of interest, issues dealing with dynamic range usually encountered by DDA mode can be circumvented, and low-copy number proteins in complex sample mixtures are analyzed with high precision [16, 454, 469]. Another advantage of targeted proteomics over discovery-based approaches is its reproducibility. Once target peptides are selected and corresponding fragment ions chosen, the resulting SRM assay can be applied in many different research labs and on different machines with minimal variability, making results comparable across the research community [3]. On the other hand, SRM is limited to the measurement of around thousand transitions per LC-MS/MS run, thus restricting the analysis to a maximum of several hundred peptides/proteins [352, 404]. Furthermore, SRM requires the careful selection and validation of peptides. Optimally, target peptides should be easily detectable, unique to the protein of interest, and not modified by PTMs. Finally, to create a transition list for the SRM assay, one relies on the knowledge of suitable fragment ions for each peptide of interest.

As an alternative method of targeted quantification, the parallel reaction monitoring (PRM) assay has emerged. PRM is performed in a high resolution and high mass accuracy mode, which make it a highly specific and selective method. In contrast to SRM, all transitions of the selected precursor ion are detected, thus not requiring the determination of specific product ions prior to MS analysis.

1.5.4 Data-independent acquisition approaches

Another recent development has been the emergence of data-independent acquisition (DIA) approaches that alleviate the limitations of both DDA and SRM. These methods operate via unbiased cyclic recording of consecutive survey scans and fragment ion spectra for all the precursors contained in predetermined isolation windows [338, 438]. This results in accurate peptide quantification without being limited to profiling predefined peptides of interest. In such full-ion scans, the link between the fragment ions and the precursor from which they originate is lost, and the resulting MS2 spectra are complex. Thus, DIA relies on efficient algorithms and software tools for deconvolution of the datasets [126, 373]. The data

is analyzed in a targeted mode, where pre-compiled spectral libraries are used to filter the fragment ion chromatography maps [159]. Similar to SRM, quantification is performed on the fragment ion level (MS2), in contrast to DDA where quantification occurs on precursor level (MS1). One key advantage of DIA approaches is that the same dataset can be mined repeatedly retrospectively, without requiring the re-analysis of the sample.

1.5.5 Identification and quantification of PTMs by MS

Mounting evidence suggests that PTMs or combinations thereof, rather than the pure protein abundance, are responsible for regulation and fine-tuning of protein function and activity (the tau protein being a prominent example (see section 1.3.4)) [51, 213]. Thus the interest in PTM analysis of proteins is growing rapidly. However, the identification and quantification of PTMs is associated with several analytical challenges. First of all, modified proteins, and thus the modified peptides, are often of lower abundance compared to the overall pool of proteins inside the cell. This is particularly problematic when using DDA methods as these rely on the "flyability" of the peptide species of interest relative to all other peptides analyzed at the same time. Peptides are typically selected for fragmentation according to their abundance in the MS spectrum, thus the analysis is biased towards higher abundant peptides which are often not the modified species. Furthermore, relative or absolute abundance of the PTM can only be based on the modified peptide, which might not be readily detectable (e.g. due to low abundance, issues in ionization or interference). In addition, modified peptides can be more difficult to identify from their fragmentation spectra than corresponding non-modified peptides. Finally, the MS2 spectra sometimes contain insufficient information to localize the modification with single AA resolution.

To overcome the problem of low stoichiometry, specific enrichment can be performed where the PTM of interest is retained with respect to the unmodified or otherwise modified peptides. For phosphorylation, there are protocols with high specificity that can lead to a phosphopeptide proportion of more than 90% [375, 417]. Other enrichment protocols now exist for ubiquitination [84, 387] and acetylation [93, 184], but these are less efficient. For many other PTMs, no enrichment strategies exist yet.

Analysis of enriched samples may increase the identification of more modified peptides and proteins in the sample of interest. However, enrichment steps introduce systematic errors that lead to a quantification bias. Furthermore, PTM quantification requires a correction by protein quantification to avoid misinterpretation arising from changes in overall protein expression over the course of an experiment. Attempts to identify modifications on a proteome-wide scale, in contrast to focusing on specific PTMs, are very challenging and resource demanding, and with current technologies unfeasible.

The above mentioned labeling techniques for quantification can be readily applied to the analysis of PTMs (reviewed for the case of phospho-proteomics in [140]). In particular, SILAC has been used in many cellular systems over the past years [203, 245, 335, 368, 374].

Because samples are combined at the earliest possible step and subsequent steps (including the enrichment) are performed together, quantification biases are minimized. In addition, in recent years both iTRAQ and TMT-based quantitative phospho-proteomics have been widely implemented [66, 226, 231, 472].

The FLEXIQuant strategy

Recently a quantitative MS-based strategy was developed that enables the precise characterization of the PTM status of a particular protein of interest. FLEXIQuant, short for Full-Length Expressed Stable Isotope-Labeled Proteins for Quantification, utilizes stable isotope-labeled full-length recombinant proteins which are expressed *in vitro* and are combined with the unlabeled endogenous sample prior to tryptic digest [401]. The method relies on quantification of unmodified peptides from the endogenous protein compared to peptides derived from the spiked-in isotope-labeled protein. A deviation from the mixing ratio indicates that a particular peptide from the endogenous protein is modified and the extent of modification can be quantified. This strategy circumvents the problems inherent to DDA-based PTM analyses, such as relying on the detectability of the modified species, and for quantification, the different response factor for modified and unmodified peptide. In FLEXIQuant, the presence of a modification can be deduced (and quantified) even when no PTM is detected, and the possible modified species can be investigated by targeted follow-up experiments. This approach has been applied to analyze phosphorylation events of APC-dependant degradation during mitosis [401, 402] and was further expanded to analyze mechanisms of multi-kinase substrate phosphorylation [400].

1.6 Approaches to analyze tau and tau PTMs

As described in previous sections, tau is a highly modified protein, and although the mechanisms are not yet fully understood, abnormalities in PTM patterns have been linked to the rate and extent of tau aggregation in AD and other tauopathies (see section 1.3.4). The characterization of tau PTMs and their relationship to tau pathology has been a major goal in the field of neurodegeneration, as understanding their exact role will help identifying molecular targets for tau-based therapeutic or diagnostic approaches (see also section 1.4.6). Traditionally, studies for the analysis of tau PTMs employed immunochemistry approaches, but advances in tandem mass spectrometry and enrichment techniques for tau have aided the identification of tau PTMs significantly. Below the current approaches and their limitations are summarized.

1.6.1 Antibody-based approaches

There exists a large number of anti-tau antibodies that have been developed over the course of several decades, some of which are now routinely used for research and diagnostic purposes

(see also section 1.4.5). Many of these antibodies are specific to tau tangles and recognize the epitope of singly or multiply phosphorylated residues, as is the case with the most commonly used AD-diagnostic antibodies (see also Fig. 1.6). Others recognize conformation-specific epitopes [282], C- and N-terminal truncation epitopes [153], as well as specific acetylated lysines [222]. Several studies have successfully used a combination of these antibodies to characterize the formation of NFTs and sequential appearance of hyperphosphorylation, providing the hierarchical model of tangle progression [307, 489]. Large panels of antibodies have also been used to characterize tau phosphorylation in post-mortem brain from patients with tauopathies such as CBD [149] or AD in comparison to PD and DLB [131]. In another study, the variability of pathological tau burden and its distribution in PSP variants was investigated, with AT8 antibody staining being one of the main criteria [463]. In addition, there has been a substantial effort in designing immunoassays that use multiple detection antibodies to infer total tau quantities in combination with phosphorylated tau levels as a diagnostic biomarker for AD [236] (see also section 1.4.5). Finally, in the context of immunotherapy approaches, several antibodies are being raised to clear toxic extracellular or intracellular tau aggregates [344].

Although immune-based assays have been an invaluable tool in the study of tau pathology in neurodegeneration, many drawbacks exist: 1) Immunochemistry methods are restricted to a limited number of antibodies that can be used simultaneously, and therefore are not suited for high-throughput and comprehensive studies; 2) a priori knowledge of particular PTMs is required, hampering the identification of novel modifications and their sites; 3) there may be known sites for which no antibodies are available, the development of new antibodies being laborious and cost-intensive; for some sites, no antibody can be raised due to sequence; 4) although often employed for relative abundance measurements of total tau and/or modified tau species, antibodies suffer from varying affinity and analytical specificity, which is particularly relevant because of the many tau PTMs and tau splice forms; and 5) there is currently no standardized reference method for antibody-based quantification that can be used for normalization between samples, further hampering precise quantification. These limitations severely limit the potential of immuno-based methods as tools to study tau PTMs in a comprehensive and quantitative manner.

1.6.2 MS-based approaches

Mass spectrometry (MS)-based proteomics approaches are a powerful alternative method used to identify proteins and characterize modifications (see also section 1.5.5). In the case of tau, exploitation of this technology over the last 20 years led to the discovery of many novel tau modifications, in particular phosphorylation sites [108, 112, 193, 196]. In some cases multiple types of modifications were characterized simultaneously, for example lysine methylation and ubiquitination [423] and phosphorylation and glycosylation [237]. However, usually not more than 2-3 types are analyzed simultaneously, typically with the

strongest focus on phosphorylation and little focus on less common PTMs.

So far, all MS tau PTM studies primarily aimed for the identification of modifications and the localization of modified sites. The latter is not often straightforward due to suboptimal quality of MS/MS spectra, especially when analyzing low-abundant species. The assignment of phosphorylation sites is particularly difficult because of the dense clustering of phosphorylation sites, which leads to peptides with multiple phospho-moieties. Information about stoichiometry of the identified modifications is sometimes provided by spectral counting of modified species relative to unmodified species [423], however this approach can be inaccurate, as the modified and unmodified species may have very different MS response factors (signal produced relative to quantity of peptide).

The vast majority of these MS-based tau PTM studies employed DDA. As mentioned above, a limitation of DDA mode is the stochastic selection of ions for fragmentation, handicapping the identification of PTMs, as the modified species can be present in very low stoichiometries compared to the unmodified counterpart (see also section 1.5.5). To overcome this limitation, several of the studies employed protein and peptide enrichment methods such as immunopurification and affinity separation [108, 112, 237, 423]. Apart from being laborious, these techniques introduce a bias into the peptide population and are thus not compatible with absolute quantification of the modification relative to their unmodified species [334, 439, 449]. Another drawback of enriching for particular modifications, such as phosphorylation, is that other modifications are neglected.

In summary, despite the extensive efforts using the existing antibody repertoire and recent progress in MS-based technologies, the study of tau PTM is hampered by the complexity and the heterogeneity of its modifications. For a start, the analysis of tau PTMs is extremely challenging due to the large number of modified sites. In the case of phosphorylation, the best studied tau PTM, over 70 sites (out of the 85 putative sites) have been described [196, 293]. It is widely accepted that in disease, tau phosphorylation occurs to an increased extent and on more sites (see also section 1.3.4). However, information about occupancy, total number of phosphorylations, and other modifications present is not only scarce, but also difficult to resolve with existing techniques. For some less studied PTMs, the location of occupied sites *in vivo* is not even identified. A further challenge are the many types of modifications that can co-exist. Several PTMs have even been reported to compete for same sites, e.g. glycosylation and phosphorylation on serines and threonines, or acetylation, ubiquitination and methylation on lysines [310, 376, 423]. Analysis of such crosstalk is not possible when enrichment of modified species is performed. Thus, a novel analytical method is urgently needed that is able to detect and quantitatively describe the PTM landscape in an unbiased, complete manner, without the need for enriching for particular PTM species.

1.7 Aim of this work

It is widely accepted that tau PTMs are involved in early as well as late stages of disease progression of AD and other tauopathies. Distinctive PTM patterns may exist for each tauopathy that could allow for their differentiation, and the modulation of distinct PTMs could be effective therapeutic targets. Nevertheless, despite extensive research it is still unclear which PTMs are preferentially implicated in tau pathology and whether a specific PTM distribution leads to disease. This is mainly due to the fact that current approaches to study tau modifications are not capable of capturing the many possible combinations of PTMs, let alone in a quantitative manner.

The overall objective of this thesis is to develop a novel quantitative tool for studying tau PTMs and to illustrate its utility by application to relevant biological questions. In Chapter 2, the development of FLEXITau is presented, a novel assay for the MS-based analysis of tau PTMs. Based on the FLEXIQuant strategy, the key to this method is the addition of an isotope labeled heavy tau standard to the endogenous mixture prior to enzymatic digest and MS analysis. Rather than aiming for the direct detection and quantification of modified tau peptide species, FLEXITau aims for the measurement of all unmodified tau peptides relative to their heavy counterpart, thus providing an indirect measure of the amount of modification present. Improving upon the original FLEXIQuant workflow, SRM acquisition is implemented to maximize sensitivity and reproducibility of quantification. The performance of the FLEXITau assay is illustrated by measuring the stoichiometry of highly phosphorylated tau expressed in a cellular model, mapping and calculating site occupancies for over 20 phosphorylation sites. The versatility of FLEXITau and its applicability to disease is then demonstrated by defining the PTM landscape present in AD post-mortem brain tissue.

The excellent accuracy and reproducibility even in complex samples was then exploited to apply the assay to the analysis of tau in non-AD tauopathies. In Chapter 3, FLEXITau is used to investigate whether tau from post-mortem brain from CBD, PSP, PiD, AD patients and non-demented individuals can be distinguished on the basis of the measured PTM landscape. The results indicate that each tauopathy presents with a unique signature. For each disease category, a computational diagnostic tool is then developed based on a subset of features, reaching accuracy of above 90%. These results have far-reaching implications in the post-mortem diagnosis of tauopathies and the development of novel *in vivo* diagnostic tools. Furthermore, the PTMs corresponding to the disease signature are mapped, providing a foundation for the development of PTM-targeted tau-modulating therapeutic approaches.

2 FLEXITau: Quantifying Hyperphosphorylation of Tau *in Vitro* and in Human Disease

2.1 Summary

Tauopathies, including Alzheimer's Disease (AD), are associated with the aggregation of modified microtubule associated protein tau. This pathological state of tau is often referred to as "hyperphosphorylated". Due to limitations in technology, an accurate quantitative description of this state is lacking. Here, a mass spectrometry-based assay, FLEXITau, is presented to measure phosphorylation stoichiometry and provide an unbiased quantitative view of the tau post-translational modification (PTM) landscape. The power of this assay is demonstrated by measuring the state of hyperphosphorylation from tau in a cellular model for AD pathology, mapping and calculating site occupancies for over 20 phosphorylations. FLEXITau was further employed to define the tau PTM landscape present in AD post-mortem brain. As shown in this study, the application of this assay provides mechanistic understanding of tau pathology that could lead to novel therapeutics, and one can envision its further use in prognostic and diagnostic approaches for tauopathies.

2.2 Introduction

Tau is a microtubule (MT)-associated protein that is predominantly expressed in neurons, where it mostly localizes to axonal regions. Major functions of tau include MT stabilization, maintenance of axonal transport and regulation of neurite outgrowth [31, 127]. Perturbation of tau regulation can lead to the formation of intra-neuronal insoluble aggregates of abnormally phosphorylated tau, in the form of paired helical filaments (PHFs). Tau aggregates are the pathological hallmark of a number of neurodegenerative disorders that are collectively called tauopathies, the most common being AD, a so-called "secondary tauopathy". Phosphorylation on multiple sites is considered to be a major early event in the formation of tau inclusions [34, 256]. Apart from phosphorylation, several other post-translational modifications (PTMs) have been implicated in disease pathogenesis, including acetylation [98, 303], ubiquitination [108, 220], methylation [423], and glycosylation [415, 450], among others.

The characterization of tau PTMs and their exact relationship to tau pathology has been a major goal in the field of neurodegeneration, as understanding the nature of tau biochem-

istry will identify molecular targets for therapeutics or diagnostic approaches, however a comprehensive picture is missing. The study of tau PTMs is extremely challenging due to the large number of modified sites and by the coexistence of multiple types of modifications, sometimes competing for same sites [310, 376, 423]. In the case of phosphorylation, to date over 70 sites (out of the 85 putative sites) have been described [196, 293]. While 28 phosphorylation sites have been exclusively found in tau from AD brain, many others overlap between AD and normal adult brain, but are phosphorylated to a different extent, in most cases higher in AD compared to control. In this context, the term "hyperphosphorylation" has been used widely in the literature, often when a positive signal is obtained from specific antibodies. One prominent example is the AT8 antibody, which binds to phosphorylated residues pS202/pT205. However, the term "hyperphosphorylation" is ambiguous, as in most cases phosphorylation stoichiometry is not measured. Moreover, information about total number of phosphorylations or other modifications, as well as their occupancy is lacking. To untangle the PTM landscape, many possible sites have to be analyzed in a qualitative as well as quantitative level. Thus the complexity of the tau PTM landscape poses a major analytical challenge.

Immunochemistry approaches are the traditional methods used to analyze tau PTMs and a large array of tau antibodies specific to phosphorylated or otherwise modified epitopes are available, such as the above mentioned AT8. While these antibodies are useful in the study of tau pathology, rigorous quantification using antibodies is difficult because of variable affinity specificity and selectivity, which complicates quantification [296, 350, 356]. Finally, a priori knowledge of particular PTMs is required, and for some sites, no antibodies exist while for other sites antibodies cannot be raised. These limitations severely constrain the potential of antibody-based methods as tools to study tau PTMs in a comprehensive and quantitative manner.

Emerging MS-based proteomics approaches are powerful alternative methods used to identify proteins and characterize modifications. In the case of tau, exploitation of this technology resulted in greatly enhanced protein sequence coverage. Many MS-based tau PTM studies led to the discovery of thus far undescribed tau modifications as well as novel phosphorylation sites, and allowed for the simultaneous analysis of dozens of modification sites [108, 193, 196, 237, 423]. Although they enabled the parallel analysis of different types of modification, these studies generally characterized only a limited number of PTM types, with the strongest emphasis on phosphorylation and little focus on less common PTMs. Furthermore, the majority of these MS-based experiments employed data-dependent-acquisition (DDA), a data collection mode that relies on the "detectability" of the peptide species of interest, biasing the analysis towards peptides of highest intensity. This particularly handicaps the identification of PTMs, as the modified species can be present in very low stoichiometries and/or exhibit decreased flyability compared to the unmodified counterpart. To address a critical need for an analytical method to measure tau PTMs, FLEXITau (Full-length expressed stable isotope-labeled Tau) assay was developed, based on the FLEXIQuant

strategy [401]. The FLEXITau assay allows for the unbiased analysis of tau modifications in a highly quantitative fashion, where the addition of a stable isotope labeled tau standard to the biological sample is key to the quantification. To maximize reproducibility and sensitivity, the original workflow was expanded by implementing a selected reaction monitoring (SRM) acquisition method and developed a sensitive, robust, tau-specific assay. The assay was then used to study human tau expressed in Sf9 insect cells, a cellular model system that generates tau in a highly phosphorylated, AD-like state [32, 419]. The precise phosphorylation state of Sf9-tau was measured, mapping and quantifying 23 phosphorylations in a site-specific manner. To demonstrate the versatility of the assay, the workflow was then applied to tau aggregates derived from post-mortem AD brain tissue. These results show that the performance of the assay is not compromised by the complexity of the human sample or the heterogeneity of the modifications on tau. Due to its sensitivity and versatility, FLEXITau is a powerful, robust tool for investigating tau modifications both *in vitro* and *in vivo*. The application of this method will greatly enhance our understanding of tau modifications and their role in pathogenesis. Thus FLEXITau provides a foundation for the development of better diagnostic tools and tau-modulating therapeutic strategies.

2.3 Experimental procedures

Cells and viruses

Sf9 cells were obtained from Invitrogen (San Diego, CA) and grown at 27 °C in monolayer culture Grace's medium (Life Technologies, Gaithersburg, MD) supplemented with 10% fetal bovine serum, 50 µg/ml Gentamycin, and 2.5 µg/ml Amphotericin. Sapphire™ baculovirus DNA was obtained from Orbigen/Biozol (Eching, Germany), and pVL1392 was from Invitrogen.

Baculovirus construction

The hTau40 cDNA, the longest tau isoform in human CNS (2N4R), was excised from the bacterial expression vector pNG2 [53] with XbaI and BamHI and inserted into the baculovirus transfer vector pVL1392. For the construction of tau containing baculovirus vectors, Sapphire™ baculovirus DNA was used for homologous recombination with pVLhtau40 plasmid in Sf9 cells.

Sf9-tau protein preparation and purification

Phosphorylated Sf9-tau ("P-tau") was purified as described before [419]. Briefly, Sf9-cells were infected with recombinant virus at a MOI of 1-5, typically in six T150 cell culture flasks containing 75% confluent Sf9 cells. Cells were incubated for three days at 27 °C and collected directly in lysis buffer (50 mM Tris HCl pH 7.4, 500 mM NaCl, 10% glycerol, 1%

Nonidet-P40, 5 mM dithiothreitol (DTT), 10 mM ethylene glycol tetra-acetic acid (EGTA), 20 mM NaF, 1 mM orthovanadate, 5 μ M microcystin, 10 μ g/ml each of protease inhibitors leupeptin, aprotinin, and pepstatin). For the generation of "PP-tau" (hyperphosphorylated Sf9 P-tau), Sf9 cells were treated for 1 h with 0.2 μ M okadaic acid (OA, a phosphatase inhibitor, Enzo-Lifescience) 1 h prior to harvesting. Lysates were boiled in a water bath at 100 °C for 10 min and cell debris was removed by centrifugation for 15 min at 16,000 x g. The supernatant containing soluble tau protein was concentrated in Millipore Amicon Ultra-4 Centrifugal filter units (MW cutoff 3 kDa). The concentrated material was applied to a size exclusion column Superdex G200 (GE Healthcare) and eluted with PBS Buffer (pH 7.4; 1 mM DTT), collecting 1 ml fractions. A second purification step was performed, using anion exchange chromatography on a MonoQ HR 16/10 column (GE Healthcare). For this purpose the tau-containing fractions of the G200-column were pooled and dialyzed against buffer A (100 mM MES (pH 6.8), 2 mM DTT, 1 mM NaEGTA, 1 mM MgSO₄, 0.1 mM PMSF), before loading onto the MonoQ column. Tau protein was eluted by a three step salt gradient (Buffer A supplemented with 1 M NaCl was used to create salt gradient steps of 0-0.2 M, 0.2-0.3 M and 0.3-1 M NaCl). To generate dephosphorylated Sf9-tau ("deP-tau") 30 μ g purified P-tau protein was incubated with 10 U of alkaline phosphatase (FastAP, Invitrogen) for ~16 h at 37 °C. The enzyme was removed afterwards by precipitation (5 mM DTT, 0.5 M NaCl), followed by centrifugation and dialysis to PBS. Protein amounts were estimated by a bicinchoninic acid test (BCA, Sigma). Samples were additionally analyzed by SDS-PAGE to verify purity and protein degradation (data not shown). The preparation and purification of Sf9-tau was performed by Dr. Katharina Tepper.

Preparation of human Tau40 from *E. coli*

Expression and purification of human Tau40 from *E. coli* cells was carried out as described in [36]. Note that human Tau40 is purified differently to Sf9-tau, as it does not carry the negative charges of phosphates. Human Tau40 was first purified by cation exchange chromatography (SP sepharose; GE Healthcare), and then by size exclusion chromatography (G200), as described above. The preparation and purification of *E. coli* tau was performed by Dr. Katharina Tepper.

SDS-PAGE and silver staining

Samples were boiled 5 min at 98 °C in 2x Laemmli buffer and separated by SDS-PAGE (4-12% Bis-Tris, NuPage, Invitrogen) at 120 V. Gels were stained with colloidal blue (Nuvex, Invitrogen). Silver staining was performed by fixing the gels in 30% ethanol / 10% acidic acid solution, cross-linking the proteins (in 0.5% glutarealdehyde) and staining in 0.1% AgNO₃ solution, followed by development with 2.5% Na₂CO₃ / 1% formaldehyde until the protein marker was visible.

Extraction of AD-tau

Human AD brain tissue was obtained from the Human Brain and Spinal Fluid Resource Center, VA West Los Angeles Healthcare Center, Los Angeles, and the Neurodegenerative Disease Brain Bank, University of California, San Francisco (see Table 2.4). AD cases had advanced disease, meeting NIA-Reagan criteria for high likelihood AD [326]. Tissue blocks representing the angular gyrus (1-3 g) were dissected from frozen brain slabs and shipped overnight to Boston Children's Hospital on dry ice. While still frozen, 0.3 g sections were homogenized in 5 volumes 25 mM Tris-HCl buffer, pH 7.4, containing 150 mM NaCl, 10 mM ethylene diamine tetraacetic acid (EDTA), 10 mM EGTA, 1 mM DTT, 10 mM nicotinamide, 2 μ M trichostatin A, phosphatase inhibitor cocktail (Sigma), protease inhibitor cocktail (Roche). Crude brain homogenates were then clarified by centrifugation at 11,000 x g for 30 min at 4 °C. Pellets were re-homogenized in half the volume of buffer used before and re-centrifuged at 11,000 x g for 30 min at 4 °C. Supernatants were pooled and used as a crude tau fraction (unfractionated homogenate). Part of the crude tau fraction was treated with sarkosyl (1% final concentration) for 60 min at 4 °C and ultracentrifuged at 100,000 x g for 2 h at 4 °C. The supernatant was transferred to a new tube (sarkosyl soluble fraction). The pellet was air-dried, washed twice with 50 μ l ddH₂O and solubilized in Tris buffer containing 1% SDS, 10 mM nicotinamide, 2 μ M trichostatin A, and phosphatase and protease inhibitor cocktail (0.3 μ l buffer per mg wet weight of the starting material). Solubilized pellets were used as the sarkosyl insoluble tau fraction. All samples were stored at -80 °C until use.

Preparation of heavy tau standard

Full-length human 2N4R (GI:294862262) was subcloned into the previously generated pEU-E01-TEV-N1-AQUA vector [401]. After verification by DNA sequencing (Molecular Genetics Core Facility, Children's Hospital Boston), tau was *in vitro* transcribed and translated in a cell-free wheat germ expression (WGE) system according to the manufacturer's protocols (Cell Free Sciences, Wheat Germ Expression H Kit-NA). Expression was carried out in the presence of isotope labeled amino acids (AAs), namely lysine K8 (13C6 15N2), arginine R10 (13C6 15N4) and aspartate D5 (13C4 15N1). Heavy tau standard was batch-purified using Ni-Sepharose beads (Ni-Sepharose High Performance resin, GE Healthcare). Briefly, after a prewash in binding buffer (20 mM phosphate buffer, pH 7.5, 500 mM NaCl, 10 mM imidazole) beads were incubated with WGE (ratio 1:4) for 1 h rotating head-over-head at 4 °C for binding. After removal of the unbound fraction, beads were washed once with 50 μ l and 3 times with 500 μ l wash buffer (20 mM phosphate buffer, pH 7.5, 500 mM NaCl, 10 mM imidazole). Elution of tau was carried out in three steps (50 μ l binding buffer with 100/300/500 mM imidazole, respectively). Purification was verified by SDS-PAGE and western blot analysis (data not shown). Pooled eluates were stored at -20 °C in 50 μ l aliquots.

Sample preparation for MS

Heavy tau standard was subjected to incubation with lambda protein phosphatase (New England Biolabs) for 30 min at 30 °C at 300 rpm. Digestion [467] was performed using 1 μ g of Sf9-tau or 50 μ g of AD sarkosyl insoluble pellet. For spikes, dephosphorylated standard was added prior to digest. Protein mixtures were reduced with 50 mM DTT (20 min, 56 °C) and alkylated with 1% acrylamide (30 min, room temperature). Samples were diluted with 8 M urea and processed using FASP following the manufacturer's protocol (FASP Protein Digestion Kit, Expedeon). Briefly, proteins were loaded on the filters, followed by washing with 8 M urea and 50 mM ammonium bicarbonate (ABC). Samples were digested with 2 ng/ μ l trypsin (sequencing grade modified trypsin, Promega) overnight at 37 °C. For LysC digest, the last two washes were performed using LysC buffer (0.1 M Tris, pH 9.2, 1 mM EDTA), followed by overnight incubation at 37 °C with 4 ng/ μ l LysC (endoproteinase LysC sequencing grade, Roche) in LysC buffer. After digestion, peptides were eluted from the membrane by two washes with 50 mM ABC (or LysC buffer for LysC samples) and one wash with 0.5 M NaCl. Peptides were acidified with formic acid (FA), desalted using C18 microspin tips (Nest Group) and dried under vacuum. Peptides were reconstituted in sample buffer (5% FA, 5% acetonitrile (ACN)) containing 10 fmol/ μ l non-labeled FLEX-peptide (TENLYFQGDISR, synthesized by Sigma Life Science, quantified via AA analysis of Molecular Biology Core Facilities, Dana Farber Cancer Institute, Boston) and indexed retention time (iRT) peptides (Biognosys) [138].

LC-MS/MS measurements

To identify the most sensitive and selective transitions (pair of peptide and their fragment ion masses), we performed high-resolution liquid chromatography tandem MS (LC-MS/MS) of purified, digested heavy tau standard in DDA mode and generated a collection of experimentally detected peptides and their fragment ions (spectral library). Multiple measurements of up to 400 fmol of tau were performed using two different instruments platforms: First, a quadrupole Orbitrap tandem mass spectrometer (Q Exactive, Thermo Fisher Scientific) was used to maximize the number of peptide identifications. Tau was analyzed on a Q Exactive hyphenated with a micro-autosampler AS2 and a nanoflow HPLC pump (both Eksigent), using the trap-elute chip system (cHiPLC nanoflex, Eksigent). Peptides were first loaded onto the trap-chip (200 μ m x 75 μ m, ChromXP C18-CL 3 μ m 120 A, Nano cHiPLC Eksigent) and then separated using an analytical column-chip (75 μ m x 15 cm, ChromXP C18-CL 3 μ m 120 Å, Nano cHiPLC Eksigent) by a linear 30 min gradient from 95% buffer A (0.1% (v/v) FA in HPLC-H₂O) and 5% buffer B (0.2% (v/v) FA in ACN) to 35% buffer B. A full mass spectrum with resolution of 70,000 (relative to an m/z of 200) was acquired in a mass range of 300-1500 m/z (AGC target 3 x 10⁶, maximum injection time 20 ms). The 10 most intense ions were selected for fragmentation via higher-energy c-trap dissociation (HCD, resolution 17,500, AGC target 2 x 10⁵, maximum injection time

250 ms, isolation window 1.6 m/z, normalized collision energy 27%). The dynamic exclusion time was set to 20 s and unassigned/singly charged ions were not selected.

In addition, the purified tau standard was analyzed on an Sciex Triple TOF 5600 to generate fragment-ion spectra comparable to the employed SRM instrument (Sciex QTRAP 5500), using the same LC setup as described above. The Triple TOF was operated in data-dependent TOP30 mode with following settings: MS1 mass range 350-1300 Th with 175 ms accumulation time; MS2 mass range 100-1500 Th with 25 ms accumulation time and following MS2 selection criteria: UNIT resolution, intensity threshold 8 cts; charge states 2-5. To identify sites of modifications on tau, Sf9-tau digests were analyzed on the Q Exactive applying the settings described above, replacing the chip-system with an in-house packed C18 analytical column (Magic C18 particles, 3 μ m, 200Å, Michrom Bioresource). After initial measurements, an inclusion list containing all identified phosphorylated tau peptides was created using Skyline. For final measurements, following settings were used in order to increase peptide identification: AGC target 5 x 10⁶, maximum injection time 120 ms, MS/MS resolution 35,000, AGC target 2 x 10⁵, maximum injection time 200 ms, isolation window 2 m/z. The dynamic exclusion time was set to 4 s and unassigned and charge state 1 and >5 ions were rejected. The inclusion list was turned on allowing picking others if idle.

LC-MS/MS data processing

Q Exactive raw files were converted into mgf data format using ProteoWizard [244]. The spectra were centroided and filtered using ms2preproc to select the 6 most intense peaks in a 30 Th window (Renard et al., 2009). MS/MS spectra from mgf or wiff files were assigned to peptides and corresponding proteins using ProteinPilot™ Software 4.5 Beta (Paragon Algorithm 4.5.0.0. 1575, Sciex). The following settings were applied: sample type 'SILAC (Lys+8, Arg+10, Asp+5)', instrument: 'Orbi MS (1-3ppm)', 'Orbi MS/MS' and 'TripleTOF 5600' respectively; 'Urea denaturation'; 'rapid' search mode. Spectra were searched against a custom database containing wheat germ proteins and the human 2N4R tau sequence tagged with the FLEX peptide. For the mapping of Sf9-tau PTMs, raw files were converted and processed in ProteinPilot as described above except for following search parameters: 'thorough' search mode, 'phosphorylation emphasis', 'acetylation emphasis', 'ID focus on biological modifications' and using Homo Sapiens database (downloaded from uniprot.org on 11/01/2011). Note that ProteinPilot doesn't allow the user to pick mass tolerances and number of missed cleavages. All MS/MS spectra of identified post-translationally modified peptides were subjected to manual verification.

SRM assay development

To generate a spectral library from the generated LC-MS/MS datasets, xml files were extracted from ProteinPilot and loaded into Skyline [286] using cut off score of 0.5. A

FASTA file containing the 2N4R tau protein sequence tagged with the FLEX-peptide was imported, using a wheat germ protein database as a background proteome. Filter settings for tryptic peptides (Trypsin/P KR|-) were as follows: a maximum of 2 missed cleavages, a peptide length between 5 and 40 AAs, a maximum of 3 variable structural modifications (cysteine propionamidation, serine/threonine phosphorylation, methionine oxidation and asparagine/glutamine deamidation) and a maximum of 1 neutral loss. The spectra were used to confirm identities, extract the optimal fragment ions for SRM analysis and obtain retention times. An initial transition list for each tryptic and LysC samples were generated choosing 8 most intense product ions from the library spectrum, considering only y ions with charges 1 and 2 (from precursor ions with charges 2, 3 and 4) from ion 3 to last ion -1. The transition lists were validated and optimized after SRM measurements, as described below.

SRM measurements and data processing

The SRM assay using the transition lists developed above was tested using the tau standard. Measurements were performed on a triple quadrupole mass spectrometer (5500 QTRAP, Sciex) using the same LC trap-elute chip setup as described above. Initial measurements for optimization of transitions were done using a scheduled SRM mode, a retention time window of 7 min, a gradient of 30 min and a maximum of 250 transitions per method. Resulting SRM data were analyzed and manually validated in Skyline. Transition groups corresponding to the targeted peptides were evaluated based on specific parameters (in order of importance): co-elution of light and heavy peptides; rank correlation between the SRM relative intensities and the intensities obtained in the MS/MS spectra; and consistence among technical and biological replicates. Using these criteria, the transition lists were reduced from 8 to 4-5 most intense product ions per peptide.

To assess linearity of product ion signals and to determine detection limit of the assay, a dilution series of heavy tau standard was performed. Absolute quantification of the standard was carried out using SRM relative intensities between the heavy FLEX-peptide and its light counterpart FLEX-peptide, as described previously [401]. Samples containing different amounts of heavy tau spanning four orders of magnitude (from 0.8 - 800 fmol) were prepared and measured in triplicates using the optimized transition list (Fig. 2.3).

Final FLEXITau measurements of mixed peptide samples were performed using the validated scheduled transition lists for a 30 min gradient (see appendix, Table A1), a retention time window of 5 min and a total scan time of 1.2 s, which ensured a dwell time of over 20 ms per transition. To achieve the desired concentration range (as elaborated below in section 2.4.2) initially data was collected from a 1:10 dilution of the samples and the injection amount adjusted appropriately. Blank runs between SRM measurements ensured minimal sample carry over, and three replicate injections were measured per sample (MS injection on separate days).

SRM data were analyzed and manually curated in Skyline. Peptide transitions were re-evaluated for variability, similarity between y-ion ratios, elution times, and interfering signals by manual analysis. For quantification, the 3 highest intense transitions were used. For each individual run, ratios of L/H peak intensities were normalized using the average of the 3 peptides with highest ratio. The same normalization factor was used for the LysC sample as calculated for the trypsin-digested sample. To assess quantification precision of technical and biological replicates, averages of normalized L/H ratio as well as light peak area of each peptide were calculated from the triplicate measurements for each biological replicate (Fig. 2.4), and subsequently the average and %CV from the three biological replicates was calculated for each species (Fig. 2.5). For the calculation of the modification extent of each peptide, first the average of technical replicates (normalized L/H ratio) was taken, followed by normalization of each sample by the average of all control samples. The modification extent for each biological replicate was then calculated by subtracting this value from 1. Negative values were transformed to zero and averages of the three biological replicates were calculated. FLEXITau data was expressed as mean +/- standard deviation (SD) of normalized L/H ratio of biological replicates and analyzed by the Student's t test (two-sided) between two groups (Fig. 2.6). Statistical significance was accepted at the $p < 0.05$ level.

Calculation of site-occupancy and number of phosphates per molecule

Individual site occupancies of the mapped phosphorylation sites were calculated for each biological replicate using the equations listed in Fig. 2.7A. Then the average for each tau species was calculated (Fig. 2.7B). Next a recursive approach was used to calculate the polynomial probability distribution of observing a specific number of phosphorylations per tau molecule (see Fig. 2.8). The input data consisted of site occupancies X_{ij} for a total number of $N = 22$ sites for each biological replicate (three replicates each). The probability p_j of a site j ($j = 1, 2, \dots, N$) being modified from a total of $r = 3$ replicates ($i = 1, 2, 3$) was calculated as

$$p_j = \frac{1}{r} \sum_{i=1}^r X_{ij} \quad (2.1)$$

Given $D = \{p_1, p_2, \dots, p_N\}$ the entire list of probability values for all N sites, $P(1|p_m) = p_m$ the probability of observing site m in a particular tau species, and $P(0|p_m) = 1 - p_m$ the probability of not observing site m , the probability of seeing k sites to be modified in that particular species out of all N sites was calculated as

$$P(k|D) = p_1(k-1|D-p_1) + (1-p_1) \cdot P(k|D-p_1) \quad (2.2)$$

with $P(0|D) = \prod_{j=1}^{17} (1-p_j)$ being the probability of observing 0 sites. The above mentioned

approach for the calculation of site-occupancy was developed and implemented by Dr. Shaojun Tang.

2.4 Results

2.4.1 Development of the quantitative SRM FLEXITau assay

The overall goal of this study was to develop an SRM workflow to quantify tau modifications in an unbiased manner. Based on the FLEXIQuant strategy [401], this approach utilizes a stable isotope-labeled ("heavy") full-length tau protein standard that is added to biological specimens prior to sample processing and MS analysis (Fig. 2.1A). The premise of FLEXITau is to measure the change in the unmodified peptide species rather than measuring the modified species. For example, if 66.7% of a particular site carries a specific modification then the abundance of the unmodified species is decreased to 33.3%.

The heavy tau standard is generated by cloning the longest tau isoform (2N4R) into the FLEX-vector, introducing an artificial tag at the N-terminal of tau, which is used for purification as well as for absolute quantification of the endogenous tau. Heavy tau protein is expressed in a cell free expression system in the presence of isotopically labeled aspartic acid, lysine and arginine. The triple labeling strategy allowed us to minimize co-expressed light tau standard that could lead to a bias in quantification of endogenous tau.

In a FLEXITau experiment, the tau standard is purified and added to the unlabeled endogenous ("light") sample, which is digested using trypsin or other enzymes (Fig. 2.1A). Notably, due to the mixing of light and heavy species early in the sample processing, quantification errors are minimized that might arise due to sample loss and technical variability between samples during preparation. Notably, variability in various batches of extraction/purification prior to mixing may lead to differences in absolute amount of the light and heavy proteins, however this does not affect the relative quantification by FLEXITau which occurs on peptide level. The digested peptide mixture, containing light and heavy tau peptides species, is then analyzed by MS. All observed tau peptides are present as pairs, featuring the light and the heavy isotopologues. The initial mixing ratio is calculated by determining the light-to-heavy (L/H) ratio of unmodified peptides. As mentioned above, if a peptide from the sample is modified, this modification results in a reduction in the amount of unmodified peptide, thus, any deviation of the L/H ratio indicates modification. The extent of modification of a peptide is calculated by measuring the difference in L/H ratio of the unmodified peptide species and the mixing ratio. Plotting the FLEXITau data for all tau peptides sorted from N- to C-terminal results in an intuitive representation of the PTM landscape across the entire protein. This plot indicates where individual modifications occur and which domains of a protein are highly modified (Fig. 2.1B).

The quality of the FLEXITau data strongly depends on the sensitive and reproducible MS-based detection of the unmodified peptide species. To ensure this, targeted assay was

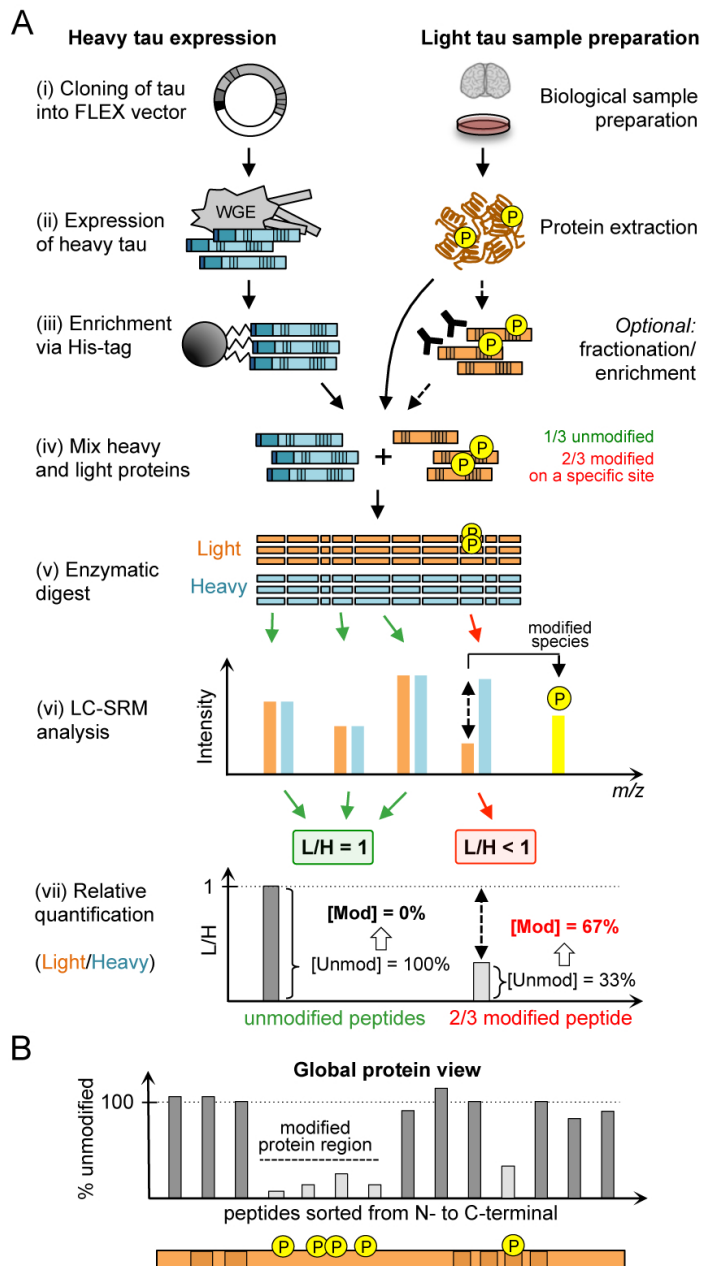


Figure 2.1: FLEXITau experimental workflow. **A.** In a typical FLEXITau experiment the heavy tau standard is generated in the presence of heavily labeled AAs and added to unlabeled endogenous sample in a ratio of approximately 1:1. After enzymatic digest and LC-MS analysis all unmodified tau peptides will be observed as pairs, featuring the light and heavy isotopologue. For modified peptides, the modification causes a mass shift, reducing the amount of detectable unmodified peptide and causing a deviation of the mixing ratio. The extent of modification on that peptide can be inferred by the amount of "missing" unmodified species. **B.** Plotting of peptide L/H ratios sorted from protein N- to C-terminus allows for a global visualization of modified peptides and protein regions. Blue, heavy tau; dark orange, light tau; P, phosphorylation

devised specifically tailored to monitor the unmodified tau, using SRM. SRM is increasingly being used in protein quantification because of its outstanding specificity, reproducibility and sensitivity [3, 243, 353, 357, 436].

A crucial step in developing SRM assays is the identification of the most sensitive and selective transitions (pair of peptide and their fragment ion masses). The expressed full-length tau standard was utilized to create a spectral library in order to find suitable transitions. To this end high-resolution liquid chromatography tandem MS (LC-MS/MS) of purified, digested tau standard in DDA mode was performed, generating a collection of experimentally detected peptides and their fragment ions (Fig. 2.2A). To maximize the

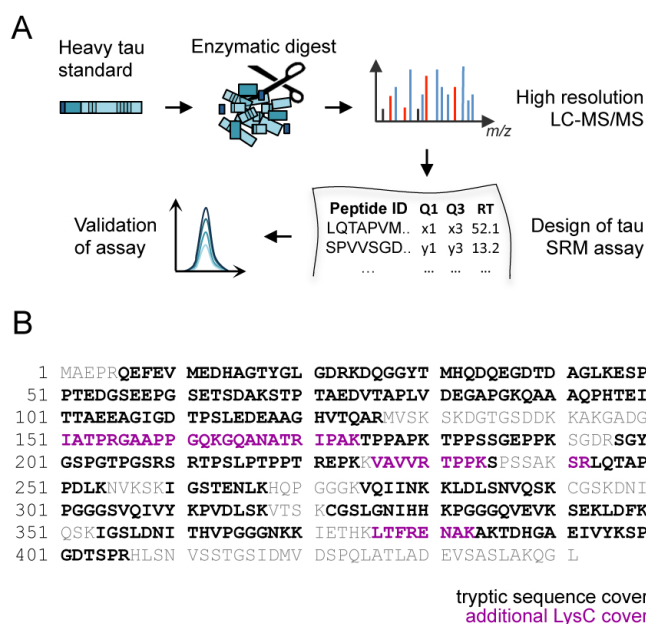


Figure 2.2: FLEXITau SRM assay development and sequence coverage. **A.** For the development of the tau SRM assay, an enzymatic digest of His-tag purified heavy tau is analyzed by high resolution LC-MS/MS and used to generate a transition list. **B.** Sequence coverage of quantifiable tau peptides by SRM is shown in bold black for trypsin, additional coverage using LysC is shown in purple (tau sequence of human 2N4R).

sequence coverage of tau, the tau standard was digested by trypsin and LysC. Collectively the spectral library peptides covered 84.6% of tau sequence. This spectral library was then used to develop a quantitative SRM assay for these peptides, choosing the transitions with highest intensity without interfering signals (for more details about the SRM assay development, see section 2.3).

The sensitivity of the SRM method can be maximized by acquisition of the transitions in a small retention time window (termed scheduled SRM). Therefore a scheduled 30 min LC-SRM method was developed. This method is suitable for pure/low complex tau samples and enables tau modification profile quantification from pure/low complex tau samples in a sensitive and time efficient manner (see appendix Table A1 for scheduled SRM transition lists). When analyzing high concentrations of purified trypsin-digested standard using the developed SRM assay, a sequence coverage of 71% was reproducibly achieved (23 peptides), and the 5 complementary LysC peptides increased this number to 75.3% (Fig. 2.2B). Notably, for the analysis of highly complex samples, it is recommended to use longer gradient in order to maintain specificity and minimize interfering background signals. Both the tau peptides or the iRT standard peptides (Biognosys) implemented in the assay allow for quick and accurate peptide retention time calculation in other gradient lengths

2.4.2 Sensitivity of the FLEXITau assay

To determine the detection limit of the assay and the dependence of the sequence coverage on concentration, a dilution series of digested heavy tau standard from 800 fmol to 8 amol in 11 dilution steps was analyzed. The FLEX peptide was used as described previously to determine initial tau concentrations [401]. Samples were measured in triplicate using the developed scheduled SRM assay and the signal intensities of the heavy peptides were

monitored. For maximal sequence coverage at least 2 fmol of tau must be injected (Fig. 2.3A); any concentrations below 2 fmol resulted in a decrease in sequence coverage. At 80 amol, a sequence coverage of 51% (25 quantifiable peptides) was measured and at the lowest end of the dilution series of 8 amol, the sequence coverage was 38.7% with 15 quantifiable peptides (Fig. 2.3B). Figure 2.3C shows representative dilution curves for 8 peptides. The peptide quantification was linear over the range of the dilution series for most peptides, with some deviation from linearity at the lower and/or higher end of the series (data not shown). The average R2 value for the peptides assayed in the dilution curve experiment was 0.97. For a concentration range with highest linearity (0.4 to 400 fmol injected on column), a R2 value of > 0.98 was observed for approximately 90% of the targeted peptides.

In summary, the sensitivity of the assay is highlighted by the successful quantification of peptides across 5 orders of magnitude, down to 8 amol of injected tau. To achieve maximum sequence coverage and linearity of quantification, a working range between 2 and 400 fmol of tau is required. It is worth noting that the optimal working range and reproducibility of the assay can be affected by interfering signals and should be reassessed in each individual sample background, particularly in highly complex samples.

2.4.3 Analytical precision of the FLEXITau assay

To evaluate precision of the assay, an *in vitro* tau expression system was used in which the modifications present are well defined, i.e. human tau protein produced in insect Sf9 cells via baculovirus transfection [32, 54, 258]. Tau expressed in these cells is phosphorylated at multiple sites and is thought to have a similar phosphorylation pattern as PHF tau from

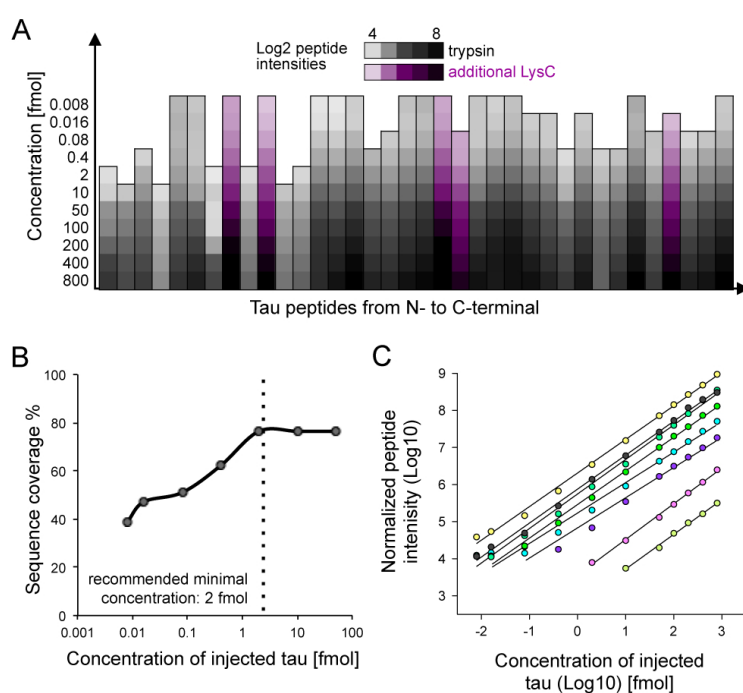


Figure 2.3: FLEXITau sequence coverage and detection limit. **A.** A dilution series of tau was performed and peptide intensities measured using the developed FLEXITau SRM assay. Log₂ peptide abundances (mean value of triplicate measurements) are shown as a heat map for the quantified peptides, sorted from N- to C-terminus. **B.** Achieved sequence coverage of tau relative to injection amount. Minimal concentration for maximum sequence coverage is indicated by dotted line. **C.** Shown are representative curves of 8 peptides (mean value of triplicate measurements).

AD [54]. This Sf9 cellular model system has been used to study tau aggregation [419] and sequential phosphorylation by multiple kinases [489]. This state of phosphorylated tau is often called "hyperphosphorylated", and despite its ambiguity, this term is used throughout this chapter for the sake of simplicity.

Four different species were analyzed: (i) tau from untreated Sf9 cells, phosphorylated at a native level (hereafter termed P-tau), (ii) tau from Sf9 cells treated with a phosphatase inhibitor (okadaic acid, OA), resulting in an increased level of phosphorylation (PP-tau), (iii) tau purified from Sf9 cells subsequently treated with alkaline phosphatase (AP) to remove the phosphorylations (deP-tau), and (iv) tau expressed in *E. coli* as unmodified control (ctrl-tau) (Fig. 2.4A). 3 independent preparations of each species were subjected to the FLEXITau workflow and each sample was analyzed 3 times. This analysis resulted in the quantification of 28 targeted peptides in all samples achieving a sequence coverage of 75%. To ensure a high level of precision in peptide quantification, the data were manually curated. For modified species (P-tau and PP-tau), L/H ratios were normalized by the average of the 3 highest L/H ratios among all peptides for each individual sample, and for control species normalization was performed using all ratios above the median ratio. The same normalization factor was used for the LysC sample as calculated for the trypsin-digested sample (for more details, see section 2.3).

First the quantification precision of technical replicates (replicate injections) and biological replicates (different Sf9 cell batches) was assessed. On average, the median coefficient of variation (CV) across replicate injections was 3.9% (Fig. 2.4B). Ctrl-tau presented the lowest (3%), and PP-tau the highest variability (5.2%). On average, the biological variability was higher than the technical variability, with a median %CV of 13.2% (3.5-fold compared to CV of technical replicates). Again, ctrl-tau presented the lowest variability (median %CV of 8.2%). In comparison to the technical variability, apart from the increase in median %CV, a broadening of the CV distribution could also be observed (Fig. 2.5A and 2.5B).

Next, to evaluate if the use of an internal standard improves the quantification reproducibility, the FLEXITau results were compared to quantification using only peak intensities of endogenous tau peptides. To this end, light peak areas were extracted for all monitored peptides in the same dataset. Quantification using peak area intensity resulted in a 4-fold increase of technical variability (15.3 %CV) and 2-fold increase in biological variability (25.3 %CV) compared to the FLEXITau quantification of 3.9 %CV and 13.2 %CV respectively (Fig. 2.4C). This corroborates that the employment of the internal standard is highly beneficial to the precision of the analysis.

2.4.4 Quantitative PTM profiling of "hyperphosphorylated" tau

Next, the peptide modification landscape in these Sf9-tau samples was quantitatively assessed. Fig. 2.6A shows the quantification of unmodified tau peptides in the global FLEXITau representation. Peptides were defined as "modified" if the average of the biological

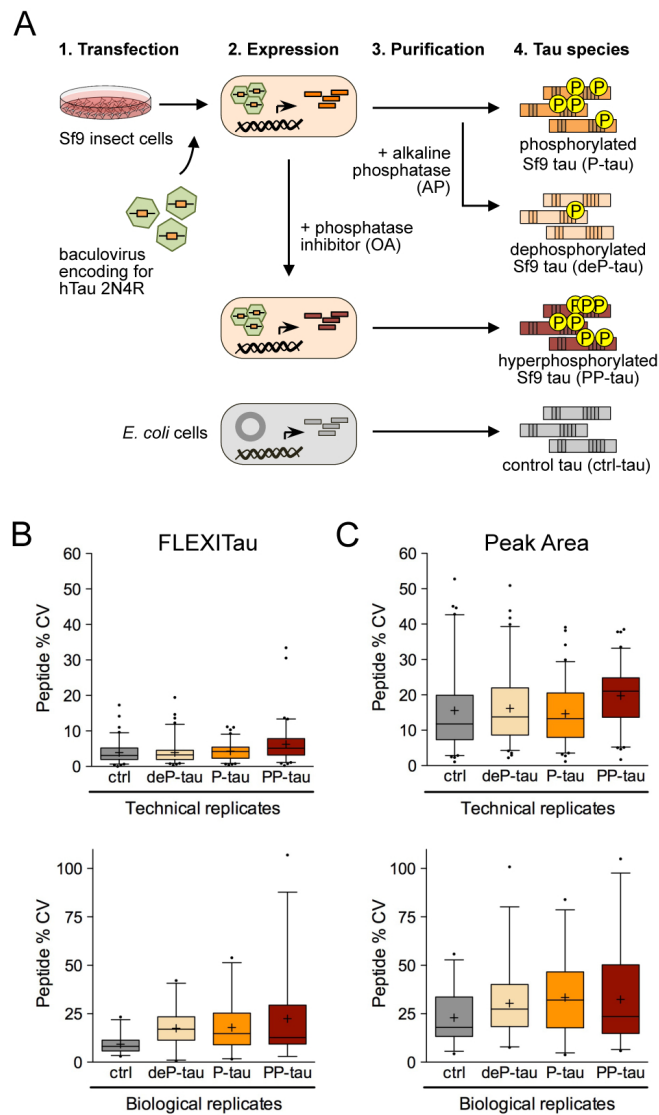


Figure 2.4: Sf9-tau sample preparation. **A.** Sf9 insect cells were transfected with recombinant baculovirus encoding for human 2N4R wild type tau. Purified Sf9-tau (P-tau) was treated with AP to generate dephosphorylated Sf9-tau (deP-tau). Phosphatase inhibition by OA prior to cell harvest and tau purification gives rise to hyperphosphorylated Sf9 (PP-tau). As control, unmodified tau was expressed in *E. coli*. **B.** Three independent preparations of Sf9-tau were subjected to FLEXITau SRM analysis (three SRM measurements each). Technical reproducibility (top panel) and biological reproducibility (bottom panel) of L/H ratio was calculated as %CV. Data is represented in a boxplot (5% - 95% whiskers, mean indicated by +). **C.** Peak areas were extracted from the same dataset and the %CV calculated. Data is represented as boxplot (5% - 95% whiskers, mean indicated by +)

replicates resulted in a value below 100% and were significantly different from ctrl-tau (student t-test, $p < 0.05$). Table 2.1 lists all quantified peptides and their respective modification extent, including the significance value. On average (mean value of all modified peptides), the modification extent of PP-tau was 25% higher compared to P-tau (33.0% for P-tau, compared to 42.7% for PP-tau). 9 peptides (39% of the quantified sequence) appeared to be unmodified in both species, while the remaining 19 peptides (nearly half of the quantified sequence) were found to be modified in P-tau and/or PP-tau. From these, the vast majority was modified both in P-tau and PP-tau; only 3 peptides (peptides F, R and T) were modified in PP-tau only, suggesting that phosphorylation sites in these regions are more accessible to phosphatases, which are inhibited by the okadaic acid ($_{151}\text{IATPRGAAPPGQK}_{163}$, $_{322}\text{CGSLGNIHHKPGGGQVEVK}_{340}$, and $_{354}\text{IGSLDNITHVPGGGNK}_{369}$, Table 2.1, peptides highlighted in red).

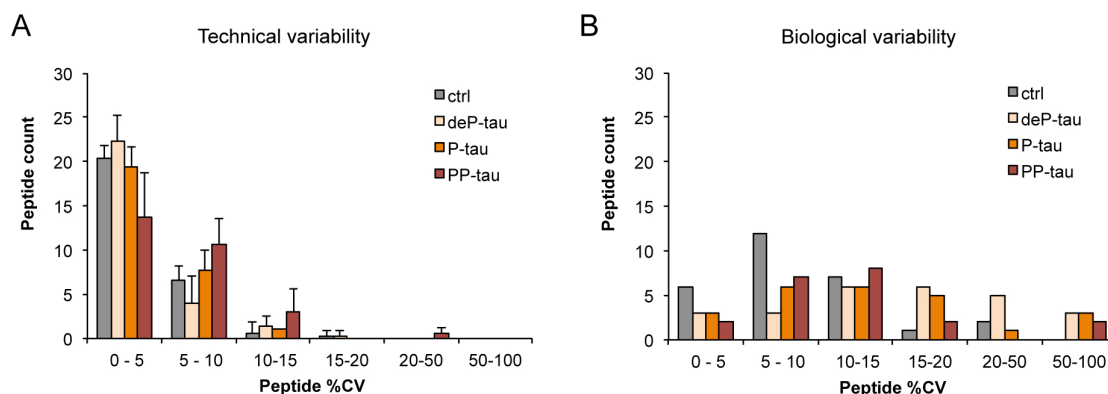


Figure 2.5: Distribution of peptide %CV. To assess variability of peptide quantification, three independent preparations of each tau species (biological replicates) were subjected to the FLEXITau workflow and analyzed in triplicates (technical replicates). %CV distributions of normalized L/H ratio of technical (**A.**) and biological (**B.**) replicates are shown. For the technical replicates, the average across the 3 biological batches is shown for each bin (mean \pm SD).

To gain a more functional view of the data, the peptides were projected to their corresponding tau domains, from N- to C-terminal: acidic region, proline-rich region, repeat region, and C-terminal tail (Fig. 2.6A, bottom). This data indicated that each tau domain presented with a characteristic modification extent (and this trend was maintained upon treatment with phosphatase inhibitor). The repeat region was the least modified with an average modification extent of 10.1% and 14.8% for P-tau and PP-tau, respectively; most of the peptides in this region were unmodified (student t-test, $p > 0.05$, see above). The acidic region and C-terminal tail showed moderate modification extents (acidic region: 23.1% and 24.5% and c-terminal tail: 48.9% and 55.9%, for P-tau and PP-tau, respectively). The proline-rich region depicted the highest modification extent (on average 55.2% and 71.0% for P-tau and PP-tau, respectively). Interestingly, this region contains residual phosphorylation in the dephosphorylated Sf9-tau species, deP-tau (consistent with previous reports [419]). The highest modification extent for deP-tau was observed on peptide K and L at 27% for both. This region also harbored the peptide with the highest modification extent of all peptides, with 90.6% in P-tau and 97.2% in PP-tau (peptide L, ${}_{226}\text{VAVVRTPPK}_{234}$, Fig. 2.6A and Table 2.1).

2.4.5 Creating a quantitative PTM map

The FLEXITau experiments measured the absolute extent of modification of tau peptides and relative differences between P-tau and PP-tau. The next goal was to identify the modifications present on these peptides and to associate these with the quantitative data. To this end, these samples were analyzed using DDA workflows and mapped the identified PTMs to their corresponding quantification data (Fig. 2.6B and Table 2.1). At this point it

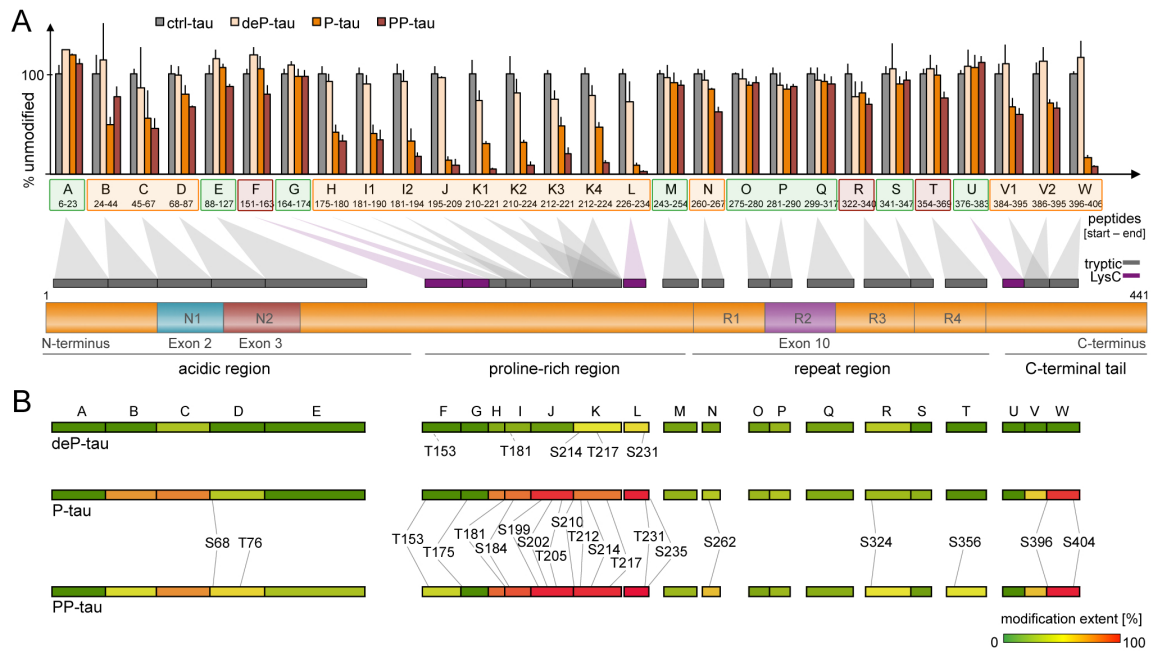


Figure 2.6: Quantification of "hyperphosphorylated" tau by FLEXITau. A. FLEXITau data is shown for each tau species (average of three independent Sf9-tau preparations, bar shows relative error (%CV)). Peptides sorted from N- to C-terminus are projected onto a schematic of 2N4R tau protein, respective to their AA location. Exons prone to splicing (exon 2, 3 and 10) are depicted in dark brown. Peptides not modified in P-tau and PP-tau are shown in green, peptides significantly different from ctrl-tau in orange, and peptides different in PP-tau only in red (student t-test, $p < 0.05$). **B.** Phosphorylated sites identified by LC-MS/MS shotgun analysis were mapped onto tau peptides that are color coded according to their modification extent as quantified by the SRM analysis. For the full list of modified peptides see Table 2.2.

is important to note that if an identified phosphorylation is located on the first AA after a tryptic cleavage site, this phosphorylation leads to a miscleavage producing a longer peptide. Thus this modification will contribute to the reduction in the abundance of the modified peptide (containing the modified site) as well as its N-terminal neighboring peptide. In these cases, the respective site is listed twice in Table 2.1.

In total, 21 phosphorylation sites were identified on Sf9 P-tau - 12 serine and 7 threonine phosphorylation sites; on PP-tau, 23 phosphorylation sites were identified, including all P-tau sites, with 2 additional phosphorylation sites being mapped at T76 and S356. Biological modifications other than phosphorylation, such as ubiquitination, acetylation or glycosylation, were not identified in this analysis (nor has it been previously reported for Sf9 tau [419]). Consistent with the FLEXITau data, the proline-rich domain depicted the highest density of phosphorylation sites with 13 sites total, for both P-tau and PP-tau (this is also consistent with previous reports [196]). A comprehensive list of detected modified peptide species can be found in Table 2.2. Of the 16 peptides identified as significantly "modified" by FLEXITau (in both P-tau and PP-tau) 15 were associated with the presence of one or

Table 2.1: Peptides quantified by the FLEXITau assay (A-W) and corresponding PTMs identified by complementary DDA. Peptide modification extent was determined by the difference of normalized L/H ratio to ctrl-tau, where 100% represents a peptide that is fully modified. Peptides were defined as "unmodified" (green shade) if the difference to control samples was insignificant (student t-test, $p > 0.05$), and as "modified" if difference was significant (orange shade, peptides modified in P-tau and PP-tau; red shade, peptides modified in PP-tau only). Corresponding phosphorylation sites detected by complementary LC-MS/MS analysis are shown (see also Fig. 3E). Note that a modification site on the first AA after the cleavage site will contribute to the N-terminal peptide as well and will be listed twice (e.g. T175). Phosphorylations only detected in PP-tau are written in red. * p -value < 0.05 ; ** p -value < 0.005 ; *** p -value < 0.0005

Region	ID	Location [AA]		FLEXITau peptide	Peptide modification extent [%]				PTM contributing to modification extent	
		Start	End		P-tau	p-value	PP-tau	p-value	detected	hypothesized
acidic	A	6	23	QEFEVMEDHAGTYGLGDR					-	
	B	24	44	KDQGGYTMHQDQEGDTDAGLK	50.8	*	22.2	*	-	Y29, T30, T39
	C	45	67	ESPLQPTEDGSEEPGSETSDAK	44.7	*	54.0	**	S68	S46, T50, T52, S58
	D	68	87	STPTAEDVTAPLVDEGAPGK	19.9	*	33.4	**	S68, T76	
	E	88	126	QAAQPHTEIPEGTTAAEEAGIGDTPSLEDEAA GHVTQAR			12.9		-	
proline-rich	F	151	163	IATPRGAAPPQK	4.2		20.1	*	T153	
	G	164	174	GQANATRIPAK	2.1		3.0		T175	
	H	175	180	TPPAPK	58.4	**	67.4	**	T175, T181	
	I1	181	190	TPPSSGEPPK	59.1	**	66.0	**	T181, S184	
	I2	181	194	TPPSSGEPPKSGDR	66.4	**	82.3	***	T181, S184	S195
	J	195	209	SGYSSPGSPGTPGSR	86.1	***	90.7	**	S199, S202, T205, S210	S195
	K1	210	221	SRTPSLTPPTR	69.7	**	94.8	**	S210, T212, S214, T217	
	K2	210	224	SRTPSLTPPTREP	68.8	*	91.1	**	S210, T212, S214, T217	
	K3	212	221	TPSLTPPTR	52.2	**	80.1	***	T212, S214, T217	
	K4	212	224	TPSLTPPTREP	53.7	**	88.0	**	T212, S214, T217	
binding repeats	L	226	234	VAVVRTPPK	90.6	***	97.2	***	T231, S235	
	M	243	254	LQTAPVMPDLK	9.2		12.0		-	
	N	260	267	IGSTENLK	15.7	*	38.6	**	S262	
	O	275	280	VQIINK	11.6		9.0		-	
	P	281	290	KLDLSNVQSK	15.2		13.2		-	
	Q	299	317	HVPGGGSQIVYKPVDSLK	7.9		10.2		-	
	R	322	340	CGSLGNIIHKPGGGQVEVK	12.4		31.0	*	S324	
	S	341	347	SEKIDFK	10.2		6.4		-	
	T	354	369	IGSLDNITHVPGGGNK	1.8		23.8	*	S356	
	C-terminal	U	376	383	LTFRENAK					-
V1		384	395	AKTDHGAEIVYK	33.2	*	41.1	*	S396	
V2		386	395	TDHGAEIVYK	29.4	*	34.2	*	S396	
W		396	406	SPVVGSDTSPR	84.1	***	92.4	***	S396, S404	

more phosphorylation site. Only for peptide B (₂₄KDQGGYTMHQDQEGDTDAGLK₄₄) no corresponding modification could be identified. In this case, FLEXITau analysis showed a significant modification extent in both P-tau and PP-tau (51%, $p=0.008$ and 22%, $p=0.046$, respectively), clearly indicating the presence of a modification. Putative phosphorylation sites on peptide B include Y29, T30 and T39 (see Table 2.1).

FLEXITau showed 3 peptides to be exclusively modified in PP-tau but not on P-tau (see 2.1, peptide sequences highlighted in red). In the DDA data phosphorylation sites T153, S324 and S356 were identified on these peptides. Unexpectedly, T153 and S324 were not only detected in PP-tau but also on P-tau. However, the quantitative FLEXITau data showed that the extent of modification of these peptides in P-tau is minimal (4.2% and 12.4%, respectively; p -value across biological replicates non-significant).

The DDA data did not map any PTMs to peptides that were determined to be "unmodified" by FLEXITau, corroborating the quantitative results. The only exception is the peptide ₁₆₄GQANATRIPAK₁₇₄, on which T175 was detected as being phosphorylated both in P-tau and PP-tau. However, the FLEXITau data determined that the modification stoichiometry

Table 2.2: Sf9-tau phosphorylation sites Summary of phosphorylated tau peptide species and phosphorylation sites detected in Sf9 deP-tau, P-tau, and PP-tau.
z, charge state; x, peptide species detected; red, site not detected; green, site detected

PTM site		Peptide species			Peptide species detected			Site detected		
AA	Site	Sequence	Precursor MW	z	deP-tau	P-tau	PP-tau	deP-tau	P-tau	PP-tau
S	68/69	STPTAEDVTAPLVDEGAPGK	2033.9055	2		x	x		yes	yes
T	76	STPTAEDVTAPLVDEGAPGK	2033.9055	2			x			yes
T	153	TKIATPR	865.4415	2		x	x	yes	yes	yes
		TKIATPRGAAPPQK	1571.8176	3			x			
		IATPR	636.2993	2			x			
		IATPRGAAPPQK	1342.6716	2		x	x			
T	175	GQANATRIPAKTPPAPK	1796.9287	3			x	red	yes	yes
		IPAKTPPAPK	1098.587	2		x	x			
		TPPAPKTPSSGEPKSGDR	2081.9709	4			x			
T / T	175 / 181	GQANATRIPAKTPPAPKTPSSGEPK	2854.3762	4		x	x	red	yes	yes
		IPAKTPPAPKTPSSGEPK	2156.0305	3			x			
T	181	IPAKTPPAPKTPSSGEPK	2156.0305	3		x	x	yes	yes	yes
		TPPAPKTPSSGEPK	1666.7997	3	x	x	x			
		TPPAPKTPSSGEPKSGDR	2081.9709	4			x			
		TPSSGEPK	1075.462	2		x	x			
		TPSSGEPKSGDR	1490.6445	2		x				
S	184	TPPAPKTPSSGEPKSGDR	2081.9709	4		x	x	red	yes	yes
		TPPAPKTPSSGEPK	1666.7997	3		x				
S	199	SGYSSPGSPGTPGSR	1472.5914	2		x	x	red	yes	yes
S	202	SGYSSPGSPGTPGSR	1472.5914	2		x	x	red	yes	yes
S	210	SRTPSLTPPTR	1388.6807	2		x	x	red	yes	yes
		SRTPSLTPPTREP	1822.8362	3		x				
T	212	SRTPSLTPPTR	1388.6807	2		x	x	red	yes	yes
		SRTPSLTPPTREP	1822.8362	3		x				
T / S	212 / 214	SRTPSLTPPTREP	1822.8362	3		x	x	red	yes	yes
T / T	212 / 217	SRTPSLTPPTREP	1822.8362	3			x	red		yes
S	214	SRTPSLTPPTR	1388.6807	2		x	x	yes	yes	yes
		SRTPSLTPPTREP	1822.8362	3		x				
		TPSLTPPTR	1145.5465	2		x	x			
		TPSLTPPTREP	1499.7394	3	x	x	x			
T	217	SRTPSLTPPTREP	1822.8362	3	x	x	x	yes	yes	yes
		TPSLTPPTR	1145.5465	2	x	x	x			
		TPSLTPPTREP	1499.7394	3	x	x	x			
T	231	KVAVVRTPPK	1173.6621	2	x	x	x	yes	yes	yes
		KVAVVRTPPKSPSSAK	1730.9443	3	x	x	x			
		TPPKSPSSAK	1078.5077	2	x	x	x			
		VAVVRTPPKSPSSAK	1602.8481	3		x	x			
T / S	231/235	KVAVVRTPPKSPSSAK	1730.9443	3		x	x	red	yes	yes
S	235	VAVVRTPPKSPSSAK	1602.8481	3		x	x	red	yes	yes
		TPPKSPSSAK	1078.5077	2		x	x			
S	262	VAVVRTPPKSPSSAK	1602.8481	3		x	x	red	yes	yes
		IGSTENLKHQGGGK	1601.7526	3		x				
		SKIGSTENLK	1155.5531	2		x	x			
S	293	SKIGSTENLKHQGGGK	1816.8882	4		x	x	red	yes	yes
		CGSKDNIK	1014.4178	2			x			
S	324	CGSLGNIHHPGGGQVEVK	2066.9736	3		x	x	red	yes	yes
S	356	IGSLDNITHVPGGGNK	1657.7806	2			x	red	red	yes
		DRVQSKIGSLDNITHVPGGGNK	2371.1626	4			x			
		KIGSLDNITHVPGGGNK	1785.8754	3			x			
S	396	AKTDHGAEIVYKSPVVSQDTSR	2493.2092	4		x	x	red	yes	yes
		TDHGAEIVYKSPVVSQDTSR	2294.0759	3		x	x			
S / S	396 / 404	TDHGAEIVYKSPVVSQDTSR	2294.0759	3				red	yes	yes
S	404	AKTDHGAEIVYKSPVVSQDTSR	2493.2092	4		x		red	yes	yes
		SPVVSQDTSR	1180.509	2		x	x			
S	422	HLSNVSSTGSIDMVDSPQLATLADEVASLAK	3322.6108	4		x	x	red	yes	yes

is low (<3% for both species), which is below the precision of the assay (%CV = 3.9%, see above).

The quantitative precision of FLEXITau can point to additional PTMs that are not detected in DDA experiments as for peptide B above. In one special case (peptide C, ₄₅ESPLQTPTEGSEEPGSETSDAK₆₇), a matching modification was identified as S68, however FLEXITau data suggested an additional PTM. S68 is located on the first AA after the cleavage site where this phosphorylation contributes to a reduction in the abundance of unmodified peptide C as well as the following peptide D (₆₈STPTAEDVTAPLVDEGAPGK₈₇), as described above. Peptide D carries an additional modification thus the abundance of unmodified peptide D was expected to be lower than that of peptide C. However, the abundance of unmodified peptide D was higher than that of peptide C, reflected by the smaller modification extent (P-tau - 19.9%; PP-tau - 33.4%), compared to that of peptide C (P-tau - 44.7%; PP-tau - 54.0%). This led us to speculate that peptide C harbored an additional modification site that was not detected by the DDA experiment. In the literature, many studies of *in vitro* and *in vivo* phosphorylated tau, often employing enrichment strategies, have been performed [108, 112, 237, 423]. Remarkably, despite the vast amount of information (see also <http://cnr.iop.kcl.ac.uk/hangerlab/tautable>, an up-to-date list of all tau phosphorylation sites), in the N-terminal region only one site has been previously described *in vivo* [195, 470]. Putative phosphorylation sites in this region are T50, T52 and S56. Importantly, although PTMs other than phosphorylation can be found in the baculovirus infected insect expression system neither we nor others have identified these. In summary, although normal workflows such as DDA experiments cannot possibly map all modified sites at once [310], the quantitative unbiased view of the modification landscape provided by FLEXITau can point to additional areas of tau that might be modified, independent of the type of modification.

2.4.6 Calculation of site occupancy using FLEXITau

In the above analysis, peptide abundance data for the unmodified peptides was obtained and modification sites were mapped. For peptides harboring a single modification, the peptide modification extent directly reflects the occupancy of the modified site. Notably this only holds true under the premise that no modification other than the one detected is present on the respective peptide. In this dataset, this situation applies to T175, S262, S324, S356, and S416/422. However, for many peptides multiple phosphorylated sites were identified, in particular in the proline-rich region, as well as in the C-terminal tail (see Table 2.1 and Fig. 2.6). In these cases, the direct correlation of peptide modification extent and site occupancy cannot be made. Each site may contribute to the overall peptide modification extent. Thus, for multiply modified peptides, the peptide modification extent is the sum of all individual site occupancies.

To determine the individual site occupancies for multiply phosphorylated peptides, a

combinatorial strategy that uses information from "overlapping" peptides was employed (for a schematic see Fig. 2.7A). Overlapping peptides are produced by a missed tryptic

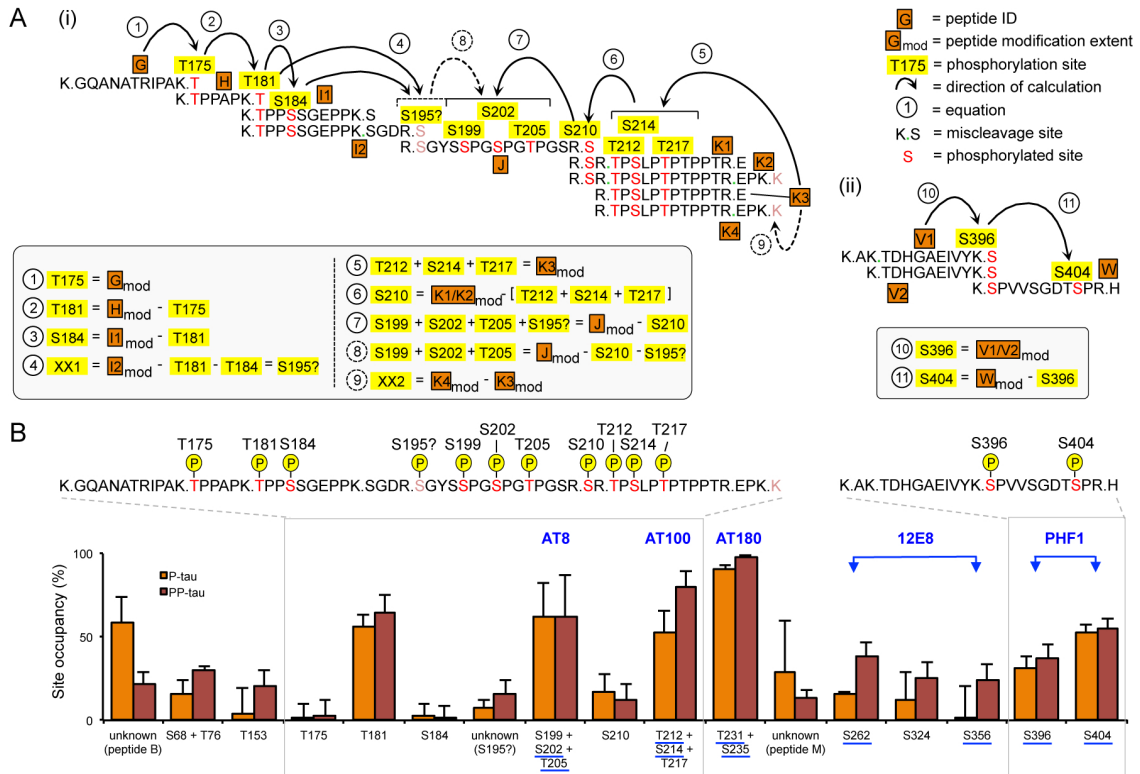


Figure 2.7: Calculation of site occupancies for singly and multiply modified peptides. **A.** For peptides containing a single modification site, the site occupancy equals the peptide modification extent calculated by the FLEXITau assay (see Table 2.1). For multiply modified peptides, a combinatorial approach was designed to stepwise calculate individual site occupancies by using quantitative information from overlapping peptides. (i) the proline-rich region; equations 1-9, with equation 1 starting from N-terminus and equation 5 starting from the C-terminus. (ii) the C-terminal tail; equations 10-11. **B.** Phosphorylation extents for all identified sites are shown in % (average \pm SD of 3 biological replicates, 3 measurements each). Sites are sorted by the AA location in the tau sequence N- to C-terminus. Commonly used diagnostic AD antibodies are shown in blue, with binding epitopes underlined. The grey boxes indicate the highly modified region (i) and (ii) shown in **A**. P, phosphate group

cleavage - typically caused by closely located lysines and arginines (peptides I1/I2, K1-K4, and V1/V2). In these cases, when trypsin is used, the primary tryptic peptide has a miscleaved counterpart whose sequence encompasses the primary tryptic peptide species with an addition of the following AAs until the next cleavage site. A missed cleavage can also occur if a phosphorylation is present on the AA in the first position after the cleavage site (see peptides G/H, I2/J, J/K, and V2/W). In these cases, cleavage is impaired due to the presence of the phosphate group. Thus, the phosphate on the second peptide causes the reduction in the abundance of both unmodified peptides, N- and C-terminal to the cleavage

site.

The strategy to calculate site occupancy of multiply phosphorylated peptides is to start with a single peptide with a single modification, whose site occupancy is therefore defined (see Fig. 2.7A). The stoichiometries of additional sites are then calculated stepwise by using the quantitative information of each subsequent "overlapping" peptide. For example, in the case of the proline-rich region, one starts at the N-terminus of this region with peptide G. Its modification extent equals the occupancy of its single phosphorylation site on residue T175. The adjacent overlapping peptide (peptide H) contained two detected phosphorylations, T175 as well as T181. Here, the modification extent of T181 is the difference in modification extent of peptide G (T175) and peptide H (T181+T175), in this case 56.3% (P-tau) and 64.4% (PP-tau). This combinatorial strategy allowed the successful quantification of the individual stoichiometry of sites T181, S184, S210, S396 and S404. In the case of peptide I (₁₈₁TPPSSGEPPKSGDR₁₉₅), 2 phosphorylation sites were mapped, T181 and S184, using DDA experiments. However, the total modification extent was higher than the sum of its quantified single components. Thus, one can speculate that the remaining value (7.3% and 16.3% in P-tau and PP-tau, respectively) corresponds to an additional modification, tentatively assigned as S195, a site reported previously in AD [131].

A summary of site occupancies for all phosphorylations detected in P-tau and PP-tau is shown in Figure 2.7B (see also Table 2.3). The average amino acid resolved site occupancy was 29.5% (P-tau) and 35.7% (PP-tau). As expected, these values are lower than the peptide modification extent mentioned above (33.0% and 42.7%, P-tau and PP-tau respectively), as there are peptides containing several sites. The strategy to determine specific AA resolved site occupancies described above cannot always be applied for two reasons i) the sites are in close proximity and/or ii) there are no adjacent miscleaved peptides. This is the case for the following regions: S68/T76, S199/S202/T205, T212/S214/T217 and T231/S235. For these sites the joined occupancy is determined.

In general, the quantitative PTM landscape suggests that most of the phosphorylation sites present with low stoichiometries. In P-tau, nearly two thirds (and in PP-tau, a third) of all sites are phosphorylated to an extent below 20%. The combination of sites T231/S235 has the highest occupancy (90.6% and 97.3% for P-tau and PP-tau, respectively). Four other sites are also phosphorylated at a stoichiometry larger than 50% (T181, S199/S202/T205, T212/S214/T217, and S404). Notably, all these are epitopes of commonly used AD diagnostic antibodies (AT8, AT100, AT180, and PHF1) (see also Fig. 2.7B). Thus, apart from validating the elevated extent of phosphorylation for these regions, FLEXITau is also able to precisely quantify this state referred to as "hyperphosphorylated" by antibodies used ubiquitously in the study of tauopathies.

Table 2.3: Summary of calculated site occupancies for tau phosphorylation sites of P-tau and PP-tau, in % Shown are values for each biological replicate (average of technical replicates), their average and SD.

Site(s)	P-tau					PP-tau				
	P-tau1	P-tau2	P-tau3	mean	stdev	PP-tau1	PP-tau2	PP-tau3	mean	stdev
unknown (peptide B)	75.72	54.72	46.80	59.08	14.94	29.50	21.15	16.07	22.24	6.78
S68 + T76	8.51	14.50	24.81	15.94	8.24	27.82	31.89	30.84	30.18	2.11
T153	2.05	0.00	6.33	2.80	3.23	16.41	12.27	31.56	20.08	10.16
T175	0.00	0.00	11.55	3.85	6.67	0.00	6.46	9.85	5.44	5.00
T181	49.29	62.23	57.42	56.31	6.54	73.49	51.66	67.91	64.35	11.34
S184	0.90	0.00	11.17	4.02	6.21	0.00	1.59	9.16	3.58	4.90
unknown (S195?)	2.07	12.52	7.34	7.31	5.23	13.74	25.04	10.07	16.28	7.80
S199 + S202 + T205	77.63	38.76	68.94	61.78	20.40	75.62	31.92	77.36	61.63	25.75
S210	6.11	28.33	16.71	17.05	11.12	5.71	22.44	10.30	12.82	8.64
T212 + S214 + T217	62.19	36.92	57.47	52.19	13.44	84.13	69.66	86.61	80.13	9.15
T231 + S235	89.04	89.03	93.70	90.59	2.69	97.79	95.30	98.56	97.22	1.71
unknown (peptide M)	64.28	17.97	2.98	28.41	31.96	15.50	17.01	7.17	13.23	5.30
S262	14.29	17.39	15.28	15.65	1.58	40.77	29.95	45.06	38.59	7.79
S324	0.00	30.09	7.97	12.69	15.59	32.48	14.96	28.59	25.34	9.20
S356	0.00	20.60	1.83	7.47	11.40	24.45	13.45	33.60	23.83	10.09
S396	24.70	39.50	29.78	31.33	7.52	33.94	31.86	47.23	37.68	8.34
S404	53.58	47.72	56.93	52.74	4.66	57.05	59.60	47.49	54.71	6.38

2.4.7 Using FLEXITau to determine the average number of phosphorylations per tau molecule

The above results showed that FLEXITau provides the stoichiometries of identified phosphorylation sites. Using a recursive approach, next the polynomial probability distribution of a particular number of sites being phosphorylated at a given time was calculated (Fig. 2.8A, for details, see section 2.3). A shift in the distribution of PP-tau towards to a higher phosphorylation state by 1 phosphate compared to P-tau was observed, with PP-tau showing a maximum likelihood of 8 phosphates per tau molecule, compared to 7 for P-tau. The broad base observed for both P-tau and PP-tau shows that there is a wide range of phosphorylation states for tau ranging from 1-14 phosphates for P-tau, and 2-15 for PP-tau (full width at half maximum (FWHM) of 4.7 and 5, P-tau and PP-tau, respectively). For joined occupancies, two possible extreme scenarios are assumed: either the respective sites are present exclusively alone, or exclusively together (Fig. 2.8B and 2.8C). Notably, it is possible that some of the phosphorylations sites that were quantified are dependent on one another i.e. a priming site is required for another phosphorylation to occur [489]. The probability estimation does not take into account any site dependencies; if such data is available, it should be incorporated into this calculation, as this will provide additional accuracy for the distribution estimation.

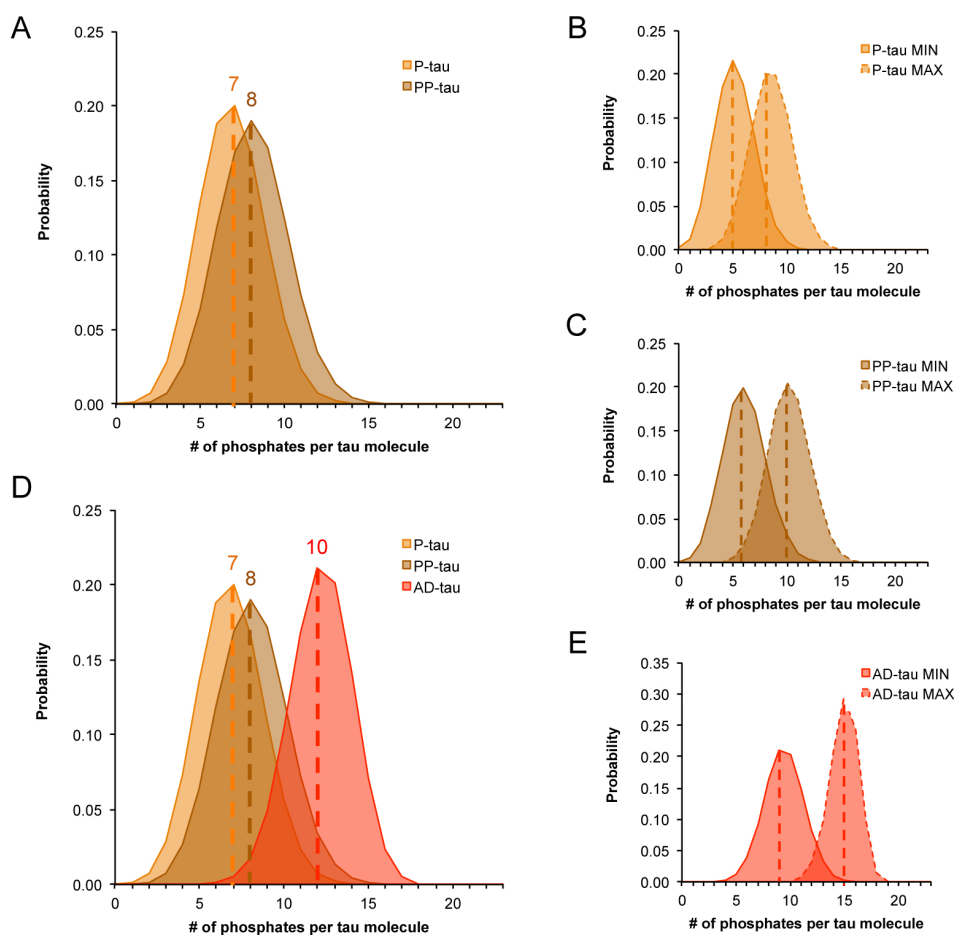


Figure 2.8: Frequency distribution of number of phosphates per tau molecule. Joined occupancies (more than 1 site per quantified occupancy) were assumed to be either exclusively occupied (MIN) or jointly occupied (MAX), and average distribution was determined by measuring the mean of MIN and MAX values for joined sites. Maximum likelihood estimate is indicated by vertical line. For details of calculation, see section 2.3. **A.** Average for Sf9 P-tau and PP-tau; **B.** and **C.** MIN/MAX distributions for P-tau and PP-tau, respectively; **D.** average for Sf9 P-tau and PP-tau, and AD-tau; **E.** MIN/MAX for AD-tau.

2.4.8 Using FLEXITau to examine the PTM landscape of human AD-tau

Above, the power of the FLEXITau approach is exemplified by quantifying the modification landscape of purified, hyperphosphorylated Sf9-tau, i.e. an "artificial" substrate. However, this assay could be applied in many biological settings, including more complex mixtures. Thus, to show its versatility, the next goal was to apply FLEXITau to a tau species in a complex, disease-related human sample. To this end, the FLEXITau assay was used to evaluate tau aggregates derived from AD patient brains, and the quantitative data was compared to the Sf9-tau to evaluate this cellular model as a proxy to disease.

A traditional sarkosyl fractionation of post-mortem cortical brain tissue was used to enrich for insoluble AD tau species (AD-tau) (see 2.4). AD-tau was subjected to the FLEXITau

Table 2.4: Characteristics of AD patient material UCSF, Neurodegenerative Disease Brain Bank, University of California, San Francisco; HBSFRC, Human Brain and Spinal Fluid Resource Center, West Los Angeles; PMI, post-mortem interval

Brain bank	Sample purpose	Brain #	Age	Gender	PMI	Location	Neuropathology Diagnosis
UCSF	initial optimization	AD1	75	F	8.8	BA39	Alzheimer's Disease
UCSF	initial optimization	AD2	80	M	6.5	BA39	Alzheimer's Disease
HBSFRC	final dataset	AD3	78	F	12.3	BA39	Alzheimer's Disease
HBSFRC	final dataset	AD4	74	F	10.5	BA39	Alzheimer's Disease
HBSFRC	final dataset	AD5	89	F	18.4	BA39	Alzheimer's Disease

workflow and quantitative data was acquired. The overall modification extent of AD-tau was more than 2-fold higher than that of the Sf9 model tau (AD-tau 77.2%, compared to 34.1% in P-tau and 42.4% PP-tau, respectively). Figure 2.9A shows the AD-tau FLEXITau data in a heatmap presentation from N- to C-terminus in comparison to P-tau and PP-tau. The data indicates that the N-terminus is considerably more modified in AD-tau compared with Sf9-tau. Notably, the proline-rich region shows high modification extent for both Sf9- and AD-tau, while the repeat regions are less modified in both, particularly R3 and R4. To systematically assess the quantitative differences in the extent of modification for Sf9-tau and AD-tau, a hierarchical cluster analysis of the FLEXITau data was performed (Euclidean Distance, Ward criteria). This analysis grouped the peptides into 6 distinct classes (I-VI, Fig. 2.9B). Class I and II contained peptides with no or little modification extent in Sf9-tau (below 15%), with class I showing none at all and class II showing minor modification in AD-tau (below 60%). Class III and IV peptides showed drastic differences between Sf9-tau and AD-tau: peptides in class III and IV showed high modification stoichiometry in AD-tau (on average 88%), while Sf9-tau showed little or no modification respectively. Finally, class V and VI peptides were highly modified in all three species: class V contained peptides that showed enhanced modification in AD-tau and class VI peptides were modified to a similar extent in all tau samples. In summary, one third of the quantified peptides (31% of tau sequence analyzed) were modified to a similar extent in AD-tau as in the Sf9 species, while the remaining two thirds of the peptides showed significantly higher modification extent in AD-tau.

As mentioned above, many PTMs of PHF-tau from AD brain have been described using different types of enrichment strategies [98, 108, 112, 179, 196, 423] (reviewed in [292, 329]). To investigate the quantitative differences between AD-tau and Sf9 qualitatively, these available datasets were compiled and all reported modifications were mapped to the peptides from the FLEXITau dataset (Fig. 2.9B, right panel). Most of the differences of AD-tau to Sf9-tau could be explained by additional modifications on the respective peptides. The peptides that reflected the biggest changes between Sf9-tau and AD-tau (class III and class IV peptides) harbor multiple additional phosphorylation as well as acetylation (ac) sites (such as acK274 and acK280), highlighting the importance of modifications other than

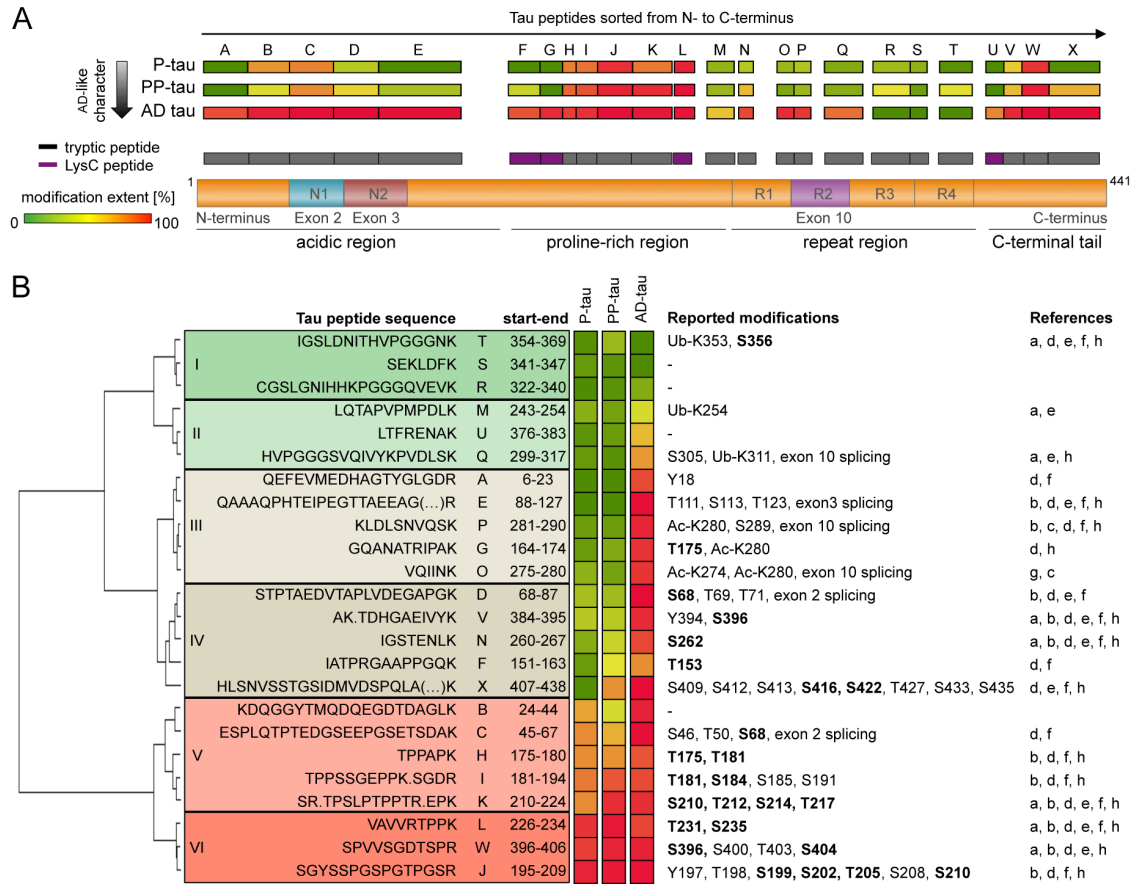


Figure 2.9: Applicability of FLEXITau to human disease. **A.** Sarkosyl insoluble tau from post-mortem brain of three different AD patients was subjected to the FLEXITau workflow (triplicate SRM measurements). The modification extent of each peptide was compared to Sf9-tau (see also Fig. 2.6B) and in-scale mapped to a schematic tau protein. The color code depicts respective modification extent (green, no modification; red, 100% modification). **B.** Peptides were sorted using hierarchical clustering of the FLEXITau data (Euclidean distance, Ward's criteria). PTMs reported on AD-tau in the literature are listed next to the corresponding peptide. If no prefix is present, AA site refers to phosphorylation; ub, ubiquitination, ac, acetylation, bold, modifications detected in Sf9-tau. References: (a) Cripps 2006 [108], (b) Hanger 2007 [196], (c) Cohen 2011 [97], (d) Martin 2011 [292], (e) Thomas 2012 [423], (f) Noble 2013 [329], (g) Grinberg 2013 [179], (h) Dammer 2015 [112]

phosphorylation when studying tau aggregation. In addition, it should be noted that class III and IV include peptides from exons 2,3 and 10 that can be spliced out, and can thus contribute to the reduced levels of unmodified peptides in these regions. Interestingly, all ubiquitination sites reported so far [108] are located on peptides that contain few other modifications and display low modification extent (class I and II peptides). Furthermore, peptides highly modified in both AD-tau and Sf9-tau (class V and VI) exclusively harbored phosphorylation (and no other type of modification). With few exceptions, most of these phosphorylation sites are present in both Sf9 and AD-tau. Notably, the epitopes of the most commonly used AD diagnostic antibodies are located on these peptides. However,

multiple additional phosphorylation sites are present on AD-tau that were not identified on Sf9-tau.

Finally, the recursive approach mentioned above (described in section 2.3) was applied to calculate the distribution of the average number of phosphates per tau molecule. This calculation showed that on average, AD-tau contains 10 phosphates per tau molecule and the distribution of sites per tau molecule ranges between a minimum of 4 to a maximum of 19 (Fig. 2.8D, and 2.8E).

Altogether, while possibly representing a model for several AD-specific phosphorylation sites in the proline-rich domain, altogether these data reveal significant qualitative and quantitative differences between Sf9-tau and AD-tau, even with respect to phosphorylation. These findings corroborate the usefulness and necessity of a global unbiased assay such as FLEXITau when assessing and comparing the PTM state of model systems to their disease equivalent.

2.5 Conclusion

The number and diversity of tau modifications is large, and misregulation of tau PTMs is believed to directly or indirectly lead to tau aggregation. However, current approaches to study tau modifications are not capable of capturing the many possible combinations of PTMs simultaneously, let alone in a quantitative manner. Here, FLEXITau was designed, a highly sensitive and robust SRM-based assay that measures unmodified peptide species of tau relative to a heavy standard, rather than aiming for identification of specific PTMs. The key advantage herein is that FLEXITau can be used to study a limitless number of modification sites and species without requiring prior information, thus circumventing many issues typically encountered when using other approaches [401].

Unlike other methods, this assay provides an unbiased, comprehensive understanding of the existing PTM landscape. The resulting "signature" can be used to determine relative differences between tau species in a precise manner. In combination with DDA data, site-specific occupancies as well as the average number of occupied sites at a given time can be calculated. Due to its unbiased quantification the assay can also point towards undetected or even undescribed modifications; those hypothetical sites can be followed up using directed and targeted analysis, emphasizing the versatility of the assay as a tool to identify novel modifications without relying on their immediate detection.

Given its precision and versatility, in the future one can envision the application of this assay to a wide range of biological and clinical settings. For examples, with its ability to measure small changes in the PTM landscape, the assay could facilitate the screening of small compounds and monitoring the effect of treatment. This is especially important given the recent interest in tau-targeted therapeutic approaches since the failure of many amyloid-beta-targeted therapeutics in phase III clinical trials [79]. Offering both the necessary sensitivity and specificity, FLEXITau also has potential as *in vivo* diagnostic biomarker

for tau derived from peripheral fluids such as cerebrospinal fluid or blood, an effort that has been hampered so far by the lack of methods capable of dealing with the molecular heterogeneity and low abundance of tau present in body fluids.

In summary, this study reports a method that provides a comprehensive, global analysis of tau PTMs. With its ability to resolve both distribution and occupancy of tau PTMs, FLEXITau might massively enhance the mechanistic understanding of tau function and untangle the role of tau modifications in physiological and pathological conditions. As such, it will provide a foundation for the development of better diagnostic tools and tau-modulating therapeutic approaches for tauopathies.

Acknowledgments

The author is grateful for the contribution of the following people for this particular chapter: to Dr. Katharina Tepper for preparation of Sf9-tau and valuable input in experimental considerations and tau biochemistry; to Dr. Katharina Tepper and Prof. Dr. Eckhard Mandelkow for fruitful discussions regarding differences of the FLEXITau analyses to MALDI-TOF analyses; Dr. Jan Muntel for collaboration and valuable support in the development of the SRM assay and other aspects of mass spectrometry; and to Dr. Shaojun Tang for developing the multimodal approach for the calculation of site-occupancy and implementation using R, and useful feedback regarding statistical questions.

This chapter contains published work which is reprinted with permission from Analytical Chemistry, copyright 2016 American Chemical Society. The original article can be accessed [here](#).

3 Quantitative Profiling of Tau Peptides Identifies Diagnostic Signatures for Neurodegenerative Tauopathies

3.1 Summary

The aggregation of tau protein in the brain is the hallmark of a diverse group of neurodegenerative diseases with overlapping clinical and pathological phenotypes. Currently, there is no accurate means of differentially diagnosing these diseases. Here, a computational classifier is presented that can identify specific tauopathies using mass spectrometry data quantifying the post-translational modification (PTM) state of tau. A total of 129 post-mortem brain samples from 5 different brain banks encompassing patients with Alzheimer's Disease (AD), progressive supranuclear palsy (PSP), corticobasal degeneration (CBD), Pick's Disease (PiD), and non-demented control subjects (ctrl) were analyzed to quantify tau modification and isoform patterns using a targeted MS assay. Supervised machine-learning approaches identified relevant peptide combinations and associated PTMs that distinguish each disease category using a training set of 68 patients. The classifier was then validated on an independent heterogeneous dataset of 61 patients. The final classifier developed achieved excellent diagnostic accuracy of 96% for AD, 94% for CBD and ctrl, and 92% for PiD. Good diagnostic accuracy was achieved for PSP with 80% accuracy. The majority of discriminating peptide features are located in the MT-binding region of tau, including exon 10 which is prone to alternative splicing leading to 3R and 4R isoforms. In summary, tau modification and isoform abundance quantified at the peptide level provides a tauopathy specific signature that can distinguish tauopathies and could be used as a novel diagnostic test.

3.2 Introduction

Neurodegenerative diseases are a major cause of disability and premature death among older people worldwide [58, 211, 380]. These conditions usually cause dementia and are clinically characterized by progressive behavioral changes, executive dysfunction and impairment of cognition and memory, ultimately affecting many of the body's activities. Today, an estimate of 44 million people worldwide live with dementia; driven by a rapidly aging

population and due to the lack of prevention and cure, its frequency is expected to double by 2030, and to triple by 2050 [359]. Alzheimer's Disease (AD) is the most common degenerative disease. Accounting for 60-70% of cases, it represents a major medical, social, and financial burden to the society. A growing body of evidence suggests that the atypical deposition of characteristic proteins into insoluble aggregates inside or among specific neurons and glial cells is a shared feature of neurodegenerative diseases, thus also referred to as proteinopathies [148, 372, 446, 447]. The most common group of proteinopathies are tauopathies, where an altered form of the microtubule associated protein tau forms aggregates. This pathological tau aggregation is a shared molecular mechanism in many neurodegenerative conditions [33, 406]; more than 20 tauopathies, including AD, have been described [317, 461].

Several non-AD tauopathies fall into the spectrum of sporadic frontotemporal lobe dementia (FTLD) with tau pathology (FTLD-tau) and are characterized by selective atrophy of the frontal and temporal cortex, together with neuronal loss and gliosis [125, 389]. The most prominent FTLD-tau disorders include corticobasal degeneration (CBD), progressive supranuclear palsy (PSP) and Pick's disease (PiD) [167, 422]. The clinical presentation is typically determined by the analysis of symptoms such as progressive deficits in behavior, executive function, or language, while the pathology of each disorder is defined by characteristic types and distribution of the tau inclusions [35, 125]. This abnormal tau protein accumulating in characteristic insoluble structures is known to carry many post-translational modifications (PTMs). Thus, it can be hypothesized that the characteristic types and distribution of the tau inclusions have underpinnings which may be defined by the molecular nature of tau, whereby specific PTMs and PTMs found in specific stoichiometries result in these characteristic tau inclusions specific to each tauopathy. Profiling the specific molecular characteristics of tau in these tauopathies will enable the diagnosis, prognosis and the development of directed therapies.

Substantial overlap in clinical phenotypes and the recent recognition of many atypical manifestations have complicated clinical diagnosis of these disorders [272, 317, 366, 464]. Despite significant progress in developing diagnostic biomarkers for some of these conditions, in particular AD [212, 251, 291] and PSP [327, 364, 444, 457], currently no method exists to permit their reliable differentiation. To date, an accurate diagnosis is often reached post-mortem by the investigation of specific types and location of inclusions among the diseases by neuropathological techniques. Post-mortem classification is a time consuming and labor intensive as it involves rigorous investigation of anatomical distributions and abnormalities using an array of immunohistological and biochemical staining methods [280, 317, 461]. Often, even a post-mortem diagnosis is difficult due to pathological heterogeneity, disease-overlapping histopathological features, and co-morbidities [62, 124, 125, 316, 433, 445].

Given these described complications, the development of patient stratification tools both *in vivo* and post-mortem will have an immense impact on the assessment, treatment, and characterization of tauopathies for multiple reasons: not only will they provide means

for future inexpensive and accurate diagnosis of new autopsies; they will also allow for fast re-evaluation of existing samples in brain banks, a key and indispensable tool for the study of neurodegenerative diseases by the research community [262, 362]. Moreover, the extension of these methods for *in vivo* patient classification approaches such as biomarker detection in CSF or blood and novel agents targeting specific molecular characteristics of tau for PET imaging will allow the stratification of patients in clinical trials and provide a quantitative means to assess efficacy of drugs in clinical trials. Finally the underlying distinct pathobiology may be unraveled, thus ultimately opening new roads for disease-modifying or even preventative therapeutics.

Stratification or diagnosis using MS-based quantitative proteomics employs specific patterns of proteins or peptides in body fluids or other tissues to uniquely define a disease state. MS is currently the most quantitative and specific tool for the measurement of proteins and thus offers enhanced diagnostic accuracy. In addition MS-based proteomics can accommodate biological heterogeneity in disease expression, with successful applications to cancer diagnostics [1, 2, 348, 410], alcoholism [172], schizophrenia [266], and several other diseases [7, 241, 242, 315, 341]. In the current study, the mapping of the PTM landscape on tau is pioneered for the classification of tauopathies. Given the prevalent disease-specific modifications of tau [223, 376], the variety of tau structures, as well as distinct isoform distributions found in sporadic tauopathies [339, 390, 392, 477], it is hypothesized that each condition may present with a distinct profile of modifications on tau. A targeted quantitative MS-based assay [288] was employed to precisely and accurately measure this tau signature and the associated PTMs. Supervised machine learning approaches were then used to evaluate the data and determine if specific features could accurately classify the disease categories.

3.3 Experimental procedures

Selection of tauopathy patients and controls

Human post-mortem brain specimens from patients with AD, PSP, PiD and CBD, and non-demented controls were obtained from 5 different brain banks through the NIH NeuroBioBank (U.S. Department of Health and Human Services, National Institutes of Health): 1) the University of Maryland Brain & Tissue Bank at the University of Maryland School of Medicine, Baltimore, MD; 2) the Harvard Brain Tissue Resource Center, McLean Hospital, Harvard Medical School, Belmont, MA; 3) the Neurodegenerative Disease Brain Bank (NDBB), Memory and Aging Center, University of California, San Francisco (UCSF), CA; 4) the University of Miami (UM) Brain Endowment Bank, Miller School of Medicine, Miami, MD; 5) the Human Brain and Spinal Fluid Resource Center (HBSFRC), VA West Los Angeles Healthcare Center, Los Angeles, CA. Pathological and clinical information, if available, was de-identified. Human brain tissue samples from the Brodmann Area (BA)

39 (angular gyrus) were obtained for this study. This tissue was selected as it would likely avoid overlapping AD-type pathology in PSP, PiD and CBD, while presenting strong AD-pathology in AD cases (personal communication, WW Seeley, UCSF). In all cases, brain blocks of 1-4 g were dissected from frozen brain slabs and shipped to Boston Children's Hospital on dry ice. Demographic details of patients and control individuals are given in Table 3.1.

Table 3.1: Patient demographics in entire cohort of 129 cases. Percentages refer to the proportion of cases from each brain bank in the entire cohort. *no PMI value was available for 5 cases (1 PSP, 3 CBD, 1 PiD).

	AD	PSP	CBD	PiD	control	Total
Total number of patients	28	29	22	21	29	129
Age at death (years)						
Mean (SD)	77.7 (10.1)	75.3 (7.9)	71.2 (7.2)	68.5 (9.6)	75.0 (12.8)	74.0 (10.2)
Range	41-90	58-93	58-88	51-92	45-97	41-97
PMI (hours)*						
Mean (SD)	13.4 (5.5)	13.4 (4.9)	11.5 (6.6)	14.8 (6.2)	16.5 (5.0)	14.1 (5.7)
Range	4.9-23.0	6.17-23.8	2.0-24	4.0-25.5	7.8-30.3	2.0-30.3
Sex						
(male:female)	11:17	21:8	10:12	16:5	19:10	77:52
Brain Bank						
UCSF	5	5	9	7	3	29 (22.5%)
UCLA	14	15	0	5	17	51 (39.5%)
McLean	9	9	5	7	9	39 (30.2%)
MIAMI	0	0	1	2	0	3 (2.3%)
UMB	0	0	7	0	0	7 (5.4%)

Extraction of sarkosyl insoluble tau from brain tissue

While still frozen, 0.25-0.35 g sections of cortical brain specimens were homogenized in 5 volumes lysis buffer (25 mM Tris-HCl buffer, pH 7.4, containing 150 mM NaCl, 10 mM ethylene diamine tetraacetic acid (EDTA), 10 mM EGTA, 1 mM DTT, 10 mM nicotinamide, 2 μ M trichostatin A, phosphatase inhibitor cocktail (Sigma), and protease inhibitor cocktail (Roche)), using Precellys® tissue homogenizer. Crude brain homogenates were clarified by centrifugation at 11,000 x g for 30 min at 4 °C. To obtain insoluble tau fractions, part of the crude tau fraction was treated with sarkosyl (1% final concentration) for 60 min at 4 °C and ultracentrifuged at 100,000 x g for 2 h at 4 °C. The supernatant was transferred to a fresh tube (sarkosyl soluble fraction). The sarkosyl insoluble pellet was carefully washed twice with 10 μ l ddH₂O, air-dried, and solubilized in 100 μ l 50 mM Tris buffer containing 1% SDS, 10 mM nicotinamide, 2 μ M trichostatin A, and phosphatase and protease inhibitor cocktail. The protein concentration in the extracts was determined by bicinchoninic acid assay (BCA Protein Assay Kit, Thermo Scientific).

Preparation of heavy tau standard

Full-length human 4R2N (GI:294862262) was subcloned into the previously generated pEU-E01-TEV-N1-AQUA vector.⁵⁰ After verification by DNA sequencing (Molecular Genetics Core Facility, Children's Hospital Boston), tau was *in vitro* transcribed and translated in a cell-free wheat germ expression (WGE) system according to the manufacturer's protocols (Cell Free Sciences, Wheat Germ Expression H Kit-NA). Expression was carried out in the presence of heavy isotope labeled lysine (13C6 15N2), arginine (13C6 15N4) and aspartate (13C4 15N1). Heavy tau standard was purified using Ni-Sepharose beads (Ni-Sepharose High Performance resin, GE Healthcare). Briefly, after a prewash in binding buffer (20 mM phosphate buffer, pH 7.5, 500 mM NaCl, 10 mM imidazole) beads were incubated with WGE (ratio 1:4) for 1 h rotating head-over-head at 4 °C for binding. After removal of the unbound fraction, beads were washed once with 1x volume and 3 times with 10x volume wash buffer (20 mM phosphate buffer, pH 7.5, 500 mM NaCl, 10 mM imidazole). Elution of tau was carried out in three consecutive steps (binding buffer with 100/300/500 mM imidazole, respectively). Success of enrichment was verified by SDS-PAGE and western blot analysis (data not shown). Pooled elutes were stored at -20 °C.

FLEXITau sample preparation for MS

Sarkosyl insoluble fractions were processed using the FLEXITau workflow in order to quantify absolute tau amounts and determine the level of tau modifications, as described in [288]. FLEXITau is an MS-based strategy that is based on the addition of a full-length tau protein standard containing the N-terminally tagged artificial tryptic FLEX-peptide to the biological sample of interest. Light FLEX-peptide is added in predetermined concentration to calculate absolute quantity of endogenous tau. The relative peptide abundance of light and heavy tau peptides can be used to infer modification extent of tau for each peptide. For FLEXITau experiments, heavy tau standard was first subjected to incubation with lambda protein phosphatase (New England Biolabs) for 30 min at 30 °C at 300 rpm for dephosphorylation. Dephosphorylated tau standard and sarkosyl protein fractions were processed separately using filter-aided sample preparation (FASP) (FASP Protein Digestion Kit, Expedeon). Briefly, samples were reduced with 50 mM DTT (20 min, 56 °C) and alkylated with 1% acrylamide (30 min, RT). Samples were diluted with 8 M urea, loaded onto the filter and washed twice with 8 M urea, 3 times with 50 mM ammonium bicarbonate (ABC). Samples were digested with 12.5 ng/ μ l trypsin (sequencing grade modified trypsin, Promega, Madison, WI) overnight at 37 °C. After digestion, peptides were eluted from the membrane by two washes with 50 mM ABC and one wash with 0.5 M NaCl. Peptides were acidified with formic acid to a final pH <3 and desalted using C18 extraction plates (Waters). Peptide samples were evaporated on a vacuum centrifuge to dryness and reconstituted in sample buffer (5% formic acid, 5% acetonitrile) containing indexed retention time (iRT) peptides (Biognosys) [138] and 50 fmol/ μ l non-labeled FLEX-peptide (TENLYFQGGDISR,

synthesized by Sigma Life Science, quantified via amino acid analysis of Molecular Biology Core Facilities, Dana Farber Cancer Institute, Boston). An initial test SRM analysis of peptide samples was performed to assess approximate tau abundance in each individual sample (see below). Heavy tau and endogenous samples were then mixed accordingly to achieve approximately a 1:1 ratio of light-to-heavy (L/H) tau.

Optimization of the FLEXITau SRM assay for brain tissue samples

For LC-SRM analysis of peptide mixtures, the tau SRM assay as developed in [288] was used as initial template (see also appendix Table A1). Optimization of the FLEXITau SRM assay for the analysis of post-mortem brain tissue was guided by a spectral library generated in-house through a LC-MS/MS analysis of sarkosyl fractions from brain protein extract (all tauopathies) on a tandem mass. To this end, samples were analyzed on a quadrupole Orbitrap tandem mass spectrometer (Q Exactive, Thermo Fisher Scientific) hyphenated with a micro-autosampler AS2 and a nanoflow HPLC pump (both Eksigent). Peptides were separated using an in-house packed C-18 analytical column (Magic C18 particles, 3 μ m, 200 Å, Michrom Bioresource) by a linear 120 min gradient from 95% buffer A (0.1% (v/v) formic acid in HPLC-H₂O) and 5% buffer B (0.2% (v/v) formic acid in ACN) to 35% buffer B. A full mass spectrum with resolution of 70,000 (relative to an m/z of 200) was acquired in a mass range of 300-1500 m/z (AGC target 3 x 10⁶, maximum injection time 20 ms). The 10 most intense ions were selected for fragmentation via higher-energy c-trap dissociation (HCD, resolution 17,500, AGC target 2 x 10⁵, maximum injection time 250 ms, isolation window 1.6 m/z, normalized collision energy 27%). The dynamic exclusion time was set to 20 s and unassigned/singly charged ions were not selected.

Q Exactive raw files were converted into mgf data format using ProteoWizard [244]. The spectra were centroided and filtered using ms2preproc to select the 6 most intense peaks in a 30 Th window [365]. Collected spectra were searched against a Homo Sapiens database (downloaded from uniprot.org on 11/01/2011) with ProteinPilot™ Software 4.5 Beta (Paragon Algorithm 4.5.0.0. 1575, Sciex). The following settings were applied: instrument type 'Orbi MS (1-3ppm)'; 'Urea denaturation'; 'rapid' search mode. For files from heavy tau, spectra were searched against a custom database containing wheat germ proteins and the human 2N4R tau sequence tagged with the FLEX peptide, and the sample type set to 'SILAC (Lys+8, Arg+10, Asp+5)'.

Xml files were extracted from ProteinPilot and loaded into Skyline [286] (version 2.6, MacCoss Lab Software, University of Washington) using cut off score of 0.5, to build a spectral library. The FLEXITau peptide tree was populated with transitions according to the spectral library. The transition lists were experimentally validated and optimized to select the most suitable transitions for quantification experiments, as described in 2.3 (see also [288]).

LC-SRM measurements and data analysis

Prior to mixing of heavy and light, individual samples were separately analyzed with the validated transition list and using a 30 min gradient (RT window 7 min). Absolute concentration of tau in the samples was determined using the FLEX peptide as described before [401]. Sarkosyl insoluble fractions were then mixed with heavy tau in a 1:1 ratio according to relative intensities. For final measurements, 200-400 fmol tau was used per injection.

Peptide mixtures were analyzed on a triple quadrupole mass spectrometer (5500 QTRAP, Sciex) using a micro-autosampler AS3 and a nanoflow UPLC pump (both Eksigent/Sciex), using the trap-elute chip system (cHiPLC nanoflex, Eksigent). Briefly, peptides were first loaded onto the trap-chip (200 μm x 75 μm , ChromXP C18-CL 3 μm 120 A, Nano cHiPLC Eksigent) and then separated using a 120 min gradient from 95% buffer A (0.1% (v/v) formic acid in HPLC- H_2O) and 5% buffer B (0.2% (v/v) formic acid in ACN) to 35% buffer B on the analytical column-chip (75 μm x 15 cm, ChromXP C18-CL 3 μm 120 A, Nano cHiPLC Eksigent). The retention time window was set to 5 min and total scan time to 1.2 s, which ensured a dwell time over 20 ms per transition. To avoid sample carry over, blanks were analyzed between every SRM run. To ensure no bias in acquisition, samples were run in randomized order (three technical replicates per sample).

SRM data were analyzed and validated in Skyline (version 2.6, MacCoss Lab Software, University of Washington, Seattle, WA) [286]. All peptide transitions were evaluated for variability, similarity between y-ion ratios, elution times, and interfering signals by manual analysis. Peak boundaries were manually inspected and reassigned as needed to ensure correct peak detection and accurate integration. Peptides were considered "quantifiable" if the peptide transitions had a signal-to-noise of >3 and at least three light and three heavy high-quality SRM transitions were observed. Peptides were kept for further downstream analysis if quantifiable in every patient sample. The final peptide list consisted of 17 tau peptides. To compensate for differences in mixing ratio, samples were normalized by the L/H ratio of the least modified peptides. To this end, in each sample, the L/H ratio of peak intensities of each peptide was divided by the average of the three tau peptides with highest ratio in that particular sample. Absolute abundance of tau was calculated using the FLEX peptide L/H ratio as described before [401]. Amounts of insoluble tau in each patient samples was calculated in the unit of fmol tau per mg brain wet weight (average of technical replicates).

PTM analysis using shotgun LC-MS/MS

Insoluble fractions of AD patient samples were also analyzed on a quadrupole Orbitrap tandem mass spectrometer (Q Exactive, Thermo Fisher Scientific) by a linear 120 min gradient as described above. In addition, in two independent experiments, insoluble tau fractions from three different patients were pooled and fractionated by off-gel fractionation

into 24 fractions, and analyzed on the Q Exactive using the same LC-setup as described above (section 3.3). Q Exactive raw files were converted into processed in Protein Pilot as described above (section 3.3) except for following search parameters: 'thorough' search mode, 'phosphorylation emphasis', 'acetylation emphasis', 'ID focus on biological modifications'. All MS/MS spectra of identified post-translationally modified peptides were subjected to manual verification (fractionation and final PTM data analysis was performed by Dr. Melissa Rotunno).

Analytical procedure

A computational classifier for each patient group was developed based on supervised machine learning. The input data consisted of normalized L/H peptide intensity ratios of each peptide measured by SRM, i.e. each sample was represented by a vector of 17 peptides (features). Absolute abundance was considered as an 18th feature, however results showed the performance of the classifier did not improve (see Fig. 3.5). A supervised machine learning model was constructed for each disease category using the following procedures (the workflow is summarized in Fig. 3.1): First, a binary dataset was created consisting of the case category of interest (e.g. AD) and the remaining reference category (e.g. a combination of all non-AD samples). Then, a recursive feature elimination method based on the Random Forest (RF) algorithm was used to select the feature set that provides optimal separation of the case category and reference category in the training dataset. Finally, the optimized RF classifier was evaluated using an independent testing dataset. This approach was repeated for each case category, i.e. also PSP, PiD, CBD, and ctrl.

The performance of the classifiers was assessed by accuracy, defined as the total number of correctly classified cases (TTrue Positives, TP, and TTrue Negatives, TN) relative to the total number of cases in the testing set. Sensitivity (se) of the classifier was calculated as the number of TP divided by the total number of cases with given condition, that is TP and False Negatives (FN) ($se = TP/(TP+FN)$). Specificity (sp) was determined as the proportion of TN to the number of cases without given condition, that is TN plus False Positives (FP) ($sp = TN/(TN+FP)$). The performance (the positive diagnostic likelihood ratio) of a classifier, expressed by its true positive rate (TPR, or sensitivity), and false positive rate (FPR, or 1 - specificity), was plotted in a receiver operator curve (ROC) space. The predictive power of each classifier was further assessed by calculating the area under the ROC curve (AUC; AUC: 0.9-1.0 = excellent; 0.8-0.9 = good; 0.7-0.8 = fair; 0.6-0.7 = poor; 0.5-0.6 = fail) [399].

The entire patient cohort of 129 cases was divided into a training and a test dataset with a similar number of patients in each dataset (Table 3.2). For the training set, only samples that showed typical pathological features were included in order to achieve a reliable classifier. An additional requirement was that the training dataset contained similar numbers of specimens for each category (68 cases total). For the test dataset an

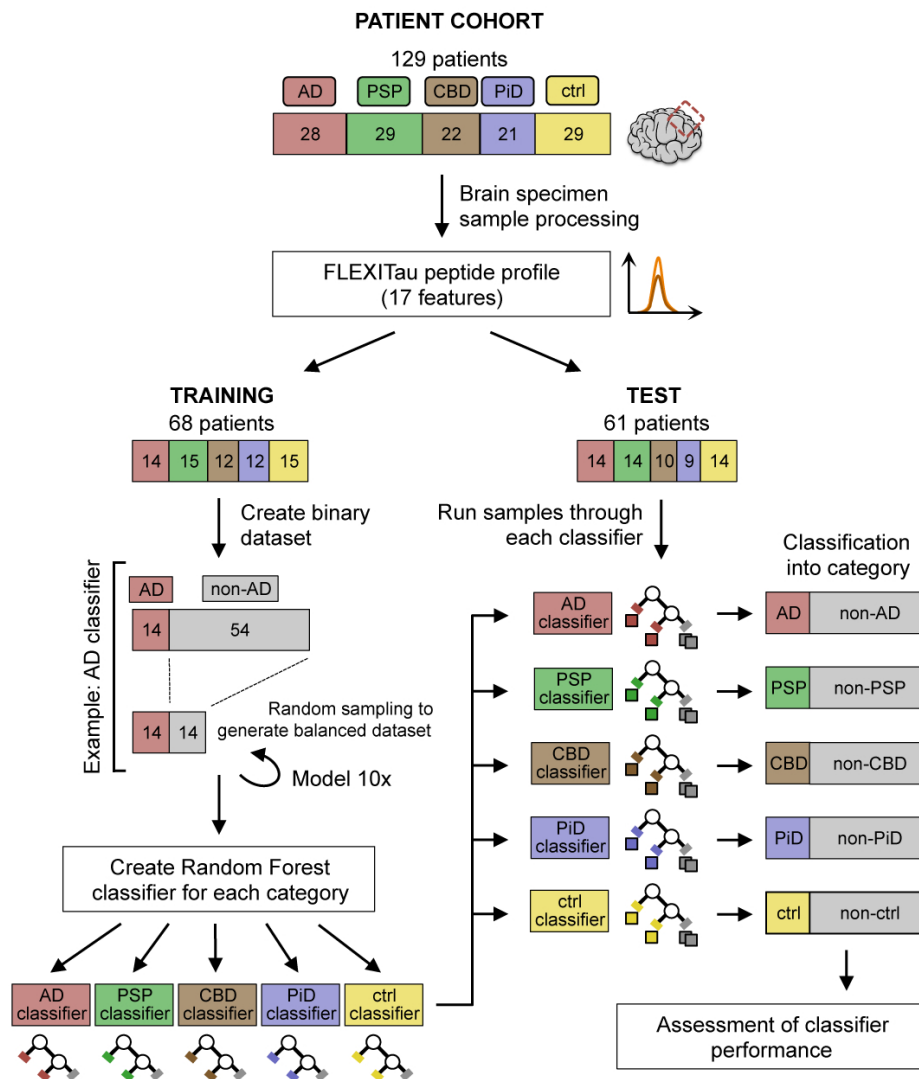


Figure 3.1: Flow diagram showing the training and test phases involved in the classifier development. After sample processing of brain specimens, the training cohort was used to construct a computational classifier to discriminate each category using RF. The modeled classifier was then applied to an independent test data set and its performance in correctly predicting the category of each sample was evaluated.

inclusive approach was taken, whereby all remaining tauopathy specimens received from the brain banks were utilized without further exclusion criteria, resulting in a heterogeneous set of samples (61 cases total): These included cases that had been diagnosed over 15 years ago when criteria for diagnoses were less advanced (5 cases). For other samples, the pathology reports described co-occurring pathologies, i.e. the patient brain showed the pathologies of two different tauopathies (5 cases). Finally there were patient brains with less confident diagnosis, i.e. that displayed less pronounced or atypical pathological features (4 cases), or reported unavailability of sections routinely evaluated as part of the diagnosis

Table 3.2: Patient demographics in training and testing set.

	AD		PSP		CBD		PiD		control		Total	
	Train	Test	Train	Test	Train	Test	Train	Test	Train	Test	Train	Test
Total number of patients	14	14	15	14	12	10	12	9	15	14	68	61
Age (years)												
Mean (SD)	79.1 (8.8)	76.4 (11.4)	73.3 (6.7)	77.5 (8.72)	70.3 (5.7)	72.3 (8.9)	67.8 (9.5)	69.4 (10.4)	70.5 (13.9)	79.9 (9.7)	72.4 (10.0)	75.7 (10.2)
Range	61-90	41-89	58-84	65-93	63-83	58-88	51-84	58-92	45-90	59-97	45-90	41-97
PMI (hours)												
Mean (SD)	12.5 (5.1)	14.3 (5.9)	11.6 (4.1)	15.3 (5.2)	10.3 (6.2)	12.5 (7.1)	17.1 (5.4)	11.9 (6.1)	15.7 (6.0)	17.4 (3.6)	13.6 (5.7)	14.6 (5.7)
Range	6.5- 20.6	4.9- 23.0	6.17- 20.5	7.0- 23.8	4.0- 21.9	2.0- 24.0	10.2- 25.5	4.0- 20.0	7.8- 30.3	10.5- 22.2	4.0- 30.3	2.0- 24.0
Sex												
(male:female)	7:7	4:10	11:4	10:4	5:7	5:5	9:3	7:2	8:7	3:21	40:28	37:24
Brain Bank												
UCSF	5	0	5	0	9	0	7	0	3	0	29	0
UCLA	6	8	8	7	0	0	0	5	9	8	23	28
McLean	3	6	2	7	2	3	5	2	3	6	15	24
MIAMI	0	0	0	0	0	1	0	2	0	0	0	3
UMB	0	0	0	0	1	6	0	0	0	0	1	6

(1 case). Given this heterogeneity, it was hypothesized that the output of the developed classifier for the test set would reflect the ambiguity of the sample set and perhaps allow the reclassification of the same cases.

A supervised classifier was computed for each of the five patient categories under study, i.e. for AD, CBD, PSP, PiD and ctrl. For the training of a classifier for a certain disease category a binary approach was used whereby the case category (for example AD) is classified against the remaining "mixed" reference category (consisting of all non-AD samples, e.g. CBD, PSP, PiD and ctrl). Given that the number of samples of each category in the training dataset is similar, the binary dataset is highly unbalanced. To remove the bias of training an unbalanced dataset, the "mixed" reference category was downsampled to create a unique balanced dataset with equal number of samples in both the case category and reference category in all subsequent model training and testing (Fig. 3.1). The training process was repeated 10 times, i.e. each time a different subset of the reference category was randomly selected in order to obtain a stable classifier.

Five widely used supervised machine learning methods were initially evaluated: RF, [76], Neural Networks (Nnet) [59], k-Nearest Neighbor (KNN) [15], Learning Vector Quantization (LVQ) [252], Linear Discriminant Analysis (LDA) [147], and Support Vector Machines (SVM) [102]. To determine performance, the average and standard deviation (SD) of accuracy and area under the ROC curve of 10 models were calculated. While the supervised classifiers performed comparably in the given data set, suggesting that the dataset does not favor a particular method, slightly better results were obtained for RF and SVM classifiers

(Fig. 3.4 and supplementary Table S1). Variance of below 5% for both accuracy and AUC indicated that both RF and SVM performed robustly with different randomly selected subsets of the dataset. The RF method holds the advantage over SVM that features associated with the discrimination of the groups can be easily extracted and was thus selected as method for the classification. Another reason for selecting the RF classifier is that the method provides an unbiased estimate of the classification error named the "Out Of Bag" (OOB) error. The development and computational implementation of the classifier using supervised machine learning was performed by Dr. Shaojun Tang.

Other statistical methods

To test whether features differed across groups, the Kruskal-Wallis test was used, which is a nonparametric multigroup comparison test, followed by Dunn's multiple comparisons test with adjusted p-value for comparison between two groups. All p-values were two-sided and $p < 0.05$ was considered significant (Fig. 3.2). FLEXITau peptide data was represented as boxplots for each category, showing the median of all samples with boxes representing 25% and 75% percentiles, and whiskers 5% and 95% percentiles. For the analysis of 4R-tau specific peptides, for each disease the average value of the three Exon 10 spanning peptides was calculated and normalized by the average value of that particular peptide in ctrl. Data is presented as average of the three peptides +/- relative error. Significance was analyzed by ANOVA, followed by the post hoc pairwise Bonferroni test with adjusted p-value for multiple comparisons. Analyses were carried out in Microsoft Excel (version 14.2.2), Prism 6.0 (GraphPad Software, La Jolla, CA) and the freely available software R (versions 3.2.1) (<http://www.r-project.org/>) [215].

3.4 Results

3.4.1 Profiling of tau peptides identifies molecular signature of tauopathies

It is well established that pathological tau carries a large number of PTMs and that in certain tauopathies, tau splice form homeostasis is perturbed [139, 292, 392, 477]. Thus it was hypothesized that the pathological tau in each tauopathy presents with a unique molecular composition (a signature), determined by its modification state and isoform distribution [355], and that this signature can be used to distinguish between tauopathies. However, identification and quantification of the different PTM states and splice forms of tau is challenging even with the most advanced analytical methods due to the complexity and molecular heterogeneity of tau. To circumvent this challenge, an alternative strategy was employed, FLEXITau, an MS-based assay that measures the abundance of the portion of tau peptides which are left unmodified, relative to heavy tau peptides from an isotope labeled tau standard that is added to the sample. Using this method, one can accurately infer the extent of modification on each endogenous tau peptide [288] (see section 3.3 for

details).

To assess the PTM and splice landscape of tau in the various tauopathies, the FLEXITau assay was used to profile the peptide landscape of tau from a total of 129 post-mortem cortical brain specimens from 5 different brain banks including the following 5 diagnostic groups: 28 AD, 29 PSP, 22 CBD, 21 PiD, and 29 non-demented controls (Table 3.1). Insoluble tau was isolated by classical sarkosyl fractionation from each specimen and processed using the FLEXITau workflow, which requires the addition of an isotope-labeled heavy tau standard, followed by SRM analysis of the L/H peptide ratio. A total of 17 tau peptides, which were quantified robustly in each patient sample across the entire cohort, were selected for further analysis (see section 3.3 for details).

First the molecular characteristics of each disease was investigated (Fig. 3.2). The FLEXITau data obtained by targeted SRM allows for the quantification of peptide modification extent. Clear quantitative differences in the modification extent could be observed for all categories (Fig. 3.2A). Tau from AD patients presented a distinct quantitative molecular signature that was unique compared to all other categories. Amongst all diseases it displayed the highest modification stoichiometry, particularly in the acidic region, the proline-rich region and the C-terminal tail. When the significance of peptide modification extent from one disease to other tauopathies was calculated, 75% of all AD peptide modification extent were found to be significant from the other categories ($p < 0.05$) (Fig. 3.2B, first panel). The two categories with the least difference from each other were PSP and ctrl samples, with only two peptides whose modification extent was significantly different from each other (Fig. 3.2B, second panel). It is important to note that these results also showed that every single peptide has a different modification extent in two or more categories. Analysis of the exon-10 spanning peptides revealed that both for CBD and PSP, these peptides are significantly enriched in the insoluble tau, whereas for PiD, they are reduced (Fig. 3.2C). This corroborates notion that CBD and PSP are so-called 4R tauopathies, where exon 10-containing 4R-tau is preferentially incorporated into tangles, whereas PiD is a 3R tauopathy, in which mostly 3R-tau accumulates.

The FLEXITau workflow also enables the absolute quantification of total tau present in the analyzed samples independent of its modification state [288]. Absolute quantification of tau in the insoluble tau samples showed that in AD, CBD, and PiD, the amount of tau was significantly higher than in ctrl (Fig. 3.2D). PSP showed insignificantly higher tau levels than control, but significantly lower levels than AD and CBD. AD contained the highest amount of tau, with the majority of AD samples containing 5-10 times higher tau levels than the samples of the other categories.

3.4.2 Mapping of PTMs in human insoluble brain-derived tau

Next possible PTMs associated with these samples were determined by creating a cumulative PTM map. Using shotgun MS, 17 AD patients were analyzed, three of which were extensively

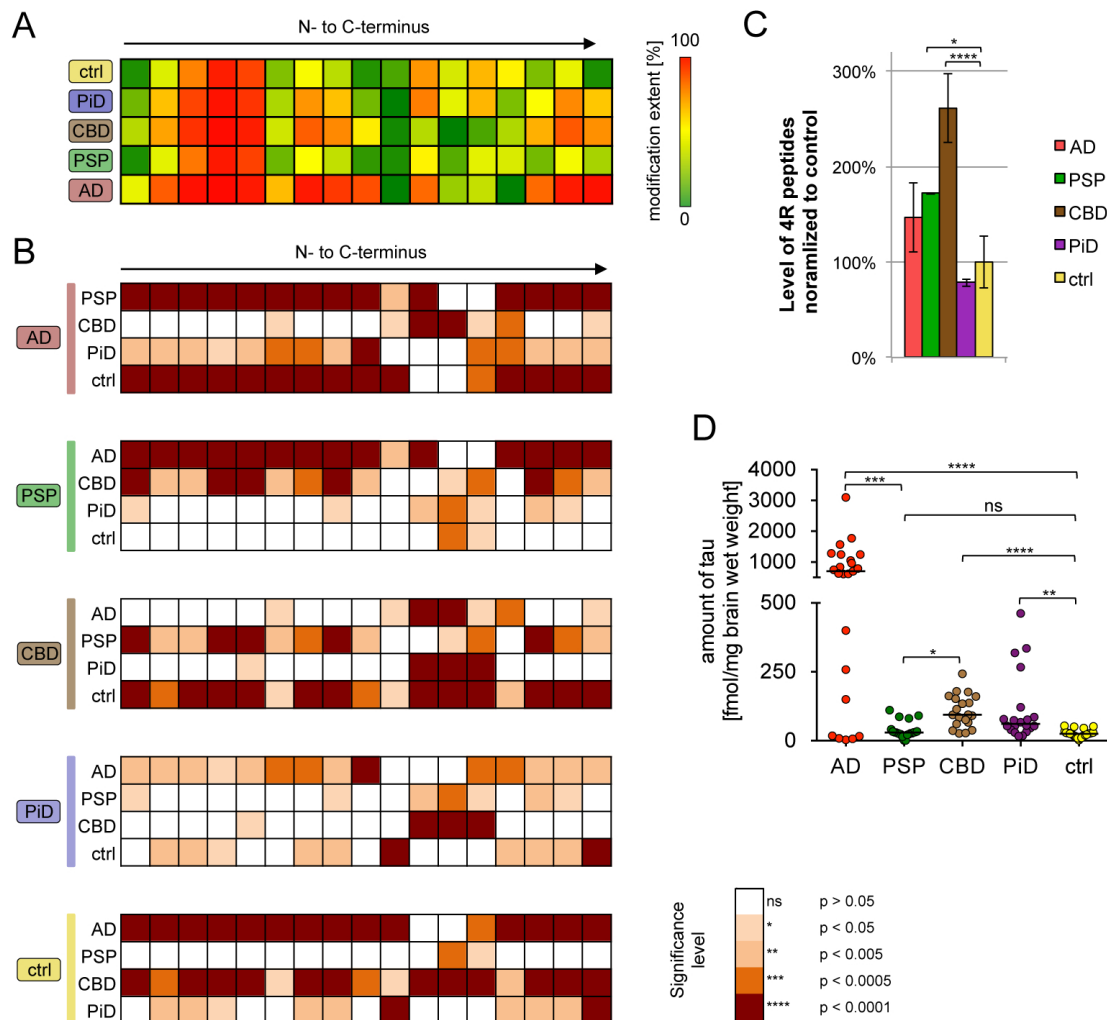


Figure 3.2: Quantitative FLEXITau analysis reveals differences in modification extents, isoform distribution and absolute amount of tau in tauopathies. Sarkosyl insoluble tau from each category was subjected to the FLEXITau workflow involving the addition of heavy isotope labeled tau to each sample and SRM analysis of light and heavy peptides. **A.** Normalized light-to-heavy ratio of signal intensities for the 17 targeted peptides was calculated for each sample. Shown is the median peptide modification extent for each category, represented in a heatmap. **B.** For each category, the peptide modification extent is compared to another category and the significance determined (Kruskal-Wallis followed by pairwise Dunn's multiple comparisons test). **C.** Mean values of 4R-tau specific peptides, relative to ctrl values +/- relative error (significance determined by ANOVA followed by post hoc pairwise Bonferroni). **D.** Absolute amounts of tau were determined using the FLEX peptide as described in [288]. Tau levels were calculated as fmol tau per mg cortical brain wet weight. Shown is average of the technical replicates for each sample (significance determined by Kruskal-Wallis followed by pairwise Dunn's multiple comparisons test).

* $p \leq 0.05$, ** $p \leq 0.01$, *** $p \leq 0.001$, **** $p \leq 0.0001$, ns = non-significant

fractionated prior to analysis. The reason for choosing AD samples for the cumulative map is twofold: 1) tau abundance in sarkosyl insoluble samples was much higher than in any of the other diseases, facilitating the identification of PTMs, and 2) according to current knowledge, so far all PTMs discovered in non-AD tauopathies have been also identified in AD. In this analysis, a total of 74 PTMs were identified with high confidence (Fig. 3.3). The PTM map included 31 phosphorylations, 10 ubiquitinations, 11 acetylations,

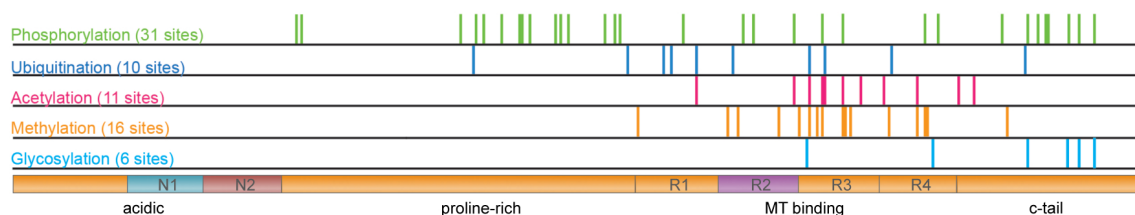


Figure 3.3: PTM map of AD insoluble tau. Cumulative PTM map derived by MS shotgun analysis from the sarkosyl insoluble fraction of 17 AD patient samples, 3 of which were extensively fractionated to increase sequence coverage. Bars represent sites occupied by respective modifications. The sequence shown is 2N4R, with the exons prone to alternative splicing marked in blue (exon 2, N1), red (exon 3, N2), and purple (exon 10, R2). Image courtesy of Dr. Melissa Rotunno.

16 methylations and 6 glycosylation sites. Apart from phosphorylation that has its highest frequency in the proline-rich region and the C-terminal tail, the other modifications cluster in the microtubule-binding region. From the 74 mapped PTMs, 46 have not yet been described before in human brain-derived tau. These include 11 novel acetylation and 6 novel ubiquitination sites.

3.4.3 Development of a computational classifier for tauopathies

Overall these analyses described above show that there are clear differences in the quantitative peptide landscape of tau that arises from different modification stoichiometries and isoform distribution of tau in these diseases, resulting in a molecular signature for each disease. The next goal was to test whether these quantitative peptide features could be used to accurately classify the disease categories. To this end the FLEXITau data was used to construct a binary classifier for each disease category using a supervised machine learning strategy (see workflow in Fig. 3.1). The patient cohort was divided into an independent training and test set, consisting of similar numbers of patients in each patient group (Table 3.2). The process of supervised machine learning consisted of two phases, the first phase was the training of the classifiers using the training dataset and the second is the testing of the classifiers on the independent test set.

First, the samples in the training set were used to construct a binary classifier for each chosen category that enables optimal separation of the case category (e.g. AD) from the remaining "mixed" reference category (e.g. all non-AD). In order to remove the bias of training with an unbalanced dataset, during the training process the reference category

was down-sampled to create a balanced dataset with an equal number of samples in both the case and reference category (Fig. 3.1). Different supervised machine learning methods were tested (RF, Nnet, KNN, LVQ, LDA, and SVM). The methods performed similarly for the dataset, with RF and SVM performing slightly better (Fig. 3.5 and supplementary Table S2, for details see section 3.3). The Random Forest (RF) method holds the advantage

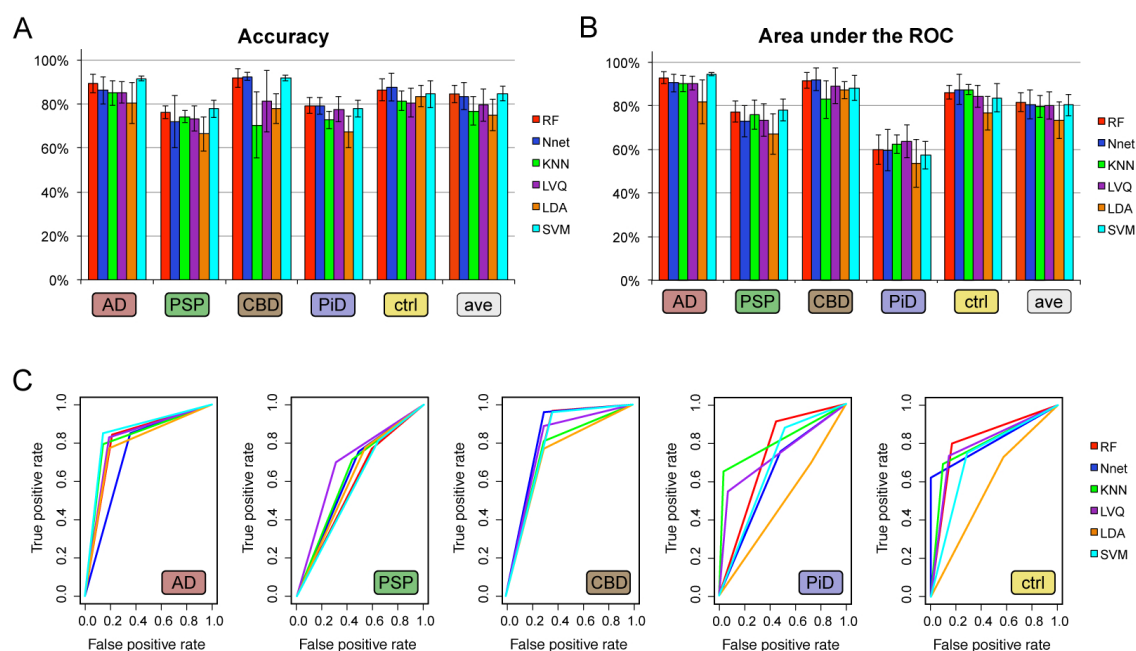


Figure 3.4: Comparison of diagnostic performance of unsupervised learning methods. Performance of RF, Nnet, KNN, LVQ, LDA, and SVM in correctly predicting each category from all others within the training set was assessed by accuracy (A.) and AUC (B.) of the ROC curve. Shown is the mean \pm SD after tenfold training with different subsets of the reference categories for each disease category, and the average performance over all categories of each method (gray). C. Classifier performance plotted in ROC space (representative curves shown). Raw values are supplied in supplementary Table S1.

over Support Vector Machine (SVM) method as features associated with the discrimination of the groups can be easily extracted and thus RF was selected for the analysis presented here. Another reason for selecting the RF classifier is that the method provides an unbiased estimate of the classification error named the "Out Of Bag" (OOB) error.

To maximize the performance of the RF classifier, the best number of features used to build the decision trees was determined. In RF classification, peptides are selected based on importance as features that can split the data into stable groups by building each bootstrap tree (using random sampling with replacement). If features are highly correlated, only a subset is needed to achieve good performance. A small number of features may improve the performance and avoid overfitting. The number of peptides features required to develop a robust classifier was tested by evaluating the performance of each classifier. The average accuracy and AUC of the ROC curve for each patient group was calculated after

ten iterations of training and testing on random subsets of the training set (Fig. 3.5). The

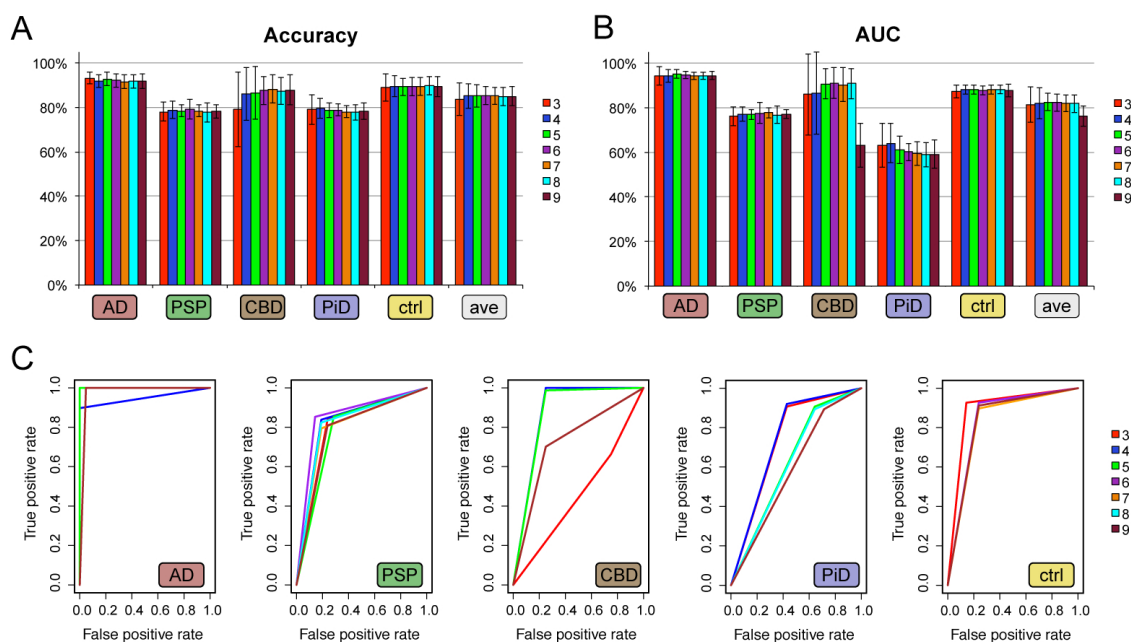


Figure 3.5: Determination of optimal number of features for the RF decision trees. Accuracy (A.) and area under the ROC curve (B.) after tenfold training and testing of RF classifier on randomly chosen test sets with a predetermined maximum number of splitter variables. Shown are the mean (\pm SD) for each condition and the average of all conditions for each classifier (gray). C. Classifier performance plotted in ROC space (representative curves shown). Raw values are supplied in supplementary Table S2.

robustness of the RF classification based on tau peptides is emphasized by minimal changes in performance upon altering the number of features (on average, less than 1% SD, see supplementary Table S2). Overall, limiting the number of features to 6 peptides minimized variance while maximizing performance for each patient group and thus was used for the remaining data analysis.

We next investigated whether the abundance of insoluble tau in each sample represents an important feature that would improve the diagnostic performance of the classifier. To this end, the absolute tau levels present in each sample were included as additional feature into the feature set. The RF classifier was then retrained and tested, either including or excluding this 18th feature. On average, the inclusion of the abundance feature led to a decrease in both accuracy and AUC (reduction by 0.5% and 6.3%) (Fig. 3.6). The decrease in performance was highest for the PSP category (reduction of AUC by 22.2%) and PiD (reduction of AUC by 9.8%). When included, the abundance feature was chosen as feature by all classifiers with the exception of CBD (supplementary Table S3). As no improvement in performance was observed, for the final model the abundance feature was not included in the feature set.

This final optimized RF classifier was then trained using the entire training set of 68 patients

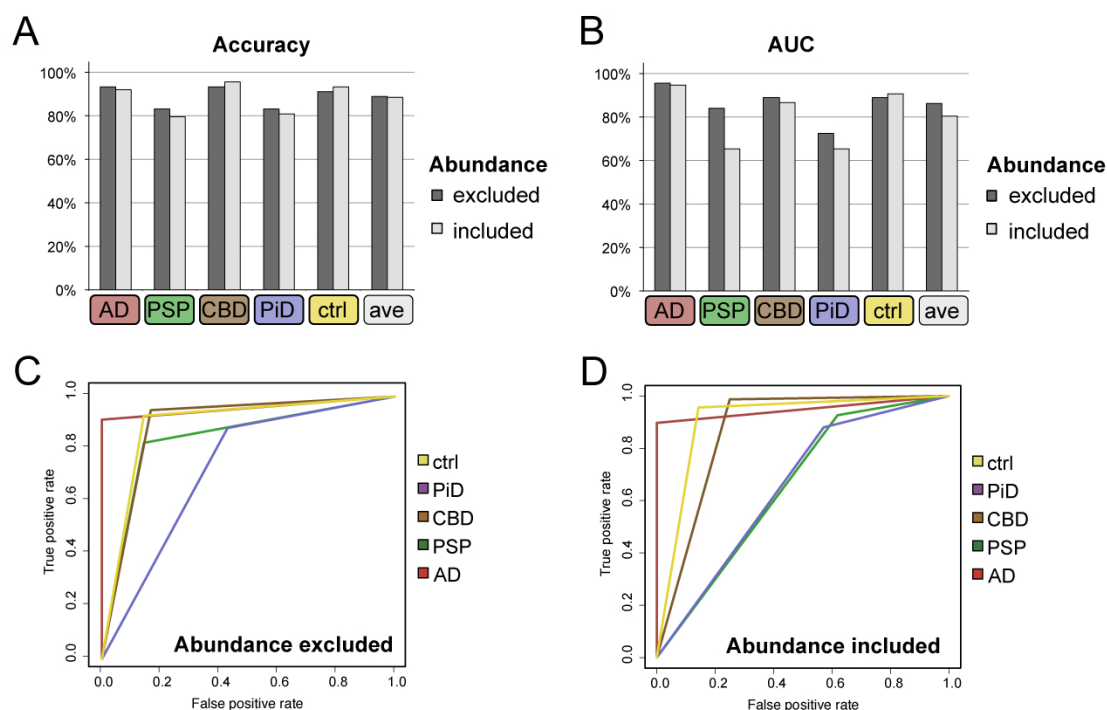


Figure 3.6: Evaluation of absolute abundance of tau as diagnostic feature. Performance of the RF classifier was evaluated upon inclusion of abundance of as additional feature into the feature set and accuracy (A.) and AUC (B.) were determined. Performance of each classifier in ROC space upon exclusion (C.) and inclusion (D.) of the abundance feature. Raw values are supplied in supplementary Table S3.

samples. The best OOB error rate achieved for this training data set was 1.5% for AD, while the average OOB error rate was 8.3% (Fig. 3.7A; out of bag error - an estimate of the error rate for RF supervised learning). This trained classifier was then applied to the independent test cohort of 61 patient samples (see Table 3.2). In contrast to the training set, which contained validated cases with typical pathological features, the test set contained patient specimens received from the brain banks without any exclusion criteria. As such, it

Table 3.3: Initial diagnostic performance of optimized classifier on independent testing sets. Table showing diagnostic performance of Random Forest trained with on the entire training set and applied to the entire independent test set, including asymptomatic and atypical samples.

Category	Performance (%)	OOB	Accuracy	Sensitivity	Specificity	AUC
AD	Train	1.5	86.9	78.6	89.4	84.0
PSP	Train	16.6	70.5	50.0	76.6	63.3
CBD	Train	9.6	93.4	80.0	96.1	88.0
PiD	Train	5.2	86.9	55.6	92.3	73.9
ctrl	Train	8.7	82.0	85.7	80.9	83.3
ave	Train	8.3	83.9	70.0	87.0	78.5

included samples with less confident diagnoses, diagnoses dating back more than a decade, and brains displaying mixed dementia (see section 3.3 for details). These samples were included at this stage of testing to determine if the classifier could detect heterogeneity at the molecular level or perhaps determine a conclusive diagnosis. A summary of the initial classification results is presented in Fig. 3.7 and Table 3.3.

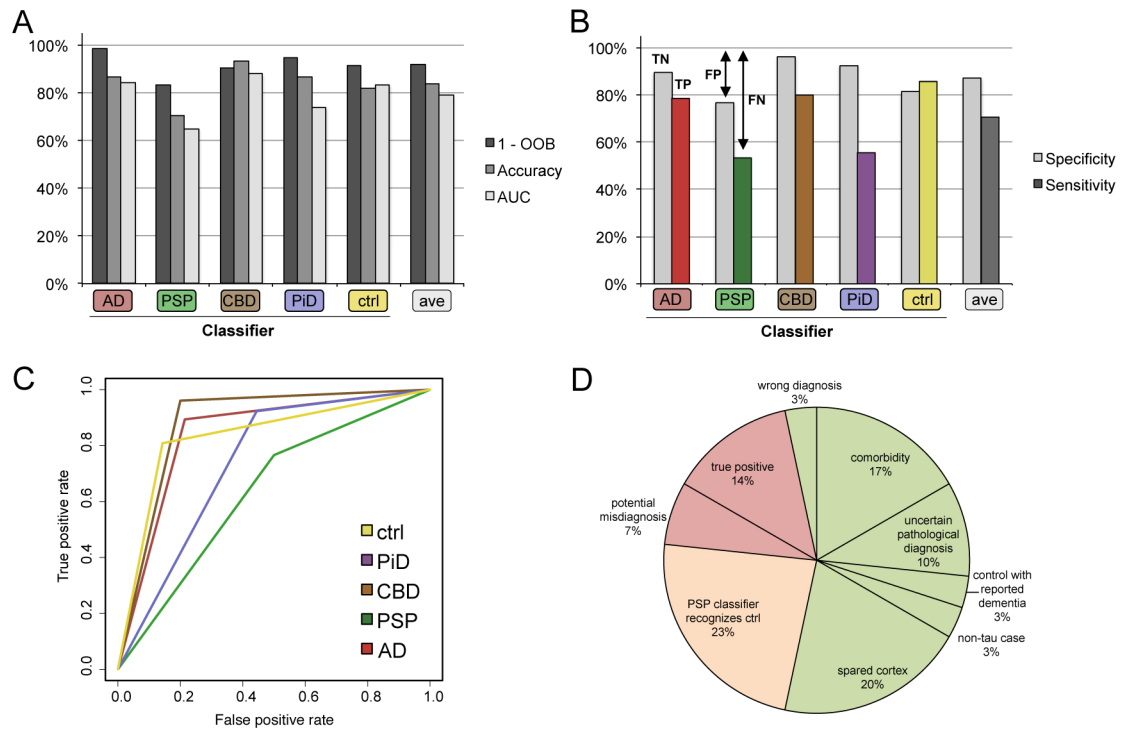


Figure 3.7: Performance of RF classifiers on the test set and identification of misclassified samples. A classifier based on the random forest method was trained for each disease group using the entire training set and its performance assessed on the entire independent test set. **A.** OOB accuracy, accuracy and AUC. **B.** Specificity and sensitivity. **C.** Performance in ROC space. **D.** Summary of all re-classified samples. Unexplained cases, red; explained cases, green; ctrl cases that were assigned to PSP, orange.

3.4.4 Detection of co-pathologies and misdiagnoses

Overall, 16.1% of the samples (31 cases total) were assigned to a category other than that of their primary diagnosis (FP) and/or were not assigned to the category of their primary diagnosis (FN) (supplementary Table S4 and S5). 15 of these cases were not assigned to the category of their primary diagnosis but to another one (FP and FN). In 13 cases, the primary diagnosis was confirmed but the sample was also assigned to another category (FP only) (i.e. samples were selected by two classifiers). 3 samples were not selected by any of the classifiers (FN only). To determine if these FP and/or FN assignments had underlying pathologies that were not explained by the primary diagnosis, the outcome

from the classifiers was cross-referenced with pathology reports and clinical information, if available and followed up with the neuropathologists at each brain bank. Remarkably, for more than half of these specimens (17 cases) the classification by the model could be explained by underlying pathological characteristics or other reasons (see supplementary Table S4 and Fig. 3.7D, green). We categorized these samples into three groups, which are summarized below. 1) Co-occurring pathology (5 cases): Several samples were assigned as AD by the AD classifier although their primary diagnoses were PSP (1 case) or PiD (4 cases); for all 5 cases the pathology reports described evidence of overlapping AD pathology (4 cases) or family history of AD (1 case). This result corroborates the accuracy of the diagnosis by the AD classifier as notably for the other 101 non-AD cases no evidence of AD was described in the pathology reports. Remarkably the 4 PiD cases were also recognized by the PiD classifier, and the pathology reports also describe typical PiD features (Fig. 3.8A and 3.8B). 2) Asymptomatic or atypical pathology (this group comprises several

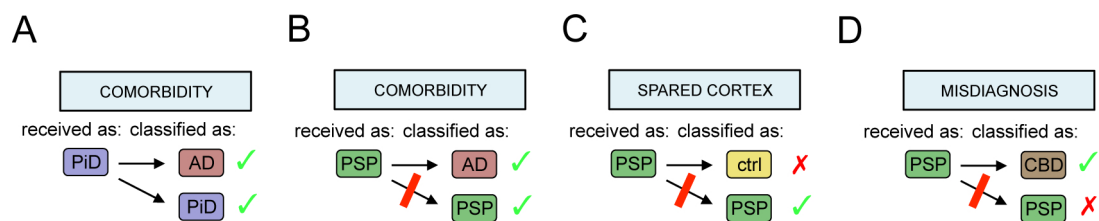


Figure 3.8: Schematic for the re-categorization of mis-assigned cases **A.** Comorbidity: 3 PiD cases were classified as PiD and as AD by the RF classifiers. Pathology reports show that all three cases had AD co-pathology that was insufficient according to CERAD criteria (Cases 2, 3 and 4 in supplementary Table S4). **B.** Comorbidity: 1 PSP case that was not recognized by the PSP classifier was instead classified as AD by the AD classifier. Pathology report lists early AD as secondary diagnosis (Case 1 in supplementary Table S4). **C.** Spared cortex: Several PSP cases provide evidence of cortical area being spared by tau pathology (e.g. Case 12 in supplementary Table S4). **D.** Misdiagnosis: One case diagnosed as PSP with unusual severe pathology was classified as CBD, which was confirmed after re-evaluation by the pathologist using current immunohistochemistry techniques (Case 17 in supplementary Table S4).

Green tickmark, diagnosis confirmed; red cross, diagnosis proven wrong; red bar, sample not assigned to category.

types of samples, 11 cases total): For several samples whose primary diagnosis was not recognized by the respective classifier (5 PSP cases and 1 PiD case) "cortical sparing" was described in the reports or stated upon re-evaluation of the samples by the pathologist, i.e. missing pathological hallmarks in the brain region received for this study, thus explaining this result (Fig. 3.8C). For additional three cases that were reassigned by the classifiers to another disease group, the final pathological diagnosis was stated to be not definite or atypical (1 AD, 1 PSP, 1 PiD). One other PiD case that was assigned to ctrl instead of PiD turned out to be a tau-negative FTD case, positive for TDP-43 (FTD-TDP-43). Furthermore, a ctrl case that was not recognized as control by the ctrl classifier, reported

a recent history of dementia, suggesting that the classifier picked up tau-related changes in the brain of this individual. This shows the sensitivity of the classifier, as this was the only ctrl case with evidence of dementia in the cohort. 3) Wrong diagnosis (1 case): Finally, a PSP case that was classified as CBD by the CBD classifier was re-evaluated using current immunohistochemistry techniques and this case was re-diagnosed as CBD by the pathologist (personal communication with JC Hedreen, McLean) (Fig. 3.8D). Overall, these results corroborate the specificity and sensitivity of the classifiers enabling the detection of comorbid pathologies and the reclassification of misdiagnosed samples.

Of the remaining 45% of reclassified specimens (14 cases), half were ctrl cases that were inaccurately classified as PSP by the PSP classifier, while being correctly being classified as ctrl by the ctrl classifier (supplementary Table S5 and Fig. 3.7D, orange). These findings, in combination with the relatively high OOB error rate for the PSP test set compared to the other categories, led to the conclusion that the cause for these mis-assignments was the performance of the PSP classifier. Possible causes for this low performance are elaborated in section 3.5.

3.4.5 Performance of the computational classifier on the testing set

To accurately assess the performance of the classifiers, the trained classifier was re-applied to the test set after 1) assigning two different categories to the cases where co-occurring pathologies were described in the pathology reports (5 cases), 2) excluding the cases with asymptomatic or atypical pathology (11 cases), and 3) assigning the correct diagnosis for the misdiagnosed case (1 case) (supplementary Table S4). Diagnostic performance of the AD classifier was highest, with an accuracy of 96.0% (88.9% sensitivity and 100.0% specificity) (Fig. 3.9 and Table 3.4). Both the CBD and the ctrl classifier achieved an

Table 3.4: Final diagnostic performance of optimized classifier on independent testing sets. Table showing diagnostic performance of RF trained with on the entire training set and applied to the independent test set after excluding the cases with asymptomatic or atypical pathology (11 cases), assigning two different diseases to the cases where comorbidity was described (5 cases) and assigning the corrected diagnosis for misdiagnosed cases (1 case) (Fig. 3.7 and supplementary Table S4).

Performance (%)	OOB	Accuracy	Sensitivity	Specificity	AUC
AD	1.5	96.0	88.9	100.0	94.4
PSP	16.6	80.0	71.4	81.4	76.4
CBD	9.6	94.0	81.8	97.4	89.6
PiD	5.2	92.0	83.3	93.2	88.3
ctrl	8.7	94.0	92.3	94.6	93.5
ave	8.3	91.2	83.6	93.3	88.4

accuracy of 94.0%, with a sensitivity of 81.8% and 92.3%, and a specificity of 97.4% and 94.6%, respectively. PiD achieved an accuracy of 92.0% (sensitivity of 83.3% and specificity of 93.4%). The performance of the PSP classifier remained the lowest with 80.0% accuracy

(71.4% sensitivity and 81.4% specificity).

Finally, the selection of peptides that were used by the classifiers to distinguish the disease categories was examined. As described above, for each binary classifier that was built, a distinct subset of 6 peptides was selected out of the 17 tau peptides. Of the 17 peptides, 5 peptides were not used by any classifier (Fig. 3.9D). From the remaining 12 discriminating peptides, 4 peptides were unique to one of the classifiers, suggesting that these peptides carry important disease-specific information. Notably, 3 out of these 4 peptides were located in the acidic n-terminal region of tau, including exon 2 and 3, which can be alternatively spliced. The other 8 peptides were shared among the classifiers, indicating that these peptides harbor characteristic information that discriminate several of the disease groups from each other. The majority of these peptides is located in the repeat region of tau, a region that harbors exon 10, the third exon prone to alternative splicing.

3.5 Discussion

We exploited a well-known common pathological hallmark of tauopathies, the abnormal tau deposition, to identify and stratify this group of neurodegenerative diseases. Based on reports of disease-specific modifications and reported differences in splice form homeostasis, it was hypothesized that the molecular nature of tau may show disease specificity. The analyses using post-mortem cortical brain tissue from patients included subjects with AD, CBD, PSP, and PiD as well as non-demented control subjects. To identify this molecular signature from these diseases, a targeted FLEXITau SRM strategy was used to profile the peptide landscape of tau in a total of 129 post-mortem brain samples. These data included identification and quantification of specific tau peptides that provided a unique molecular readout of tau across the tauopathies in this study (Fig. 3.2). In addition, the associated modifications were identified, producing the most comprehensive PTM map of tau in diseased tissue. The FLEXITau data were then used to build and test a diagnostic classifier for each disease group. A supervised RF machine learning method was trained on a well-characterized group of patients and subsequently tested on a highly heterogeneous, independent test set.

Cases identified by more than one classifier and those that did not match the primary diagnosis in the pathology reports were evaluated by referencing pathology reports and clinical data, if available, and by personal correspondence with neuropathologists at each brain bank. This analysis showed that the majority of these mis-assigned samples fell into three categories 1) mixed pathology - pathological features of two tauopathies were noted, 2) samples with uncertain diagnosis or with spared pathology in the region of the cortex analyzed - this was common for PSP, and 3) samples that were reclassified and confirmed. To obtain an accurate assessment of the classifiers, cases presenting uncertain or asymptomatic pathologies were excluded and cases with co-occurring pathologies were assigned to two categories. The final classification achieved an accuracy of 96.0% for AD

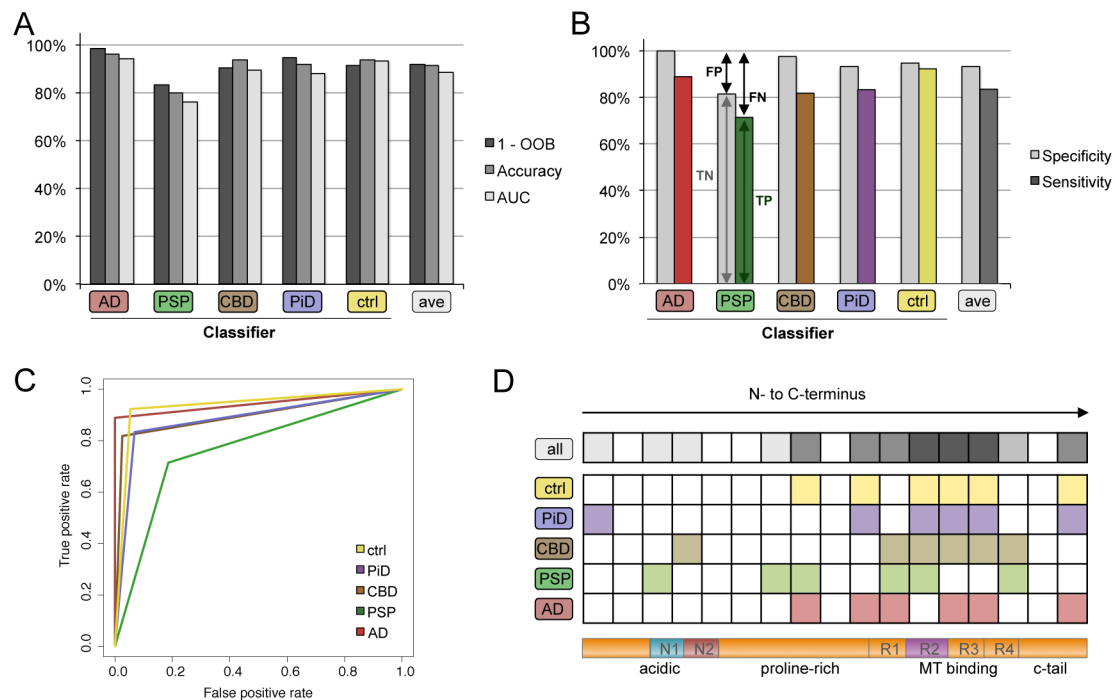


Figure 3.9: Performance of RF classifiers on the test set and identification of best discriminating peptide features. A classifier based on the RF method was trained for each category using the training set and its performance assessed on the independent test set. Explained misclassified cases were removed (Fig. 3.7D and supplementary Table S4). **A.** OOB accuracy, accuracy and AUC for each category and the average of all categories. **B.** Specificity and sensitivity for each category and the average of all categories. **C.** Performance of all classifiers in ROC space. **D.** Discriminating peptide features for each classifier (bottom), and accumulative count (top), shown in a heat map representation. Peptides are mapped to a schematic of 2N4R tau; alternatively spliced exons 2 (N1), 3 (N2) and 10 (R2) are shown in blue, red, and purple.

and 94.0% for both CBD and ctrl, while PiD had an accuracy of 92.0% and PSP 80.0% (Fig. 3.9 and Table 3.4).

These analyses show that AD patient tau possesses a distinct quantitative molecular signature that resulted in 100% specificity of the AD classifier (Fig. 3.2 and Fig. 3.9B). Interestingly the AD classifier also recognized 5 cases where the primary diagnoses were either PiD (4 cases) or PSP (1 case). The pathology reports of these samples were investigated to better understand these results. One of the PiD cases had a family history and clinical evidence of AD, while the pathology of the three remaining PiD cases indicated clear AD pathology (neuritic plaques, flame-like NFTs). The PSP case stated evidence of "early" AD. None of the remaining 101 non-AD cases documented evidence of AD pathology in addition to the primary underlying diagnosis. This indicates that the developed AD classifier is highly sensitive to AD co-morbidity and may recognize AD in its early stages, thus suggesting amending current diagnostic criteria. Importantly, all 4 PiD cases were correctly identified as TP with the PiD classifier, indicating that the performance of the

PiD classifier is not hampered by the co-existing AD. These results exemplify that the combination of individual classifiers serves as a powerful tool to detect co-pathologies.

CBD is a disorder that is clinically heterogeneous presenting with various clinical syndromes. Corticobasal syndrome (CBS), the classical clinical manifestation of CBD, is neither predictive nor specific for CBD pathology. Efforts are being made to improve CBD clinical diagnosis clinically and recently new consensus criteria were established, however these were reported as unspecific and not sensitive to early CBD [14, 24, 337]. In fact, CBS is more likely to be caused by a pathology other than CBD, e.g. PSP, AD, PiD, or is unrelated to tau when evaluated post-mortem [63, 273, 443]. At a neuropathological level, diagnosis of CBD is complicated by the heterogeneity and variability of tau pathology, as well as overlapping pathological features with other tauopathies [149, 432, 445]. In particular, CBD and PSP have recently been suggested as being part of a clinicopathological disease spectrum, as these disease groups show similar clinicopathological features, i.e. both present with neuronal, oligodendroglial, and astrocytic lesions immunoreactive for 4R tau, which may make a correct classification difficult [120, 233, 445, 464]. Considering these issues, it is noteworthy that in this analysis the only 2 FP cases recognized by the CBD classifier in the test set were 2 PSP cases, consistent with the suggested molecular overlap of these two diseases. No other non-CBD patient (out of 51 total) was misclassified as CBD, resulting in excellent specificity (97.4%). These results highlight the power of using the tau peptide signature to accurately differentiate heterogeneous, overlapping disease phenotypes.

The classic form of PSP is Richardson's syndrome, also known as Steele-Richardson-Olszewski syndrome; however, similar to CBD, several clinical variants fall under pathologically defined PSP. Defining a classifier for this disease is challenging for multiple reasons: First of all, studies of PSP have reported relative sparing of cerebral cortex in typical PSP cases, both in terms of atrophy and tau pathology [431]. Furthermore, each variant of PSP has variations in the type of tau lesion, the load of tau and the distribution of tau pathology [72, 206, 351, 431, 440, 464]. For example, the "brain-stem predominant" atypical PSP presents with significantly lower pathological tau burden in cortical regions, especially temporal and parietal lobes [124, 229, 445, 460]. In contrast, the "cortical predominant" atypical PSP (which often present with clinical presentations of CBS) displays greater cortical tau pathology compared to typical PSP [431]. The variability in tau burden might not only explain difficulties in developing a PSP classifier based on cortical tissue, but may also explain why the addition of tau abundance into the feature set failed to improve the performance of the classifier. Given these issues, it was surprising that the PSP classifier achieved an accuracy as high as 80%. To confirm that the underlying performance was affected by the tau load, the severity of tau pathology was investigated using the pathology reports and follow-up silver staining and immunohistochemistry analyses of tissue in the parietal cortex used in this study (personal communication with neuropathologists JC Hedreen, McLean and WW Seeley, UCSF). The majority of misclassified PSP tissue samples showed evidence of the cortex as being spared of tau pathology, suggesting that the

tau analyzed in the assay was closer to normal tau than pathological tau. In conclusion, the classifier was trained and applied on a heterogeneous set of samples including those with "normal" tau in this region. Given this issue, it is plausible that the PSP classifier also recognizes ctrl cases as PSP. A focused FLEXITau study of PSP variants would be extremely informative and important to understanding the disease. This study would investigate the different regions of the brain in different variants of PSP patient tissue in statistically relevant numbers to map the regions of the brain with respect to tau pathology and molecular signature.

Interestingly, of all classifiers, the ctrl classification clearly achieved the highest sensitivity of 92.3%. This reflects the ability of the ctrl classifier to confidently predict true positive ctrl cases. The excellent sensitivity of the ctrl classifier provides evidence that tau found in ctrl patient tissue has unique molecular properties that distinguishes it from pathological tau. The characterization of the distinct molecular entities (i.e. particular modifications) responsible for the discrimination of controls from diseased cases may yield valuable insights for developing tau-directed therapeutic strategies against tauopathies, such as immunotherapy approaches [344, 479].

Several bioinformatics models were explored for the construction of a classifier to distinguish each disease class. All tested algorithms obtained accuracies of 75 - 85% in separating the diseases (Fig. 3.4 and supplementary Table S1). The RF tree model was selected not only because it was superior in performance but also because it is intuitive to interpret. In RF, the features used in the classifier are easily attainable, compared to classifiers built on neural networks and support vector machines that require deconvolution steps for identification of relevant features. In the present study, the best number of features to construct each decision tree was 6 peptides (Fig. 3.5 and supplementary Table S2). It is important to note that the majority of discriminatory peptides are shared amongst the classifiers, indicating that the assay is able to measure a distinct quantitative pattern of each peptide, rather than assessing binary states (on/off). This allows for three possible scenarios of the modification landscape on each peptide in tauopathies 1) the same modification(s) is/are present in each disease, but at different stoichiometries, 2) the same modifications are present with similar stoichiometries, but additional unique modifications exist, and 3) different modifications are present in each disease with specific stoichiometries.

In sum these results demonstrate that tauopathies with distinct histopathologies carry different pathological tau species with unique molecular signatures that can be measured by the FLEXITau assay. A particular combination of the peptide features can be used to distinguish between these diseases. One can speculate that the developed classifiers recognize a mix of PTMs and isoform distribution characteristic for each condition. Although it is plausible that these differences emerge from modifications unique for each disease, it cannot be excluded that they underlie common modifications present in all tauopathies that exhibit distinct stoichiometry, strongly undermining the need for quantitative analyses of tau, as exemplified here by the use of FLEXITau. Further studies are warranted to identify the

tauopathy-specific PTMs that are responsible for the differentiation between the diseases.

Acknowledgments

The author is grateful for the contribution of the following people for this particular chapter: Dr. Shaojun Tang for the development of the classifier and writing of the R code for the computational analysis; Dr. Melissa Rotunno for the mapping of tau PTMs, in particular for the off-gel fractionation, and for PTM data analysis, and for kindly providing Figure 3.3 and allowing me to use it in my thesis, and to Dr. Jan Muntel for his help in critiquing the data and MS methodology. The author is also thankful to Dr. John C Hedreen (Harvard McLean), Dr. William W Seeley (UCSF), Dr. Lea Grinberg (UCSF), and Dr. Deborah Mash (Miami) for pathological evaluation of human brain specimens, and for their advice and guidance in developing the study from the pathology perspective. All the above mentioned people contributed to discussions and the direction of this project.

3.6 Supplementary Tables

The following pages contain supplementary Tables [S1](#) to [S5](#).

Table S1: Diagnostic performance of several supervised machine-learning methods. Table showing diagnostic performance of RF, Nnet, KNN, LVQ, LDA, and SVM in correctly predicting each category from all others was assessed by accuracy (ac) and area under the curve (AUC) of the ROC curve. Mean value and SD of ten models (trained with different subsets of the reference category) are listed for each disease category.

Classifier		RF		Nnet		KNN		LVQ		LDA		SVM		average	
Performance		ac (%)	AUC (%)	ac (%)	AUC (%)	ac (%)	AUC (%)	ac (%)	AUC (%)	ac (%)	AUC (%)	ac (%)	AUC (%)	ac (%)	AUC (%)
AD	mean	89.2	93.0	86.2	90.5	85.1	90.2	85.2	90.3	80.4	81.8	91.7	94.5	86.3	90.1
	SD	4.3	2.8	6.2	4.1	5.7	3.7	4.9	3.2	9.4	10.0	1.1	0.7	3.9	4.4
PSP	mean	76.2	77.3	72.0	73.0	74.3	75.9	73.4	73.5	66.3	67.1	77.8	78.2	73.3	74.2
	SD	2.8	4.8	12.0	7.3	2.9	6.7	5.8	7.5	7.7	9.4	3.9	5.1	4.0	4.0
CBD	mean	91.8	91.7	92.5	92.2	70.4	82.9	81.3	89.2	77.9	87.2	91.8	88.2	84.3	88.6
	SD	4.3	3.7	1.7	5.2	14.9	8.6	14.0	8.1	6.9	4.0	1.3	5.8	9.2	3.4
PiD	mean	79.3	59.8	79.1	59.7	72.8	62.4	77.5	63.7	67.3	53.6	78.0	57.3	75.7	59.4
	SD	3.6	6.7	3.9	9.5	4.0	4.3	5.8	7.5	7.4	11.0	3.9	6.4	4.7	3.6
ctrl	mean	86.5	86.2	87.8	87.5	81.5	87.5	80.5	84.3	83.6	76.7	84.6	83.7	84.1	84.3
	SD	5.1	3.1	6.4	6.8	4.4	2.4	6.5	5.1	4.8	7.7	6.3	6.4	2.8	4.0
average	mean	84.6	81.6	83.5	80.6	76.8	79.8	79.6	80.2	75.1	73.3	84.7	80.4	80.7	79.3
	SD	4.0	4.2	6.0	6.6	6.4	5.1	7.4	6.3	7.2	8.4	3.3	4.9	4.2	3.0

Table S2: Optimization of number of split features in RF classification. Table showing diagnostic performance of RF trained with distinct number of split variables for the decision trees. Mean and SD of ten models (trained with different undersampled subsets of the reference category) are shown for each disease category.

Number of splitter variables		3		4		5		6		7		8		9		average	
Performance		ac (%)	AUC (%)	ac (%)	AUC (%)	ac (%)	AUC (%)	ac (%)	AUC (%)	ac (%)	AUC (%)	ac (%)	AUC (%)	ac (%)	AUC (%)	ac (%)	AUC (%)
AD	mean	93.3	94.4	91.8	94.3	92.8	95.3	92.1	94.7	91.6	94.3	91.8	94.5	91.8	94.5	92.2	94.6
	SD	2.6	4.2	2.8	2.8	3.1	2.0	3.0	1.6	3.1	1.7	3.1	1.6	3.2	1.7	0.6	0.4
PSP	mean	78.1	76.1	78.9	77.3	78.4	77.0	79.2	77.7	78.5	77.7	77.8	76.9	78.2	77.2	78.4	77.1
	SD	4.2	4.2	3.9	3.3	2.7	2.3	4.4	4.8	2.7	2.3	4.3	4.1	3.0	2.0	0.5	0.6
CBD	mean	79.1	86.0	86.1	86.6	86.6	90.7	87.6	91.1	88.3	90.3	87.5	90.9	87.9	63.1	86.2	89.3
	SD	16.8	18.2	11.9	18.5	11.9	6.8	6.3	6.9	6.5	7.5	6.1	6.9	6.7	10.0	3.2	2.3
PiD	mean	79.0	63.1	79.6	64.0	78.7	61.2	78.9	60.2	78.1	59.4	77.8	58.9	78.2	59.2	78.6	61.1
	SD	6.6	10.0	4.5	8.9	3.3	6.3	2.7	3.9	2.8	5.3	3.5	5.4	3.8	6.3	0.6	2.1
ctrl	mean	89.0	87.2	89.6	88.1	89.3	88.0	89.3	87.9	89.4	88.1	89.8	88.4	89.4	87.8	89.4	87.9
	SD	6.2	2.9	4.7	2.0	3.9	2.1	4.1	2.0	3.9	2.1	4.0	2.0	4.6	2.8	0.2	0.4
ave	mean	83.7	81.4	85.2	82.1	85.2	82.5	85.4	82.3	85.2	82.0	84.9	81.9	85.1	76.3	84.9	82.0
	SD	7.3	7.9	5.6	7.1	5.0	3.9	4.1	3.9	3.8	3.8	4.2	4.0	4.3	4.6	0.6	0.4

Table S3: Evaluation of absolute abundance of tau as diagnostic feature. Table showing diagnostic performance when absolute abundance of tau in each sample is included, or excluded as 18th feature. The six split features chosen by the RF classifier in each category are shown in the order of descending importance.

		Performance		Chosen features (descending importance)					
		ac (%)	AUC (%)	1	2	3	4	5	6
AD	excluded	93.3	95.6	17	14	8	3	10	9
	included	92.1	94.9	14	18	17	13	8	10
PSP	excluded	83.1	84.0	15	12	8	13	11	3
	included	79.8	65.4	18	15	12	13	7	11
CBD	excluded	93.3	89.1	5	13	12			
	included	95.5	86.9	12	5	11	9	13	7
PiD	excluded	83.1	72.6	13	12	9	17	14	5
	included	80.9	65.4	13	17	18	9	12	14
ctrl	excluded	91.0	89.2	17	14	13	8	10	2
	included	93.3	90.7	17	14	10	13	18	7
ave	excluded	94.4	86.1						
	included	93.5	80.6						

Table S4: FN and/or FP assignments in the test set that were explained by underlying pathological characteristics. For the final testing, samples with confirmed co-occurring pathologies were re-assigned to both categories. Misdiagnosed samples were re-assigned to the correct category. Samples with asymptomatic or atypical pathologies were excluded from the final testing. TDP-43, TAR DNA-binding protein 43; ICH, immunohistochemistry

Case #	Category	Brain bank	FN	FP	FP in category:	Details from pathology reports and clinical information	Explanation	Hypothesized diagnosis	Diagnosis for final testing
1	PSP	Harvard	yes	yes	AD	early AD as secondary pathological diagnosis	co-occurring pathology	PSP+AD	re-assign to both
2	PiD	UCLA	no	yes	AD	AD pathological changes	co-occurring pathology	AD+PiD	re-assign to both
3	PiD	UCLA	no	yes	AD	AD pathological changes	co-occurring pathology	AD+PiD	re-assign to both
4	PiD	UCLA	no	yes	AD	AD pathological changes	co-occurring pathology	AD+PiD	re-assign to both
5	PiD	Miami	no	yes	AD	cause of death endstage AD and family history	co-occurring pathology	PiD+AD	re-assign to both
6	AD	UCLA	yes	yes	PSP	"probable" AD, minimal to mild NFT pathology	uncertain pathological diagnosis	PSP	exclude
7	PSP	UCLA	no	yes	ctrl	atypical	uncertain pathological diagnosis	PSP	exclude
8	PiD	UCLA	yes	yes	PSP, ctrl	no Picks bodies or any other pathological evidence for PiD	uncertain pathological diagnosis	non-tau FTD	exclude
9	ctrl	UCLA	yes	no	-	recent history of dementia	control with reported dementia	tauopathy	exclude
10	PiD	Miami	yes	yes	ctrl	TDP-43 positive	non-tau case	FTD-TDP (TDP-43)	exclude
11	PSP	UCLA	yes	yes	ctrl	no pathology in parietal cortex	spared cortex	PSP	exclude
12	PSP	Harvard	yes	yes	PiD, ctrl	no NFTs in BA39	spared cortex	PSP	exclude
13	PSP	Harvard	yes	no	-	no NFTs in BA39	spared cortex	PSP	exclude
14	PSP	Harvard	yes	yes	ctrl	no NFTs in BA39	spared cortex	PSP	exclude
15	PSP	UCLA	no	yes	ctrl	spared cortex	spared cortex	PSP	exclude
16	PiD	Harvard	yes	yes	PSP	rare to sparse Picks bodies, family history indicates	spared cortex	PiD	exclude
17	PSP	Harvard	yes	yes	CBD	unusually severe. Reevaluation by IHC	wrong diagnosis	CBD	re-assign to CBD

Table S5: Misclassified samples in final testing (FN and/or FP). Probable cause of misclassification is given.

Case #	Category	Brain bank	FN	FP	FP in category:	Details from pathology reports and clinical information	Explanation	Hypothesized diagnosis
1	ctrl	Harvard	yes	yes	PSP	-	unexplained	ctrl
2	ctrl	Harvard	no	yes	PSP	-	ctrl TP in ctrl classifier	ctrl
3	ctrl	Harvard	no	yes	PSP	-	ctrl TP in ctrl classifier	ctrl
4	ctrl	UCLA	no	yes	PSP	-	ctrl TP in ctrl classifier	ctrl
5	ctrl	UCLA	no	yes	PSP	-	ctrl TP in ctrl classifier	ctrl
6	ctrl	UCLA	no	yes	PSP	-	ctrl TP in ctrl classifier	ctrl
7	ctrl	UCLA	no	yes	PSP	-	ctrl TP in ctrl classifier	ctrl
8	PSP	UCLA	yes	yes	CBD	-	potential misdiagnosis	PSP
9	CBD	Maryland	yes	yes	PSP, ctrl	-	potential misdiagnosis	CBD
10	AD	UCLA	yes	yes	ctrl	"definite AD"	unexplained	AD
11	AD	UCLA	yes	yes	PiD	"definite AD"	unexplained	AD
12	PiD	Harvard	yes	no	no FP	many Picks bodies	unexplained	PiD
13	CBD	Maryland	yes	yes	PiD	-	unexplained	CBD
14	ctrl	Harvard	no	yes	PiD	-	unexplained	ctrl

4 Discussion

Tau is a protein abundant in neuronal axons where it localizes to and stabilizes microtubules (MTs). It has received increased attention in the last years due to its link to a group of neurodegenerative diseases called tauopathies, with the most prevalent being Alzheimer's Disease (AD). A common hallmark in the pathogenesis of these conditions is the aggregation of excessively phosphorylated and otherwise modified tau protein into filamentous and/or fibrillar structures inside neuronal and glial cells in the brain.

The diversity and number of tau post-translational modifications (PTMs) is large; more than a dozen different types of modifications have been described. Over 70 sites have been identified for phosphorylation alone, and more than half of these are implicated in disease (see also section 1.3.4). Although the advance in current technologies, in particular mass-spectrometry (MS)-based strategies, enabled the mapping of many tau PTMs, it is not known which sites are relevant to disease, as information pertaining to function cannot be inferred by these qualitative analyses. Furthermore, not all PTMs are detectable using current workflows.

To overcome these limitations a quantitative method was developed that can accurately quantify the tau PTM landscape and even point to modifications that are not detected using common workflows. As proof of principle, this method was used to measure the stoichiometry of highly phosphorylated tau expressed in a cellular model system, as well as of insoluble tau from AD patient brain (Chapter 2). Its power was then further illustrated by application to the study of tau PTMs in several other tauopathies, where specific PTM features were utilized to develop a diagnostic tool to differentiate these diseases (Chapter 3). Below the results and implications of these two studies are discussed.

4.1 Development of FLEXITau and proof of principle

The goal of the first study was to design a method that enables a quantitative, unbiased modification analysis of tau. Based on the MS-based FLEXIQuant strategy [401], the FLEXITau assay was designed which, rather than aiming for identification of specific PTMs, measures unmodified peptide species of the endogenous sample relative to a heavy peptide from an isotope-labeled tau standard. The key advantage herein is that a limitless number of modification sites can be studied, without requiring prior information about the number and types of modification present. To maximize reproducibility and sensitivity, the selected reaction monitoring (SRM) acquisition method was implemented, resulting in a

highly sensitive, robust assay that can measure tau peptides down to attomolar quantities (section 2.4.2, Fig. 2.3).

Quantitative PTM profiling of "hyperphosphorylated" tau

As a proof of principle experiment, the FLEXITau assay was employed to analyze human tau expressed in Sf9 insect cells, a cellular expression system that generates tau in a distinct and highly phosphorylated state [419]. Incubation of Sf9 cells with phosphatase inhibitors prior to cell harvesting results in an even higher state of phosphorylation. These tau species are herein termed P-tau and PP-tau, respectively. Using the FLEXITau approach, the precise phosphorylation state of Sf9 P-tau and PP-tau was assessed. In combination with traditional data-dependent acquisition (DDA) analyses, over 20 phosphorylation sites were mapped and the corresponding stoichiometries calculated (section 2.4.6, Fig. 2.7). For tau peptides that harbor multiple phosphorylations, as is the case for the densely phosphorylated proline-rich region, a consecutive approach was taken to extract site occupancies for each site. Altogether, this data showed that most of the phosphorylation sites present with low stoichiometries. Furthermore, the completeness of this data enabled the measurement of average moles of phosphates per moles of tau by calculating the polynomial probability distribution of how many sites are phosphorylated at a given time. These results showed that on average, each molecule of P-tau carries 7 phosphates, whereas PP-tau carries 8 (section 2.4.7, Fig. 2.8).

Overall, the Sf9 P-tau and PP-tau species showed little difference in extent of phosphorylation, as well as number of sites per molecule. This is in contrast to previous studies, which reported that P-tau and PP-tau carry an average of 12 and 20 phosphates, respectively, using MALDI-TOF MS [419]. The discrepancy to the results presented here may be explained by the limited accuracy of low-resolution MALDI-TOF analyses, and by the lack of a labeled standard for the different phospho-protein species [342]. The FLEXITau assay, in contrast, provides accurate quantification due to the use of an internal standard for each peptide. On the other hand, it has to be kept in mind that the FLEXITau assay covers 75% of the amino acid sequence of tau - hence the FLEXITau calculation may underestimate the total number of phosphates present on tau, as one cannot exclude the possibility of additional phosphorylated residues in the undetected sequence. Additionally, a multimodal distribution of tau with differing numbers of tau modifications may exist. To characterize this, information for site-specific dependencies (e.g. phosphorylation on site X only occurs when site Y is phosphorylated) should be included in the probability analysis. Combinatorial PTM patterns can be deduced using complementary top-down MS [191, 403].

Using FLEXITau to measure the PTM landscape of human AD-tau

The FLEXITau assay was then used to study the extent of modification on insoluble tau derived from post-mortem AD brain tissue (AD-tau). Many PTMs have been described for tau aggregates from AD brain, and the existing literature was compiled to map PTMs to the quantitative FLEXITau data. This enabled a comparison of the AD-tau PTM landscape to that of Sf9-tau in a qualitative and quantitative manner (section 2.4.8, Fig. 2.9). These results show that FLEXITau is well suited not only for the analysis of purified tau from *in vitro* systems, but also for the analysis of complex biological samples, and the precise comparison of two tau species. As such it represents a powerful tool to investigate tau PTMs in a wide range of biological settings. Notably, the sensitivity of the assay, paired with the targeted (i.e. non-stochastic) measurement of tau peptides, allows for the analysis of samples in which tau is less abundant, avoiding the need of enrichment. Importantly, in order to maintain maximum sequence coverage, it is recommended to inject more than 2 femtomol of tau per MS run (section 2.4.2, Fig. 2.3).

Phosphorylated tau from Sf9-cells has been described as being "AD-like" due to 1) the generally high number of phosphorylation sites that were identified and 2) a pattern of phosphorylation similar to AD-tau, visualized by so-called AD-diagnostic antibodies, such as AT8, AT100, AT180, 12E8 and PHF1 (see also section 1.3.4, 1.6) [54, 419]. As such, it has been used as a model system for pathological tau, for instance to investigate the relationship of tau hyperphosphorylation and aggregation [419, 489]. These studies concluded that even high states of phosphorylation do not lead to aggregation. The FLEXITau analysis confirmed that Sf9-tau is highly phosphorylated at specific sites, in particular the proline-rich region, including sites recognized by the commonly used AD-diagnostic antibodies listed above (Fig. 2.7). However, the FLEXITau data showed that the overall modification extent of Sf9-tau is considerably lower than that of AD-tau aggregates, especially in the C-terminal acidic region and the MT-binding domain. This may indicate that the phosphorylation extent in Sf9 is not sufficient to mimic the state of AD-tau. Furthermore, in addition to the 23 phosphorylation sites mapped on Sf9-tau, more than 20 other phosphorylation sites have been described for AD-tau, whose relevance in respect to aggregation is neglected when using the Sf9 model system. Finally, the data showed that other types of PTMs, such as acetylation, are located in regions that showed the biggest difference in modification extent when comparing AD-tau to Sf9-tau, indicating that these may contribute to aggregation, as supported by previous studies [98, 303]. Overall one can conclude that the Sf9 possibly represents a model for particular phosphorylation sites in the proline-rich domain, however it is limited as a general model system for pathological tau. These findings indicate that restricting the PTM analysis of tau to few sites or to phosphorylation only can be misleading as an incomplete picture is generated. Altogether this corroborates the usefulness and even necessity of a global unbiased assay such as FLEXITau when assessing the PTM state of tau from a model system as a proxy for disease.

Conclusions and outlook

The application of the FLEXITau assay to the Sf9-tau and the AD-tau exemplifies several key advantages of this method over existing strategies to analyze tau PTMs. First of all, because FLEXITau provides a global, complete picture of the PTM landscape, one can use the quantitative data as a signature to compare different species to each other in a very precise manner. The major improvement of FLEXITau, in particular when complemented by DDA analyses, is that tau modifications are identified both on a qualitative and quantitative level, and additionally the number of occupied sites per molecule can be determined. Thus FLEXITau delivers information on three levels: 1) how many and what sites are present 2) to what extent are they modified, and 3) what is the average number of modified moieties. The results also highlight that a reliable detection of a particular phosphorylation site by traditional DDA analyses poorly reflects its abundance, and that quantification is indispensable. For example, phosphorylation on T175 was identified with high confidence, while FLEXITau revealed the extent of modification being only 2-3%. Conversely, the completeness of the quantitative data obtained can also point towards the presence of modifications although none is identified with the complementary DDA shotgun analysis. For example, this study revealed that the acidic N-terminal tail of Sf9 tau is modified to a high extent (approximately 50%), but no modification was detected by the complementary DDA shotgun analysis and also previous reports concluded that this region was unmodified [419]. In fact, it is striking how little PTM data is available for this particular region, despite the overall vast amount of information of both *in vivo* tau or *in vitro* modified tau [192, 470] (see also <http://cnr.iop.kcl.ac.uk/hangerlab/tautable>, an up-to-date list of all tau phosphorylation sites). With other words, this study suggests that to date the analysis of tau PTMs has been biased towards sites that either can be targeted by site-specific antibodies or that are detectable by discovery-based MS approaches. Because FLEXITau overcomes these limitations, targeted follow-up experiments (such as peak-chasing methods or biochemical enrichment strategies) can be performed to identify these unknown modifications.

The only requisite for the FLEXITau approach is the relatively straightforward expression of the isotopically labeled tau protein. In this study, the longest tau isoform was chosen as standard, as the assay was specifically conceived to accommodate the measurement of 2N4R expressed in Sf9 cells. However, FLEXITau is not limited to full-length tau and the extension of the assay to other splice variants is feasible, allowing for precise quantification of tau isoforms. In cases where a particular set of PTMs is of interest, the SRM assay can conveniently be modified to incorporate the respective modified peptide species for additional PTM information. Here special care should be paid to densely modified regions, where all possible combinations of modifications must be taken into account to maintain unbiased quantification of the site of interest. Moreover, one can imagine the design of other variants to include alternate tau species (e.g. mouse tau), given that the respective heavy standards are readily cloned and expressed, and provided that the additional SRM

transitions are validated such that specificity and sensitivity of the assay are maintained.

Overall, this study highlights that FLEXITau is a versatile, useful tool to assess tau PTMs in a reproducible manner. With the possibility of obtaining quantitative data for both distribution and occupancy, the analysis of tau phosphorylation and other PTMs can be performed with unprecedented precision and accuracy. With this, FLEXITau will not only enhance mechanistic understanding of tau function but also open the door for development of diagnostic tools and tau-modulating therapeutic strategies for tauopathies, as discussed further below.

4.2 Using FLEXITau to identify tau PTM signatures for the diagnosis of tauopathies

Usually, proteomics studies for the detection of diagnostic markers make no previous assumptions about the identities of proteins and peptides constituting an informative signature. In the case of neurodegenerative tauopathies, the well-known pathological hallmark is abnormal tau deposition. Although common to all diseases, disease-specific modifications and differences in isoform distribution are reported. Thus it was hypothesized that in different diseases, insoluble tau presents with a distinct molecular signature. The goal of the second study was to extract this signature using the FLEXITau assay and use it to differentially diagnose several tauopathies.

Development of a computational classifier for tauopathies

To this end, post-mortem cortical brain tissue specimens from a total of 129 patients were analyzed. These included AD, the most common tauopathy, as well as several other conditions that fall into the spectrum of frontotemporal lobar degeneration (FTLD), including Pick's disease (PiD), corticobasal degeneration (CBD), and progressive supranuclear palsy (PSP), as well as non-demented control (ctrl) subjects. For each patient, the peptide landscape of insoluble tau was profiled using the developed assay. This quantitative data was then used to build and test a computational classifying tool for each disease (i.e. 5 classifiers were built). The classifiers were computed by the Random Forest machine learning method by training on a well-characterized group of patients and subsequently tested on an independent test set containing a heterogeneous group of samples.

Cases in the test set were designated as "mis-assigned" if they were assigned to a category that did not match their primary diagnosis. This included cases that were classified correctly, but additionally were assigned to a second category (e.g. a sample received with the primary diagnosis of PSP was classified as AD and as PSP). To determine if these mis-assignments had underlying pathologies that were not explained by the primary diagnosis, for all mis-assigned cases the classification outcome was cross-referenced with

pathology reports and clinical data, if available, and followed up by personal correspondence with neuropathologists at the brain bank from which the specimens were obtained. Interestingly, for the majority of cases, an explanation for the mis-assignment could be found. These cases fell into 3 different categories: 1) patients were reported to display co-occurring pathologies (e.g. in addition to PSP features, further pathological alterations were observed in the brain that indicated AD), 2) the pathological diagnosis of the patient was uncertain, atypical or asymptomatic in the region of the cortex analyzed, and 3) cases that were re-diagnosed by the pathologist after re-evaluation using immunohistochemistry techniques (this was the case for one sample only). The final performance of the classifiers were evaluated after re-assigning these cases, i.e. in the case of co-occurring pathologies, each diagnosis was included, and cases with uncertain or spared pathology were eliminated. The final classification achieved accuracies of above 90% for AD, CBD, PiD and ctrl, and 80% for PSP.

Performance of the classifiers: Detection of co-pathologies, misdiagnoses, and cortical sparing

Several conclusions could be drawn from this study. First of all, it was intriguing that in the AD classifier, all false positive (FP) cases (i.e. samples that were classified as AD although their primary diagnosis was another) were actually specimens with reported AD pathologies (these were 4 PiD cases and one PSP case). With a single exception, none of the remaining non-AD cases documented evidence of AD pathology in addition to the primary diagnosis, indicating that the developed AD classifier is highly sensitive and specific to AD co-morbidity. Importantly, all 4 PiD cases were correctly assigned to PiD by the PiD classifier, indicating that the combination of individual classifiers is a powerful method to detect co-pathologies.

Neuropathological diagnosis of CBD and PSP is usually hampered by overlapping features, little correlation with clinical diagnosis, and a large heterogeneity and variability of tau pathology, in particular in the parietal cortex region under study here [120, 233, 445, 464]. Considering these issues, it is impressive that the CBD classifier achieved a specificity of 97.4%, highlighting the power of using the tau peptide signature for differentiation of these heterogeneous disease phenotypes. The CBD classifier also revealed the misdiagnosed case mentioned above, further corroborating the specificity of the classifier. This case was received with a primary diagnosis of PSP, and was assigned to CBD and not to PSP by the respective classifiers. Re-evaluation by immunohistochemistry analyses at the brain bank then confirmed a CBD diagnosis. A possible reason for the initial misdiagnosis is that the autopsy and evaluation of this case dated back to the year 2009, when diagnostic phospho-tau antibodies were not yet commonly used for diagnostic purposes and pathological evaluation was restricted to silver staining, particularly hampering the differential diagnosis of CBD and PSP.

In contrast to the CBD classifier, the PSP classifier performed significantly lower than all other classifiers (accuracy of 80%). As discussed in more detail in Chapter 3, section 3.5, the main reason for this low performance may be relatively low tau burden in the cortical regions of typical PSP cases [431]. Thus the extracted PSP tau signature from these regions would be similar to that of ctrl cases. Corroborating this, in the PSP classification, most FP cases (non-PSP samples that were recognized as PSP) were from the ctrl group. Reversely, in the ctrl classifier, most FP cases were from the PSP category. The tau burden of several of these PSP cases was investigated using follow-up silver stainings and immunohistochemistry and confirmed the absence of tau pathology in this particular cortical region. Severity of tau pathology in cortical areas is also a major difference among PSP variants, complicating further the extraction of a typical PSP signature [72, 206, 351, 431, 440, 463, 464]. Altogether these findings suggest that while for the other tauopathies under study the chosen cortical region is well-suited for diagnosis, for PSP the analysis of other brain regions should be considered to improve diagnostic specificity and sensitivity.

The differential PTM signature of tauopathies

Phosphorylation is the best studied disease-related tau PTM. Most phosphorylation sites cluster in domains surrounding the MT-binding region, i.e. in the proline-rich region and the c-terminal tail (section 1.3.4, Fig. 1.6). Detection of specific phosphorylated epitopes using antibodies is widely accepted as an indicator for tau-mediated neurodegeneration, and as mentioned earlier, today some of these antibodies are used in diagnostic practices for the evaluation of tauopathies, such as AT8 and AT100, both targeting phosphorylated serines (S) and threonines (T) in the proline-rich region (pS202/pT205 and pT212/pS214). Remarkably, in this study, the majority of the peptides selected as discriminating features were not located in this region, but inside the MT-binding region of tau, including exon 10 (section 3.4.5, Fig. 3.9D). This indicates that the MT-binding region harbors molecular characteristics that are unique to each tauopathy. In contrast to phosphorylation, most of the *in vivo* acetylation and ubiquitination sites identified so far are located inside the MT-binding region (Fig. 3.3) [108, 220, 303, 423]. Overall this suggests that acetylated and ubiquitinated tau may serve as biomarker to distinguish different tauopathies, while phosphorylation on characteristic sites is a common marker for tau pathology, but unspecific for individual tauopathies. Supporting this, PiD as well as AGD, a less well-understood tauopathy, have been shown to lack acetylation on specific sites in the first MT-binding repeat compared to other tauopathies (acetylated lysine (acK) acK280 and acK274, respectively) [97, 179, 223]. Furthermore, ubiquitination in glial lesions has also been reported to be useful for distinguishing between various types of tauopathies [145].

Another PTM that has been recently linked to the early pathogenesis of AD and other tauopathies is proteolytic cleavage, in particular at the C-terminus of tau, i.e. glutamate (E) E391 and aspartate (D) D421 [154, 331]. Notably in this study, the two peptides covering

these sites contribute to all classifiers (the former to CBD and PSP, the latter to ctrl, PiD and AD). This implies that in addition to the above-mentioned PTMs, C-terminal truncation could be used to biochemically classify tauopathies, as suggested by previous studies [185]. Finally, recently it was reported that in sarkosyl insoluble tau, the MT-binding region harbors distinct conformational modifications and protease-resistant fragments that are different among tauopathies [416]. This further supports the findings of this study that the MT-binding region is useful for differentiation of tauopathies.

Apart from PTMs, disturbance in tau isoform homeostasis has been suggested to be an important mechanistic basis in tauopathies, in particular the alternative splicing of exon 10 in the MT-binding region. Exon 10 encodes for one of the four MT-binding repeats. Alternative splicing of exon 10 therefore produces two isoforms: tau containing 3 MT-binding repeats (3R-tau) or 4 MT-binding repeats (4R-tau). Under physiological conditions, 3R-tau and 4R-tau exist in a 1:1 ratio. In tau pathology of AD, this ratio is maintained, as both isoforms are equally incorporated into tangles. In contrast, in CBD and PSP brains predominantly 4R-tau is deposited inside neuronal and glial lesions, whereas in PiD, preferentially 3R-tau isoforms accumulate [117, 390, 392] (see also section 1.4). Consistent with this, for CBD and PSP samples, the three 4R-tau specific peptides that cover the exon 10 sequence were significantly enriched compared to control (section 3.4.1, Fig. 3.2C). In addition, these peptides were selected by the classifiers as discriminatory features in each disease category under study (section 3.4.5, Fig. 3.9D).

Application of FLEXITau as a post-mortem diagnostic tool

Currently, diagnosis of tauopathies relies on time-consuming post-mortem investigation of the autopsied brain by a neuropathologist, involving stepwise gross and histological findings to confirm clinical diagnosis, if available. Diagnosis is based on the identification of characteristic morphological changes, as well as distribution and types of specific lesions using histological and immunohistochemical staining techniques, e.g. silver staining and, more recently, antibody-based detection of phosphorylated tau and tau isoforms (reviewed in [260], see also section 1.4.5). Overlapping features and heterogeneities hamper unequivocal findings [233]. Another issue of the current post-mortem diagnosis is variability in protocols and staining qualities as well as the manual evaluation of histopathological findings by each pathologist that may cause inter-brain bank inconsistencies in diagnosis [11, 12, 262]. Today, MS is being widely used in clinical laboratories, in particular for the detection of small molecules with diverse applications such as drug/toxicology, newborn screening and endocrinology [177, 453]. However for protein analysis, apart from biomarker discovery and validation, the use of MS has not yet been adopted in clinical practice [199, 278]. Importantly, the use of MS-based protein analysis is a natural progression from antibody-based protein staining, as diagnosis relies on the analysis of cellular and morphological features which are related to changes at the peptide or protein level.

The use of the MS-based FLEXITau assay for the post-mortem diagnosis of tauopathies circumvents many of the issues associated with traditional histopathological assessments. The sensitivity of the technique allows for detection of attomolar amounts of tau, thus requiring minimal amount of tissue. In particular, SRM does not rely on specific antibodies, which suffer from varying sensitivity and specificity. The FLEXITau approach is relatively simple to implement, requiring a recombinant protein and a state-of-the-art mass spectrometer, and dozens of samples can be processed in parallel. The use of an internal standard and the monitoring of multiple product ions for each peptide ensure excellent specificity. Furthermore, the SRM quantification methodology is recognized for its robustness and reproducibility within and across laboratories [99, 357]. Notably, the testing of a single cortical brain specimen (in contrast to multiple sections) proves to be sufficient to achieve excellent accuracy of diagnosis (with the exception of PSP). In summary, the use of the FLEXITau assay coupled with the computational classifier provides a uniform diagnostic framework and represents an attractive alternative to classification of tauopathies using histopathological means, possibly yielding results much more rapidly and cost-efficiently than current approaches.

An immediate application of such MS-based diagnostic tools is the re-evaluation of stored post-mortem brain specimens in tissue banks. Systematic brain banking represents an indispensable resource for the study of neurodegenerative diseases [262, 362, 427]. The concept of brain repositories exists since the 1960s, therefore, stored specimens distributed to the researcher upon tissue request can date back several decades, and thereby the diagnosis. However, over the last decade, the understanding of tauopathies has changed and many diagnostic neuropathological concepts have been updated [24, 121, 214, 299]. Thus a re-classification of stored specimens is of paramount importance to ensure quality and accuracy of documented cases consistent with current standards. While this endeavor is difficult to conceive using traditional approaches, the multiplexing capabilities and simplicity of the developed diagnostic classifier may enable inexpensive, systematic re-evaluation of entire cohorts in different brain banks.

4.3 Future perspective

In this thesis the development of FLEXITau is presented, a novel quantitative tau PTM assay. FLEXITau was first used to measure the PTM landscape from hyperphosphorylated tau expressed in Sf9 cells, in comparison to tau from AD. Next the assay was successfully applied to insoluble tau of tauopathy brain, where disease-specific diagnostic profiles were determined. Due to its precision and versatility, in the future the FLEXITau assay could be applied to a wide range of other biological and clinical settings.

The use of FLEXITau for benchmarking tau model systems

For instance, FLEXITau could enable the evaluation of other tau model systems and the assessment of their proximity to disease tau, similar to the Sf9 tau, for instance transgenic mouse models carrying human mutant tau, such as the commonly used P301L and P301S mice. Less characterized or novel tau model systems could be systematically prototyped, allowing to define which model is most reflective of a particular disease. Similarly, aged populations of induced pluripotent stem cells (iPSC)-derived neurons carrying mutations could be compared to each other and wild-type (WT) neurons. As a matter of fact, as part of a collaborative project which is not part of this thesis, I investigated the differences between iPSC-derived WT neurons and neurons carrying the A152T variant, which is found in a small population of PSP patients. The goal was to define the tau PTM signature of these cells and to evaluate the effect of specific autophagy-targeting drugs on this signature and total amounts of tau (manuscript in preparation).

Application of FLEXITau for *in vivo* diagnostics

Importantly, the findings in this study may be translated into *in vivo* diagnostic tools, i.e. the diagnosis of the disease in the living patient. The main approach for *in vivo* diagnostics is the identification of disease-indicative biochemical analytes (called biomarkers) that are measured in peripheral fluids such as cerebrospinal fluid (CSF) or plasma (see also section 1.4.5). Quantification of tau in CSF is currently used as a highly sensitive biomarker for AD diagnosis [20]. However, currently this analysis relies on immunoassays (ELISA), which suffer from lack of specificity in regards to the molecular heterogeneity of tau which is caused by the multiple isoforms and PTMs. Furthermore, in a large-cohort CSF biomarker study it became apparent that perhaps as many as 30% of clinical FTLD patients, including PSP syndrome and CBS, are also AD biomarker positive [383]. Efforts using alternative, MS-based approaches have been hampered so far by the low concentration of tau present in CSF. Two promising studies that were published during the writing of this thesis presented a novel extraction workflow without the use of affinity reagents, that, coupled with SRM analysis, enabled the detection of up to 19 tau peptides in endogenous CSF [40, 78]. Additionally, relative differences in the abundance of specific peptides were observed, suggesting that tau in CSF might present a signature, just as in tauopathy post-mortem brains [40]. The incorporation of the FLEXITau strategy into this workflow might enable the detection of disease-specific CSF signatures and thus lead to the development of highly specific biomarkers for AD and other tauopathies. Increasing efforts are also being made towards neuroimaging strategies that visualize distinct patterns in the brain using different brain-scanning techniques (see also section 1.4.5). These methodologies either measure tau pathology directly by using tau positron emission tomography (PET) ligands, or indirectly by measuring tau-mediated neuronal injury by magnetic resonance imaging (MRI). These methods are promising as they are non-invasive and could detect changes in

its early symptomatic stage. However, the complexity and heterogeneity of tau pathology and the limited knowledge of disease-specific molecular species have presented a major challenge for the development of effective ligands [317, 441]. The tauopathy FLEXITau data obtained in this study offers great potential for the design of novel PET imaging ligands specific for the differentially modified protein regions. These *in vivo* biomarkers and imaging reagents could then be used for staging of disease progress, and for measuring benefits of treatments in clinical trials.

Development of novel therapeutic strategies

Of equal importance as diagnosis is the ability to treat individuals once a particular disease is diagnosed. Tau-targeted therapeutic strategies have received increased attention since the failure of many amyloid- β -targeted therapeutics in phase III clinical trials for AD [79] (see also section 1.4.6). However, a critical confound for the development of effective therapeutics is the unclarity surrounding tau toxicity. To date, it is not yet fully understood which of the many morphological species of tau (e.g. oligomers, pretangles, or fibrillar or aggregate forms) is the primary cause for tau pathogenesis and neuronal toxicity, ultimately leading to brain atrophy and cognitive decline (see also section 1.3). It is also unclear whether there is one main toxicity mechanism or whether there are multiple toxic species (which is quite probable given the wide range of modifications that tau undergoes), and finally whether the toxic species is the same in all tauopathies or whether each disease is characterized by a different molecular process. Investigating the involvement of PTMs in the formation of distinct morphological tau assemblies may lead to a better mechanistic understanding of tau toxicity and how this process can be stopped or reverted. Moreover, with its ability to measure small changes in the PTM landscape, FLEXITau could also facilitate the screening of small molecule inhibitors of oligomer formation or fibrillization, and could even be used to monitor the progress and effect of treatment.

Another promising therapeutic avenue is the removal of pathological tau using immunotherapy. Treatment with antibodies targeting intracellular or extracellular tau species has been shown to suppress tau pathology and improve phenotypes in several transgenic models of tauopathy [30, 52, 65, 67, 90, 396]. Immunotherapy strategies rely on precisely identifying the species, and/or epitope of this species, that is responsible for toxicity. A successful application in human disease will rely on the resolution of this issue. The FLEXITau assay represents a valuable tool for defining disease-indicative epitopes and guiding the selection and development of therapeutic tau antibodies. Whether tau immunotherapy will be effective in clinical trials has to be seen.

4.4 Closing remarks

Today there are around 44 million people living with dementia worldwide, and with the current trend of a rapidly aging population and no cure, this number is expected to triple by 2050 [29]. A key problem in the care of AD and other forms of dementia is the high impact on caregivers and the society. While the affected individuals usually are able to live a relatively unperturbed life over many years, their family and friends become increasingly involved over the course of the disease, facing pragmatic challenges and emotional stress that often leads to depression and burnout. At later stages of the disease progression, assisted living or nursing homes provide round-the-clock care and long-term medical service for the affected individual. Thus, care for demented people is extremely resource and cost demanding. In fact, in the US, AD is considered the most expensive disease - it costs more than 200 billion dollars every year, and by 2050 this number is expected to exceed 1 trillion dollars each year [29].

Clearly, dementia is one of the biggest medical, social and financial challenges of our generation, and neither health care nor financial systems are prepared to face the magnitude of the situation [133]. Despite these disturbing facts, there is a lack of consciousness worldwide - e.g. the US government spends 10 times more money each year on cancer research than on AD. This lack of awareness may be due to the slow, progressive onset of disease. In addition, in the past, and still today in countries where information is lacking, dementia is confused with senility-related mental decline, i.e. mistaken as part of normal aging, implying that it cannot be cured. A new study found that these misconceptions are particularly high in low-income to middle-income countries and among racial and ethnic minority groups [86]. Altogether these findings point to the substantial need for governments not only to invest more money into dementia research, but also to incorporate more educational and advocacy programs on dementia into public health campaigns.

Clinical trials for AD have generally reached the conclusion that medication is more effective in slowing the cognitive decline if administered early in the course of disease. Understanding which elderly individuals are at highest risk for eventually developing dementia will thus be essential to the ultimate goal of preventing it, apart from this being extremely advantageous from an economic perspective. This requires studies in pre-symptomatic patients as the appearance of pathology precedes the manifestation of clinical symptoms, potentially more than 10 years [42, 169]. To this end it is imperative to find means able to measure minimal changes in the molecular landscape early in the continuum from healthy cognition to dementia, where the diagnostic line is still "blurry". Current advancements and sophistication of technology, such as the FLEXITau assay presented in this work, represent a promising step towards this goal.

List of Abbreviations

0N	0 N-terminal inserts containing tau
1N	1 N-terminal inserts containing tau
2N	2 N-terminal inserts containing tau
3R	3 MT-binding repeats containing tau
4R	4 MT-binding repeats containing tau
A β	amyloid β
AA	amino acid
ABC	ammonium bicarbonate
ac	accuracy
ACN	acetonitrile
AD	Alzheimer's disease
AGD	argyrophilic Grain disease
AGE	advanced glycation end products
ALS	amyotrophic lateral sclerosis
AP	alkaline phosphatase
Asp	aspartic acid
AUC	area under the ROC curve
BA	Brodmann Area
bvFTD	behavioral variant FTD
C	cysteine
C-terminal	carboxy-terminal
CBD	corticobasal degeneration

CBS	corticobasal syndrom
CDK5	cyclin-dependent kinase-5
CE	collision energy
CJD	Creutzfeldt-Jakob Disease
CNS	central nervous system
CSF	cerebrospinal fluid
CV	coefficient of variance
D	aspartate
DDA	data-dependent acquisition
DIA	data-independent acquisition
DLB	dementia with Lewy bodies
DP	declustering potential
DTT	dithiothreitol
E	glutamate
EDTA	ethylene diamine tetraacetic acid
EGTA	ethylene glycol tetraacetic acid
ESI	electrospray ionization
FA	formic acid
FASP	filter aided sample preparation
FLEXIQuant	Full-Length Expressed Stable Isotope-labeled Proteins for Quantification
FLEXITau	Full-Length Expressed Stable Isotope-labeled Tau for Quantification
FN	false negative
FP	false positive
FPR	false positive rate
FTD-MND	frontotemporal dementia with motor neuron disease
FTDP	frontotemporal dementia with parkinsonism

FTDP-17	frontotemporal dementia with parkinsonism linked to chromosome 17
FTLD	frontotemporal lobe dementia
FUS	fused in sarcoma protein
FWHM	full width at half maximum
GSK3	glycogen synthase kinase 3
HAT	histone acetyltransferases
HD	Huntington's disease
HDAC	histone deacetylases
HSP90	heat shock protein 90
ICAT	isotope coded affinity tag
ICH	immunohistochemistry
iRT	indexed retention time
iTRAQ	isobaric tags for relative and absolute quantitation
K	lysine
KNN	k-Nearest Neighbor
L/H	light-to-heavy
LC	liquid chromatography
LC-MS/MS	tandem mass spectrometry
LC-SRM	liquid chromatography-selected reaction monitoring
LDA	Linear Discriminant Analysis
LVQ	Learning Vector Quantization
m/z	mass-to-charge ratio
MALDI	matrix-assisted laser desorption/ionization
MAP	microtubule associated protein
MAPK	mitogen-activated protein kinase
MAPT	microtubule associated protein tau

MARK	MAP/microtubule affinity-regulating kinase
MCI	mild cognitive impairment
MRI	magnetic resonance imaging
MRM	multiple reaction monitoring
MS	mass spectrometry
MT	microtubule
MW	molecular weight
N-terminal	amino-terminal
NFT	neurofibrillary tangle
Nnet	Neural Networks
ns	non-significant
O-GlcNAc	O-linked attachment of N-acetylglucosamine
O-GlcNAcase	β -N-acetylglucosaminidase
OA	okadaic acid
OOB	Out-of-Bag
P	proline
PAGE	polyacrylamide gel electrophoresis
PD	Parkinson's disease
PET	positron emission tomography
PHF	paired helical filaments
PiD	Pick's disease
PKA	protein kinase A
PMI	post-mortem interval
PNFA	progressive nonfluent aphasia
PRP ^{SC}	cellular and scrapie form of prion protein
PSA	puromycin-sensitive aminopeptidase

PSP	progressive supranuclear palsy
QconCATs	concatenated synthetic peptides
R	arginine
RF	Random Forest
ROC	receiver operator curve
RT	retention time
S	serine
SAP	stress-activated protein
SD	standard deviation
SDS	sodium dodecyl sulfate
se	sensitivity
SF	straight filaments
SILAC	stable isotope labeling with amino acids in cell culture
sp	specificity
SRM	selected reaction monitoring
SUMO1	small ubiquitin-like modifier protein-1
T	threonine
TDP-43	TAR DNA-binding protein 43
TMT	tandem mass tags
TN	true negative
TP	true positive
TPR	true positive rate
UPS	ubiquitin-proteasome-system
WGE	wheat germ expression
Y	tyrosine

Bibliography

- [1] ABRAMOWICZ, Agata ; WOJAKOWSKA, Anna ; GDOWICZ-KLOSOK, Agnieszka ; POLANSKA, Joanna ; RODZIEWICZ, Pawel ; POLANOWSKI, Pawel ; NAMYSL-KALETKA, Agnieszka ; PIETROWSKA, Monika ; WYDMANSKI, Jerzy ; WIDLAK, Piotr: Identification of serum proteome signatures of locally advanced and metastatic gastric cancer: a pilot study. In: *J Transl Med* 13 (2015), Jan, S. 304. <http://dx.doi.org/10.1186/s12967-015-0668-9>. – DOI 10.1186/s12967-015-0668-9
- [2] ADAM, Bao-Ling ; QU, Yinsheng ; DAVIS, John W. ; WARD, Michael D. ; CLEMENTS, Mary A. ; CAZARES, Lisa H. ; SEMMES, O J. ; SCHELLHAMMER, Paul F. ; YASUI, Yutaka ; FENG, Ziding ; WRIGHT, George L.: Serum protein fingerprinting coupled with a pattern-matching algorithm distinguishes prostate cancer from benign prostate hyperplasia and healthy men. In: *Cancer Res* 62 (2002), Jul, Nr. 13, 3609–14. <http://cancerres.aacrjournals.org/content/62/13/3609.long>
- [3] ADDONA, T ; ABBATIELLO, S ; SCHILLING, B ; SKATES, S ; MANI, D ; BUNK, D ; SPIEGELMAN, C ; ZIMMERMAN, L ; HAM, A ; KESHISHIAN, H ; HALL, S ; ALLEN, S ; BLACKMAN, R ; BORCHERS, C ; BUCK, C ; CARDASIS, H ; CUSACK, M ; DODDER, N ; GIBSON, B ; HELD, J ; HILTKE, T ; JACKSON, A ; JOHANSEN, E ; KINSINGER, C ; LI, J ; MESRI, M ; NEUBERT, T ; NILES, R ; PULSIPHER, T ; RANSOHOFF, D ; RODRIGUEZ, H ; RUDNICK, P ; SMITH, D ; TABB, D ; TEGELER, T ; VARIYATH, A ; VEGA-MONTOTO, L ; WAHLANDER, A ; WALDEMARSON, S ; WANG, M ; WHITEAKER, J ; ZHAO, L ; ANDERSON, N ; FISHER, S ; LIEBLER, D ; PAULOVICH, A ; REGNIER, F ; TEMPST, P ; CARR, S: Multi-site assessment of the precision and reproducibility of multiple reaction monitoring-based measurements of proteins in plasma. In: *Nat Biotechnol* 27 (2009), Jul, Nr. 7, 633–41. <http://dx.doi.org/10.1038/nbt.1546>. – DOI 10.1038/nbt.1546
- [4] AEBERSOLD, R ; GOODLETT, D R.: Mass spectrometry in proteomics. In: *Chem Rev* 101 (2001), Feb, Nr. 2, 269–95. <http://pubs.acs.org/doi/abs/10.1021/cr990076h>
- [5] AEBERSOLD, R ; MANN, M: Mass spectrometry-based proteomics. In: *Nature* 422 (2003), Mar, Nr. 6928, 198–207. <http://dx.doi.org/10.1038/nature01511>. – DOI 10.1038/nature01511
- [6] AGDEPPA, E D. ; KEPE, V ; LIU, J ; FLORES-TORRES, S ; SATYAMURTHY, N ; PETRIC, A ; COLE, G M. ; SMALL, G W. ; HUANG, S C. ; BARRIO, J R.: Binding characteristics of radiofluorinated 6-dialkylamino-2-naphthylethylidene derivatives as positron emission tomography imaging probes for beta-amyloid plaques in Alzheimer's disease. In: *The Journal of neuroscience : the official journal of the Society for Neuroscience* 21 (2001), Dec, Nr. 24, S. RC189
- [7] AGRANOFF, Dan ; FERNANDEZ-REYES, Delmiro ; PAPAPOPOULOS, Marios C. ; ROJAS, Sergio A. ; HERBSTER, Mark ; LOOSEMORE, Alison ; TARELLI, Edward ; SHELDON, Jo ; SCHWENK, Achim ; POLLOK, Richard ; RAYNER, Charlotte F J. ; KRISHNA, Sanjeev: Identification of diagnostic markers for tuberculosis by proteomic fingerprinting of serum. In: *Lancet* 368 (2006), Sep, Nr. 9540, S. 1012–21. [http://dx.doi.org/10.1016/S0140-6736\(06\)69342-2](http://dx.doi.org/10.1016/S0140-6736(06)69342-2). – DOI 10.1016/S0140-6736(06)69342-2
- [8] AHMED, Farid E.: Utility of mass spectrometry for proteome analysis: part I. Conceptual and experimental approaches. In: *Expert Rev Proteomics* 5 (2008), Dec, Nr. 6, S. 841–64. <http://dx.doi.org/10.1586/14789450.5.6.841>. – DOI 10.1586/14789450.5.6.841
- [9] AHMED, Zeshan ; JOSEPHS, Keith A. ; GONZALEZ, John ; DELLEDONNE, Anthony ; DICKSON, Dennis W.: Clinical and neuropathologic features of progressive supranuclear palsy with severe pallido-nigro-luysial degeneration and axonal dystrophy. In: *Brain* 131 (2008), Feb, Nr. Pt 2, S. 460–72. <http://dx.doi.org/10.1093/brain/awm301>. – DOI 10.1093/brain/awm301
- [10] AKIYAMA, H ; BARGER, S ; BARNUM, S ; BRADT, B ; BAUER, J ; COLE, G M. ; COOPER, N R. ; EIKELENBOOM, P ; EMMERLING, M ; FIEBICH, B L. ; FINCH, C E. ; FRAUTSCHY, S ; GRIFFIN, W S. ; HAMPEL, H ; HULL, M ; LANDRETH, G ; LUE, L ; MRAK, R ; MACKENZIE, I R. ; MCGEER, P L. ;

- O'BANION, M K. ; PACHTER, J ; PASINETTI, G ; PLATA-SALAMAN, C ; ROGERS, J ; RYDEL, R ; SHEN, Y ; STREIT, W ; STROHMAYER, R ; TOOYOMA, I ; MUISWINKEL, F L V. ; VEERHUIS, R ; WALKER, D ; WEBSTER, S ; WEGRZYNIAK, B ; WENK, G ; WYSS-CORAY, T: Inflammation and Alzheimer's disease. In: *Neurobiol Aging* 21 (2000), Jan, Nr. 3, S. 383–421
- [11] ALAFUZOFF, I ; ARZBERGER, T ; AL-SARRAJ, S ; BODI, I ; BOGDANOVIC, N ; BRAAK, H ; BUGIANI, O ; DEL-TREDICI, K ; FERRER, I ; GELPI, E ; GIACCONE, G ; GRAEBER, M ; INCE, P ; KAMPHORST, W ; KING, A ; KORKOLOPOULOU, P ; KOVACS, G ; LARIONOV, S ; MEYRONET, D ; MONORANU, C ; PARCHI, P ; PATSOURIS, E ; ROGGENDORF, W ; SEILHEAN, D ; TAGLIAVINI, F ; STADELMANN, C ; STREICHENBERGER, N ; THAL, D ; WHARTON, S ; KRETZSCHMAR, H: Staging of neurofibrillary pathology in Alzheimer's disease: a study of the BrainNet Europe Consortium. In: *Brain Pathol* 18 (2008), Oct, Nr. 4, 484–96. <http://dx.doi.org/10.1111/j.1750-3639.2008.00147.x>. – DOI 10.1111/j.1750-3639.2008.00147.x
- [12] ALAFUZOFF, I ; PIKKARAINEN, M ; AL-SARRAJ, S ; ARZBERGER, T ; BELL, J ; BODI, I ; BOGDANOVIC, N ; BUDKA, H ; BUGIANI, O ; FERRER, I ; GELPI, E ; GIACCONE, G ; GRAEBER, M ; HAUW, J ; KAMPHORST, W ; KING, A ; KOPP, N ; KORKOLOPOULOU, P ; KOVACS, G ; MEYRONET, D ; PARCHI, P ; PATSOURIS, E ; PREUSSER, M ; RAVID, R ; ROGGENDORF, W ; SEILHEAN, D ; STREICHENBERGER, N ; THAL, D ; KRETZSCHMAR, H: Interlaboratory comparison of assessments of Alzheimer disease-related lesions: a study of the BrainNet Europe Consortium. In: *J Neuropathol Exp Neurol* 65 (2006), Aug, Nr. 8, 740–57. <http://dx.doi.org/10.1097/01.jnen.0000229986.17548.27>. – DOI 10.1097/01.jnen.0000229986.17548.27
- [13] ALBERT, Marilyn S. ; DEKOSKY, Steven T. ; DICKSON, Dennis ; DUBOIS, Bruno ; FELDMAN, Howard H. ; FOX, Nick C. ; GAMST, Anthony ; HOLTZMAN, David M. ; JAGUST, William J. ; PETERSEN, Ronald C. ; SNYDER, Peter J. ; CARRILLO, Maria C. ; THIES, Bill ; PHELPS, Creighton H.: The diagnosis of mild cognitive impairment due to Alzheimer's disease: recommendations from the National Institute on Aging-Alzheimer's Association workgroups on diagnostic guidelines for Alzheimer's disease. In: *Alzheimers Dement* 7 (2011), May, Nr. 3, S. 270–9. <http://dx.doi.org/10.1016/j.jalz.2011.03.008>. – DOI 10.1016/j.jalz.2011.03.008
- [14] ALEXANDER, S ; RITTMAN, T ; XUEREB, J ; BAK, T ; HODGES, J ; ROWE, J: Validation of the new consensus criteria for the diagnosis of corticobasal degeneration. In: *Journal of neurology, neurosurgery, and psychiatry* 85 (2014), Aug, Nr. 8, 925–9. <http://dx.doi.org/10.1136/jnnp-2013-307035>. – DOI 10.1136/jnnp-2013-307035
- [15] ALTMAN, N: An Introduction to Kernel and Nearest-Neighbor Nonparametric Regression. In: *The American Statistician* 46 (1992), Nr. 3, S. 175–185
- [16] ANDERSON, Leigh ; HUNTER, Christie L.: Quantitative mass spectrometric multiple reaction monitoring assays for major plasma proteins. In: *Mol Cell Proteomics* 5 (2006), Apr, Nr. 4, S. 573–88. <http://dx.doi.org/10.1074/mcp.M500331-MCP200>. – DOI 10.1074/mcp.M500331-MCP200
- [17] ANDORFER, Cathy ; ACKER, Christopher M. ; KRESS, Yvonne ; HOF, Patrick R. ; DUFF, Karen ; DAVIES, Peter: Cell-cycle reentry and cell death in transgenic mice expressing nonmutant human tau isoforms. In: *J Neurosci* 25 (2005), Jun, Nr. 22, S. 5446–54. <http://dx.doi.org/10.1523/JNEUROSCI.4637-04.2005>. – DOI 10.1523/JNEUROSCI.4637-04.2005
- [18] ANDREADIS, A ; BRODERICK, J ; KOSIK, K: Relative exon affinities and suboptimal splice site signals lead to non-equivalence of two cassette exons. In: *Nucleic Acids Res* 23 (1995), Sep, Nr. 17, 3585–93. <http://www.ncbi.nlm.nih.gov/pubmed/7567473>
- [19] ANDREADIS, A ; BROWN, W ; KOSIK, K: Structure and novel exons of the human tau gene. In: *Biochemistry* 31 (1992), Nov, Nr. 43, 10626–33. <http://www.ncbi.nlm.nih.gov/pubmed/1420178>
- [20] ANDREASEN, Niels ; BLENNOW, Kaj: CSF biomarkers for mild cognitive impairment and early Alzheimer's disease. In: *Clin Neurol Neurosurg* 107 (2005), Apr, Nr. 3, S. 165–73. <http://dx.doi.org/10.1016/j.clineuro.2004.10.011>. – DOI 10.1016/j.clineuro.2004.10.011

- [21] ARAI, Tetsuaki ; IKEDA, Kenji ; AKIYAMA, Haruhiko ; NONAKA, Takashi ; HASEGAWA, Masato ; ISHIGURO, Koichi ; IRITANI, Shuji ; TSUCHIYA, Kuniaki ; ISEKI, Eizo ; YAGISHITA, Saburo ; ODA, Tatsuro ; MOCHIZUKI, Akihide: Identification of amino-terminally cleaved tau fragments that distinguish progressive supranuclear palsy from corticobasal degeneration. In: *Ann Neurol* 55 (2004), Jan, Nr. 1, 72–9. <http://dx.doi.org/10.1002/ana.10793>. – DOI 10.1002/ana.10793
- [22] ARENDT, Thomas ; STIELER, Jens ; STRIJKSTRA, Arjen M. ; HUT, Roelof A. ; RÜDIGER, Jan ; ZEE, Eddy A V. ; HARKANY, Tibor ; HOLZER, Max ; HÄRTIG, Wolfgang: Reversible paired helical filament-like phosphorylation of tau is an adaptive process associated with neuronal plasticity in hibernating animals. In: *J Neurosci* 23 (2003), Aug, Nr. 18, S. 6972–81
- [23] ARIMA, K ; IZUMIYAMA, Y ; NAKAMURA, M ; NAKAYAMA, H ; KIMURA, M ; ANDO, S ; IKEDA, K ; TAKAHASHI, K: Argyrophilic tau-positive twisted and non-twisted tubules in astrocytic processes in brains of Alzheimer-type dementia: an electron microscopical study. In: *Acta Neuropathol* 95 (1998), Jan, Nr. 1, S. 28–39
- [24] ARMSTRONG, Melissa J. ; LITVAN, Irene ; LANG, Anthony E. ; BAK, Thomas H. ; BHATIA, Kailash P. ; BORRONI, Barbara ; BOXER, Adam L. ; DICKSON, Dennis W. ; GROSSMAN, Murray ; HALLETT, Mark ; JOSEPHS, Keith A. ; KERTESZ, Andrew ; LEE, Suzee E. ; MILLER, Bruce L. ; REICH, Stephen G. ; RILEY, David E. ; TOLOSA, Eduardo ; TRÖSTER, Alexander I. ; VIDAILHET, Marie ; WEINER, William J.: Criteria for the diagnosis of corticobasal degeneration. In: *Neurology* 80 (2013), Jan, Nr. 5, S. 496–503. <http://dx.doi.org/10.1212/WNL.0b013e31827f0fd1>. – DOI 10.1212/WNL.0b013e31827f0fd1
- [25] ARNAUD, L ; MYEKU, N ; FIGUEIREDO-PEREIRA, M: Proteasome-caspase-cathepsin sequence leading to tau pathology induced by prostaglandin J2 in neuronal cells. In: *J Neurochem* 110 (2009), Jul, Nr. 1, 328–42. <http://dx.doi.org/10.1111/j.1471-4159.2009.06142.x>. – DOI 10.1111/j.1471-4159.2009.06142.x
- [26] ARNOLD, C ; JOHNSON, G ; COLE, R ; DONG, D ; LEE, M ; HART, G: The microtubule-associated protein tau is extensively modified with O-linked N-acetylglucosamine. In: *J Biol Chem* 271 (1996), Nov, Nr. 46, 28741–4. <http://www.ncbi.nlm.nih.gov/pubmed/8910513>
- [27] ARNOLD, S E. ; HYMAN, B T. ; FLORY, J ; DAMASIO, A R. ; HOESEN, G W V.: The topographical and neuroanatomical distribution of neurofibrillary tangles and neuritic plaques in the cerebral cortex of patients with Alzheimer's disease. In: *Cereb Cortex* 1 (1991), Jan, Nr. 1, S. 103–16
- [28] ARRIAGADA, P V. ; MARZLOFF, K ; HYMAN, B T.: Distribution of Alzheimer-type pathologic changes in nondemented elderly individuals matches the pattern in Alzheimer's disease. In: *Neurology* 42 (1992), Sep, Nr. 9, S. 1681–8
- [29] ASSOCIATION, Alzheimer's: 2015 Alzheimer's disease facts and figures. In: *Alzheimer's & dementia : the journal of the Alzheimer's Association* 11 (2015), Mar, Nr. 3, 332–84. http://www.ncbi.nlm.nih.gov/entrez/query.fcgi?db=pubmed&cmd=Retrieve&dopt=AbstractPlus&list_uids=25984581
- [30] ASUNI, Ayodeji A. ; BOUTAJANGOUT, Allal ; QUARTERMAIN, David ; SIGURDSSON, Einar M.: Immunotherapy targeting pathological tau conformers in a tangle mouse model reduces brain pathology with associated functional improvements. In: *J Neurosci* 27 (2007), Aug, Nr. 34, 9115–29. <http://dx.doi.org/10.1523/JNEUROSCI.2361-07.2007>. – DOI 10.1523/JNEUROSCI.2361-07.2007
- [31] AVILA, Jesus ; LUCAS, Jose J. ; PEREZ, Mar ; HERNANDEZ, Felix: Role of tau protein in both physiological and pathological conditions. In: *Physiol Rev* 84 (2004), Apr, Nr. 2, 361–84. <http://dx.doi.org/10.1152/physrev.00024.2003>. – DOI 10.1152/physrev.00024.2003
- [32] BAAS, P W. ; PIENKOWSKI, T P. ; KOSIK, K S.: Processes induced by tau expression in Sf9 cells have an axon-like microtubule organization. In: *J Cell Biol* 115 (1991), Dec, Nr. 5, S. 1333–44
- [33] BALLATORE, Carlo ; LEE, Virginia ; TROJANOWSKI, John: Tau-mediated neurodegeneration in Alzheimer's disease and related disorders. In: *Nat Rev Neurosci* 8 (2007), Sep, Nr. 9, 663–72. <http://dx.doi.org/10.1038/nrn2194>. – DOI 10.1038/nrn2194

- [34] BANCHER, C ; BRUNNER, C ; LASSMANN, H ; BUDKA, H ; JELLINGER, K ; WICHE, G ; SEITELBERGER, F ; GRUNDKE-IQBAL, I ; IQBAL, K ; WISNIEWSKI, H M.: Accumulation of abnormally phosphorylated tau precedes the formation of neurofibrillary tangles in Alzheimer's disease. In: *Brain Res* 477 (1989), Jan, Nr. 1-2, S. 90–9
- [35] BANG, J ; SPINA, S ; MILLER, B: Frontotemporal dementia. In: *Lancet* 386 (2015), Oct, Nr. 10004, 1672–82. [http://dx.doi.org/10.1016/S0140-6736\(15\)00461-4](http://dx.doi.org/10.1016/S0140-6736(15)00461-4). – DOI 10.1016/S0140-6736(15)00461-4
- [36] BARGHORN, S ; BIERNAT, J ; MANDELKOW, E: Purification of recombinant tau protein and preparation of Alzheimer-paired helical filaments in vitro. In: *Methods Mol Biol* 299 (2005), 35–51. <http://www.ncbi.nlm.nih.gov/pubmed/15980594>
- [37] BARGHORN, S ; ZHENG-FISCHHÖFER, Q ; ACKMANN, M ; BIERNAT, J ; BERGEN, M von ; MANDELKOW, E M. ; MANDELKOW, E: Structure, microtubule interactions, and paired helical filament aggregation by tau mutants of frontotemporal dementias. In: *Biochemistry* 39 (2000), Sep, Nr. 38, 11714–21. <http://pubs.acs.org/doi/abs/10.1021/bi000850r>
- [38] BARKER, Warren W. ; LUIS, Cheryl A. ; KASHUBA, Alice ; LUIS, Mercy ; HARWOOD, Dylan G. ; LOEWENSTEIN, David ; WATERS, Carol ; JIMISON, Pat ; SHEPHERD, Eugene ; SEVUSH, Steven ; GRAFF-RADFORD, Neil ; NEWLAND, Douglas ; TODD, Murray ; MILLER, Bayard ; GOLD, Michael ; HELLMAN, Kenneth ; DOTY, Leilani ; GOODMAN, Ira ; ROBINSON, Bruce ; PEARL, Gary ; DICKSON, Dennis ; DUARA, Ranjan: Relative frequencies of Alzheimer disease, Lewy body, vascular and frontotemporal dementia, and hippocampal sclerosis in the State of Florida Brain Bank. In: *Alzheimer Dis Assoc Disord* 16 (2002), Jan, Nr. 4, S. 203–12
- [39] BARTEN, Donna M. ; FANARA, Patrizia ; ANDORFER, Cathy ; HOQUE, Nina ; WONG, P Y A. ; HUSTED, Kristofor H. ; CADELINA, Gregory W. ; DECARR, Lynn B. ; YANG, Ling ; LIU, Victoria ; FESSLER, Chancy ; PROTASSIO, Joan ; RIFF, Timothy ; TURNER, Holly ; JANUS, Christopher G. ; SANKARANARAYANAN, Sethu ; POLSON, Craig ; MEREDITH, Jere E. ; GRAY, Gemma ; HANNA, Amanda ; OLSON, Richard E. ; KIM, Soong-Hoon ; VITE, Gregory D. ; LEE, Francis Y. ; ALBRIGHT, Charles F.: Hyperdynamic microtubules, cognitive deficits, and pathology are improved in tau transgenic mice with low doses of the microtubule-stabilizing agent BMS-241027. In: *J Neurosci* 32 (2012), May, Nr. 21, S. 7137–45. <http://dx.doi.org/10.1523/JNEUROSCI.0188-12.2012>. – DOI 10.1523/JNEUROSCI.0188-12.2012
- [40] BARTHÉLEMY, Nicolas R. ; FENAILE, François ; HIRTZ, Christophe ; SERGEANT, Nicolas ; SCHRAEN-MASCHKE, Susanna ; VIALARET, Jérôme ; BUÉE, Luc ; GABELLE, Audrey ; JUNOT, Christophe ; LEHMANN, Sylvain ; BECHER, François: Tau Protein Quantification in Human Cerebrospinal Fluid by Targeted Mass Spectrometry at High Sequence Coverage Provides Insights into Its Primary Structure Heterogeneity. In: *J Proteome Res* 15 (2016), Feb, Nr. 2, S. 667–76. <http://dx.doi.org/10.1021/acs.jproteome.5b01001>. – DOI 10.1021/acs.jproteome.5b01001
- [41] BASURTO-ISLAS, Gustavo ; LUNA-MUÑOZ, Jose ; GUILLOZET-BONGAARTS, Angela L. ; BINDER, Lester I. ; MENA, Raul ; GARCÍA-SIERRA, Francisco: Accumulation of aspartic acid421- and glutamic acid391-cleaved tau in neurofibrillary tangles correlates with progression in Alzheimer disease. In: *J Neuropathol Exp Neurol* 67 (2008), May, Nr. 5, S. 470–83. <http://dx.doi.org/10.1097/NEN.0b013e31817275c7>. – DOI 10.1097/NEN.0b013e31817275c7
- [42] BATEMAN, Randall J. ; XIONG, Chengjie ; BENZINGER, Tammie L S. ; FAGAN, Anne M. ; GOATE, Alison ; FOX, Nick C. ; MARCUS, Daniel S. ; CAIRNS, Nigel J. ; XIE, Xianyun ; BLAZEY, Tyler M. ; HOLTZMAN, David M. ; SANTACRUZ, Anna ; BUCKLES, Virginia ; OLIVER, Angela ; MOULDER, Krista ; AISEN, Paul S. ; GHETTI, Bernardino ; KLUNK, William E. ; MCDADE, Eric ; MARTINS, Ralph N. ; MASTERS, Colin L. ; MAYEUX, Richard ; RINGMAN, John M. ; ROSSOR, Martin N. ; SCHOFIELD, Peter R. ; SPERLING, Reisa A. ; SALLOWAY, Stephen ; MORRIS, John C. ; NETWORK, Dominantly Inherited A.: Clinical and biomarker changes in dominantly inherited Alzheimer's disease. In: *N Engl J Med* 367 (2012), Aug, Nr. 9, S. 795–804. <http://dx.doi.org/10.1056/NEJMoa1202753>. – DOI 10.1056/NEJMoa1202753
- [43] BECKER, R E. ; GREIG, N H.: Why so few drugs for Alzheimer's disease? Are methods failing drugs? In: *Curr Alzheimer Res* 7 (2010), Nov, Nr. 7, S. 642–51

- [44] BECKER, Robert E. ; GREIG, Nigel H.: Increasing the success rate for Alzheimer's disease drug discovery and development. In: *Expert Opin Drug Discov* 7 (2012), Apr, Nr. 4, S. 367–70. <http://dx.doi.org/10.1517/17460441.2012.672409>. – DOI 10.1517/17460441.2012.672409
- [45] BECKER, Robert E. ; GREIG, Nigel H. ; GIACOBINI, Ezio: Why do so many drugs for Alzheimer's disease fail in development? Time for new methods and new practices? In: *J Alzheimers Dis* 15 (2008), Oct, Nr. 2, S. 303–25
- [46] BERGEN, M von ; BARGHORN, S ; JEGANATHAN, S ; MANDELKOW, E-M ; MANDELKOW, E: Spectroscopic approaches to the conformation of tau protein in solution and in paired helical filaments. In: *Neurodegener Dis* 3 (2006), Jan, Nr. 4-5, S. 197–206. <http://dx.doi.org/10.1159/000095257>. – DOI 10.1159/000095257
- [47] BERGEN, M von ; FRIEDHOFF, P ; BIERNAT, J ; HEBERLE, J ; MANDELKOW, E M. ; MANDELKOW, E: Assembly of tau protein into Alzheimer paired helical filaments depends on a local sequence motif ((306)VQIVYK(311)) forming beta structure. In: *Proc Natl Acad Sci USA* 97 (2000), May, Nr. 10, S. 5129–34
- [48] BERGER, Zdenek ; RODER, Hanno ; HANNA, Amanda ; CARLSON, Aaron ; RANGACHARI, Vijayaraghavan ; YUE, Mei ; WSZOLEK, Zbigniew ; ASHE, Karen ; KNIGHT, Joshua ; DICKSON, Dennis ; ANDORFER, Cathy ; ROSENBERRY, Terrone L. ; LEWIS, Jada ; HUTTON, Mike ; JANUS, Christopher: Accumulation of pathological tau species and memory loss in a conditional model of tauopathy. In: *J Neurosci* 27 (2007), Apr, Nr. 14, S. 3650–62. <http://dx.doi.org/10.1523/JNEUROSCI.0587-07.2007>. – DOI 10.1523/JNEUROSCI.0587-07.2007
- [49] BERRIMAN, John ; SERPELL, Louise C. ; OBERG, Keith A. ; FINK, Anthony L. ; GOEDERT, Michel ; CROWTHER, R A.: Tau filaments from human brain and from in vitro assembly of recombinant protein show cross-beta structure. In: *Proc Natl Acad Sci USA* 100 (2003), Jul, Nr. 15, 9034–8. <http://dx.doi.org/10.1073/pnas.1530287100>. – DOI 10.1073/pnas.1530287100
- [50] BEYNON, Robert J. ; DOHERTY, Mary K. ; PRATT, Julie M. ; GASKELL, Simon J.: Multiplexed absolute quantification in proteomics using artificial QCAT proteins of concatenated signature peptides. In: *Nat Methods* 2 (2005), Aug, Nr. 8, S. 587–9. <http://dx.doi.org/10.1038/nmeth774>. – DOI 10.1038/nmeth774
- [51] BHAUMIK, Sukesh R. ; SMITH, Edwin ; SHILATIFARD, Ali: Covalent modifications of histones during development and disease pathogenesis. In: *Nat Struct Mol Biol* 14 (2007), Nov, Nr. 11, S. 1008–16. <http://dx.doi.org/10.1038/nsmb1337>. – DOI 10.1038/nsmb1337
- [52] BI, Mian ; ITTNER, Arne ; KE, Yazi D. ; GÖTZ, Jürgen ; ITTNER, Lars M.: Tau-targeted immunization impedes progression of neurofibrillary histopathology in aged P301L tau transgenic mice. In: *PLoS ONE* 6 (2011), Jan, Nr. 12, S. e26860. <http://dx.doi.org/10.1371/journal.pone.0026860>. – DOI 10.1371/journal.pone.0026860
- [53] BIERNAT, J ; GUSTKE, N ; DREWES, G ; MANDELKOW, E ; MANDELKOW, E: Phosphorylation of Ser262 strongly reduces binding of tau to microtubules: distinction between PHF-like immunoreactivity and microtubule binding. In: *Neuron* 11 (1993), Jul, Nr. 1, 153–63. <http://www.ncbi.nlm.nih.gov/pubmed/8393323>
- [54] BIERNAT, J ; MANDELKOW, E: The development of cell processes induced by tau protein requires phosphorylation of serine 262 and 356 in the repeat domain and is inhibited by phosphorylation in the proline-rich domains. In: *Mol Biol Cell* 10 (1999), Mar, Nr. 3, 727–40. <http://www.ncbi.nlm.nih.gov/pubmed/10069814>
- [55] BIERNAT, J ; MANDELKOW, E M. ; SCHRÖTER, C ; LICHTENBERG-KRAAG, B ; STEINER, B ; BERLING, B ; MEYER, H ; MERCKEN, M ; VANDERMEEREN, A ; GOEDERT, M: The switch of tau protein to an Alzheimer-like state includes the phosphorylation of two serine-proline motifs upstream of the microtubule binding region. In: *EMBO J* 11 (1992), Apr, Nr. 4, S. 1593–7
- [56] BIGIO, E H. ; BROWN, D F. ; WHITE, C L.: Progressive supranuclear palsy with dementia: cortical pathology. In: *J Neuropathol Exp Neurol* 58 (1999), Apr, Nr. 4, S. 359–64

- [57] BILLINGSLEY, M L. ; KINCAID, R L.: Regulated phosphorylation and dephosphorylation of tau protein: effects on microtubule interaction, intracellular trafficking and neurodegeneration. In: *Biochem J* 323 (Pt 3) (1997), May, 577–91. <http://www.biochemj.org/content/323/3/577.long>
- [58] BIRD, T ; KNOPMAN, D ; VANSWIETEN, J ; ROSSO, S ; FELDMAN, H ; TANABE, H ; GRAFF-RAFORD, N ; GESCHWIND, D ; VERPILLAT, P ; HUTTON, M: Epidemiology and genetics of frontotemporal dementia/Pick's disease. In: *Ann Neurol* 54 Suppl 5 (2003), S29–31. <http://dx.doi.org/10.1002/ana.10572>. – DOI 10.1002/ana.10572
- [59] BISHOP, C: *Neural Networks for Pattern Recognition*. 1995
- [60] BLENNOW, K ; VANMECHELEN, E ; HAMPEL, H: CSF total tau, Abeta42 and phosphorylated tau protein as biomarkers for Alzheimer's disease. In: *Mol Neurobiol* 24 (2001), Jan, Nr. 1-3, S. 87–97. <http://dx.doi.org/10.1385/MN:24:1-3:087>. – DOI 10.1385/MN:24:1-3:087
- [61] BLENNOW, K ; WALLIN, A ; AGREN, H ; SPENGER, C ; SIEGFRIED, J ; VANMECHELEN, E: Tau protein in cerebrospinal fluid: a biochemical marker for axonal degeneration in Alzheimer disease? In: *Mol Chem Neuropathol* 26 (1995), Dec, Nr. 3, S. 231–45. <http://dx.doi.org/10.1007/BF02815140>. – DOI 10.1007/BF02815140
- [62] BOEVE, B ; LANG, A ; LITVAN, I: Corticobasal degeneration and its relationship to progressive supranuclear palsy and frontotemporal dementia. In: *Ann Neurol* 54 Suppl 5 (2003), S15–9. <http://dx.doi.org/10.1002/ana.10570>. – DOI 10.1002/ana.10570
- [63] BOEVE, B F. ; MARAGANORE, D M. ; PARISI, J E. ; AHLKOG, J E. ; GRAFF-RADFORD, N ; CASELLI, R J. ; DICKSON, D W. ; KOKMEN, E ; PETERSEN, R C.: Pathologic heterogeneity in clinically diagnosed corticobasal degeneration. In: *Neurology* 53 (1999), Sep, Nr. 4, S. 795–800
- [64] BOHM, K ; VATER, W ; STEINMETZER, P ; KUSNETSOV, S ; RODIONOV, V ; GELFAND, V ; UNGER, E: Effect of MAP 1, MAP 2, and tau-proteins on structural parameters of tubulin assemblies. In: *Acta Histochem Suppl* 39 (1990), 357–64. <http://www.ncbi.nlm.nih.gov/pubmed/2127856>
- [65] BOIMEL, Moran ; GRIGORIADIS, Nikolaos ; LOURBOPOULOS, Athanasios ; HABER, Esther ; ABRAMSKY, Oded ; ROSENMAN, Hanna: Efficacy and safety of immunization with phosphorylated tau against neurofibrillary tangles in mice. In: *Exp Neurol* 224 (2010), Aug, Nr. 2, S. 472–85. <http://dx.doi.org/10.1016/j.expneurol.2010.05.010>. – DOI 10.1016/j.expneurol.2010.05.010
- [66] BOJA, Emily S. ; PHILLIPS, Darci ; FRENCH, Stephanie A. ; HARRIS, Robert A. ; BALABAN, Robert S.: Quantitative mitochondrial phosphoproteomics using iTRAQ on an LTQ-Orbitrap with high energy collision dissociation. In: *J Proteome Res* 8 (2009), Oct, Nr. 10, S. 4665–75. <http://dx.doi.org/10.1021/pr900387b>. – DOI 10.1021/pr900387b
- [67] BOUTAJANGOUT, Allal ; INGADOTTIR, Johanna ; DAVIES, Peter ; SIGURDSSON, Einar M.: Passive immunization targeting pathological phospho-tau protein in a mouse model reduces functional decline and clears tau aggregates from the brain. In: *J Neurochem* 118 (2011), Aug, Nr. 4, S. 658–67. <http://dx.doi.org/10.1111/j.1471-4159.2011.07337.x>. – DOI 10.1111/j.1471-4159.2011.07337.x
- [68] BOUWMAN, F H. ; FLIER, W M. d. ; SCHOONENBOOM, N S M. ; ELK, E J. ; KOK, A ; RIJMEN, F ; BLANKENSTEIN, M A. ; SCHELTENS, P: Longitudinal changes of CSF biomarkers in memory clinic patients. In: *Neurology* 69 (2007), Sep, Nr. 10, S. 1006–11. <http://dx.doi.org/10.1212/01.wnl.0000271375.37131.04>. – DOI 10.1212/01.wnl.0000271375.37131.04
- [69] BOXER, Adam L. ; LANG, Anthony E. ; GROSSMAN, Murray ; KNOPMAN, David S. ; MILLER, Bruce L. ; SCHNEIDER, Lon S. ; DOODY, Rachele S. ; LEES, Andrew ; GOLBE, Lawrence I. ; WILLIAMS, David R. ; CORVOL, Jean-Cristophe ; LUDOLPH, Albert ; BURN, David ; LORENZL, Stefan ; LITVAN, Irene ; ROBERSON, Erik D. ; HÖGLINGER, Günter U ; KOESTLER, Mary ; JACK, Clifford R. ; DEERLIN, Viviana V. ; RANDOLPH, Christopher ; LOBACH, Iryna V. ; HEUER, Hilary W. ; GOZES, Illana ; PARKER, Lesley ; WHITAKER, Steve ; HIRMAN, Joe ; STEWART, Alistair J. ; GOLD, Michael ; MORIMOTO, Bruce H. ; INVESTIGATORS, AL-108-231: Davunetide in patients with progressive supranuclear palsy: a randomised, double-blind, placebo-controlled phase 2/3 trial. In: *The Lancet Neurology* 13 (2014), Jul, Nr. 7, S. 676–85. [http://dx.doi.org/10.1016/S1474-4422\(14\)70088-2](http://dx.doi.org/10.1016/S1474-4422(14)70088-2). – DOI 10.1016/S1474-4422(14)70088-2

- [70] BRAAK, H ; BRAAK, E: Neuropathological staging of Alzheimer-related changes. In: *Acta Neuropathol* 82 (1991), Jan, Nr. 4, S. 239–59
- [71] BRAAK, H ; BRAAK, E: Argyrophilic grain disease: frequency of occurrence in different age categories and neuropathological diagnostic criteria. In: *J Neural Transm* 105 (1998), Jan, Nr. 8-9, S. 801–19
- [72] BRAAK, H ; JELLINGER, K ; BRAAK, E ; BOHL, J: Allocortical neurofibrillary changes in progressive supranuclear palsy. In: *Acta Neuropathol* 84 (1992), Nr. 5, 478–83. <http://www.ncbi.nlm.nih.gov/pubmed/1462762>
- [73] BRAAK, Heiko ; ALAFUZOFF, Irina ; ARZBERGER, Thomas ; KRETZSCHMAR, Hans ; TREDICI, Kelly D.: Staging of Alzheimer disease-associated neurofibrillary pathology using paraffin sections and immunocytochemistry. In: *Acta Neuropathol* 112 (2006), Oct, Nr. 4, S. 389–404. <http://dx.doi.org/10.1007/s00401-006-0127-z>. – DOI 10.1007/s00401-006-0127-z
- [74] BRAMBLETT, G T. ; GOEDERT, M ; JAKES, R ; MERRICK, S E. ; TROJANOWSKI, J Q. ; LEE, V M.: Abnormal tau phosphorylation at Ser396 in Alzheimer's disease recapitulates development and contributes to reduced microtubule binding. In: *Neuron* 10 (1993), Jun, Nr. 6, 1089–99. [http://www.cell.com/neuron/abstract/S0896-6273\(93\)90057-X?_returnURL=http%253A%252F%252Flinkinghub.elsevier.com%252Fretrieve%252Fpii%252F089662739390057X%253Fshowall%253Dtrue](http://www.cell.com/neuron/abstract/S0896-6273(93)90057-X?_returnURL=http%253A%252F%252Flinkinghub.elsevier.com%252Fretrieve%252Fpii%252F089662739390057X%253Fshowall%253Dtrue)
- [75] BRANDT, R ; LEE, G: The balance between tau protein's microtubule growth and nucleation activities: implications for the formation of axonal microtubules. In: *J Neurochem* 61 (1993), Sep, Nr. 3, 997–1005. <http://www.ncbi.nlm.nih.gov/pubmed/8360696>
- [76] BREIMAN, Jerome L.: Classification and Regression Trees. In: *Wadsworth Statistics/Probability* 1st Edition (1984)
- [77] BRONNER, I F. ; MEULEN, B C. ; AZMANI, A ; SEVERIJNEN, L A. ; WILLEMSSEN, R ; KAMPHORST, W ; RAVID, R ; HEUTINK, P ; SWIETEN, J C.: Hereditary Pick's disease with the G272V tau mutation shows predominant three-repeat tau pathology. In: *Brain* 128 (2005), Nov, Nr. Pt 11, S. 2645–53. <http://dx.doi.org/10.1093/brain/awh591>. – DOI 10.1093/brain/awh591
- [78] BROS, Pauline ; VIALARET, Jérôme ; BARTHELEMY, Nicolas ; DELATOUR, Vincent ; GABELLE, Audrey ; LEHMANN, Sylvain ; HIRTZ, Christophe: Antibody-free quantification of seven tau peptides in human CSF using targeted mass spectrometry. In: *Front. Neurosci.* 9 (2015), Jan, 302. <http://dx.doi.org/10.3389/fnins.2015.00302>. – DOI 10.3389/fnins.2015.00302
- [79] BRUNDEN, Kurt R. ; TROJANOWSKI, John Q. ; LEE, Virginia M-Y: Advances in tau-focused drug discovery for Alzheimer's disease and related tauopathies. In: *Nat Rev Drug Discov* 8 (2009), Oct, Nr. 10, S. 783–93. <http://dx.doi.org/10.1038/nrd2959>. – DOI 10.1038/nrd2959
- [80] BRUNDEN, Kurt R. ; ZHANG, Bin ; CARROLL, Jenna ; YAO, Yuemang ; POTUZAK, Justin S. ; HOGAN, Anne-Marie L. ; IBA, Michiyo ; JAMES, Michael J. ; XIE, Sharon X. ; BALLATORE, Carlo ; SMITH, Amos B. ; LEE, Virginia M-Y ; TROJANOWSKI, John Q.: Epopthilone D improves microtubule density, axonal integrity, and cognition in a transgenic mouse model of tauopathy. In: *J Neurosci* 30 (2010), Oct, Nr. 41, S. 13861–6. <http://dx.doi.org/10.1523/JNEUROSCI.3059-10.2010>. – DOI 10.1523/JNEUROSCI.3059-10.2010
- [81] BRUYN, G W. ; ROOS, R A.: Senile plaques in Huntington's disease: a preliminary report. In: *Clin Neurol Neurosurg* 92 (1990), Jan, Nr. 4, S. 329–31
- [82] BUÉE, L ; BUSSIÈRE, T ; BUÉE-SCHERRER, V ; DELACOURTE, A ; HOF, P R.: Tau protein isoforms, phosphorylation and role in neurodegenerative disorders. In: *Brain Res Brain Res Rev* 33 (2000), Aug, Nr. 1, S. 95–130
- [83] BUNKER, J ; WILSON, L ; JORDAN, M ; FEINSTEIN, S: Modulation of microtubule dynamics by tau in living cells: implications for development and neurodegeneration. In: *Mol Biol Cell* 15 (2004), Jun, Nr. 6, 2720–8. <http://dx.doi.org/10.1091/mbc.E04-01-0062>. – DOI 10.1091/mbc.E04-01-0062

- [84] BUSTOS, Daisy ; BAKALARSKI, Corey E. ; YANG, Yanling ; PENG, Junmin ; KIRKPATRICK, Donald S.: Characterizing ubiquitination sites by peptide-based immunoaffinity enrichment. In: *Mol Cell Proteomics* 11 (2012), Dec, Nr. 12, S. 1529–40. <http://dx.doi.org/10.1074/mcp.R112.019117>. – DOI 10.1074/mcp.R112.019117
- [85] CACERES, A ; KOSIK, K: Inhibition of neurite polarity by tau antisense oligonucleotides in primary cerebellar neurons. In: *Nature* 343 (1990), Feb, Nr. 6257, 461–3. <http://dx.doi.org/10.1038/343461a0>. – DOI 10.1038/343461a0
- [86] CAHILL, Suzanne ; PIERCE, Maria ; WERNER, Perla ; DARLEY, Andrew ; BOBERSKY, Andrea: A systematic review of the public's knowledge and understanding of Alzheimer's disease and dementia. In: *Alzheimer Dis Assoc Disord* 29 (2015), Jan, Nr. 3, S. 255–75. <http://dx.doi.org/10.1097/WAD.000000000000102>. – DOI 10.1097/WAD.000000000000102
- [87] CAMBIAZO, V ; GONZALEZ, M ; MACCIONI, R: DMAP-85: a tau-like protein from *Drosophila melanogaster* larvae. In: *J Neurochem* 64 (1995), Mar, Nr. 3, 1288–97. <http://www.ncbi.nlm.nih.gov/pubmed/7861162>
- [88] CAMERON, Brent ; LANDRETH, Gary E.: Inflammation, microglia, and Alzheimer's disease. In: *Neurobiol Dis* 37 (2010), Mar, Nr. 3, S. 503–9. <http://dx.doi.org/10.1016/j.nbd.2009.10.006>. – DOI 10.1016/j.nbd.2009.10.006
- [89] CAPPELLETTI, Graziella ; TEDESCHI, Gabriella ; MAGGIONI, Maria G. ; NEGRI, Armando ; NONNIS, Simona ; MACI, Rosalba: The nitration of tau protein in neurone-like PC12 cells. In: *FEBS Letters* 562 (2004), Mar, Nr. 1-3, S. 35–9. [http://dx.doi.org/10.1016/S0014-5793\(04\)00173-5](http://dx.doi.org/10.1016/S0014-5793(04)00173-5). – DOI 10.1016/S0014-5793(04)00173-5
- [90] CASTILLO-CARRANZA, Diana L. ; SENGUPTA, Urmi ; GUERRERO-MUÑOZ, Marcos J. ; LASAGNA-REEVES, Cristian A. ; GERSON, Julia E. ; SINGH, Gurpreet ; ESTES, D M. ; BARRETT, Alan D T. ; DINELEY, Kelly T. ; JACKSON, George R. ; KAYED, Rakez: Passive immunization with Tau oligomer monoclonal antibody reverses tauopathy phenotypes without affecting hyperphosphorylated neurofibrillary tangles. In: *The Journal of neuroscience : the official journal of the Society for Neuroscience* 34 (2014), Mar, Nr. 12, S. 4260–72. <http://dx.doi.org/10.1523/JNEUROSCI.3192-13.2014>. – DOI 10.1523/JNEUROSCI.3192-13.2014
- [91] CHEN, Feng ; DAVID, Della ; FERRARI, Alessandra ; GÖTZ, Jürgen: Posttranslational modifications of tau—role in human tauopathies and modeling in transgenic animals. In: *Curr Drug Targets* 5 (2004), Aug, Nr. 6, 503–15. <http://www.eurekaselect.com/62936/article>
- [92] CHIN, S ; GOLDMAN, J: Glial inclusions in CNS degenerative diseases. In: *J Neuropathol Exp Neurol* 55 (1996), May, Nr. 5, 499–508. <http://www.ncbi.nlm.nih.gov/pubmed/8627339>
- [93] CHOUDHARY, Chunaram ; WEINERT, Brian T. ; NISHIDA, Yuya ; VERDIN, Eric ; MANN, Matthias: The growing landscape of lysine acetylation links metabolism and cell signalling. In: *Nat Rev Mol Cell Biol* 15 (2014), Aug, Nr. 8, S. 536–50. <http://dx.doi.org/10.1038/nrm3841>. – DOI 10.1038/nrm3841
- [94] CHUNG, C W. ; SONG, Y H. ; KIM, I K. ; YOON, W J. ; RYU, B R. ; JO, D G. ; WOO, H N. ; KWON, Y K. ; KIM, H H. ; GWAG, B J. ; MOOK-JUNG, I H. ; JUNG, Y K.: Proapoptotic effects of tau cleavage product generated by caspase-3. In: *Neurobiol Dis* 8 (2001), Feb, Nr. 1, S. 162–72. <http://dx.doi.org/10.1006/nbdi.2000.0335>. – DOI 10.1006/nbdi.2000.0335
- [95] CLEVELAND, D ; HWO, S ; KIRSCHNER, M: Physical and chemical properties of purified tau factor and the role of tau in microtubule assembly. In: *J Mol Biol* 116 (1977), Oct, Nr. 2, 227–47. <http://www.ncbi.nlm.nih.gov/pubmed/146092>
- [96] CLEVELAND, D ; HWO, S ; KIRSCHNER, M: Purification of tau, a microtubule-associated protein that induces assembly of microtubules from purified tubulin. In: *J Mol Biol* 116 (1977), Oct, Nr. 2, 207–25. <http://www.ncbi.nlm.nih.gov/pubmed/599557>

- [97] COHEN, Todd ; GUO, Jing ; HURTADO, David ; KWONG, Linda ; MILLS, Ian ; TROJANOWSKI, John ; LEE, Virginia: The acetylation of tau inhibits its function and promotes pathological tau aggregation. In: *Nature Communications* 2 (2011), Jan, 252. <http://dx.doi.org/10.1038/ncomms1255>. – DOI 10.1038/ncomms1255
- [98] COHEN, Todd J. ; GUO, Jing L. ; HURTADO, David E. ; KWONG, Linda K. ; MILLS, Ian P. ; TROJANOWSKI, John Q. ; LEE, Virginia M Y.: The acetylation of tau inhibits its function and promotes pathological tau aggregation. In: *Nat Comms* 2 (2011), Jan, S. 252. <http://dx.doi.org/10.1038/ncomms1255>. – DOI 10.1038/ncomms1255
- [99] COLOMÉE, N ; CAMPOS, A ; MARTÉINEZ-BARTOLOMÉE, S ; PARADELA, A ; PROTEORED, Iscii ; OLIVEIRA, E de ; RADABAUGH, M ; WALTERS, J ; RAY, K ; ALBAR, J ; CANALS, Francesc: A Multi-Centric Study To Assess Reproducibility of Protein Quantification By SRM LC-MS Proteomic Analysis. In: *Journal of Biomolecular Techniques : JBT* 23 (2012), Nr. Suppl, S57–S57. <http://www.ncbi.nlm.nih.gov/pmc/articles/PMC3630565/>. – 202[PII] J Biomol Tech
- [100] CONSTANTINIDIS, J ; RICHARD, J ; TISSOT, R: Pick's disease. Histological and clinical correlations. In: *Eur Neurol* 11 (1974), Jan, Nr. 4, S. 208–17
- [101] CORRE, Sylvie L. ; KLAFKI, Hans W. ; PLESNILA, Nikolaus ; HÜBINGER, Gabriele ; OBERMEIER, Axel ; SAHAGÚN, Heidi ; MONSE, Barbara ; SENECI, Pierfausto ; LEWIS, Jada ; ERIKSEN, Jason ; ZEHR, Cynthia ; YUE, Mei ; MCGOWAN, Eileen ; DICKSON, Dennis W. ; HUTTON, Michael ; RÖDER, Hanno M.: An inhibitor of tau hyperphosphorylation prevents severe motor impairments in tau transgenic mice. In: *Proc Natl Acad Sci USA* 103 (2006), Jun, Nr. 25, S. 9673–8. <http://dx.doi.org/10.1073/pnas.0602913103>. – DOI 10.1073/pnas.0602913103
- [102] CORTES, Corinna ; VAPNIK, Vladimir: Support-Vector Networks. In: *Machine Learning* 20 (1995), Nr. 3, 273–297. <http://dx.doi.org/10.1023/A:1022627411411>. – DOI 10.1023/A:1022627411411
- [103] COUCHIE, D ; FAIVRE-BAUMAN, A ; PUYMIRAT, J ; GUILLEMINOT, J ; TIXIER-VIDAL, A ; NUNEZ, J: Expression of microtubule-associated proteins during the early stages of neurite extension by brain neurons cultured in a defined medium. In: *J Neurochem* 47 (1986), Oct, Nr. 4, 1255–61. <http://www.ncbi.nlm.nih.gov/pubmed/3528393>
- [104] COWAN, Catherine M. ; MUDHER, Amrit: Are tau aggregates toxic or protective in tauopathies? In: *Front. Neurol.* 4 (2013), Jan, S. 114. <http://dx.doi.org/10.3389/fneur.2013.00114>. – DOI 10.3389/fneur.2013.00114
- [105] COWAN, Catherine M. ; QURAIŠHE, Shmma ; MUDHER, Amritpal: What is the pathological significance of tau oligomers? In: *Biochem. Soc. Trans* 40 (2012), Aug, Nr. 4, S. 693–7. <http://dx.doi.org/10.1042/BST20120135>. – DOI 10.1042/BST20120135
- [106] CRARY, John F. ; TROJANOWSKI, John Q. ; SCHNEIDER, Julie A. ; ABISAMBRA, Jose F. ; ABNER, Erin L. ; ALAFUZOFF, Irina ; ARNOLD, Steven E. ; ATTEMS, Johannes ; BEACH, Thomas G. ; BIGIO, Eileen H. ; CAIRNS, Nigel J. ; DICKSON, Dennis W. ; GEARING, Marla ; GRINBERG, Lea T. ; HOF, Patrick R. ; HYMAN, Bradley T. ; JELLINGER, Kurt ; JICHA, Gregory A. ; KOVACS, Gabor G. ; KNOPMAN, David S. ; KOFLER, Julia ; KUKULL, Walter A. ; MACKENZIE, Ian R. ; MASLIAH, Eliezer ; MCKEE, Ann ; MONTINE, Thomas J. ; MURRAY, Melissa E. ; NELTNER, Janna H. ; SANTA-MARIA, Ismael ; SEELEY, William W. ; SERRANO-POZO, Alberto ; SHELANSKI, Michael L. ; STEIN, Thor ; TAKAO, Masaki ; THAL, Dietmar R. ; TOLEDO, Jonathan B. ; TRONCOSO, Juan C. ; VONSATTEL, Jean P. ; WHITE, Charles L. ; WISNIEWSKI, Thomas ; WOLTJER, Randall L. ; YAMADA, Masahito ; NELSON, Peter T.: Primary age-related tauopathy (PART): a common pathology associated with human aging. In: *Acta Neuropathol* 128 (2014), Dec, Nr. 6, S. 755–66. <http://dx.doi.org/10.1007/s00401-014-1349-0>. – DOI 10.1007/s00401-014-1349-0
- [107] CRAS, P ; KAWAI, M ; SIEDLAK, S ; PERRY, G: Microglia are associated with the extracellular neurofibrillary tangles of Alzheimer disease. In: *Brain Res* 558 (1991), Sep, Nr. 2, S. 312–4
- [108] CRIPPS, Diane ; THOMAS, Stefani N. ; JENG, Young ; YANG, Frank ; DAVIES, Peter ; YANG, Austin J.: Alzheimer disease-specific conformation of hyperphosphorylated paired helical filament-Tau is polyubiquitinated through Lys-48, Lys-11, and Lys-6 ubiquitin conjugation. In: *J Biol*

- Chem* 281 (2006), Apr, Nr. 16, 10825–38. <http://dx.doi.org/10.1074/jbc.M512786200>. – DOI 10.1074/jbc.M512786200
- [109] CROWTHER, R A. ; GOEDERT, M: Abnormal tau-containing filaments in neurodegenerative diseases. In: *J Struct Biol* 130 (2000), Jun, Nr. 2-3, S. 271–9. <http://dx.doi.org/10.1006/jsbi.2000.4270>. – DOI 10.1006/jsbi.2000.4270
- [110] CROWTHER, R A. ; WISCHIK, C M.: Image reconstruction of the Alzheimer paired helical filament. In: *EMBO J* 4 (1985), Dec, Nr. 13B, S. 3661–5
- [111] D'ALTON, Simon ; LEWIS, Jada: Therapeutic and diagnostic challenges for frontotemporal dementia. In: *Front Aging Neurosci* 6 (2014), Jan, S. 204. <http://dx.doi.org/10.3389/fnagi.2014.00204>. – DOI 10.3389/fnagi.2014.00204
- [112] DAMMER, E ; LEE, A ; DUONG, D ; GEARING, M ; LAH, J ; LEVEY, A ; SEYFRIED, N: Quantitative phosphoproteomics of Alzheimer's disease reveals cross-talk between kinases and small heat shock proteins. In: *PROTEOMICS* 15 (2015), Jan, Nr. 2-3, 508–19. <http://dx.doi.org/10.1002/pmic.201400189>. – DOI 10.1002/pmic.201400189
- [113] DAVID, Della C. ; LAYFIELD, Robert ; SERPELL, Louise ; NARAIN, Yolanda ; GOEDERT, Michel ; SPILLANTINI, Maria G.: Proteasomal degradation of tau protein. In: *J Neurochem* 83 (2002), Oct, Nr. 1, S. 176–85
- [114] DAYANANDAN, R ; SLEGTENHORST, M V. ; MACK, T G. ; KO, L ; YEN, S H. ; LEROY, K ; BRION, J P. ; ANDERTON, B H. ; HUTTON, M ; LOVESTONE, S: Mutations in tau reduce its microtubule binding properties in intact cells and affect its phosphorylation. In: *FEBS Lett* 446 (1999), Mar, Nr. 2-3, 228–32. [http://www.febsletters.org/article/S0014-5793\(99\)00222-7/abstract](http://www.febsletters.org/article/S0014-5793(99)00222-7/abstract)
- [115] DELACOURTE, A ; ROBITAILLE, Y ; SERGEANT, N ; BUÉE, L ; HOF, P R. ; WATTEZ, A ; LAROCHE-CHOLETTE, A ; MATHIEU, J ; CHAGNON, P ; GAUVREAU, D: Specific pathological Tau protein variants characterize Pick's disease. In: *J Neuropathol Exp Neurol* 55 (1996), Feb, Nr. 2, S. 159–68
- [116] DELACOURTE, A ; SERGEANT, N ; CHAMPAIN, D ; WATTEZ, A ; MAURAGE, C-A ; LEBERT, F ; PASQUIER, F ; DAVID, J-P: Nonoverlapping but synergetic tau and APP pathologies in sporadic Alzheimer's disease. In: *Neurology* 59 (2002), Aug, Nr. 3, S. 398–407
- [117] DELACOURTE, Andre: Tauopathies: recent insights into old diseases. In: *Folia Neuropathol* 43 (2005), Jan, Nr. 4, S. 244–57
- [118] DENG, Hao ; GAO, Kai ; JANKOVIC, Joseph: The role of FUS gene variants in neurodegenerative diseases. In: *Nat Rev Neurol* 10 (2014), Jun, Nr. 6, S. 337–48. <http://dx.doi.org/10.1038/nrneurol.2014.78>. – DOI 10.1038/nrneurol.2014.78
- [119] DICKEY, Chad A. ; DUNMORE, Judith ; LU, Bingwei ; WANG, Ji-Wu ; LEE, Wing C. ; KAMAL, Adeela ; BURROWS, Francis ; ECKMAN, Christopher ; HUTTON, Michael ; PETRUCELLI, Leonard: HSP induction mediates selective clearance of tau phosphorylated at proline-directed Ser/Thr sites but not KXGS (MARK) sites. In: *FASEB J* 20 (2006), Apr, Nr. 6, 753–5. <http://dx.doi.org/10.1096/fj.05-5343fje>. – DOI 10.1096/fj.05-5343fje
- [120] DICKSON, D W.: Neuropathologic differentiation of progressive supranuclear palsy and corticobasal degeneration. In: *J Neurol* 246 Suppl 2 (1999), Sep, S. II6–15
- [121] DICKSON, D W. ; BERGERON, C ; CHIN, S S. ; DUYNCKAERTS, C ; HOROUPIAN, D ; IKEDA, K ; JELLINGER, K ; LANTOS, P L. ; LIPPA, C F. ; MIRRA, S S. ; TABATON, M ; VONSATTEL, J P. ; WAKABAYASHI, K ; LITVAN, I ; HEALTH, Office of Rare Diseases of the National Institutes o.: Office of Rare Diseases neuropathologic criteria for corticobasal degeneration. In: *J Neuropathol Exp Neurol* 61 (2002), Nov, Nr. 11, S. 935–46
- [122] DICKSON, D W. ; CRYSTAL, H A. ; BEVONA, C ; HONER, W ; VINCENT, I ; DAVIES, P: Correlations of synaptic and pathological markers with cognition of the elderly. In: *Neurobiology of Aging* 16 (1995), Jan, Nr. 3, S. 285–98; discussion 298–304

- [123] DICKSON, D W. ; FEANY, M B. ; YEN, S H. ; MATTIACE, L A. ; DAVIES, P: Cytoskeletal pathology in non-Alzheimer degenerative dementia: new lesions in diffuse Lewy body disease, Pick's disease, and corticobasal degeneration. In: *J Neural Transm Suppl* 47 (1996), Jan, S. 31–46
- [124] DICKSON, Dennis W. ; AHMED, Zeshan ; ALGOM, Avi A. ; TSUBOI, Yoshio ; JOSEPHS, Keith A.: Neuropathology of variants of progressive supranuclear palsy. In: *Current Opinion in Neurology* 23 (2010), Aug, Nr. 4, S. 394–400. <http://dx.doi.org/10.1097/WCO.0b013e32833be924>. – DOI 10.1097/WCO.0b013e32833be924
- [125] DICKSON, Dennis W. ; KOURI, Naomi ; MURRAY, Melissa E. ; JOSEPHS, Keith A.: Neuropathology of Frontotemporal Lobar Degeneration-Tau (FTLD-Tau). In: *J Mol Neurosci* 45 (2011), Nov, Nr. 3, S. 384–389. <http://dx.doi.org/10.1007/s12031-011-9589-0>. – DOI 10.1007/s12031-011-9589-0
- [126] DISTLER, Ute ; KUHAREV, Jörg ; NAVARRO, Pedro ; LEVIN, Yishai ; SCHILD, Hansjörg ; TENZER, Stefan: Drift time-specific collision energies enable deep-coverage data-independent acquisition proteomics. In: *Nat Methods* 11 (2014), Feb, Nr. 2, S. 167–70. <http://dx.doi.org/10.1038/nmeth.2767>. – DOI 10.1038/nmeth.2767
- [127] DIXIT, Ram ; ROSS, Jennifer L. ; GOLDMAN, Yale E. ; HOLZBAUR, Erika L F.: Differential regulation of dynein and kinesin motor proteins by tau. In: *Science* 319 (2008), Feb, Nr. 5866, 1086–9. <http://dx.doi.org/10.1126/science.1152993>. – DOI 10.1126/science.1152993
- [128] DORVAL, Véronique ; FRASER, Paul E.: Small ubiquitin-like modifier (SUMO) modification of natively unfolded proteins tau and alpha-synuclein. In: *J Biol Chem* 281 (2006), Apr, Nr. 15, S. 9919–24. <http://dx.doi.org/10.1074/jbc.M510127200>. – DOI 10.1074/jbc.M510127200
- [129] DORVAL, Véronique ; FRASER, Paul E.: SUMO on the road to neurodegeneration. In: *Biochimica et biophysica acta* 1773 (2007), Jun, Nr. 6, S. 694–706. <http://dx.doi.org/10.1016/j.bbamcr.2007.03.017>. – DOI 10.1016/j.bbamcr.2007.03.017
- [130] DRECHSEL, D N. ; HYMAN, A A. ; COBB, M H. ; KIRSCHNER, M W.: Modulation of the dynamic instability of tubulin assembly by the microtubule-associated protein tau. In: *Mol Biol Cell* 3 (1992), Oct, Nr. 10, 1141–54. <http://www.molbiolcell.org/content/3/10/1141.long>
- [131] DUKA, Valeriy ; LEE, Jae-Hoon ; CREDLE, Joel ; WILLS, Jonathan ; OAKS, Adam ; SMOLINSKY, Ciaran ; SHAH, Ketul ; MASH, Deborah C. ; MASLIAH, Eliezer ; SIDHU, Anita: Identification of the sites of tau hyperphosphorylation and activation of tau kinases in synucleinopathies and Alzheimer's diseases. In: *PLoS ONE* 8 (2013), Jan, Nr. 9, S. e75025. <http://dx.doi.org/10.1371/journal.pone.0075025>. – DOI 10.1371/journal.pone.0075025
- [132] DUPUIS, Alain ; HENNEKINNE, Jacques-Antoine ; GARIN, Jérôme ; BRUN, Virginie: Protein Standard Absolute Quantification (PSAQ) for improved investigation of staphylococcal food poisoning outbreaks. In: *Proteomics* 8 (2008), Nov, Nr. 22, S. 4633–6. <http://dx.doi.org/10.1002/pmic.200800326>. – DOI 10.1002/pmic.200800326
- [133] DUTHEY, Béatrice: Update on 2004 Background Paper, BP 6.11 Alzheimer Disease and other Dementias. In: *Priority Medicines for Europe and the World "A Public Health Approach to Innovation"* (2013)
- [134] DUYSKAERTS, Charles ; POTIER, Marie-Claude ; DELATOUR, Benoît: Alzheimer disease models and human neuropathology: similarities and differences. In: *Acta Neuropathol* 115 (2008), Jan, Nr. 1, S. 5–38. <http://dx.doi.org/10.1007/s00401-007-0312-8>. – DOI 10.1007/s00401-007-0312-8
- [135] EBNETH, A ; GODEMANN, R ; STAMER, K ; ILLENBERGER, S ; TRINCZEK, B ; MANDELKOW, E: Overexpression of tau protein inhibits kinesin-dependent trafficking of vesicles, mitochondria, and endoplasmic reticulum: implications for Alzheimer's disease. In: *J Cell Biol* 143 (1998), Nov, Nr. 3, 777–94. <http://www.ncbi.nlm.nih.gov/pubmed/9813097>
- [136] ECKERMANN, K ; MOCANU, M ; KHLISTUNOVA, I ; BIERNAT, J ; NISSEN, A ; HOFMANN, A ; SCHONIG, K ; BUJARD, H ; HAEMISCH, A ; MANDELKOW, E ; ZHOU, L ; RUNE, G ; MANDELKOW, E: The beta-propensity of Tau determines aggregation and synaptic loss in inducible mouse models of tauopathy. In: *J Biol Chem* 282 (2007), Oct, Nr. 43, 31755–65. <http://dx.doi.org/10.1074/jbc.M705282200>. – DOI 10.1074/jbc.M705282200

- [137] ELLIOTT, Monica H. ; SMITH, Derek S. ; PARKER, Carol E. ; BORCHERS, Christoph: Current trends in quantitative proteomics. In: *J Mass Spectrom* 44 (2009), Dec, Nr. 12, S. 1637–60. <http://dx.doi.org/10.1002/jms.1692>. – DOI 10.1002/jms.1692
- [138] ESCHER, C ; REITER, L ; MACLEAN, B ; OSSOLA, R ; HERZOG, F ; CHILTON, J ; MACCOSS, M ; RINNER, O: Using iRT, a normalized retention time for more targeted measurement of peptides. In: *PROTEOMICS* 12 (2012), Apr, Nr. 8, 1111–21. <http://dx.doi.org/10.1002/pmic.201100463>. – DOI 10.1002/pmic.201100463
- [139] ESPINOZA, M ; SILVA, R de ; DICKSON, D ; DAVIES, P: Differential incorporation of tau isoforms in Alzheimer's disease. In: *J Alzheimers Dis* 14 (2008), May, Nr. 1, 1–16. <http://www.ncbi.nlm.nih.gov/pubmed/18525123>
- [140] EYRICH, Beate ; SICKMANN, Albert ; ZAHEDI, René P.: Catch me if you can: mass spectrometry-based phosphoproteomics and quantification strategies. In: *Proteomics* 11 (2011), Feb, Nr. 4, S. 554–70. <http://dx.doi.org/10.1002/pmic.201000489>. – DOI 10.1002/pmic.201000489
- [141] FASULO, Luisa ; UGOLINI, Gabriele ; CATTANEO, Antonino: Apoptotic effect of caspase-3 cleaved tau in hippocampal neurons and its potentiation by tau FTDP-mutation N279K. In: *J Alzheimers Dis* 7 (2005), Feb, Nr. 1, S. 3–13
- [142] FEANY, M B. ; DICKSON, D W.: Widespread cytoskeletal pathology characterizes corticobasal degeneration. In: *Am J Pathol* 146 (1995), Jun, Nr. 6, S. 1388–96
- [143] FEANY, M B. ; MATTIACE, L A. ; DICKSON, D W.: Neuropathologic overlap of progressive supranuclear palsy, Pick's disease and corticobasal degeneration. In: *J Neuropathol Exp Neurol* 55 (1996), Jan, Nr. 1, S. 53–67
- [144] FENN, J B. ; MANN, M ; MENG, C K. ; WONG, S F. ; WHITEHOUSE, C M.: Electrospray ionization for mass spectrometry of large biomolecules. In: *Science* 246 (1989), Oct, Nr. 4926, S. 64–71
- [145] FERRER, I ; LOPEZ-GONZALEZ, I ; CARMONA, M ; ARREGUI, L ; DALFO, E ; TORREJON-ESCRIBANO, B ; DIEHL, R ; KOVACS, G: Glial and neuronal tau pathology in tauopathies: characterization of disease-specific phenotypes and tau pathology progression. In: *J Neuropathol Exp Neurol* 73 (2014), Jan, Nr. 1, 81–97. <http://dx.doi.org/10.1097/NEN.0000000000000030>. – DOI 10.1097/NEN.0000000000000030
- [146] FISCHER, Daniela ; MUKRASCH, Marco D. ; BIERNAT, Jacek ; BIBOW, Stefan ; BLACKLEDGE, Martin ; GRIESINGER, Christian ; MANDELKOW, Eckhard ; ZWECKSTETTER, Markus: Conformational changes specific for pseudophosphorylation at serine 262 selectively impair binding of tau to microtubules. In: *Biochemistry* 48 (2009), Oct, Nr. 42, 10047–55. <http://dx.doi.org/10.1021/bi901090m>. – DOI 10.1021/bi901090m
- [147] FISHER, R: THE USE OF MULTIPLE MEASUREMENTS IN TAXONOMIC PROBLEMS. In: *Annals of Eugenics* 7 (1936), Nr. 2, 179–188. <http://dx.doi.org/10.1111/j.1469-1809.1936.tb02137.x>. – DOI 10.1111/j.1469-1809.1936.tb02137.x
- [148] FORMAN, M ; TROJANOWSKI, J ; LEE, V: Neurodegenerative diseases: a decade of discoveries paves the way for therapeutic breakthroughs. In: *Nat Med* 10 (2004), Oct, Nr. 10, 1055–63. <http://dx.doi.org/10.1038/nm1113>. – DOI 10.1038/nm1113
- [149] FORMAN, Mark S. ; ZHUKAREVA, Victoria ; BERGERON, Catherine ; CHIN, Steven S-M ; GROSSMAN, Murray ; CLARK, Chris ; LEE, Virginia M-Y ; TROJANOWSKI, John Q.: Signature tau neuropathology in gray and white matter of corticobasal degeneration. In: *Am J Pathol* 160 (2002), Jun, Nr. 6, S. 2045–53. [http://dx.doi.org/10.1016/S0002-9440\(10\)61154-6](http://dx.doi.org/10.1016/S0002-9440(10)61154-6). – DOI 10.1016/S0002-9440(10)61154-6
- [150] FUNK, Kristen E. ; THOMAS, Stefani N. ; SCHAFER, Kelsey N. ; COOPER, Grace L. ; LIAO, Zhongping ; CLARK, David J. ; YANG, Austin J. ; KURET, Jeff: Lysine methylation is an endogenous post-translational modification of tau protein in human brain and a modulator of aggregation propensity. In: *Biochem J* 462 (2014), Aug, Nr. 1, S. 77–88. <http://dx.doi.org/10.1042/BJ20140372>. – DOI 10.1042/BJ20140372

- [151] GADO, M ; HUGHES, C P. ; DANZIGER, W ; CHI, D ; JOST, G ; BERG, L: Volumetric measurements of the cerebrospinal fluid spaces in demented subjects and controls. In: *Radiology* 144 (1982), Aug, Nr. 3, S. 535–8. <http://dx.doi.org/10.1148/radiology.144.3.7100467>. – DOI 10.1148/radiology.144.3.7100467
- [152] GAMBLIN, T C. ; KING, M E. ; DAWSON, H ; VITEK, M P. ; KURET, J ; BERRY, R W. ; BINDER, L I.: In vitro polymerization of tau protein monitored by laser light scattering: method and application to the study of FTDP-17 mutants. In: *Biochemistry* 39 (2000), May, Nr. 20, 6136–44. <http://pubs.acs.org/doi/abs/10.1021/bi000201f>
- [153] GARCIA-SIERRA, F ; GHOSHAL, N ; QUINN, B ; BERRY, R ; BINDER, L: Conformational changes and truncation of tau protein during tangle evolution in Alzheimer's disease. In: *J Alzheimers Dis* 5 (2003), Apr, Nr. 2, 65–77. <http://www.ncbi.nlm.nih.gov/pubmed/12719624>
- [154] GARCIA-SIERRA, F ; MONDRAGON-RODRIGUEZ, S ; BASURTO-ISLAS, G: Truncation of tau protein and its pathological significance in Alzheimer's disease. In: *J Alzheimers Dis* 14 (2008), Aug, Nr. 4, 401–9. <http://www.ncbi.nlm.nih.gov/pubmed/18688090>
- [155] GERBER, Scott A. ; RUSH, John ; STEMMAN, Olaf ; KIRSCHNER, Marc W. ; GYGI, Steven P.: Absolute quantification of proteins and phosphoproteins from cell lysates by tandem MS. In: *Proc Natl Acad Sci USA* 100 (2003), Jun, Nr. 12, S. 6940–5. <http://dx.doi.org/10.1073/pnas.0832254100>. – DOI 10.1073/pnas.0832254100
- [156] GERHARD, Alexander ; TRENDER-GERHARD, Iris ; TURKHEIMER, Federico ; QUINN, Niall P. ; BHATIA, Kailash P. ; BROOKS, David J.: In vivo imaging of microglial activation with [¹¹C](R)-PK11195 PET in progressive supranuclear palsy. In: *Mov Disord* 21 (2006), Jan, Nr. 1, S. 89–93. <http://dx.doi.org/10.1002/mds.20668>. – DOI 10.1002/mds.20668
- [157] GERSON, Julia E. ; KAYED, Rakez: Formation and propagation of tau oligomeric seeds. In: *Front. Neurol.* 4 (2013), Jan, S. 93. <http://dx.doi.org/10.3389/fneur.2013.00093>. – DOI 10.3389/fneur.2013.00093
- [158] GHORESCHI, Kamran ; LAURENCE, Arian ; O'SHEA, John J.: Selectivity and therapeutic inhibition of kinases: to be or not to be? In: *Nat Immunol* 10 (2009), Apr, Nr. 4, S. 356–60. <http://dx.doi.org/10.1038/ni.1701>. – DOI 10.1038/ni.1701
- [159] GILLET, Ludovic C. ; NAVARRO, Pedro ; TATE, Stephen ; RÖST, Hannes ; SELEVSEK, Nathalie ; REITER, Lukas ; BONNER, Ron ; AEBERSOLD, Ruedi: Targeted data extraction of the MS/MS spectra generated by data-independent acquisition: a new concept for consistent and accurate proteome analysis. In: *Mol Cell Proteomics* 11 (2012), Jun, Nr. 6, S. O111.016717. <http://dx.doi.org/10.1074/mcp.0111.016717>. – DOI 10.1074/mcp.0111.016717
- [160] GILLETTE, Michael A. ; CARR, Steven A.: Quantitative analysis of peptides and proteins in biomedicine by targeted mass spectrometry. In: *Nat Methods* 10 (2013), Jan, Nr. 1, S. 28–34. <http://dx.doi.org/10.1038/nmeth.2309>. – DOI 10.1038/nmeth.2309
- [161] GOEDERT, M ; BAUR, C ; AHRINGER, J ; JAKES, R ; HASEGAWA, M ; SPILLANTINI, M ; SMITH, M ; HILL, F: PTL-1, a microtubule-associated protein with tau-like repeats from the nematode *Caenorhabditis elegans*. In: *J Cell Sci* 109 (Pt 11) (1996), Nov, 2661–72. <http://www.ncbi.nlm.nih.gov/pubmed/8937984>
- [162] GOEDERT, M ; JAKES, R: Expression of separate isoforms of human tau protein: correlation with the tau pattern in brain and effects on tubulin polymerization. In: *EMBO J* 9 (1990), Dec, Nr. 13, 4225–30. <http://www.ncbi.nlm.nih.gov/pubmed/2124967>
- [163] GOEDERT, M ; JAKES, R ; CROWTHER, R A. ; COHEN, P ; VANMECHELEN, E ; VANDERMEEREN, M ; CRAS, P: Epitope mapping of monoclonal antibodies to the paired helical filaments of Alzheimer's disease: identification of phosphorylation sites in tau protein. In: *Biochem J* 301 (Pt 3) (1994), Aug, S. 871–7

- [164] GOEDERT, M ; JAKES, R ; CROWTHER, R A. ; SIX, J ; LÜBKE, U ; VANDERMEEREN, M ; CRAS, P ; TROJANOWSKI, J Q. ; LEE, V M.: The abnormal phosphorylation of tau protein at Ser-202 in Alzheimer disease recapitulates phosphorylation during development. In: *Proc Natl Acad Sci USA* 90 (1993), Jun, Nr. 11, S. 5066–70
- [165] GOEDERT, M ; SPILLANTINI, M ; JAKES, R ; RUTHERFORD, D ; CROWTHER, R: Multiple isoforms of human microtubule-associated protein tau: sequences and localization in neurofibrillary tangles of Alzheimer's disease. In: *Neuron* 3 (1989), Oct, Nr. 4, 519–26. <http://www.ncbi.nlm.nih.gov/pubmed/2484340>
- [166] GOEDERT, M ; SPILLANTINI, M ; POTIER, M ; ULRICH, J ; CROWTHER, R: Cloning and sequencing of the cDNA encoding an isoform of microtubule-associated protein tau containing four tandem repeats: differential expression of tau protein mRNAs in human brain. In: *EMBO J* 8 (1989), Feb, Nr. 2, 393–9. <http://www.ncbi.nlm.nih.gov/pubmed/2498079>
- [167] GOEDERT, Michel ; GHETTI, Bernardino ; SPILLANTINI, Maria G.: Frontotemporal dementia: implications for understanding Alzheimer disease. In: *Cold Spring Harbor Perspectives in Medicine* 2 (2012), Feb, Nr. 2, S. a006254. <http://dx.doi.org/10.1101/cshperspect.a006254>. – DOI 10.1101/cshperspect.a006254
- [168] GOLD, Michael ; LORENZL, Stefan ; STEWART, Alistair J. ; MORIMOTO, Bruce H. ; WILLIAMS, David R. ; GOZES, Illana: Critical appraisal of the role of davunetide in the treatment of progressive supranuclear palsy. In: *Neuropsychiatr Dis Treat* 8 (2012), Jan, S. 85–93. <http://dx.doi.org/10.2147/NDT.S12518>. – DOI 10.2147/NDT.S12518
- [169] GOLDE, Todd E. ; SCHNEIDER, Lon S. ; KOO, Edward H.: Anti-a-beta therapeutics in Alzheimer's disease: the need for a paradigm shift. In: *Neuron* 69 (2011), Jan, Nr. 2, S. 203–13. <http://dx.doi.org/10.1016/j.neuron.2011.01.002>. – DOI 10.1016/j.neuron.2011.01.002
- [170] GÓMEZ-ISLA, T ; HOLLISTER, R ; WEST, H ; MUI, S ; GROWDON, J H. ; PETERSEN, R C. ; PARISI, J E. ; HYMAN, B T.: Neuronal loss correlates with but exceeds neurofibrillary tangles in Alzheimer's disease. In: *Ann Neurol* 41 (1997), Jan, Nr. 1, S. 17–24. <http://dx.doi.org/10.1002/ana.410410106>. – DOI 10.1002/ana.410410106
- [171] GONZALEZ-BILLAULT, C ; ENGELKE, M ; JIMENEZ-MATEOS, E ; WANDOSELL, F ; CACERES, A ; AVILA, J: Participation of structural microtubule-associated proteins (MAPs) in the development of neuronal polarity. In: *J Neurosci Res* 67 (2002), Mar, Nr. 6, 713–9. <http://www.ncbi.nlm.nih.gov/pubmed/11891784>
- [172] GORINI, Giorgio ; ROBERTS, Amanda J. ; MAYFIELD, R D.: Neurobiological signatures of alcohol dependence revealed by protein profiling. In: *PLoS ONE* 8 (2013), Jan, Nr. 12, S. e82656. <http://dx.doi.org/10.1371/journal.pone.0082656>. – DOI 10.1371/journal.pone.0082656
- [173] GÖTZ, J ; CHEN, F ; BARMETTLER, R ; NITSCH, R M.: Tau filament formation in transgenic mice expressing P301L tau. In: *J Biol Chem* 276 (2001), Jan, Nr. 1, S. 529–34. <http://dx.doi.org/10.1074/jbc.M006531200>. – DOI 10.1074/jbc.M006531200
- [174] GÖTZ, Jürgen ; DETERS, Natasha ; DOLDISSEN, Amy ; BOKHARI, Laita ; KE, Yazi ; WIESNER, Andreas ; SCHONROCK, Nicole ; ITTNER, Lars M.: A decade of tau transgenic animal models and beyond. In: *Brain Pathol* 17 (2007), Jan, Nr. 1, S. 91–103. <http://dx.doi.org/10.1111/j.1750-3639.2007.00051.x>. – DOI 10.1111/j.1750-3639.2007.00051.x
- [175] GÖTZ, Jürgen ; ITTNER, Lars M.: Animal models of Alzheimer's disease and frontotemporal dementia. In: *Nat Rev Neurosci* 9 (2008), Jul, Nr. 7, S. 532–44. <http://dx.doi.org/10.1038/nrn2420>. – DOI 10.1038/nrn2420
- [176] GRAFF-RADFORD, N R. ; DAMASIO, A R. ; HYMAN, B T. ; HART, M N. ; TRANEL, D ; DAMASIO, H ; HOESEN, G W V. ; REZAI, K: Progressive aphasia in a patient with Pick's disease: a neuropsychological, radiologic, and anatomic study. In: *Neurology* 40 (1990), Apr, Nr. 4, S. 620–6

- [177] GREBE, Stefan K. ; SINGH, Ravinder J.: LC-MS/MS in the Clinical Laboratory - Where to From Here? In: *Clin Biochem Rev* 32 (2011), Feb, Nr. 1, 5–31. http://www.ncbi.nlm.nih.gov/pubmed?Db=pubmed&Cmd=Retrieve&list_uids=21451775&dopt=abstractplus
- [178] GREENBERG, S G. ; DAVIES, P: A preparation of Alzheimer paired helical filaments that displays distinct tau proteins by polyacrylamide gel electrophoresis. In: *Proc Natl Acad Sci USA* 87 (1990), Aug, Nr. 15, S. 5827–31
- [179] GRINBERG, L ; WANG, X ; WANG, C ; SOHN, P ; THEOFILAS, P ; SIDHU, M ; AREVALO, J ; HEINSEN, H ; HUANG, E ; ROSEN, H ; MILLER, B ; GAN, L ; SEELEY, W: Argyrophilic grain disease differs from other tauopathies by lacking tau acetylation. In: *Acta Neuropathologica* 125 (2013), Apr, Nr. 4, 581–93. <http://dx.doi.org/10.1007/s00401-013-1080-2>. – DOI 10.1007/s00401-013-1080-2
- [180] GROBER, E ; DICKSON, D ; SLIWINSKI, M J. ; BUSCHKE, H ; KATZ, M ; CRYSTAL, H ; LIPTON, R B.: Memory and mental status correlates of modified Braak staging. In: *Neurobiology of Aging* 20 (1999), Jan, Nr. 6, S. 573–9
- [181] GROSSMAN, Murray ; LIBON, David J. ; FORMAN, Mark S. ; MASSIMO, Lauren ; WOOD, Elisabeth ; MOORE, Peachie ; ANDERSON, Chivon ; FARMER, Jennifer ; CHATTERJEE, Anjan ; CLARK, Christopher M. ; COSLETT, H B. ; HURDIG, Howard I. ; LEE, Virginia M-Y ; TROJANOWSKI, John Q.: Distinct antemortem profiles in patients with pathologically defined frontotemporal dementia. In: *Arch Neurol* 64 (2007), Nov, Nr. 11, S. 1601–9. <http://dx.doi.org/10.1001/archneur.64.11.1601>. – DOI 10.1001/archneur.64.11.1601
- [182] GROUP., Biomarkers Definitions W.: Biomarkers and surrogate endpoints: preferred definitions and conceptual framework. In: *Clin Pharmacol Ther* 69 (2001), Mar, Nr. 3, S. 89–95. <http://dx.doi.org/10.1067/mcp.2001.113989>. – DOI 10.1067/mcp.2001.113989
- [183] GU, Y ; OYAMA, F ; IHARA, Y: Tau is widely expressed in rat tissues. In: *J Neurochem* 67 (1996), Sep, Nr. 3, 1235–44. <http://www.ncbi.nlm.nih.gov/pubmed/8752131>
- [184] GUAN, Kun-Liang ; YU, Wei ; LIN, Yan ; XIONG, Yue ; ZHAO, Shimin: Generation of acetyllysine antibodies and affinity enrichment of acetylated peptides. In: *Nat Protoc* 5 (2010), Sep, Nr. 9, S. 1583–95. <http://dx.doi.org/10.1038/nprot.2010.117>. – DOI 10.1038/nprot.2010.117
- [185] GUILLOZET-BONGAARTS, Angela L. ; GLAJCH, Kelly E. ; LIBSON, Emilie G. ; CAHILL, Michael E. ; BIGIO, Eileen ; BERRY, Robert W. ; BINDER, Lester I.: Phosphorylation and cleavage of tau in non-AD tauopathies. In: *Acta Neuropathol* 113 (2007), May, Nr. 5, 513–20. <http://dx.doi.org/10.1007/s00401-007-0209-6>. – DOI 10.1007/s00401-007-0209-6
- [186] GUO, Ailan ; GU, Hongbo ; ZHOU, Jing ; MULHERN, Daniel ; WANG, Yi ; LEE, Kimberly A. ; YANG, Vicky ; AGUIAR, Mike ; KORNHAUSER, Jon ; JIA, Xiaoying ; REN, Jianmin ; BEAUSOLEIL, Sean A. ; SILVA, Jeffrey C. ; VEMULAPALLI, Vidyasiri ; BEDFORD, Mark T. ; COMB, Michael J.: Immunoaffinity enrichment and mass spectrometry analysis of protein methylation. In: *Mol Cell Proteomics* 13 (2014), Jan, Nr. 1, S. 372–87. <http://dx.doi.org/10.1074/mcp.O113.027870>. – DOI 10.1074/mcp.O113.027870
- [187] GYGI, S P. ; RIST, B ; GERBER, S A. ; TURECEK, F ; GELB, M H. ; AEBERSOLD, R: Quantitative analysis of complex protein mixtures using isotope-coded affinity tags. In: *Nat Biotechnol* 17 (1999), Oct, Nr. 10, S. 994–9. <http://dx.doi.org/10.1038/13690>. – DOI 10.1038/13690
- [188] HALL, Sara ; ÖHRFELT, Annika ; CONSTANTINESCU, Radu ; ANDREASSON, Ulf ; SUROVA, Yulia ; BOSTROM, Frederick ; NILSSON, Christer ; HÅKAN, Widner ; DECRAEMER, Hilde ; NÅGGA, Katarina ; MINTHON, Lennart ; LONDOS, Elisabet ; VANMECHELEN, Eugene ; HOLMBERG, Björn ; ZETTERBERG, Henrik ; BLENNOW, Kaj ; HANSSON, Oskar: Accuracy of a panel of 5 cerebrospinal fluid biomarkers in the differential diagnosis of patients with dementia and/or parkinsonian disorders. In: *Arch Neurol* 69 (2012), Nov, Nr. 11, S. 1445–52. <http://dx.doi.org/10.1001/archneurol.2012.1654>. – DOI 10.1001/archneurol.2012.1654

- [189] HAMANO, Tadanori ; GENDRON, Tania F. ; CAUSEVIC, Ena ; YEN, Shu-Hui ; LIN, Wen-Lang ; ISIDORO, Ciro ; DETURE, Michael ; KO, Li wen: Autophagic-lysosomal perturbation enhances tau aggregation in transfectants with induced wild-type tau expression. In: *Eur J Neurosci* 27 (2008), Mar, Nr. 5, S. 1119–30. <http://dx.doi.org/10.1111/j.1460-9568.2008.06084.x>. – DOI 10.1111/j.1460-9568.2008.06084.x
- [190] HAMPEL, Harald ; SHEN, Yong: Beta-site amyloid precursor protein cleaving enzyme 1 (BACE1) as a biological candidate marker of Alzheimer's disease. In: *Scand J Clin Lab Invest* 69 (2009), Jan, Nr. 1, S. 8–12. <http://dx.doi.org/10.1080/00365510701864610>. – DOI 10.1080/00365510701864610
- [191] HAN, Xuemei ; JIN, Mi ; BREUKER, Kathrin ; MCLAFFERTY, Fred W.: Extending top-down mass spectrometry to proteins with masses greater than 200 kilodaltons. In: *Science* 314 (2006), Oct, Nr. 5796, S. 109–12. <http://dx.doi.org/10.1126/science.1128868>. – DOI 10.1126/science.1128868
- [192] HANGER, D ; ANDERTON, B ; NOBLE, W: Tau phosphorylation: the therapeutic challenge for neurodegenerative disease. In: *Trends Mol Med* 15 (2009), Mar, Nr. 3, 112–9. <http://dx.doi.org/10.1016/j.molmed.2009.01.003>. – DOI 10.1016/j.molmed.2009.01.003
- [193] HANGER, D P. ; BETTS, J C. ; LOVINY, T L. ; BLACKSTOCK, W P. ; ANDERTON, B H.: New phosphorylation sites identified in hyperphosphorylated tau (paired helical filament-tau) from Alzheimer's disease brain using nanoelectrospray mass spectrometry. In: *J Neurochem* 71 (1998), Dec, Nr. 6, S. 2465–76
- [194] HANGER, D P. ; BRION, J P. ; GALLO, J M. ; CAIRNS, N J. ; LUTHER, P J. ; ANDERTON, B H.: Tau in Alzheimer's disease and Down's syndrome is insoluble and abnormally phosphorylated. In: *Biochem J* 275 (Pt 1) (1991), Apr, S. 99–104
- [195] HANGER, Diane P. ; ANDERTON, Brian H. ; NOBLE, Wendy: Tau phosphorylation: the therapeutic challenge for neurodegenerative disease. In: *Trends Mol Med* 15 (2009), Mar, Nr. 3, 112–9. <http://dx.doi.org/10.1016/j.molmed.2009.01.003>. – DOI 10.1016/j.molmed.2009.01.003
- [196] HANGER, Diane P. ; BYERS, Helen L. ; WRAY, Selina ; LEUNG, Kit-Yi ; SAXTON, Malcolm J. ; SEEREERAM, Anjan ; REYNOLDS, C H. ; WARD, Malcolm A. ; ANDERTON, Brian H.: Novel phosphorylation sites in tau from Alzheimer brain support a role for casein kinase 1 in disease pathogenesis. In: *J Biol Chem* 282 (2007), Aug, Nr. 32, S. 23645–54. <http://dx.doi.org/10.1074/jbc.M703269200>. – DOI 10.1074/jbc.M703269200
- [197] HARADA, A ; OGUCHI, K ; OKABE, S ; KUNO, J ; TERADA, S ; OHSHIMA, T ; SATO-YOSHITAKE, R ; TAKEI, Y ; NODA, T ; HIROKAWA, N: Altered microtubule organization in small-calibre axons of mice lacking tau protein. In: *Nature* 369 (1994), Jun, Nr. 6480, 488–91. <http://dx.doi.org/10.1038/369488a0>. – DOI 10.1038/369488a0
- [198] HARDY, John ; SELKOE, Dennis J.: The amyloid hypothesis of Alzheimer's disease: progress and problems on the road to therapeutics. In: *Science* 297 (2002), Jul, Nr. 5580, S. 353–6. <http://dx.doi.org/10.1126/science.1072994>. – DOI 10.1126/science.1072994
- [199] HARLAN, R ; ZHANG, H: Targeted proteomics: a bridge between discovery and validation. In: *Expert Rev Proteomics* 11 (2014), Dec, Nr. 6, 657–61. <http://dx.doi.org/10.1586/14789450.2014.976558>. – DOI 10.1586/14789450.2014.976558
- [200] HÄRTIG, Wolfgang ; STIELER, Jens ; BOEREMA, Ate S. ; WOLF, Jennifer ; SCHMIDT, Udo ; WEISSFUSS, Jana ; BULLMANN, Torsten ; STRIJKSTRA, Arjen M. ; ARENDT, Thomas: Hibernation model of tau phosphorylation in hamsters: selective vulnerability of cholinergic basal forebrain neurons - implications for Alzheimer's disease. In: *Eur J Neurosci* 25 (2007), Jan, Nr. 1, S. 69–80. <http://dx.doi.org/10.1111/j.1460-9568.2006.05250.x>. – DOI 10.1111/j.1460-9568.2006.05250.x
- [201] HASEGAWA, M ; SMITH, M J. ; GOEDERT, M: Tau proteins with FTDP-17 mutations have a reduced ability to promote microtubule assembly. In: *FEBS Lett* 437 (1998), Oct, Nr. 3, 207–10. [http://www.febsletters.org/article/S0014-5793\(98\)01217-4/abstract](http://www.febsletters.org/article/S0014-5793(98)01217-4/abstract)

- [202] HAUW, J J. ; DANIEL, S E. ; DICKSON, D ; HOROUPIAN, D S. ; JELLINGER, K ; LANTOS, P L. ; MCKEE, A ; TABATON, M ; LITVAN, I: Preliminary NINDS neuropathologic criteria for Steele-Richardson-Olszewski syndrome (progressive supranuclear palsy). In: *Neurology* 44 (1994), Nov, Nr. 11, S. 2015–9
- [203] HILGER, Maximiliane ; BONALDI, Tiziana ; GNAD, Florian ; MANN, Matthias: Systems-wide analysis of a phosphatase knock-down by quantitative proteomics and phosphoproteomics. In: *Mol Cell Proteomics* 8 (2009), Aug, Nr. 8, S. 1908–20. <http://dx.doi.org/10.1074/mcp.M800559-MCP200>. – DOI 10.1074/mcp.M800559-MCP200
- [204] HIMMLER, A ; DRECHSEL, D ; KIRSCHNER, M ; MARTIN, D: Tau consists of a set of proteins with repeated C-terminal microtubule-binding domains and variable N-terminal domains. In: *Mol Cell Biol* 9 (1989), Apr, Nr. 4, 1381–8. <http://www.ncbi.nlm.nih.gov/pubmed/2498649>
- [205] HIRANO, A: Hirano bodies and related neuronal inclusions. In: *Neuropathol Appl Neurobiol* 20 (1994), Feb, Nr. 1, S. 3–11
- [206] HOF, P R. ; DELACOURTE, A ; BOURAS, C: Distribution of cortical neurofibrillary tangles in progressive supranuclear palsy: a quantitative analysis of six cases. In: *Acta Neuropathol* 84 (1992), Jan, Nr. 1, S. 45–51
- [207] HOGG, Marion ; GRUJIC, Zoran M. ; BAKER, Matt ; DEMIRCI, Serpil ; GUILLOZET, Angela L. ; SWEET, Alison P. ; HERZOG, Laura L. ; WEINTRAUB, Sandra ; MESULAM, M-Marsel ; LAPOINTE, Nichole E. ; GAMBLIN, T C. ; BERRY, Robert W. ; BINDER, Lester I. ; SILVA, Rohan de ; LEES, Andrew ; ESPINOZA, Marisol ; DAVIES, Peter ; GROVER, Andrew ; SAHARA, Naruhiko ; ISHIZAWA, Takashi ; DICKSON, Dennis ; YEN, Shu-Hui ; HUTTON, Michael ; BIGIO, Eileen H.: The L266V tau mutation is associated with frontotemporal dementia and Pick-like 3R and 4R tauopathy. In: *Acta Neuropathologica* 106 (2003), Oct, Nr. 4, S. 323–36. <http://dx.doi.org/10.1007/s00401-003-0734-x>. – DOI 10.1007/s00401-003-0734-x
- [208] HONG, M ; ZHUKAREVA, V ; VOGELSBERG-RAGAGLIA, V ; WSZOLEK, Z ; REED, L ; MILLER, B I. ; GESCHWIND, D H. ; BIRD, T D. ; MCKEEL, D ; GOATE, A ; MORRIS, J C. ; WILHELMSEN, K C. ; SCHELLENBERG, G D. ; TROJANOWSKI, J Q. ; LEE, V M.: Mutation-specific functional impairments in distinct tau isoforms of hereditary FTDP-17. In: *Science* 282 (1998), Dec, Nr. 5395, S. 1914–7
- [209] HOROWITZ, Peleg M. ; PATTERSON, Kristina R. ; GUILLOZET-BONGAARTS, Angela L. ; REYNOLDS, Matthew R. ; CARROLL, Christopher A. ; WEINTRAUB, Susan T. ; BENNETT, David A. ; CRYNS, Vincent L. ; BERRY, Robert W. ; BINDER, Lester I.: Early N-terminal changes and caspase-6 cleavage of tau in Alzheimer's disease. In: *The Journal of neuroscience : the official journal of the Society for Neuroscience* 24 (2004), Sep, Nr. 36, S. 7895–902. <http://dx.doi.org/10.1523/JNEUROSCI.1988-04.2004>. – DOI 10.1523/JNEUROSCI.1988-04.2004
- [210] HUANG, Yunpeng ; WU, Zhihao ; ZHOU, Bing: Behind the curtain of tauopathy: a show of multiple players orchestrating tau toxicity. In: *Cellular and Molecular Life Sciences* (2015), Sep. <http://dx.doi.org/10.1007/s00018-015-2042-8>. – DOI 10.1007/s00018-015-2042-8
- [211] HUISMAN, M ; JONG, S de ; DOORMAAL, P van ; WEINREICH, S ; SCHELHAAS, H ; KOOI, A van d. ; VISSER, M de ; VELDINK, J ; BERG, L van d.: Population based epidemiology of amyotrophic lateral sclerosis using capture-recapture methodology. In: *J Neurol Neurosurg Psychiatry* 82 (2011), Oct, Nr. 10, 1165–70. <http://dx.doi.org/10.1136/jnnp.2011.244939>. – DOI 10.1136/jnnp.2011.244939
- [212] HULSTAERT, F ; BLENNOW, K ; IVANOIU, A ; SCHOONDERWALDT, H C. ; RIEMENSCHNEIDER, M ; DEYN, P P D. ; BANCHER, C ; CRAS, P ; WILTFANG, J ; MEHTA, P D. ; IQBAL, K ; POTTTEL, H ; VANMECHELEN, E ; VANDERSTICHELE, H: Improved discrimination of AD patients using beta-amyloid(1-42) and tau levels in CSF. In: *Neurology* 52 (1999), May, Nr. 8, S. 1555–62
- [213] HUNTER, Tony: The age of crosstalk: phosphorylation, ubiquitination, and beyond. In: *Mol Cell* 28 (2007), Dec, Nr. 5, S. 730–8. <http://dx.doi.org/10.1016/j.molcel.2007.11.019>. – DOI 10.1016/j.molcel.2007.11.019

- [214] HYMAN, Bradley T. ; PHELPS, Creighton H. ; BEACH, Thomas G. ; BIGIO, Eileen H. ; CAIRNS, Nigel J. ; CARRILLO, Maria C. ; DICKSON, Dennis W. ; DUYSKAERTS, Charles ; FROSCHE, Matthew P. ; MASLIAH, Eliezer ; MIRRA, Suzanne S. ; NELSON, Peter T. ; SCHNEIDER, Julie A. ; THAL, Dietmar R. ; THIES, Bill ; TROJANOWSKI, John Q. ; VINTERS, Harry V. ; MONTINE, Thomas J.: National Institute on Aging-Alzheimer's Association guidelines for the neuropathologic assessment of Alzheimer's disease. In: *Alzheimers Dement* 8 (2012), Jan, Nr. 1, S. 1–13. <http://dx.doi.org/10.1016/j.jalz.2011.10.007>. – DOI 10.1016/j.jalz.2011.10.007
- [215] IHAKA, Ross ; RGENTLEMAN, Robert: R: A language for Data Analysis and Graphics. In: *Journal of Computational and Graphical Statistics* 5 (1996), Nr. 3, S. 299–314. <http://dx.doi.org/10.2307/1390807>. – DOI 10.2307/1390807
- [216] IKEDA, K ; HAGA, C ; AKIYAMA, H ; KASE, K ; IRITANI, S: Coexistence of paired helical filaments and glial filaments in astrocytic processes within ghost tangles. In: *Neurosci Lett* 148 (1992), Dec, Nr. 1-2, S. 126–8
- [217] ILLENBERGER, S ; ZHENG-FISCHHÖFER, Q ; PREUSS, U ; STAMER, K ; BAUMANN, K ; TRINCZEK, B ; BIERNAT, J ; GODEMANN, R ; MANDELKOW, E M. ; MANDELKOW, E: The endogenous and cell cycle-dependent phosphorylation of tau protein in living cells: implications for Alzheimer's disease. In: *Mol Biol Cell* 9 (1998), Jun, Nr. 6, 1495–512. <http://www.molbiolcell.org/content/9/6/1495.long>
- [218] INGELSON, M ; VANMECHELEN, E ; LANNFELT, L: Microtubule-associated protein tau in human fibroblasts with the Swedish Alzheimer mutation. In: *Neurosci Lett* 220 (1996), Dec, Nr. 1, 9–12. <http://www.ncbi.nlm.nih.gov/pubmed/8977136>
- [219] INGRAM, Esther M. ; SPILLANTINI, Maria G.: Tau gene mutations: dissecting the pathogenesis of FTDP-17. In: *Trends Mol Med* 8 (2002), Dec, Nr. 12, S. 555–62
- [220] IQBAL, K ; GRUNDKE-IQBAL, I: Ubiquitination and abnormal phosphorylation of paired helical filaments in Alzheimer's disease. In: *Molecular Neurobiology* 5 (1991), Jan, Nr. 2-4, 399–410. http://www.ncbi.nlm.nih.gov/entrez/query.fcgi?db=pubmed&cmd=Retrieve&dopt=AbstractPlus&list_uids=1726645
- [221] IRMINGER-FINGER, I ; LAYMON, R ; GOLDSTEIN, L: Analysis of the primary sequence and microtubule-binding region of the Drosophila 205K MAP. In: *J Cell Biol* 111 (1990), Dec, Nr. 6 Pt 1, 2563–72. <http://www.ncbi.nlm.nih.gov/pubmed/1703540>
- [222] IRWIN, D ; COHEN, T ; GROSSMAN, M ; ARNOLD, S ; MCCARTY-WOOD, E ; DEERLIN, V V. ; LEE, V ; TROJANOWSKI, J: Acetylated tau neuropathology in sporadic and hereditary tauopathies. In: *The American Journal of Pathology* 183 (2013), Aug, Nr. 2, 344–51. <http://dx.doi.org/10.1016/j.ajpath.2013.04.025>. – DOI 10.1016/j.ajpath.2013.04.025
- [223] IRWIN, David J. ; COHEN, Todd J. ; GROSSMAN, Murray ; ARNOLD, Steven E. ; XIE, Sharon X. ; LEE, Virginia M-Y ; TROJANOWSKI, John Q.: Acetylated tau, a novel pathological signature in Alzheimer's disease and other tauopathies. In: *Brain* 135 (2012), Mar, Nr. Pt 3, S. 807–18. <http://dx.doi.org/10.1093/brain/aws013>. – DOI 10.1093/brain/aws013
- [224] ISHIHAMA, Yasushi ; ODA, Yoshiya ; TABATA, Tsuyoshi ; SATO, Toshitaka ; NAGASU, Takeshi ; RAPPILBER, Juri ; MANN, Matthias: Exponentially modified protein abundance index (emPAI) for estimation of absolute protein amount in proteomics by the number of sequenced peptides per protein. In: *Mol Cell Proteomics* 4 (2005), Sep, Nr. 9, S. 1265–72. <http://dx.doi.org/10.1074/mcp.M500061-MCP200>. – DOI 10.1074/mcp.M500061-MCP200
- [225] ISHIZAWA, K ; DICKSON, D W.: Microglial activation parallels system degeneration in progressive supranuclear palsy and corticobasal degeneration. In: *J Neuropathol Exp Neurol* 60 (2001), Jun, Nr. 6, S. 647–57
- [226] IWAI, Leo K. ; BENOIST, Christophe ; MATHIS, Diane ; WHITE, Forest M.: Quantitative phosphoproteomic analysis of T cell receptor signaling in diabetes prone and resistant mice. In: *J Proteome Res* 9 (2010), Jun, Nr. 6, S. 3135–45. <http://dx.doi.org/10.1021/pr100035b>. – DOI 10.1021/pr100035b

- [227] JANOCKO, Nicholas J. ; BRODERSEN, Kevin A. ; SOTO-ORTOLAZA, Alexandra I. ; ROSS, Owen A. ; LIESINGER, Amanda M. ; DUARA, Ranjan ; GRAFF-RADFORD, Neill R. ; DICKSON, Dennis W. ; MURRAY, Melissa E.: Neuropathologically defined subtypes of Alzheimer's disease differ significantly from neurofibrillary tangle-predominant dementia. In: *Acta Neuropathol* 124 (2012), Nov, Nr. 5, S. 681–92. <http://dx.doi.org/10.1007/s00401-012-1044-y>. – DOI 10.1007/s00401-012-1044-y
- [228] JELLINGER, K ; RIEDERER, P ; TOMONAGA, M: Progressive supranuclear palsy: clinico-pathological and biochemical studies. In: *J Neural Transm Suppl* (1980), Jan, Nr. 16, 111–28. http://www.ncbi.nlm.nih.gov/pubmed?Db=pubmed&Cmd=Retrieve&list_uids=6107328&dopt=abstractplus
- [229] JELLINGER, Kurt A.: Clinicopathological analysis of dementia disorders in the elderly—an update. In: *J Alzheimers Dis* 9 (2006), Jan, Nr. 3 Suppl, 61–70. http://www.ncbi.nlm.nih.gov/pubmed?Db=pubmed&Cmd=Retrieve&list_uids=16914845&dopt=abstractplus
- [230] JEUGD, Ann V. ; HOCHGRÄFE, Katja ; AHMED, Tariq ; DECKER, Jochen M. ; SYDOW, Astrid ; HOFMANN, Anne ; WU, Dan ; MESSING, Lars ; BALSCHUN, Detlef ; D'HOOGHE, Rudi ; MANDELKOW, Eva-Maria: Cognitive defects are reversible in inducible mice expressing pro-aggregant full-length human Tau. In: *Acta Neuropathol* 123 (2012), Jun, Nr. 6, S. 787–805. <http://dx.doi.org/10.1007/s00401-012-0987-3>. – DOI 10.1007/s00401-012-0987-3
- [231] JONES, Alexandra M E. ; NUEHSE, TS: Phosphoproteomics using iTRAQ. In: *Methods Mol Biol* 779 (2011), Jan, S. 287–302. <http://dx.doi.org/10.1007/978-1-61779-264-917>. – DOI 10.1007/978-1-61779-264-917
- [232] JOSEPHS, K A. ; BOEVE, B F. ; DUFFY, J R. ; SMITH, G E. ; KNOPMAN, D S. ; PARISI, J E. ; PETERSEN, R C. ; DICKSON, D W.: Atypical progressive supranuclear palsy underlying progressive apraxia of speech and nonfluent aphasia. In: *Neurocase* 11 (2005), Aug, Nr. 4, S. 283–96. <http://dx.doi.org/10.1080/13554790590963004>. – DOI 10.1080/13554790590963004
- [233] JOSEPHS, Keith A.: Key emerging issues in progressive supranuclear palsy and corticobasal degeneration. In: *J Neurol* 262 (2015), Mar, Nr. 3, S. 783–788. <http://dx.doi.org/10.1007/s00415-015-7682-y>. – DOI 10.1007/s00415-015-7682-y
- [234] JOSEPHS, Keith A. ; KATSUSE, Omi ; BECCANO-KELLY, Dayne A. ; LIN, Wen-Lang ; UTTI, Ryan J. ; FUJINO, Yasuhiro ; BOEVE, Bradley F. ; HUTTON, Michael L. ; BAKER, Matthew C. ; DICKSON, Dennis W.: Atypical progressive supranuclear palsy with corticospinal tract degeneration. In: *J Neuropathol Exp Neurol* 65 (2006), Apr, Nr. 4, S. 396–405. <http://dx.doi.org/10.1097/01.jnen.0000218446.38158.61>. – DOI 10.1097/01.jnen.0000218446.38158.61
- [235] JOSEPHS, Keith A. ; WHITWELL, Jennifer L. ; DICKSON, Dennis W. ; BOEVE, Bradley F. ; KNOPMAN, David S. ; PETERSEN, Ronald C. ; PARISI, Joseph E. ; JACK, Clifford R.: Voxel-based morphometry in autopsy proven PSP and CBD. In: *Neurobiol Aging* 29 (2008), Feb, Nr. 2, S. 280–9. <http://dx.doi.org/10.1016/j.neurobiolaging.2006.09.019>. – DOI 10.1016/j.neurobiolaging.2006.09.019
- [236] KANG, J ; KORECKA, M ; TOLEDO, J ; TROJANOWSKI, J ; SHAW, L: Clinical utility and analytical challenges in measurement of cerebrospinal fluid amyloid-beta(1-42) and tau proteins as Alzheimer disease biomarkers. In: *Clin Chem* 59 (2013), Jun, Nr. 6, 903–16. <http://dx.doi.org/10.1373/clinchem.2013.202937>. – DOI 10.1373/clinchem.2013.202937
- [237] KANG, Min J. ; KIM, Chaeyoung ; JEONG, Hyobin ; CHO, Byoung-Kyu ; RYOU, Ae L. ; HWANG, Daehae ; MOOK-JUNG, Inhee ; YI, Eugene C.: Synapsin-1 and tau reciprocal O-GlcNAcylation and phosphorylation sites in mouse brain synaptosomes. In: *Experimental & Molecular Medicine* 45 (2013), Jan, Nr. 6, e29–7. <http://dx.doi.org/10.1038/emm.2013.56>. – DOI 10.1038/emm.2013.56
- [238] KARAS, M ; HILLENKAMP, F: Laser desorption ionization of proteins with molecular masses exceeding 10,000 daltons. In: *Anal Chem* 60 (1988), Oct, Nr. 20, S. 2299–301
- [239] KAUFMAN, Sarah K. ; DIAMOND, Marc I.: Prion-like propagation of protein aggregation and related therapeutic strategies. In: *Neurotherapeutics* 10 (2013), Jul, Nr. 3, S. 371–82. <http://dx.doi.org/10.1007/s13311-013-0196-3>. – DOI 10.1007/s13311-013-0196-3

- [240] KENESSEY, A ; YEN, S H.: The extent of phosphorylation of fetal tau is comparable to that of PHF-tau from Alzheimer paired helical filaments. In: *Brain Res* 629 (1993), Nov, Nr. 1, S. 40–6
- [241] KENTSI, A ; AHMED, S ; KUREK, K ; BRENNAN, E ; BRADWIN, G ; STEEN, H ; BACHUR, R: Detection and diagnostic value of urine leucine-rich alpha-2-glycoprotein in children with suspected acute appendicitis. In: *Ann Emerg Med* 60 (2012), Jul, Nr. 1, 78–83 e1. <http://dx.doi.org/10.1016/j.annemergmed.2011.12.015>. – DOI 10.1016/j.annemergmed.2011.12.015
- [242] KENTSI, A ; SHULMAN, A ; AHMED, S ; BRENNAN, E ; MONUTEAUX, M ; LEE, Y ; LIPSETT, S ; PAULO, J ; DEDEOGLU, F ; FUHLBRIGGE, R ; BACHUR, R ; BRADWIN, G ; ARDITI, M ; SUNDEL, R ; NEWBURGER, J ; STEEN, H ; KIM, S: Urine proteomics for discovery of improved diagnostic markers of Kawasaki disease. In: *EMBO Mol Med* 5 (2013), Feb, Nr. 2, 210–20. <http://dx.doi.org/10.1002/emmm.201201494>. – DOI 10.1002/emmm.201201494
- [243] KESHISHIAN, H ; ADDONA, T ; BURGESS, M ; KUHN, E ; CARR, S: Quantitative, multiplexed assays for low abundance proteins in plasma by targeted mass spectrometry and stable isotope dilution. In: *Mol Cell Proteomics* 6 (2007), Dec, Nr. 12, 2212–29. <http://dx.doi.org/10.1074/mcp.M700354-MCP200>. – DOI 10.1074/mcp.M700354-MCP200
- [244] KESSNER, D ; CHAMBERS, M ; BURKE, R ; AGUS, D ; MALLICK, P: ProteoWizard: open source software for rapid proteomics tools development. In: *Bioinformatics* 24 (2008), Nov, Nr. 21, S. 2534–6. <http://dx.doi.org/10.1093/bioinformatics/btn323>. – DOI 10.1093/bioinformatics/btn323
- [245] KETTENBACH, Arminja N. ; SCHWEPPE, Devin K. ; FAHERTY, Brendan K. ; PECHENICK, Dov ; PLETNEV, Alexandre A. ; GERBER, Scott A.: Quantitative phosphoproteomics identifies substrates and functional modules of Aurora and Polo-like kinase activities in mitotic cells. In: *Sci Signal* 4 (2011), Jan, Nr. 179, S. rs5. <http://dx.doi.org/10.1126/scisignal.2001497>. – DOI 10.1126/scisignal.2001497
- [246] KHATOON, S ; GRUNDKE-IQBAL, I ; IQBAL, K: Brain levels of microtubule-associated protein tau are elevated in Alzheimer's disease: a radioimmuno-slot-blot assay for nanograms of the protein. In: *J Neurochem* 59 (1992), Aug, Nr. 2, S. 750–3
- [247] KHATOON, S ; GRUNDKE-IQBAL, I ; IQBAL, K: Levels of normal and abnormally phosphorylated tau in different cellular and regional compartments of Alzheimer disease and control brains. In: *FEBS Lett* 351 (1994), Aug, Nr. 1, S. 80–4
- [248] KIM, E J. ; RABINOVICI, G D. ; SEELEY, W W. ; HALABI, C ; SHU, H ; WEINER, M W. ; DEARMOND, S J. ; TROJANOWSKI, J Q. ; GORNO-TEMPINI, M L. ; MILLER, B L. ; ROSEN, H J.: Patterns of MRI atrophy in tau positive and ubiquitin positive frontotemporal lobar degeneration. In: *J Neurol Neurosurg Psychiatr* 78 (2007), Dec, Nr. 12, S. 1375–8. <http://dx.doi.org/10.1136/jnnp.2006.114231>. – DOI 10.1136/jnnp.2006.114231
- [249] KLEGERIS, Andis ; MCGEER, Patrick L.: Non-steroidal anti-inflammatory drugs (NSAIDs) and other anti-inflammatory agents in the treatment of neurodegenerative disease. In: *Curr Alzheimer Res* 2 (2005), Jul, Nr. 3, S. 355–65
- [250] KLUNK, William ; ENGLER, Henry ; NORDBERG, Agneta ; WANG, Yanming ; BLOMQVIST, Gunnar ; HOLT, Daniel ; BERGSTRÖM, Mats ; SAVITCHEVA, Irina ; HUANG, Guo feng ; ESTRADA, Sergio ; AUSÉN, Birgitta ; DEBNATH, Manik ; BARLETTA, Julien ; PRICE, Julie ; SANDELL, Johan ; LOPRESTI, Brian ; WALL, Anders ; KOIVISTO, Pernilla ; ANTONI, Gunnar ; MATHIS, Chester ; LÅNGSTRÖM, Bengt: Imaging brain amyloid in Alzheimer's disease with Pittsburgh Compound-B. In: *Annals of neurology* 55 (2004), Mar, Nr. 3, 306–19. <http://dx.doi.org/10.1002/ana.20009>. – DOI 10.1002/ana.20009
- [251] KLUNK, William E. ; ENGLER, Henry ; NORDBERG, Agneta ; WANG, Yanming ; BLOMQVIST, Gunnar ; HOLT, Daniel P. ; BERGSTRÖM, Mats ; SAVITCHEVA, Irina ; HUANG, Guo feng ; ESTRADA, Sergio ; AUSÉN, Birgitta ; DEBNATH, Manik L. ; BARLETTA, Julien ; PRICE, Julie C. ; SANDELL, Johan ; LOPRESTI, Brian J. ; WALL, Anders ; KOIVISTO, Pernilla ; ANTONI, Gunnar ; MATHIS, Chester A. ; LÅNGSTRÖM, Bengt: Imaging brain amyloid in Alzheimer's disease with Pittsburgh Compound-B. In: *Ann Neurol* 55 (2004), Mar, Nr. 3, S. 306–19. <http://dx.doi.org/10.1002/ana.20009>. – DOI 10.1002/ana.20009

- [252] KOHONEN, T: *Learning vector quantization*. 1995
- [253] KOMORI, T ; ARAI, N ; ODA, M ; NAKAYAMA, H ; MORI, H ; YAGISHITA, S ; TAKAHASHI, T ; AMANO, N ; MURAYAMA, S ; MURAKAMI, S ; SHIBATA, N ; KOBAYASHI, M ; SASAKI, S ; IWATA, M: Astrocytic plaques and tufts of abnormal fibers do not coexist in corticobasal degeneration and progressive supranuclear palsy. In: *Acta Neuropathol* 96 (1998), Oct, Nr. 4, S. 401–8
- [254] KONDRAT, R W. ; MCCLUSKY, G A. ; COOKS, R G.: Multiple Reaction Monitoring in Mass Spectrometry/Mass Spectrometry for Direct Analysis of Complex Mixtures. In: *Anal Chem* 50 (1978), Jan, Nr. 14, S. 2017–2021
- [255] KOPEIKINA, Katherine J. ; CARLSON, George A. ; PITSTICK, Rose ; LUDVIGSON, Adam E. ; PETERS, Alan ; LUEBKE, Jennifer I. ; KOFFIE, Robert M. ; FROSCHE, Matthew P. ; HYMAN, Bradley T. ; SPIRES-JONES, Tara L.: Tau accumulation causes mitochondrial distribution deficits in neurons in a mouse model of tauopathy and in human Alzheimer's disease brain. In: *The American Journal of Pathology* 179 (2011), Oct, Nr. 4, S. 2071–82. <http://dx.doi.org/10.1016/j.ajpath.2011.07.004>. – DOI 10.1016/j.ajpath.2011.07.004
- [256] KÖPKE, E ; TUNG, Y C. ; SHAIKH, S ; ALONSO, A C. ; IQBAL, K ; GRUNDKE-IQBAL, I: Microtubule-associated protein tau. Abnormal phosphorylation of a non-paired helical filament pool in Alzheimer disease. In: *J Biol Chem* 268 (1993), Nov, Nr. 32, S. 24374–84
- [257] KOSIK, K ; FINCH, E: MAP2 and tau segregate into dendritic and axonal domains after the elaboration of morphologically distinct neurites: an immunocytochemical study of cultured rat cerebrum. In: *J Neurosci* 7 (1987), Oct, Nr. 10, 3142–53. <http://www.ncbi.nlm.nih.gov/pubmed/2444675>
- [258] KOSIK, K S. ; MCCONLOGUE, L: Microtubule-associated protein function: lessons from expression in *Spodoptera frugiperda* cells. In: *Cell Motil Cytoskeleton* 28 (1994), Jan, Nr. 3, S. 195–8. <http://dx.doi.org/10.1002/cm.970280302>. – DOI 10.1002/cm.970280302
- [259] KOSMIDIS, Stylianos ; GRAMMENOUDI, Sofia ; PAPANIKOLOPOULOU, Katerina ; SKOULAKIS, Efthimios M C.: Differential effects of Tau on the integrity and function of neurons essential for learning in *Drosophila*. In: *J Neurosci* 30 (2010), Jan, Nr. 2, S. 464–77. <http://dx.doi.org/10.1523/JNEUROSCI.1490-09.2010>. – DOI 10.1523/JNEUROSCI.1490-09.2010
- [260] KOVACS, G: Invited review: Neuropathology of tauopathies: principles and practice. In: *Neuropathol Appl Neurobiol* 41 (2015), Feb, Nr. 1, 3–23. <http://dx.doi.org/10.1111/nan.12208>. – DOI 10.1111/nan.12208
- [261] KREMER, Anna ; LOUIS, Justin V. ; JAWORSKI, Tomasz ; LEUVEN, Fred V.: GSK3 and Alzheimer's Disease: Facts and Fiction... In: *Front Mol Neurosci* 4 (2011), Jan, S. 17. <http://dx.doi.org/10.3389/fnmol.2011.00017>. – DOI 10.3389/fnmol.2011.00017
- [262] KRETZSCHMAR, Hans: Brain banking: opportunities, challenges and meaning for the future. In: *Nat Rev Neurosci* 10 (2009), Jan, Nr. 1, S. 70–8. <http://dx.doi.org/10.1038/nrn2535>. – DOI 10.1038/nrn2535
- [263] KSIEZAK-REDING, H ; LIU, W ; YEN, S: Phosphate analysis and dephosphorylation of modified tau associated with paired helical filaments. In: *Brain Res* 597 (1992), Dec, Nr. 2, 209–19. <http://www.ncbi.nlm.nih.gov/pubmed/1472994>
- [264] KUUSISTO, E ; KAUPPINEN, T ; ALAFUZOFF, I: Use of p62/SQSTM1 antibodies for neuropathological diagnosis. In: *Neuropathol Appl Neurobiol* 34 (2008), Apr, Nr. 2, S. 169–80. <http://dx.doi.org/10.1111/j.1365-2990.2007.00884.x>. – DOI 10.1111/j.1365-2990.2007.00884.x
- [265] LAI, Shiao-Lin ; ABRAMZON, Yevgeniya ; SCHYMICK, Jennifer C. ; STEPHAN, Dietrich A. ; DUNCKLEY, Travis ; DILLMAN, Allissa ; COOKSON, Mark ; CALVO, Andrea ; BATTISTINI, Stefania ; GIANNINI, Fabio ; CAPONNETTO, Claudia ; MANCARDI, Giovanni L. ; SPATARO, Rossella ; MONSURRO, Maria R. ; TEDESCHI, Gioacchino ; MARINO, Kalliopi ; SABATELLI, Mario ; CONTE, Amelia ; MANDRIOLI, Jessica ; SOLA, Patrizia ; SALVI, Fabrizio ; BARTOLOMEI, Ilaria ; LOMBARDO, Federica ; CONSORTIUM, ITALSGEN ; MORA, Gabriele ; RESTAGNO, Gabriella ; CHIÒ, Adriano ; TRAYNOR, Bryan J.:

- FUS mutations in sporadic amyotrophic lateral sclerosis. In: *Neurobiology of Aging* 32 (2011), Mar, Nr. 3, S. 550.e1–4. <http://dx.doi.org/10.1016/j.neurobiolaging.2009.12.020>. – DOI 10.1016/j.neurobiolaging.2009.12.020
- [266] LAKHAN, Shaheen E.: Schizophrenia proteomics: biomarkers on the path to laboratory medicine? In: *Diagn Pathol* 1 (2006), Jan, S. 11. <http://dx.doi.org/10.1186/1746-1596-1-11>. – DOI 10.1186/1746-1596-1-11
- [267] LANG, A E. ; BERGERON, C ; POLLANEN, M S. ; ASHBY, P: Parietal Pick's disease mimicking cortical-basal ganglionic degeneration. In: *Neurology* 44 (1994), Aug, Nr. 8, S. 1436–40
- [268] LEE, G ; COWAN, N ; KIRSCHNER, M: The primary structure and heterogeneity of tau protein from mouse brain. In: *Science* 239 (1988), Jan, Nr. 4837, 285–8. <http://www.ncbi.nlm.nih.gov/pubmed/3122323>
- [269] LEE, G ; NEVE, R ; KOSIK, K: The microtubule binding domain of tau protein. In: *Neuron* 2 (1989), Jun, Nr. 6, 1615–24. <http://www.ncbi.nlm.nih.gov/pubmed/2516729>
- [270] LEE, Min J. ; LEE, Jung H. ; RUBINSZTEIN, David C.: Tau degradation: the ubiquitin-proteasome system versus the autophagy-lysosome system. In: *Progress in Neurobiology* 105 (2013), Jun, S. 49–59. <http://dx.doi.org/10.1016/j.pneurobio.2013.03.001>. – DOI 10.1016/j.pneurobio.2013.03.001
- [271] LI, F ; ISEKI, E ; ODAWARA, T ; KOSAKA, K ; YAGISHITA, S ; AMANO, N: Regional quantitative analysis of tau-positive neurons in progressive supranuclear palsy: comparison with Alzheimer's disease. In: *J Neurol Sci* 159 (1998), Jul, Nr. 1, S. 73–81
- [272] LING, Helen ; LING, H ; SILVA, R de ; MASSEY, L A. ; COURTNEY, R ; HONDHAMUNI, G ; BAJAJ, N ; LOWE, J ; HOLTON, J L. ; LEES, A ; REVESZ, T: Characteristics of progressive supranuclear palsy presenting with corticobasal syndrome: a cortical variant. In: *Neuropathol Appl Neurobiol* 40 (2014), Feb, Nr. 2, S. 149–63. <http://dx.doi.org/10.1111/nan.12037>. – DOI 10.1111/nan.12037
- [273] LING, Helen ; O'SULLIVAN, Sean S. ; HOLTON, Janice L. ; REVESZ, Tamas ; MASSEY, Luke A. ; WILLIAMS, David R. ; PAVIOUR, Dominic C. ; LEES, Andrew J.: Does corticobasal degeneration exist? A clinicopathological re-evaluation. In: *Brain* 133 (2010), Jul, Nr. Pt 7, 2045–57. <http://dx.doi.org/10.1093/brain/awq123>. – DOI 10.1093/brain/awq123
- [274] LITVAN, I ; GRIMES, D A. ; LANG, A E.: Phenotypes and prognosis: clinicopathologic studies of corticobasal degeneration. In: *Adv Neurol* 82 (2000), Jan, S. 183–96
- [275] LIU, F ; IQBAL, K ; GRUNDKE-IQBAL, I ; HART, G ; GONG, C: O-GlcNAcylation regulates phosphorylation of tau: a mechanism involved in Alzheimer's disease. In: *Proc Natl Acad Sci U S A* 101 (2004), Jul, Nr. 29, 10804–9. <http://dx.doi.org/10.1073/pnas.0400348101>. – DOI 10.1073/pnas.0400348101
- [276] LIU, Fei ; IQBAL, Khalid ; GRUNDKE-IQBAL, Inge ; GONG, Cheng-Xin: Involvement of aberrant glycosylation in phosphorylation of tau by cdk5 and GSK-3beta. In: *FEBS Lett* 530 (2002), Oct, Nr. 1-3, S. 209–14
- [277] LIU, Hongbin ; SADYGOV, Rovshan G. ; YATES, John R.: A model for random sampling and estimation of relative protein abundance in shotgun proteomics. In: *Anal Chem* 76 (2004), Jul, Nr. 14, S. 4193–201. <http://dx.doi.org/10.1021/ac0498563>. – DOI 10.1021/ac0498563
- [278] LIU, Y ; HUTTENHAIN, R ; COLLINS, B ; AEBERSOLD, R: Mass spectrometric protein maps for biomarker discovery and clinical research. In: *Expert Rev Mol Diagn* 13 (2013), Nov, Nr. 8, 811–25. <http://dx.doi.org/10.1586/14737159.2013.845089>. – DOI 10.1586/14737159.2013.845089
- [279] LIU, Ying-Hua ; WEI, Wei ; YIN, Jun ; LIU, Gong-Ping ; WANG, Qun ; CAO, Fu-Yuan ; WANG, Jian-Zhi: Proteasome inhibition increases tau accumulation independent of phosphorylation. In: *Neurobiology of Aging* 30 (2009), Dec, Nr. 12, S. 1949–61. <http://dx.doi.org/10.1016/j.neurobiolaging.2008.02.012>. – DOI 10.1016/j.neurobiolaging.2008.02.012

- [280] LOVE, S: Post mortem sampling of the brain and other tissues in neurodegenerative disease. In: *Histopathology* 44 (2004), Apr, Nr. 4, S. 309–17. <http://dx.doi.org/10.1111/j.1365-2559.2004.01794.x>. – DOI 10.1111/j.1365-2559.2004.01794.x
- [281] LU, M ; KOSIK, K: Competition for microtubule-binding with dual expression of tau missense and splice isoforms. In: *Mol Biol Cell* 12 (2001), Jan, Nr. 1, 171–84. <http://www.ncbi.nlm.nih.gov/pubmed/11160831>
- [282] LUNA-MUNOZ, J ; GARCIA-SIERRA, F ; FALCON, V ; MENENDEZ, I ; CHAVEZ-MACIAS, L ; MENA, R: Regional conformational change involving phosphorylation of tau protein at the Thr231, precedes the structural change detected by Alz-50 antibody in Alzheimer's disease. In: *J Alzheimers Dis* 8 (2005), Sep, Nr. 1, 29–41. <http://www.ncbi.nlm.nih.gov/pubmed/16155347>
- [283] LUO, Wenjie ; DOU, Fei ; RODINA, Anna ; CHIP, Sophorn ; KIM, Joungnam ; ZHAO, Qi ; MOULICK, Kamalika ; AGUIRRE, Julia ; WU, Nian ; GREENGARD, Paul ; CHIOSIS, Gabriela: Roles of heat-shock protein 90 in maintaining and facilitating the neurodegenerative phenotype in tauopathies. In: *Proc Natl Acad Sci USA* 104 (2007), May, Nr. 22, 9511–6. <http://dx.doi.org/10.1073/pnas.0701055104>. – DOI 10.1073/pnas.0701055104
- [284] MACIVER, S K. ; HARRINGTON, C R.: Two actin binding proteins, actin depolymerizing factor and cofilin, are associated with Hirano bodies. In: *Neuroreport* 6 (1995), Oct, Nr. 15, S. 1985–8
- [285] MACKENZIE, Ian R A. ; NEUMANN, Manuela ; BIGIO, Eileen H. ; CAIRNS, Nigel J. ; ALAFUZOFF, Irina ; KRIL, Jillian ; KOVACS, Gabor G. ; GHETTI, Bernardino ; HALLIDAY, Glenda ; HOLM, Ida E. ; INCE, Paul G. ; KAMPHORST, Wouter ; REVESZ, Tamas ; ROZEMULLER, Annemieke J M. ; KUMAR-SINGH, Samir ; AKIYAMA, Haruhiko ; BABORIE, Atik ; SPINA, Salvatore ; DICKSON, Dennis W. ; TROJANOWSKI, John Q. ; MANN, David M A.: Nomenclature and nosology for neuropathologic subtypes of frontotemporal lobar degeneration: an update. In: *Acta Neuropathol* 119 (2010), Jan, Nr. 1, S. 1–4. <http://dx.doi.org/10.1007/s00401-009-0612-2>. – DOI 10.1007/s00401-009-0612-2
- [286] MACLEAN, B ; TOMAZELA, D ; SHULMAN, N ; CHAMBERS, M ; FINNEY, G ; FREWEN, B ; KERN, R ; TABB, D ; LIEBLER, D ; MACCOSS, M: Skyline: an open source document editor for creating and analyzing targeted proteomics experiments. In: *Bioinformatics* 26 (2010), Apr, Nr. 7, S. 966–8. <http://dx.doi.org/10.1093/bioinformatics/btq054>. – DOI 10.1093/bioinformatics/btq054
- [287] MAEDA, Sumihiro ; SAHARA, Naruhiko ; SAITO, Yuko ; MURAYAMA, Miyuki ; YOSHIKE, Yuji ; KIM, Hyonchol ; MIYASAKA, Tomohiro ; MURAYAMA, Shigeo ; IKAI, Atsushi ; TAKASHIMA, Akihiko: Granular tau oligomers as intermediates of tau filaments. In: *Biochemistry* 46 (2007), Mar, Nr. 12, S. 3856–61. <http://dx.doi.org/10.1021/bi061359o>. – DOI 10.1021/bi061359o
- [288] MAIR, Waltraud ; MUNTEL, Jan ; TEPPER, Katharina ; TANG, Shaojun ; BIERNAT, Jacek ; SEELEY, William W. ; KOSIK, Kenneth S. ; MANDELKOW, Eckhard ; STEEN, Hanno ; STEEN, Judith A.: FLEXITau: Quantifying Post-translational Modifications of Tau Protein in vitro and in Human Disease. In: *Anal Chem* (2016), Feb. <http://dx.doi.org/10.1021/acs.analchem.5b04509>. – DOI 10.1021/acs.analchem.5b04509
- [289] MANDELKOW, E ; STAMER, K ; VOGEL, R ; THIES, E ; MANDELKOW, E: Clogging of axons by tau, inhibition of axonal traffic and starvation of synapses. In: *Neurobiol Aging* 24 (2003), Dec, Nr. 8, 1079–85. <http://www.ncbi.nlm.nih.gov/pubmed/14643379>
- [290] MANN, M ; HENDRICKSON, R C. ; PANDEY, A: Analysis of proteins and proteomes by mass spectrometry. In: *Annu Rev Biochem* 70 (2001), Jan, S. 437–73. <http://dx.doi.org/10.1146/annurev.biochem.70.1.437>. – DOI 10.1146/annurev.biochem.70.1.437
- [291] MAPSTONE, Mark ; CHEEMA, Amrita K. ; FIANDACA, Massimo S. ; ZHONG, Xiaogang ; MHYRE, Timothy R. ; MACARTHUR, Linda H. ; HALL, William J. ; FISHER, Susan G. ; PETERSON, Derick R. ; HALEY, James M. ; NAZAR, Michael D. ; RICH, Steven A. ; BERLAU, Dan J. ; PELTZ, Carrie B. ; TAN, Ming T. ; KAWAS, Claudia H. ; FEDEROFF, Howard J.: Plasma phospholipids identify antecedent memory impairment in older adults. In: *Nat Med* 20 (2014), Apr, Nr. 4, S. 415–8. <http://dx.doi.org/10.1038/nm.3466>. – DOI 10.1038/nm.3466

- [292] MARTIN, Ludovic ; LATYPOVA, Xenia ; TERRO, Faraj: Post-translational modifications of tau protein: implications for Alzheimer's disease. In: *Neurochemistry International* 58 (2011), Mar, Nr. 4, 458–71. <http://dx.doi.org/10.1016/j.neuint.2010.12.023>. – DOI 10.1016/j.neuint.2010.12.023
- [293] MARTIN, Ludovic ; LATYPOVA, Xenia ; WILSON, Cornelia M. ; MAGNAUDEIX, Amandine ; PERRIN, Marie-Laure ; YARDIN, Catherine ; TERRO, Faraj: Tau protein kinases: involvement in Alzheimer's disease. In: *Ageing Research Reviews* 12 (2013), Jan, Nr. 1, S. 289–309. <http://dx.doi.org/10.1016/j.arr.2012.06.003>. – DOI 10.1016/j.arr.2012.06.003
- [294] MATTSSON, Niklas ; INSEL, Philip S. ; LANDAU, Susan ; JAGUST, William ; DONOHUE, Michael ; SHAW, Leslie M. ; TROJANOWSKI, John Q. ; ZETTERBERG, Henrik ; BLENNOW, Kaj ; WEINER, Michael ; INITIATIVE, Alzheimer's Disease N.: Diagnostic accuracy of CSF Ab42 and florbetapir PET for Alzheimer's disease. In: *Ann Clin Transl Neurol* 1 (2014), Aug, Nr. 8, S. 534–43. <http://dx.doi.org/10.1002/acn3.81>. – DOI 10.1002/acn3.81
- [295] MAZANETZ, Michael P. ; FISCHER, Peter M.: Untangling tau hyperphosphorylation in drug design for neurodegenerative diseases. In: *Nat Rev Drug Discov* 6 (2007), Jun, Nr. 6, S. 464–79. <http://dx.doi.org/10.1038/nrd2111>. – DOI 10.1038/nrd2111
- [296] MCAVOY, Thomas ; LASSMAN, Michael E. ; SPELLMAN, Daniel S. ; KE, Zhenlian ; HOWELL, Bonnie J. ; WONG, Oitak ; ZHU, Lan ; TANEN, Michael ; STRUYK, Arie ; LATERZA, Omar F.: Quantification of tau in cerebrospinal fluid by immunoaffinity enrichment and tandem mass spectrometry. In: *Clinical Chemistry* 60 (2014), Apr, Nr. 4, S. 683–9. <http://dx.doi.org/10.1373/clinchem.2013.216515>. – DOI 10.1373/clinchem.2013.216515
- [297] MCDERMOTT, J ; AAMODT, S ; AAMODT, E: ptl-1, a *Caenorhabditis elegans* gene whose products are homologous to the tau microtubule-associated proteins. In: *Biochemistry* 35 (1996), Jul, Nr. 29, 9415–23. <http://dx.doi.org/10.1021/bi952646n>. – DOI 10.1021/bi952646n
- [298] MCINTOSH, G C. ; JAMESON, H D. ; MARKESBERY, W R.: Huntington disease associated with Alzheimer disease. In: *Ann Neurol* 3 (1978), Jun, Nr. 6, S. 545–8. <http://dx.doi.org/10.1002/ana.410030616>. – DOI 10.1002/ana.410030616
- [299] MCKHANN, G M. ; ALBERT, M S. ; GROSSMAN, M ; MILLER, B ; DICKSON, D ; TROJANOWSKI, J Q. ; FRONTOTEMPORAL DEMENTIA, Work G. ; DISEASE, Pick's: Clinical and pathological diagnosis of frontotemporal dementia: report of the Work Group on Frontotemporal Dementia and Pick's Disease. In: *Arch Neurol* 58 (2001), Nov, Nr. 11, S. 1803–9
- [300] MCKHANN, Guy M. ; KNOPMAN, David S. ; CHERTKOW, Howard ; HYMAN, Bradley T. ; JACK, Clifford R. ; KAWAS, Claudia H. ; KLUNK, William E. ; KOROSHETZ, Walter J. ; MANLY, Jennifer J. ; MAYEUX, Richard ; MOHS, Richard C. ; MORRIS, John C. ; ROSSOR, Martin N. ; SCHELTENS, Philip ; CARRILLO, Maria C. ; THIES, Bill ; WEINTRAUB, Sandra ; PHELPS, Creighton H.: The diagnosis of dementia due to Alzheimer's disease: recommendations from the National Institute on Aging-Alzheimer's Association workgroups on diagnostic guidelines for Alzheimer's disease. In: *Alzheimers Dement* 7 (2011), May, Nr. 3, S. 263–9. <http://dx.doi.org/10.1016/j.jalz.2011.03.005>. – DOI 10.1016/j.jalz.2011.03.005
- [301] MERAZ-RÍOS, Marco A. ; LEÓN, Karla I Lira-De ; CAMPOS-PEÑA, Victoria ; ANDA-HERNÁNDEZ, Martha A D. ; MENA-LÓPEZ, Raúl: Tau oligomers and aggregation in Alzheimer's disease. In: *J Neurochem* 112 (2010), Mar, Nr. 6, 1353–67. <http://dx.doi.org/10.1111/j.1471-4159.2009.06511.x>. – DOI 10.1111/j.1471-4159.2009.06511.x
- [302] MERSHIN, Andreas ; PAVLOPOULOS, Elias ; FITCH, Olivia ; BRADEN, Brittany C. ; NANOPOULOS, Dimitri V. ; SKOULAKIS, Efthimios M C.: Learning and memory deficits upon TAU accumulation in *Drosophila* mushroom body neurons. In: *Learn Mem* 11 (2004), Jan, Nr. 3, S. 277–87. <http://dx.doi.org/10.1101/lm.70804>. – DOI 10.1101/lm.70804
- [303] MIN, Sang-Won ; CHO, Seo-Hyun ; ZHOU, Yungui ; SCHROEDER, Sebastian ; HAROUTUNIAN, Vahram ; SEELEY, William W. ; HUANG, Eric J. ; SHEN, Yong ; MASLIAH, Eliezer ; MUKHERJEE, Chandrani ; MEYERS, David ; COLE, Philip A. ; OTT, Melanie ; GAN, Li: Acetylation of tau inhibits its degradation and contributes to tauopathy. In: *Neuron* 67 (2010), Sep, Nr. 6, S. 953–66. <http://dx.doi.org/10.1016/j.neuron.2010.08.044>. – DOI 10.1016/j.neuron.2010.08.044

- [304] MIRZAEI, Hamid ; MCBEE, Joshua K. ; WATTS, Julian ; AEBERSOLD, Ruedi: Comparative evaluation of current peptide production platforms used in absolute quantification in proteomics. In: *Mol Cell Proteomics* 7 (2008), Apr, Nr. 4, S. 813–23. <http://dx.doi.org/10.1074/mcp.M700495-MCP200>. – DOI 10.1074/mcp.M700495-MCP200
- [305] MITSUYAMA, Y ; SEYAMA, S: Frequency of Alzheimer's neurofibrillary tangle in the brains of progressive supranuclear palsy, postencephalitic parkinsonism, Alzheimer's disease, senile dementia and non-demented elderly person. In: *Folia Psychiatr Neurol Jpn* 35 (1981), Jan, Nr. 2, 189–204. http://www.ncbi.nlm.nih.gov/pubmed?Db=pubmed&Cmd=Retrieve&list_uids=7286861&dopt=abstractplus
- [306] MOCANU, M ; NISSEN, A ; ECKERMANN, K ; KHLISTUNOVA, I ; BIERNAT, J ; DREXLER, D ; PETROVA, O ; SCHONIG, K ; BUJARD, H ; MANDELKOW, E ; ZHOU, L ; RUNE, G ; MANDELKOW, E: The potential for beta-structure in the repeat domain of tau protein determines aggregation, synaptic decay, neuronal loss, and coassembly with endogenous Tau in inducible mouse models of tauopathy. In: *J Neurosci* 28 (2008), Jan, Nr. 3, 737–48. <http://dx.doi.org/10.1523/JNEUROSCI.2824-07.2008>. – DOI 10.1523/JNEUROSCI.2824-07.2008
- [307] MONDRAGON-RODRIGUEZ, S ; MENA, R ; BINDER, L ; SMITH, M ; PERRY, G ; GARCIA-SIERRA, F: Conformational changes and cleavage of tau in Pick bodies parallel the early processing of tau found in Alzheimer pathology. In: *Neuropathol Appl Neurobiol* 34 (2008), Feb, Nr. 1, 62–75. <http://dx.doi.org/10.1111/j.1365-2990.2007.00853.x>. – DOI 10.1111/j.1365-2990.2007.00853.x
- [308] MORISHIMA-KAWASHIMA, M ; HASEGAWA, M ; TAKIO, K ; SUZUKI, M ; TITANI, K ; IHARA, Y: Ubiquitin is conjugated with amino-terminally processed tau in paired helical filaments. In: *Neuron* 10 (1993), Jun, Nr. 6, S. 1151–60
- [309] MORRIS, H R. ; KHAN, M N. ; JANSSEN, J C. ; BROWN, J M. ; PEREZ-TUR, J ; BAKER, M ; OZANSOY, M ; HARDY, J ; HUTTON, M ; WOOD, N W. ; LEES, A J. ; REVESZ, T ; LANTOS, P ; ROSSOR, M N.: The genetic and pathological classification of familial frontotemporal dementia. In: *Arch Neurol* 58 (2001), Nov, Nr. 11, 1813–6. <http://archneur.jamanetwork.com/article.aspx?articleid=780848>
- [310] MORRIS, Meaghan ; KNUDSEN, Giselle M. ; MAEDA, Sumihiro ; TRINIDAD, Jonathan C. ; IOANOVICIU, Alexandra ; BURLINGAME, Alma L. ; MUCKE, Lennart: Tau post-translational modifications in wild-type and human amyloid precursor protein transgenic mice. In: *Nat Neurosci* (2015), Jul. <http://dx.doi.org/10.1038/nn.4067>. – DOI 10.1038/nn.4067
- [311] MORRISON, John H. ; HOF, Patrick R.: Life and death of neurons in the aging cerebral cortex. In: *Int Rev Neurobiol* 81 (2007), Jan, S. 41–57. [http://dx.doi.org/10.1016/S0074-7742\(06\)81004-4](http://dx.doi.org/10.1016/S0074-7742(06)81004-4). – DOI 10.1016/S0074-7742(06)81004-4
- [312] MOTTER, R ; VIGO-PELFREY, C ; KHOLODENKO, D ; BARBOUR, R ; JOHNSON-WOOD, K ; GALASKO, D ; CHANG, L ; MILLER, B ; CLARK, C ; GREEN, R: Reduction of beta-amyloid peptide42 in the cerebrospinal fluid of patients with Alzheimer's disease. In: *Ann Neurol* 38 (1995), Oct, Nr. 4, S. 643–8. <http://dx.doi.org/10.1002/ana.410380413>. – DOI 10.1002/ana.410380413
- [313] MUDHER, A ; SHEPHERD, D ; NEWMAN, T A. ; MILDREN, P ; JUKES, J P. ; SQUIRE, A ; MEARS, A ; DRUMMOND, J A. ; BERG, S ; MACKAY, D ; ASUNI, A A. ; BHAT, R ; LOVESTONE, S: GSK-3beta inhibition reverses axonal transport defects and behavioural phenotypes in *Drosophila*. In: *Mol Psychiatry* 9 (2004), May, Nr. 5, S. 522–30. <http://dx.doi.org/10.1038/sj.mp.4001483>. – DOI 10.1038/sj.mp.4001483
- [314] MUNGAS, D ; REED, B R. ; JAGUST, W J. ; DECARLI, C ; MACK, W J. ; KRAMER, J H. ; WEINER, M W. ; SCHUFF, N ; CHUI, H C.: Volumetric MRI predicts rate of cognitive decline related to AD and cerebrovascular disease. In: *Neurology* 59 (2002), Sep, Nr. 6, S. 867–73
- [315] MUNTEL, J ; XUAN, Y ; BERGER, S ; REITER, L ; BACHUR, R ; KENTSI, A ; STEEN, H: Advancing Urinary Protein Biomarker Discovery by Data-Independent Acquisition on a Quadrupole-Orbitrap Mass Spectrometer. In: *J Proteome Res* 14 (2015), Nov, Nr. 11, 4752–62. <http://dx.doi.org/10.1021/acs.jproteome.5b00826>. – DOI 10.1021/acs.jproteome.5b00826

- [316] MURRAY, Melissa E. ; GRAFF-RADFORD, Neill R. ; ROSS, Owen A. ; PETERSEN, Ronald C. ; DUARA, Ranjan ; DICKSON, Dennis W.: Neuropathologically defined subtypes of Alzheimer's disease with distinct clinical characteristics: a retrospective study. In: *The Lancet Neurology* 10 (2011), Sep, Nr. 9, S. 785–96. [http://dx.doi.org/10.1016/S1474-4422\(11\)70156-9](http://dx.doi.org/10.1016/S1474-4422(11)70156-9). – DOI 10.1016/S1474-4422(11)70156-9
- [317] MURRAY, Melissa E. ; KOURI, Naomi ; LIN, Wen-Lang ; JACK, Clifford R. ; DICKSON, Dennis W. ; VEMURI, Prashanthi: Clinicopathologic assessment and imaging of tauopathies in neurodegenerative dementias. In: *Alzheimers Res Ther* 6 (2014), Jan, Nr. 1, S. 1. <http://dx.doi.org/10.1186/alzrt231>. – DOI 10.1186/alzrt231
- [318] MURRELL, J R. ; SPILLANTINI, M G. ; ZOLO, P ; GUAZZELLI, M ; SMITH, M J. ; HASEGAWA, M ; REDI, F ; CROWTHER, R A. ; PIETRINI, P ; GHETTI, B ; GOEDERT, M: Tau gene mutation G389R causes a tauopathy with abundant pick body-like inclusions and axonal deposits. In: *J Neuropathol Exp Neurol* 58 (1999), Dec, Nr. 12, S. 1207–26
- [319] NACHARAJU, P ; LEWIS, J ; EASSON, C ; YEN, S ; HACKETT, J ; HUTTON, M ; YEN, S H.: Accelerated filament formation from tau protein with specific FTDP-17 missense mutations. In: *FEBS Lett* 447 (1999), Mar, Nr. 2-3, S. 195–9
- [320] NAGY, Z ; ESIRI, M M. ; JOBST, K A. ; MORRIS, J H. ; KING, E M. ; McDONALD, B ; LITCHFIELD, S ; SMITH, A ; BARNETSON, L ; SMITH, A D.: Relative roles of plaques and tangles in the dementia of Alzheimer's disease: correlations using three sets of neuropathological criteria. In: *Dementia* 6 (1995), Jan, Nr. 1, S. 21–31
- [321] NAKANO, I ; IWATSUBO, T ; OTSUKA, N ; KAMEI, M ; MATSUMURA, K ; MANNEN, T: Paired helical filaments in astrocytes: electron microscopy and immunohistochemistry in a case of atypical Alzheimer's disease. In: *Acta Neuropathol* 83 (1992), Jan, Nr. 3, S. 228–32
- [322] NELSON, P ; STEFANSSON, K ; GULCHER, J ; SAPER, C: Molecular evolution of tau protein: implications for Alzheimer's disease. In: *J Neurochem* 67 (1996), Oct, Nr. 4, 1622–32. <http://www.ncbi.nlm.nih.gov/pubmed/8858947>
- [323] NELSON, Peter T. ; ALAFUZOFF, Irina ; BIGIO, Eileen H. ; BOURAS, Constantin ; BRAAK, Heiko ; CAIRNS, Nigel J. ; CASTELLANI, Rudolph J. ; CRAIN, Barbara J. ; DAVIES, Peter ; TREDICI, Kelly D. ; DUYSCKAERTS, Charles ; FROSCHE, Matthew P. ; HAROUTUNIAN, Vahram ; HOF, Patrick R. ; HULETTE, Christine M. ; HYMAN, Bradley T. ; IWATSUBO, Takeshi ; JELLINGER, Kurt A. ; JICHA, Gregory A. ; KÖVARI, Enikő ; KUKULL, Walter A. ; LEVERENZ, James B. ; LOVE, Seth ; MACKENZIE, Ian R. ; MANN, David M. ; MASLIAH, Eliezer ; MCKEE, Ann C. ; MONTINE, Thomas J. ; MORRIS, John C. ; SCHNEIDER, Julie A. ; SONNEN, Joshua A. ; THAL, Dietmar R. ; TROJANOWSKI, John Q. ; TRONCOSO, Juan C. ; WISNIEWSKI, Thomas ; WOLTJER, Randall L. ; BEACH, Thomas G.: Correlation of Alzheimer disease neuropathologic changes with cognitive status: a review of the literature. In: *J Neuropathol Exp Neurol* 71 (2012), May, Nr. 5, S. 362–81. <http://dx.doi.org/10.1097/NEN.0b013e31825018f7>. – DOI 10.1097/NEN.0b013e31825018f7
- [324] NEUMANN, Manuela ; SAMPATHU, Deepak M. ; KWONG, Linda K. ; TRUAX, Adam C. ; MICSENYI, Matthew C. ; CHOU, Thomas T. ; BRUCE, Jennifer ; SCHUCK, Theresa ; GROSSMAN, Murray ; CLARK, Christopher M. ; MCCLUSKEY, Leo F. ; MILLER, Bruce L. ; MASLIAH, Eliezer ; MACKENZIE, Ian R. ; FELDMAN, Howard ; FEIDEN, Wolfgang ; KRETZSCHMAR, Hans A. ; TROJANOWSKI, John Q. ; LEE, Virginia M-Y: Ubiquitinated TDP-43 in frontotemporal lobar degeneration and amyotrophic lateral sclerosis. In: *Science* 314 (2006), Oct, Nr. 5796, S. 130–3. <http://dx.doi.org/10.1126/science.1134108>. – DOI 10.1126/science.1134108
- [325] NEVE, R ; HARRIS, P ; KOSIK, K ; KURNIT, D ; DONLON, T: Identification of cDNA clones for the human microtubule-associated protein tau and chromosomal localization of the genes for tau and microtubule-associated protein 2. In: *Brain Res* 387 (1986), Dec, Nr. 3, 271–80. <http://www.ncbi.nlm.nih.gov/pubmed/3103857>
- [326] NEWELL, K L. ; HYMAN, B T. ; GROWDON, J H. ; HEDLEY-WHYTE, E T.: Application of the National Institute on Aging (NIA)-Reagan Institute criteria for the neuropathological diagnosis of Alzheimer disease. In: *J Neuropathol Exp Neurol* 58 (1999), Nov, Nr. 11, S. 1147–55

- [327] NIETHAMMER, Martin ; TANG, Chris ; FEIGIN, Andrew ; ALLEN, Patricia ; HEINEN, Lisette ; HELLWIG, Sabine ; AMTAGE, Florian ; HANSPAL, Era ; VONSATTEL, Jean ; POSTON, Kathleen ; MEYER, Philipp ; LEENDERS, Klaus ; EIDELBERG, David: A disease-specific metabolic brain network associated with corticobasal degeneration. In: *Brain* 137 (2014), Nov, Nr. Pt 11, 3036–46. <http://dx.doi.org/10.1093/brain/awu256>. – DOI 10.1093/brain/awu256
- [328] NISHIMURA, M ; TOMIMOTO, H ; SUENAGA, T ; NAMBA, Y ; IKEDA, K ; AKIGUCHI, I ; KIMURA, J: Immunocytochemical characterization of glial fibrillary tangles in Alzheimer's disease brain. In: *Am J Pathol* 146 (1995), May, Nr. 5, S. 1052–8
- [329] NOBLE, Wendy ; HANGER, Diane P. ; MILLER, Christopher C J. ; LOVESTONE, Simon: The importance of tau phosphorylation for neurodegenerative diseases. In: *Front. Neurol.* 4 (2013), Jan, S. 83. <http://dx.doi.org/10.3389/fneur.2013.00083>. – DOI 10.3389/fneur.2013.00083
- [330] NOBLE, Wendy ; PLANEL, Emmanuel ; ZEHR, Cindy ; OLM, Vicki ; MEYERSON, Jordana ; SULEMAN, Farhana ; GAYNOR, Kate ; WANG, Lili ; LAFRANCOIS, John ; FEINSTEIN, Boris ; BURNS, Mark ; KRISHNAMURTHY, Pavan ; WEN, Yi ; BHAT, Ratan ; LEWIS, Jada ; DICKSON, Dennis ; DUFF, Karen: Inhibition of glycogen synthase kinase-3 by lithium correlates with reduced tauopathy and degeneration in vivo. In: *Proc Natl Acad Sci USA* 102 (2005), May, Nr. 19, S. 6990–5. <http://dx.doi.org/10.1073/pnas.0500466102>. – DOI 10.1073/pnas.0500466102
- [331] NOVAK, M ; KABAT, J ; WISCHIK, C M.: Molecular characterization of the minimal protease resistant tau unit of the Alzheimer's disease paired helical filament. In: *EMBO J* 12 (1993), Jan, Nr. 1, S. 365–70
- [332] OKAMURA, Nobuyuki ; SUEMOTO, Takahiro ; FURUMOTO, Shozo ; SUZUKI, Masako ; SHIMADZU, Hiroshi ; AKATSU, Hiroyasu ; YAMAMOTO, Takayuki ; FUJIWARA, Hironori ; NEMOTO, Miyako ; MARUYAMA, Masahiro ; ARAI, Hiroyuki ; YANAI, Kazuhiko ; SAWADA, Tohru ; KUDO, Yukitsuka: Quinoline and benzimidazole derivatives: candidate probes for in vivo imaging of tau pathology in Alzheimer's disease. In: *The Journal of neuroscience : the official journal of the Society for Neuroscience* 25 (2005), Nov, Nr. 47, S. 10857–62. <http://dx.doi.org/10.1523/JNEUROSCI.1738-05.2005>. – DOI 10.1523/JNEUROSCI.1738-05.2005
- [333] OLD, William M. ; MEYER-ARENDT, Karen ; AVELINE-WOLF, Lauren ; PIERCE, Kevin G. ; MENDOZA, Alex ; SEVINSKY, Joel R. ; RESING, Katheryn A. ; AHN, Natalie G.: Comparison of label-free methods for quantifying human proteins by shotgun proteomics. In: *Mol Cell Proteomics* 4 (2005), Oct, Nr. 10, S. 1487–502. <http://dx.doi.org/10.1074/mcp.M500084-MCP200>. – DOI 10.1074/mcp.M500084-MCP200
- [334] OLSEN, J ; MANN, M: Status of large-scale analysis of post-translational modifications by mass spectrometry. In: *Mol Cell Proteomics* 12 (2013), Dec, Nr. 12, 3444–52. <http://dx.doi.org/10.1074/mcp.0113.034181>. – DOI 10.1074/mcp.0113.034181
- [335] OLSEN, Jesper V. ; BLAGOEV, Blagoy ; GNAD, Florian ; MACEK, Boris ; KUMAR, Chanchal ; MORTENSEN, Peter ; MANN, Matthias: Global, in vivo, and site-specific phosphorylation dynamics in signaling networks. In: *Cell* 127 (2006), Nov, Nr. 3, S. 635–48. <http://dx.doi.org/10.1016/j.cell.2006.09.026>. – DOI 10.1016/j.cell.2006.09.026
- [336] ONG, Shao-En ; BLAGOEV, Blagoy ; KRATCHMAROVA, Irina ; KRISTENSEN, Dan B. ; STEEN, Hanno ; PANDEY, Akhilesh ; MANN, Matthias: Stable isotope labeling by amino acids in cell culture, SILAC, as a simple and accurate approach to expression proteomics. In: *Mol Cell Proteomics* 1 (2002), May, Nr. 5, S. 376–86
- [337] OUCHI, H ; TOYOSHIMA, Y ; TADA, M ; OYAKE, M ; AIDA, I ; TOMITA, I ; SATOH, A ; TSUJIHATA, M ; TAKAHASHI, H ; NISHIZAWA, M ; SHIMOHATA, T: Pathology and sensitivity of current clinical criteria in corticobasal syndrome. In: *Mov Disord* 29 (2014), Feb, Nr. 2, 238–44. <http://dx.doi.org/10.1002/mds.25746>. – DOI 10.1002/mds.25746
- [338] PANCHAUD, Alexandre ; SCHERL, Alexander ; SHAFFER, Scott A. ; HALLER, Priska D. ; KULASEKARA, Hemantha D. ; MILLER, Samuel I. ; GOODLETT, David R.: Precursor acquisition independent from ion count: how to dive deeper into the proteomics ocean. In: *Anal Chem* 81 (2009), Aug, Nr. 15, S. 6481–8. <http://dx.doi.org/10.1021/ac900888s>. – DOI 10.1021/ac900888s

- [339] PANDA, Dulal ; SAMUEL, Jonathan C. ; MASSIE, Michelle ; FEINSTEIN, Stuart C. ; WILSON, Leslie: Differential regulation of microtubule dynamics by three- and four-repeat tau: implications for the onset of neurodegenerative disease. In: *Proc Natl Acad Sci USA* 100 (2003), Aug, Nr. 16, S. 9548–53. <http://dx.doi.org/10.1073/pnas.1633508100>. – DOI 10.1073/pnas.1633508100
- [340] PANDEY, A ; MANN, M: Proteomics to study genes and genomes. In: *Nature* 405 (2000), Jun, Nr. 6788, S. 837–46. <http://dx.doi.org/10.1038/35015709>. – DOI 10.1038/35015709
- [341] PAPADOPOULOS, Marios C. ; ABEL, Paulo M. ; AGRANOFF, Dan ; STICH, August ; TARELLI, Edward ; BELL, B A. ; PLANCHE, Timothy ; LOOSEMORE, Alison ; SAADOUN, Samira ; WILKINS, Peter ; KRISHNA, Sanjeev: A novel and accurate diagnostic test for human African trypanosomiasis. In: *Lancet* 363 (2004), Apr, Nr. 9418, 1358–63. [http://dx.doi.org/10.1016/S0140-6736\(04\)16046-7](http://dx.doi.org/10.1016/S0140-6736(04)16046-7). – DOI 10.1016/S0140-6736(04)16046-7
- [342] PARKER, Laurie ; ENGEL-HALL, Aaron ; DREW, Kevin ; STEINHARDT, George ; HELSETH, Donald L. ; JABON, David ; MCMURRY, Timothy ; ANGULO, David S. ; KRON, Stephen J.: Investigating quantitation of phosphorylation using MALDI-TOF mass spectrometry. In: *J Mass Spectrom* 43 (2008), Apr, Nr. 4, S. 518–27. <http://dx.doi.org/10.1002/jms.1342>. – DOI 10.1002/jms.1342
- [343] PASINETTI, Giulio M.: From epidemiology to therapeutic trials with anti-inflammatory drugs in Alzheimer's disease: the role of NSAIDs and cyclooxygenase in beta-amyloidosis and clinical dementia. In: *J Alzheimers Dis* 4 (2002), Oct, Nr. 5, S. 435–45
- [344] PEDERSEN, J ; SIGURDSSON, E: Tau immunotherapy for Alzheimer's disease. In: *Trends Mol Med* 21 (2015), Jun, Nr. 6, 394–402. <http://dx.doi.org/10.1016/j.molmed.2015.03.003>. – DOI 10.1016/j.molmed.2015.03.003
- [345] PEI, J J. ; GRUNDKE-IQBAL, I ; IQBAL, K ; BOGDANOVIC, N ; WINBLAD, B ; COWBURN, R F.: Accumulation of cyclin-dependent kinase 5 (cdk5) in neurons with early stages of Alzheimer's disease neurofibrillary degeneration. In: *Brain Res* 797 (1998), Jun, Nr. 2, S. 267–77
- [346] PEREIRA, J M S. ; WILLIAMS, G B. ; ACOSTA-CABRONERO, J ; PENGAS, G ; SPILLANTINI, M G. ; XUEREB, J H. ; HODGES, J R. ; NESTOR, P J.: Atrophy patterns in histologic vs clinical groupings of frontotemporal lobar degeneration. In: *Neurology* 72 (2009), May, Nr. 19, S. 1653–60. <http://dx.doi.org/10.1212/WNL.0b013e3181a55fa2>. – DOI 10.1212/WNL.0b013e3181a55fa2
- [347] PERRY, G ; KAWAI, M ; TABATON, M ; ONORATO, M ; MULVIHILL, P ; RICHEY, P ; MORANDI, A ; CONNOLLY, J A. ; GAMBETTI, P: Neuropil threads of Alzheimer's disease show a marked alteration of the normal cytoskeleton. In: *The Journal of neuroscience : the official journal of the Society for Neuroscience* 11 (1991), Jun, Nr. 6, S. 1748–55
- [348] PETRICOIN, Emanuel F. ; ARDEKANI, Ali M. ; HITT, Ben A. ; LEVINE, Peter J. ; FUSARO, Vincent A. ; STEINBERG, Seth M. ; MILLS, Gordon B. ; SIMONE, Charles ; FISHMAN, David A. ; KOHN, Elise C. ; LIOTTA, Lance A.: Use of proteomic patterns in serum to identify ovarian cancer. In: *Lancet* 359 (2002), Feb, Nr. 9306, S. 572–7. [http://dx.doi.org/10.1016/S0140-6736\(02\)07746-2](http://dx.doi.org/10.1016/S0140-6736(02)07746-2). – DOI 10.1016/S0140-6736(02)07746-2
- [349] PETRUCELLI, L ; DICKSON, D ; KEHOE, K ; TAYLOR, J ; SNYDER, H ; GROVER, A ; LUCIA, M D. ; MCGOWAN, E ; LEWIS, J ; PRIHAR, G ; KIM, J ; DILLMANN, W ; BROWNE, S ; HALL, A ; VOELLMY, R ; TSUBOI, Y ; DAWSON, T ; WOLOZIN, B ; HARDY, J ; HUTTON, M: CHIP and Hsp70 regulate tau ubiquitination, degradation and aggregation. In: *Human Molecular Genetics* 13 (2004), Apr, Nr. 7, 703–14. <http://dx.doi.org/10.1093/hmg/ddh083>. – DOI 10.1093/hmg/ddh083
- [350] PETRY, Franck R. ; PELLETIER, Jérôme ; BRETTEVILLE, Alexis ; MORIN, Françoise ; CALON, Frédéric ; HÉBERT, Sébastien S ; WHITTINGTON, Robert A. ; PLANEL, Emmanuel: Specificity of anti-tau antibodies when analyzing mice models of Alzheimer's disease: problems and solutions. In: *PLoS ONE* 9 (2014), Jan, Nr. 5, S. e94251. <http://dx.doi.org/10.1371/journal.pone.0094251>. – DOI 10.1371/journal.pone.0094251

- [351] PIAO, Y ; HAYASHI, S ; WAKABAYASHI, K ; KAKITA, A ; AIDA, I ; YAMADA, M ; TAKAHASHI, H: Cerebellar cortical tau pathology in progressive supranuclear palsy and corticobasal degeneration. In: *Acta Neuropathol* 103 (2002), May, Nr. 5, 469–74. <http://dx.doi.org/10.1007/s00401-001-0488-2>. – DOI 10.1007/s00401-001-0488-2
- [352] PICOTTI, P ; AEBERSOLD, R: Selected reaction monitoring-based proteomics: workflows, potential, pitfalls and future directions. In: *Nat Methods* 9 (2012), Jun, Nr. 6, 555–66. <http://dx.doi.org/10.1038/nmeth.2015>. – DOI 10.1038/nmeth.2015
- [353] PICOTTI, P ; BODENMILLER, B ; MUELLER, L ; DOMON, B ; AEBERSOLD, R: Full dynamic range proteome analysis of *S. cerevisiae* by targeted proteomics. In: *Cell* 138 (2009), Aug, Nr. 4, 795–806. <http://dx.doi.org/10.1016/j.cell.2009.05.051>. – DOI 10.1016/j.cell.2009.05.051
- [354] PLANEL, Emmanuel ; MIYASAKA, Tomohiro ; LAUNAY, Thomas ; CHUI, De-Hua ; TANEMURA, Kentaro ; SATO, Shinji ; MURAYAMA, Ohoshi ; ISHIGURO, Koichi ; TATEBAYASHI, Yoshitaka ; TAKASHIMA, Akihiko: Alterations in glucose metabolism induce hypothermia leading to tau hyperphosphorylation through differential inhibition of kinase and phosphatase activities: implications for Alzheimer's disease. In: *J Neurosci* 24 (2004), Mar, Nr. 10, S. 2401–11. <http://dx.doi.org/10.1523/JNEUROSCI.5561-03.2004>. – DOI 10.1523/JNEUROSCI.5561-03.2004
- [355] PRABAKARAN, S ; LIPPENS, G ; STEEN, H ; GUNAWARDENA, J: Post-translational modification: nature's escape from genetic imprisonment and the basis for dynamic information encoding. In: *Wiley Interdiscip Rev Syst Biol Med* 4 (2012), Nov, Nr. 6, 565–83. <http://dx.doi.org/10.1002/wsbm.1185>. – DOI 10.1002/wsbm.1185
- [356] PRABAKARAN, Sudhakaran ; EVERLEY, Robert A. ; LANDRIEU, Isabelle ; WIERUSZESKI, Jean-Michel ; LIPPENS, Guy ; STEEN, Hanno ; GUNAWARDENA, Jeremy: Comparative analysis of Erk phosphorylation suggests a mixed strategy for measuring phospho-form distributions. In: *Mol Syst Biol* 7 (2011), Apr, S. 482. <http://dx.doi.org/10.1038/msb.2011.15>. – DOI 10.1038/msb.2011.15
- [357] PRAKASH, A ; REZAI, T ; KRASTINS, B ; SARRACINO, D ; ATHANAS, M ; RUSSO, P ; ROSS, M ; ZHANG, H ; TIAN, Y ; KULASINGAM, V ; DRABOVICH, A ; SMITH, C ; BATRUCH, I ; LIOTTA, L ; PETRICOIN, E ; DIAMANDIS, E ; CHAN, D ; LOPEZ, M: Platform for establishing interlaboratory reproducibility of selected reaction monitoring-based mass spectrometry peptide assays. In: *J Proteome Res* 9 (2010), Dec, Nr. 12, 6678–88. <http://dx.doi.org/10.1021/pr100821m>. – DOI 10.1021/pr100821m
- [358] PREUSS, U ; MANDELKOW, E M.: Mitotic phosphorylation of tau protein in neuronal cell lines resembles phosphorylation in Alzheimer's disease. In: *Eur J Cell Biol* 76 (1998), Jul, Nr. 3, S. 176–84. [http://dx.doi.org/10.1016/S0171-9335\(98\)80032-0](http://dx.doi.org/10.1016/S0171-9335(98)80032-0). – DOI 10.1016/S0171-9335(98)80032-0
- [359] PRINCE, M ; WIMO, Anders ; GUERCHET, Maelenn ; ALI, Gemma-Claire ; WU, Yu-Tzu ; PRINA, Matthew: The World Alzheimer Report 2015. In: *Alzheimer's Disease International* (2015)
- [360] PROBST, A ; TOLNAY, M ; LANGUI, D ; GOEDERT, M ; SPILLANTINI, M G.: Pick's disease: hyperphosphorylated tau protein segregates to the somatoaxonal compartment. In: *Acta Neuropathologica* 92 (1996), Dec, Nr. 6, 588–96. <http://link.springer.de/link/service/journals/00401/bibs/6092006/60920588.htm>
- [361] PROFENNO, Louis A. ; PORSTEINSSON, Anton P. ; FARAONE, Stephen V.: Meta-analysis of Alzheimer's disease risk with obesity, diabetes, and related disorders. In: *Biol Psychiatry* 67 (2010), Mar, Nr. 6, S. 505–12. <http://dx.doi.org/10.1016/j.biopsych.2009.02.013>. – DOI 10.1016/j.biopsych.2009.02.013
- [362] RAVID, Rivka: The uniqueness of biobanks for neurological and psychiatric diseases: potentials and pitfalls. In: *Pathobiology* 81 (2014), Jan, Nr. 5-6, 237–44. <http://dx.doi.org/10.1159/000369886>. – DOI 10.1159/000369886
- [363] REBEIZ, J J. ; KOLODNY, E H. ; RICHARDSON, E P.: Corticodentatonigral degeneration with neuronal achromasia. In: *Arch Neurol* 18 (1968), Jan, Nr. 1, S. 20–33

- [364] REGINOLD, William ; LANG, Anthony E. ; MARRAS, Connie ; HEYN, Chris ; ALHARBI, Mohammed ; MIKULIS, David J.: Longitudinal quantitative MRI in multiple system atrophy and progressive supranuclear palsy. In: *Parkinsonism Relat Disord* 20 (2014), Feb, Nr. 2, S. 222–5. <http://dx.doi.org/10.1016/j.parkreldis.2013.10.002>. – DOI 10.1016/j.parkreldis.2013.10.002
- [365] RENARD, B ; KIRCHNER, M ; MONIGATTI, F ; IVANOV, A ; RAPPILBER, J ; WINTER, D ; STEEN, J ; HAMPRECHT, F ; STEEN, H: When less can yield more - Computational preprocessing of MS/MS spectra for peptide identification. In: *PROTEOMICS* 9 (2009), Nov, Nr. 21, S. 4978–84. <http://dx.doi.org/10.1002/pmic.200900326>. – DOI 10.1002/pmic.200900326
- [366] RESPONDEK, Gesine ; STAMELOU, Maria ; KURZ, Carolin ; FERGUSON, Leslie W. ; RAJPUT, Alexander ; CHIU, Wan Z. ; SWIETEN, John C. ; TROAKES, Claire ; SARRAJ, Safa A. ; GELPI, Ellen ; GAIG, Carles ; TOLOSA, Eduardo ; OERTEL, Wolfgang H. ; GIESE, Armin ; ROEBER, Sigrun ; ARZBERGER, Thomas ; WAGENPFEIL, Stefan ; HÖGLINGER, Günter U ; PSP STUDY GROUP, Movement Disorder S.: The phenotypic spectrum of progressive supranuclear palsy: a retrospective multicenter study of 100 definite cases. In: *Mov Disord* 29 (2014), Dec, Nr. 14, S. 1758–66. <http://dx.doi.org/10.1002/mds.26054>. – DOI 10.1002/mds.26054
- [367] REYNOLDS, Matthew R. ; REYES, Juan F. ; FU, Yifan ; BIGIO, Eileen H. ; GUILLOZET-BONGAARTS, Angela L. ; BERRY, Robert W. ; BINDER, Lester I.: Tau nitration occurs at tyrosine 29 in the fibrillar lesions of Alzheimer’s disease and other tauopathies. In: *The Journal of neuroscience : the official journal of the Society for Neuroscience* 26 (2006), Oct, Nr. 42, S. 10636–45. <http://dx.doi.org/10.1523/JNEUROSCI.2143-06.2006>. – DOI 10.1523/JNEUROSCI.2143-06.2006
- [368] RIGBOLT, Kristoffer T G. ; PROKHOROVA, Tatyana A. ; AKIMOV, Vyacheslav ; HENNINGSSEN, Jeanette ; JOHANSEN, Pia T. ; KRATCHMAROVA, Irina ; KASSEM, Moustapha ; MANN, Matthias ; OLSEN, Jesper V. ; BLAGOEV, Blagoy: System-wide temporal characterization of the proteome and phosphoproteome of human embryonic stem cell differentiation. In: *Sci Signal* 4 (2011), Jan, Nr. 164, S. rs3. <http://dx.doi.org/10.1126/scisignal.2001570>. – DOI 10.1126/scisignal.2001570
- [369] RINNE, J O. ; LEE, M S. ; THOMPSON, P D. ; MARSDEN, C D.: Corticobasal degeneration. A clinical study of 36 cases. In: *Brain* 117 (Pt 5) (1994), Oct, S. 1183–96
- [370] RIZZU, P ; SWIETEN, J C V. ; JOOSSE, M ; HASEGAWA, M ; STEVENS, M ; TIBBEN, A ; NIERMEIJER, M F. ; HILLEBRAND, M ; RAVID, R ; OOSTRA, B A. ; GOEDERT, M ; DUIJN, C M. ; HEUTINK, P: High prevalence of mutations in the microtubule-associated protein tau in a population study of frontotemporal dementia in the Netherlands. In: *Am J Hum Genet* 64 (1999), Feb, Nr. 2, 414–21. <http://dx.doi.org/10.1086/302256>. – DOI 10.1086/302256
- [371] RODRIGUEZ, RD ; GRINBERG, LT: Argyrophilic grain disease: An underestimated tauopathy. In: *Dement Neuropsychol* 9 (2015), Dec, Nr. 1, S. 2–8
- [372] ROSS, Philip L. ; HUANG, Yulin N. ; MARCHESE, Jason N. ; WILLIAMSON, Brian ; PARKER, Kenneth ; HATTAN, Stephen ; KHAINOVSKI, Nikita ; PILLAI, Sasi ; DEY, Subhakar ; DANIELS, Scott ; PURKAYASTHA, Subhasish ; JUHASZ, Peter ; MARTIN, Stephen ; BARTLET-JONES, Michael ; HE, Feng ; JACOBSON, Allan ; PAPPIN, Darryl J.: Multiplexed protein quantitation in *Saccharomyces cerevisiae* using amine-reactive isobaric tagging reagents. In: *Mol Cell Proteomics* 3 (2004), Dec, Nr. 12, S. 1154–69. <http://dx.doi.org/10.1074/mcp.M400129-MCP200>. – DOI 10.1074/mcp.M400129-MCP200
- [373] RÖST, Hannes L. ; ROSENBERGER, George ; NAVARRO, Pedro ; GILLET, Ludovic ; MILADINović, Saša M ; SCHUBERT, Olga T. ; WOLSKI, Witold ; COLLINS, Ben C. ; MALMSTRÖM, Johan ; MALMSTRÖM, Lars ; AEBERSOLD, Ruedi: OpenSWATH enables automated, targeted analysis of data-independent acquisition MS data. In: *Nat Biotechnol* 32 (2014), Mar, Nr. 3, S. 219–23. <http://dx.doi.org/10.1038/nbt.2841>. – DOI 10.1038/nbt.2841
- [374] RUBBI, Liudmilla ; TITZ, Björn ; BROWN, Lauren ; GALVAN, Erica ; KOMISOPOULOU, Evangelia ; CHEN, Sharon S. ; LOW, Tracey ; TAHMASIAN, Martik ; SKAGGS, Brian ; MÜSCHEN, Markus ; PELLEGRINI, Matteo ; GRAEBER, Thomas G.: Global phosphoproteomics reveals crosstalk between Bcr-Abl and negative feedback mechanisms controlling Src signaling. In: *Sci Signal* 4 (2011), Jan, Nr. 166, S. ra18. <http://dx.doi.org/10.1126/scisignal.2001314>. – DOI 10.1126/scisignal.2001314

- [375] RUPRECHT, Benjamin ; KOCH, Heiner ; MEDARD, Guillaume ; MUNDT, Max ; KUSTER, Bernhard ; LEMEER, Simone: Comprehensive and reproducible phosphopeptide enrichment using iron immobilized metal ion affinity chromatography (Fe-IMAC) columns. In: *Mol Cell Proteomics* 14 (2015), Jan, Nr. 1, S. 205–15. <http://dx.doi.org/10.1074/mcp.M114.043109>. – DOI 10.1074/mcp.M114.043109
- [376] RUSSELL, Claire L. ; KONCAREVIC, Sasa ; WARD, Malcolm A.: Post-translational modifications in Alzheimer's disease and the potential for new biomarkers. In: *J Alzheimers Dis* 41 (2014), Jan, Nr. 2, 345–64. <http://dx.doi.org/10.3233/JAD-132312>. – DOI 10.3233/JAD-132312
- [377] SAHARA, Naruhiko ; DETURE, Michael ; REN, Yan ; EBRAHIM, Abdul-Shukkur ; KANG, Dongcheul ; KNIGHT, Joshua ; VOLBRACHT, Christiane ; PEDERSEN, Jan T. ; DICKSON, Dennis W. ; YEN, Shu-Hui ; LEWIS, Jada: Characteristics of TBS-extractable hyperphosphorylated tau species: aggregation intermediates in rTg4510 mouse brain. In: *J Alzheimers Dis* 33 (2013), Jan, Nr. 1, S. 249–63. <http://dx.doi.org/10.3233/JAD-2012-121093>. – DOI 10.3233/JAD-2012-121093
- [378] SANDERS, David W. ; KAUFMAN, Sarah K. ; DEVOS, Sarah L. ; SHARMA, Apurwa M. ; MIRBAHA, Hilda ; LI, Aimin ; BARKER, Scarlett J. ; FOLEY, Alex C. ; THORPE, Julian R. ; SERPELL, Louise C. ; MILLER, Timothy M. ; GRINBERG, Lea T. ; SEELEY, William W. ; DIAMOND, Marc I.: Distinct Tau Prion Strains Propagate in Cells and Mice and Define Different Tauopathies. In: *Neuron* 82 (2015), Sep, Nr. 6, 1271–1288. <http://dx.doi.org/10.1016/j.neuron.2014.04.047>. – DOI 10.1016/j.neuron.2014.04.047
- [379] SANTACRUZ, K ; LEWIS, J ; SPIRES, T ; PAULSON, J ; KOTILINEK, L ; INGELSSON, M ; GUIMARAES, A ; DETURE, M ; RAMSDEN, M ; MCGOWAN, E ; FORSTER, C ; YUE, M ; ORNE, J ; JANUS, C ; MARIASH, A ; KUSKOWSKI, M ; HYMAN, B ; HUTTON, M ; ASHE, K H.: Tau suppression in a neurodegenerative mouse model improves memory function. In: *Science* 309 (2005), Jul, Nr. 5733, S. 476–81. <http://dx.doi.org/10.1126/science.1113694>. – DOI 10.1126/science.1113694
- [380] SAVICA, R ; GROSSARDT, B ; BOWER, J ; BOEVE, B ; AHLKOG, J ; ROCCA, W: Incidence of dementia with Lewy bodies and Parkinson disease dementia. In: *JAMA Neurol* 70 (2013), Nov, Nr. 11, 1396–402. <http://dx.doi.org/10.1001/jamaneurol.2013.3579>. – DOI 10.1001/jamaneurol.2013.3579
- [381] SCHNEIDER, A ; BIERNAT, J ; BERGEN, M von ; MANDELKOW, E ; MANDELKOW, E: Phosphorylation that detaches tau protein from microtubules (Ser262, Ser214) also protects it against aggregation into Alzheimer paired helical filaments. In: *Biochemistry* 38 (1999), Mar, Nr. 12, 3549–58. <http://dx.doi.org/10.1021/bi981874p>. – DOI 10.1021/bi981874p
- [382] SCHOENFELD, T ; OBAR, R: Diverse distribution and function of fibrous microtubule-associated proteins in the nervous system. In: *Int Rev Cytol* 151 (1994), 67–137. <http://www.ncbi.nlm.nih.gov/pubmed/7912236>
- [383] SCHOONENBOOM, N S M. ; REESINK, F E. ; VERWEY, N A. ; KESTER, M I. ; TEUNISSEN, C E. ; VEN, P M. d. ; PIJNENBURG, Y A L. ; BLANKENSTEIN, M A. ; ROZEMULLER, A J. ; SCHELTENS, P ; FLIER, W M. d.: Cerebrospinal fluid markers for differential dementia diagnosis in a large memory clinic cohort. In: *Neurology* 78 (2012), Jan, Nr. 1, 47–54. <http://dx.doi.org/10.1212/WNL.0b013e31823ed0f0>. – DOI 10.1212/WNL.0b013e31823ed0f0
- [384] SCHULTE, Eva C. ; FUKUMORI, Akio ; MOLLENHAUER, Brit ; HOR, Hyun ; ARZBERGER, Thomas ; PERNECZKY, Robert ; KURZ, Alexander ; DIEHL-SCHMID, Janine ; HÜLL, Michael ; LICHTNER, Peter ; ECKSTEIN, Gertrud ; ZIMPRICH, Alexander ; HAUBENBERGER, Dietrich ; PIRKER, Walter ; BRÜCKE, Thomas ; BEREZNAI, Benjamin ; MOLNAR, Maria J. ; LORENZO-BETANCOR, Oswaldo ; PASTOR, Pau ; PETERS, Annette ; GIEGER, Christian ; ESTIVILL, Xavier ; MEITINGER, Thomas ; KRETZSCHMAR, Hans A. ; TRENKWALDER, Claudia ; HAASS, Christian ; WINKELMANN, Juliane: Rare variants in Amyloid precursor protein (APP) and Parkinson's disease. In: *Eur J Hum Genet* 23 (2015), Oct, Nr. 10, S. 1328–33. <http://dx.doi.org/10.1038/ejhg.2014.300>. – DOI 10.1038/ejhg.2014.300
- [385] SCHULZE, Waltraud X. ; USADEL, Björn: Quantitation in mass-spectrometry-based proteomics. In: *Annu Rev Plant Biol* 61 (2010), Jan, S. 491–516. <http://dx.doi.org/10.1146/annurev-arplant-042809-112132>. – DOI 10.1146/annurev-arplant-042809-112132

- [386] SCHWEERS, O ; MANDELKOW, E M. ; BIERNAT, J ; MANDELKOW, E: Oxidation of cysteine-322 in the repeat domain of microtubule-associated protein tau controls the in vitro assembly of paired helical filaments. In: *Proc Natl Acad Sci USA* 92 (1995), Aug, Nr. 18, S. 8463–7
- [387] SCHWERTMAN, Petra ; BEZSTAROSTI, Karel ; LAFFEBER, Charlie ; VERMEULEN, Wim ; DEMMERS, Jeroen A A. ; MARTEIJN, Jurgen A.: An immunoaffinity purification method for the proteomic analysis of ubiquitinated protein complexes. In: *Anal Biochem* 440 (2013), Sep, Nr. 2, S. 227–36. <http://dx.doi.org/10.1016/j.ab.2013.05.020>. – DOI 10.1016/j.ab.2013.05.020
- [388] SCOTT, Kerry B. ; TURKO, Illarion V. ; PHINNEY, Karen W.: Quantitative performance of internal standard platforms for absolute protein quantification using multiple reaction monitoring-mass spectrometry. In: *Anal Chem* 87 (2015), Apr, Nr. 8, S. 4429–35. <http://dx.doi.org/10.1021/acs.analchem.5b00331>. – DOI 10.1021/acs.analchem.5b00331
- [389] SEELAAR, Harro ; ROHRER, Jonathan D. ; PIJNENBURG, Yolande A L. ; FOX, Nick C. ; SWIETEN, John C.: Clinical, genetic and pathological heterogeneity of frontotemporal dementia: a review. In: *J Neurol Neurosurg Psychiatr* 82 (2011), May, Nr. 5, S. 476–86. <http://dx.doi.org/10.1136/jnnp.2010.212225>. – DOI 10.1136/jnnp.2010.212225
- [390] SERGEANT, N ; DAVID, J P. ; LEFRANC, D ; VERMERSCH, P ; WATTEZ, A ; DELACOURTE, A: Different distribution of phosphorylated tau protein isoforms in Alzheimer's and Pick's diseases. In: *FEBS Letters* 412 (1997), Aug, Nr. 3, S. 578–82
- [391] SERGEANT, N ; WATTEZ, A ; DELACOURTE, A: Neurofibrillary degeneration in progressive supranuclear palsy and corticobasal degeneration: tau pathologies with exclusively "exon 10" isoforms. In: *J Neurochem* 72 (1999), Mar, Nr. 3, S. 1243–9
- [392] SERGEANT, Nicolas ; DELACOURTE, André ; BUÉE, Luc: Tau protein as a differential biomarker of tauopathies. In: *Biochim Biophys Acta* 1739 (2005), Jan, Nr. 2-3, S. 179–97. <http://dx.doi.org/10.1016/j.bbadis.2004.06.020>. – DOI 10.1016/j.bbadis.2004.06.020
- [393] SHANKAR, S K. ; YANAGIHARA, R ; GARRUTO, R M. ; GRUNDKE-IQBAL, I ; KOSIK, K S. ; GAJDUSEK, D C.: Immunocytochemical characterization of neurofibrillary tangles in amyotrophic lateral sclerosis and parkinsonism-dementia of Guam. In: *Ann Neurol* 25 (1989), Feb, Nr. 2, S. 146–51. <http://dx.doi.org/10.1002/ana.410250207>. – DOI 10.1002/ana.410250207
- [394] SHEFFIELD, L G. ; MARQUIS, J G. ; BERMAN, N E.: Regional distribution of cortical microglia parallels that of neurofibrillary tangles in Alzheimer's disease. In: *Neurosci Lett* 285 (2000), May, Nr. 3, S. 165–8
- [395] SHOGHI-JADID, Kooresh ; SMALL, Gary W. ; AGDEPPA, Eric D. ; KEPE, Vladimir ; ERCOLI, Linda M. ; SIDDARTH, Prabha ; READ, Stephen ; SATYAMURTHY, Nagichettiar ; PETRIC, Andrej ; HUANG, Sung-Cheng ; BARRIO, Jorge R.: Localization of neurofibrillary tangles and beta-amyloid plaques in the brains of living patients with Alzheimer disease. In: *Am J Geriatr Psychiatry* 10 (2002), Jan, Nr. 1, S. 24–35
- [396] SIGURDSSON, Einar M.: Immunotherapy targeting pathological tau protein in Alzheimer's disease and related tauopathies. In: *J Alzheimers Dis* 15 (2008), Oct, Nr. 2, S. 157–68
- [397] SILVA, R de ; LASHLEY, T ; GIBB, G ; HANGER, D ; HOPE, A ; REID, A ; BANDOPADHYAY, R ; UTTON, M ; STRAND, C ; JOWETT, T ; KHAN, N ; ANDERTON, B ; WOOD, N ; HOLTON, J ; REVESZ, T ; LEES, A: Pathological inclusion bodies in tauopathies contain distinct complements of tau with three or four microtubule-binding repeat domains as demonstrated by new specific monoclonal antibodies. In: *Neuropathol Appl Neurobiol* 29 (2003), Jun, Nr. 3, S. 288–302
- [398] SILVA, Rohan de ; LASHLEY, Tammaryn ; STRAND, Catherine ; SHIARLI, Anna-Maria ; SHI, Jing ; TIAN, Jinzhou ; BAILEY, Kathryn L. ; DAVIES, Peter ; BIGIO, Eileen H. ; ARIMA, Kunimasa ; ISEKI, Eizo ; MURAYAMA, Shigeo ; KRETZSCHMAR, Hans ; NEUMANN, Manuela ; LIPPA, Carol ; HALLIDAY, Glenda ; MACKENZIE, James ; RAVID, Rivka ; DICKSON, Dennis ; WSZOLEK, Zbigniew ; IWATSUBO, Takeshi ; PICKERING-BROWN, Stuart M. ; HOLTON, Janice ; LEES, Andrew ; REVESZ, Tamas ; MANN, David M A.: An immunohistochemical study of cases of sporadic and inherited frontotemporal lobar degeneration

- using 3R- and 4R-specific tau monoclonal antibodies. In: *Acta Neuropathologica* 111 (2006), Apr, Nr. 4, S. 329–40. <http://dx.doi.org/10.1007/s00401-006-0048-x>. – DOI 10.1007/s00401-006-0048-x
- [399] SING, T ; SANDER, O ; BEERENWINKEL, N ; LENGAUER, T: ROCR: visualizing classifier performance in R. In: *Bioinformatics* 21 (2005), Oct, Nr. 20, 3940–1. <http://dx.doi.org/10.1093/bioinformatics/bti623>. – DOI 10.1093/bioinformatics/bti623
- [400] SINGH, S ; WINTER, D ; BILIMORIA, P ; BONNI, A ; STEEN, H ; STEEN, J: FLEXIQinase, a mass spectrometry-based assay, to unveil multikinase mechanisms. In: *Nat Methods* 9 (2012), May, Nr. 5, 504–8. <http://dx.doi.org/10.1038/nmeth.1970>. – DOI 10.1038/nmeth.1970
- [401] SINGH, Sasha ; SPRINGER, Michael ; STEEN, Judith ; KIRSCHNER, Marc W. ; STEEN, Hanno: FLEXI-Quant: a novel tool for the absolute quantification of proteins, and the simultaneous identification and quantification of potentially modified peptides. In: *J Proteome Res* 8 (2009), May, Nr. 5, S. 2201–10. <http://dx.doi.org/10.1021/pr800654s>. – DOI 10.1021/pr800654s
- [402] SINGH, Sasha A. ; WINTER, Dominic ; KIRCHNER, Marc ; CHAUHAN, Ruchi ; AHMED, Saima ; OZLU, Nurhan ; TZUR, Amit ; STEEN, Judith A. ; STEEN, Hanno: Co-regulation proteomics reveals substrates and mechanisms of APC/C-dependent degradation. In: *EMBO J* 33 (2014), Feb, Nr. 4, S. 385–99. <http://dx.doi.org/10.1002/embj.201385876>. – DOI 10.1002/embj.201385876
- [403] SIUTI, Nertila ; KELLEHER, Neil L.: Decoding protein modifications using top-down mass spectrometry. In: *Nat Meth* 4 (2007), Oct, Nr. 10, S. 817–821. <http://dx.doi.org/10.1038/nmeth1097>. – DOI 10.1038/nmeth1097
- [404] SOSTE, Martin ; HRABAKOVA, Rita ; WANKA, Stefanie ; MELNIK, Andre ; BOERSEMA, Paul ; MAIOLICA, Alessio ; WERNAS, Timon ; TOGNETTI, Marco ; MERING, Christian von ; PICOTTI, Paola: A sentinel protein assay for simultaneously quantifying cellular processes. In: *Nature Methods* (2014), Jul, 1–8. <http://dx.doi.org/10.1038/nmeth.3101>. – DOI 10.1038/nmeth.3101
- [405] SPILLANTINI, M G. ; GOEDERT, M: Tau protein pathology in neurodegenerative diseases. In: *Trends Neurosci* 21 (1998), Oct, Nr. 10, 428–33. <http://www.sciencedirect.com/science/article/pii/S016622369801337X>
- [406] SPILLANTINI, Maria G. ; GOEDERT, Michel: Tau pathology and neurodegeneration. In: *Lancet Neurol* 12 (2013), Jun, Nr. 6, S. 609–22. [http://dx.doi.org/10.1016/S1474-4422\(13\)70090-5](http://dx.doi.org/10.1016/S1474-4422(13)70090-5). – DOI 10.1016/S1474-4422(13)70090-5
- [407] SPIRES, Tara L. ; ORNE, Jennifer D. ; SANTA CRUZ, Karen ; PITSTICK, Rose ; CARLSON, George A. ; ASHE, Karen H. ; HYMAN, Bradley T.: Region-specific dissociation of neuronal loss and neurofibrillary pathology in a mouse model of tauopathy. In: *The American Journal of Pathology* 168 (2006), May, Nr. 5, S. 1598–607. <http://dx.doi.org/10.2353/ajpath.2006.050840>. – DOI 10.2353/ajpath.2006.050840
- [408] STEELE, J C. ; RICHARDSON, J C. ; OLSZEWSKI, J: PROGRESSIVE SUPRANUCLEAR PALSY. A HETEROGENEOUS DEGENERATION INVOLVING THE BRAIN STEM, BASAL GANGLIA AND CEREBELLUM WITH VERTICAL GAZE AND PSEUDOBULBAR PALSY, NUCHAL DYSTONIA AND DEMENTIA. In: *Arch Neurol* 10 (1964), Apr, S. 333–59
- [409] STEEN, Hanno ; MANN, Matthias: The ABC's (and XYZ's) of peptide sequencing. In: *Nat Rev Mol Cell Biol* 5 (2004), Sep, Nr. 9, S. 699–711. <http://dx.doi.org/10.1038/nrm1468>. – DOI 10.1038/nrm1468
- [410] STEPHENSON, Barney ; SHIMWELL, Neil ; HUMPHREYS, Elizabeth ; WARD, Douglas ; ADAMS, David ; MARTIN, Ashley ; AFFORD, Simon: Quantitative assessment of the cell surface proteome to identify novel therapeutic targets in cholangiocarcinoma. In: *Lancet* 385 Suppl 1 (2015), Feb, S94. [http://dx.doi.org/10.1016/S0140-6736\(15\)60409-3](http://dx.doi.org/10.1016/S0140-6736(15)60409-3). – DOI 10.1016/S0140-6736(15)60409-3
- [411] STIELER, Jens T. ; BULLMANN, Torsten ; KOHL, Franziska ; TØIEN, Øivind ; BRÜCKNER, Martina K. ; HÄRTIG, Wolfgang ; BARNES, Brian M. ; ARENDT, Thomas: The physiological link between metabolic rate depression and tau phosphorylation in mammalian hibernation. In: *PLoS ONE* 6 (2011), Jan, Nr. 1, S. e14530. <http://dx.doi.org/10.1371/journal.pone.0014530>. – DOI 10.1371/journal.pone.0014530

- [412] SUN, Anyang ; NGUYEN, Xuan V. ; BING, Guoying: Comparative analysis of an improved thioflavin-s stain, Gallyas silver stain, and immunohistochemistry for neurofibrillary tangle demonstration on the same sections. In: *J Histochem Cytochem* 50 (2002), Apr, Nr. 4, S. 463–72
- [413] SYDOW, Astrid ; JEUGD, Ann V. ; ZHENG, Fang ; AHMED, Tariq ; BALSCHUN, Detlef ; PETROVA, Olga ; DREXLER, Dagmar ; ZHOU, Lepu ; RUNE, Gabriele ; MANDELKOW, Eckhard ; D’HOOGHE, Rudi ; ALZHEIMER, Christian ; MANDELKOW, Eva-Maria: Tau-induced defects in synaptic plasticity, learning, and memory are reversible in transgenic mice after switching off the toxic Tau mutant. In: *J Neurosci* 31 (2011), Feb, Nr. 7, S. 2511–25. <http://dx.doi.org/10.1523/JNEUROSCI.5245-10.2011>. – DOI 10.1523/JNEUROSCI.5245-10.2011
- [414] TAKAHASHI, Kaoru ; ISHIDA, Mami ; KOMANO, Hajime ; TAKAHASHI, Hiroshi: SUMO-1 immunoreactivity co-localizes with phospho-Tau in APP transgenic mice but not in mutant Tau transgenic mice. In: *Neuroscience letters* 441 (2008), Aug, Nr. 1, S. 90–3. <http://dx.doi.org/10.1016/j.neulet.2008.06.012>. – DOI 10.1016/j.neulet.2008.06.012
- [415] TAKAHASHI, M ; TSUJIOKA, Y ; YAMADA, T ; TSUBOI, Y ; OKADA, H ; YAMAMOTO, T ; LIPOSITS, Z: Glycosylation of microtubule-associated protein tau in Alzheimer’s disease brain. In: *Acta Neuropathol* 97 (1999), Jun, Nr. 6, 635–41. http://www.ncbi.nlm.nih.gov/pubmed?Db=pubmed&Cmd=Retrieve&list_uids=10378383&dopt=abstractplus
- [416] TANIGUCHI-WATANABE, Sayuri ; ARAI, Tetsuaki ; KAMETANI, Fuyuki ; NONAKA, Takashi ; MASUDA-SUZUKAKE, Masami ; TARUTANI, Airi ; MURAYAMA, Shigeo ; SAITO, Yuko ; ARIMA, Kunimasa ; YOSHIDA, Mari ; AKIYAMA, Haruhiko ; ROBINSON, Andrew ; MANN, David M A. ; IWATSUBO, Takeshi ; HASEGAWA, Masato: Biochemical classification of tauopathies by immunoblot, protein sequence and mass spectrometric analyses of sarkosyl-insoluble and trypsin-resistant tau. In: *Acta Neuropathologica* (2015), Nov. <http://dx.doi.org/10.1007/s00401-015-1503-3>. – DOI 10.1007/s00401-015-1503-3
- [417] TAPE, Christopher J. ; WORBOYS, Jonathan D. ; SINCLAIR, John ; GOURLAY, Robert ; VOGT, Janis ; MCMAHON, Kelly M. ; TROST, Matthias ; LAUFFENBURGER, Douglas A. ; LAMONT, Douglas J. ; JØRGENSEN, Claus: Reproducible automated phosphopeptide enrichment using magnetic TiO₂ and Ti-IMAC. In: *Anal Chem* 86 (2014), Oct, Nr. 20, S. 10296–302. <http://dx.doi.org/10.1021/ac5025842>. – DOI 10.1021/ac5025842
- [418] TARKOWSKI, E ; ANDREASEN, N ; TARKOWSKI, A ; BLENNOW, K: Intrathecal inflammation precedes development of Alzheimer’s disease. In: *J Neurol Neurosurg Psychiatr* 74 (2003), Sep, Nr. 9, S. 1200–5
- [419] TEPPER, K ; BIERNAT, J ; KUMAR, S ; WEGMANN, S ; TIMM, T ; HUBSCHMANN, S ; REDECKE, L ; MANDELKOW, E.-M ; MULLER, D. J. ; MANDELKOW, E: Oligomer Formation of Tau Protein Hyperphosphorylated in Cells. In: *J Biol Chem* 289 (2014), Dec, Nr. 49, S. 34389–34407. <http://dx.doi.org/10.1074/jbc.M114.611368>. – DOI 10.1074/jbc.M114.611368
- [420] TERRY, R D.: Do neuronal inclusions kill the cell? In: *J Neural Transm Suppl* 59 (2000), Jan, S. 91–3
- [421] THAL, D ; ARNIM, C von ; GRIFFIN, W ; MRAK, R ; WALKER, L ; ATTEMS, J ; ARZBERGER, T: Frontotemporal lobar degeneration FTLD-tau: preclinical lesions, vascular, and Alzheimer-related co-pathologies. In: *J Neural Transm (Vienna)* 122 (2015), Jul, Nr. 7, 1007–18. <http://dx.doi.org/10.1007/s00702-014-1360-6>. – DOI 10.1007/s00702-014-1360-6
- [422] THAL, Dietmar R. ; ARNIM, Christine A F. ; GRIFFIN, W Sue T. ; MRAK, Robert E. ; WALKER, Lauren ; ATTEMS, Johannes ; ARZBERGER, Thomas: Frontotemporal lobar degeneration FTLD-tau: preclinical lesions, vascular, and Alzheimer-related co-pathologies. In: *Journal of neural transmission* (2015), Apr, 1–12. <http://dx.doi.org/10.1007/s00702-014-1360-6>. – DOI 10.1007/s00702-014-1360-6
- [423] THOMAS, Stefani N. ; FUNK, Kristen E. ; WAN, Yunhu ; LIAO, Zhongping ; DAVIES, Peter ; KURET, Jeff ; YANG, Austin J.: Dual modification of Alzheimer’s disease PHF-tau protein by lysine methylation and ubiquitylation: a mass spectrometry approach. In: *Acta Neuropathol* 123 (2012), Jan, Nr. 1, S. 105–17. <http://dx.doi.org/10.1007/s00401-011-0893-0>. – DOI 10.1007/s00401-011-0893-0

- [424] THOMPSON, Andrew ; SCHÄFER, Jürgen ; KUHN, Karsten ; KIENLE, Stefan ; SCHWARZ, Josef ; SCHMIDT, Günter ; NEUMANN, Thomas ; JOHNSTONE, R ; MOHAMMED, A Karim A. ; HAMON, Christian: Tandem mass tags: a novel quantification strategy for comparative analysis of complex protein mixtures by MS/MS. In: *Anal Chem* 75 (2003), Apr, Nr. 8, S. 1895–904
- [425] TOLNAY, M ; SCHWIETERT, M ; MONSCH, A U. ; STAEHELIN, H B. ; LANGUI, D ; PROBST, A: Argyrophilic grain disease: distribution of grains in patients with and without dementia. In: *Acta Neuropathol* 94 (1997), Oct, Nr. 4, 353–8. <http://link.springer.com/>
- [426] TOMLINSON, B E. ; BLESSED, G ; ROTH, M: Observations on the brains of demented old people. In: *J Neurol Sci* 11 (1970), Sep, Nr. 3, S. 205–42
- [427] TOURELLOTTE, W: Avant-propos: a human specimen bank and a brain biopsier. In: *Riv Patol Nerv Ment* 91 (1970), Oct, Nr. 5, 255–62. <http://www.ncbi.nlm.nih.gov/pubmed/5525770>
- [428] TOWNSEND, Kirk P. ; PRATICÒ, Domenico: Novel therapeutic opportunities for Alzheimer's disease: focus on nonsteroidal anti-inflammatory drugs. In: *FASEB J* 19 (2005), Oct, Nr. 12, S. 1592–601. <http://dx.doi.org/10.1096/fj.04-3620rev>. – DOI 10.1096/fj.04-3620rev
- [429] TRINCZEK, B ; BIERNAT, J ; BAUMANN, K ; MANDELKOW, E M. ; MANDELKOW, E: Domains of tau protein, differential phosphorylation, and dynamic instability of microtubules. In: *Mol Biol Cell* 6 (1995), Dec, Nr. 12, 1887–902. <http://www.molbiolcell.org/content/6/12/1887.long>
- [430] TSUBOI, Y ; SLOWINSKI, J ; JOSEPHS, K A. ; HONER, W G. ; WSZOLEK, Z K. ; DICKSON, D W.: Atrophy of superior cerebellar peduncle in progressive supranuclear palsy. In: *Neurology* 60 (2003), Jun, Nr. 11, S. 1766–9
- [431] TSUBOI, Yoshio ; JOSEPHS, Keith A. ; BOEVE, Bradley F. ; LITVAN, Irene ; CASELLI, Richard J. ; CAVINESS, John N. ; UTTI, Ryan J. ; BOTT, Allen D. ; DICKSON, Dennis W.: Increased tau burden in the cortices of progressive supranuclear palsy presenting with corticobasal syndrome. In: *Mov Disord* 20 (2005), Aug, Nr. 8, 982–8. <http://dx.doi.org/10.1002/mds.20478>. – DOI 10.1002/mds.20478
- [432] TSUCHIYA, K ; IKEDA, K ; UCHIHARA, T ; ODA, T ; SHIMADA, H: Distribution of cerebral cortical lesions in corticobasal degeneration: a clinicopathological study of five autopsy cases in Japan. In: *Acta Neuropathol* 94 (1997), Nov, Nr. 5, 416–24. <http://www.ncbi.nlm.nih.gov/pubmed/9386773>
- [433] TSUCHIYA, Kuniaki ; PIAO, Yue-Shan ; ODA, Tatsuro ; MOCHIZUKI, Akihide ; ARIMA, Kunimasa ; HASEGAWA, Kazuko ; HAGA, Chie ; KAKITA, Akiyoshi ; HORI, Koji ; TOMINAGA, Itaru ; YAGISHITA, Saburo ; AKIYAMA, Haruhiko ; TAKAHASHI, Hitoshi: Pathological heterogeneity of the precentral gyrus in Pick's disease: a study of 16 autopsy cases. In: *Acta Neuropathol* 112 (2006), Jul, Nr. 1, S. 29–42. <http://dx.doi.org/10.1007/s00401-005-0028-6>. – DOI 10.1007/s00401-005-0028-6
- [434] TUCKER, R: The roles of microtubule-associated proteins in brain morphogenesis: a review. In: *Brain Res Brain Res Rev* 15 (1990), May, Nr. 2, 101–20. <http://www.ncbi.nlm.nih.gov/pubmed/2282447>
- [435] UCHIHARA, Toshiki: Silver diagnosis in neuropathology: principles, practice and revised interpretation. In: *Acta Neuropathol* 113 (2007), May, Nr. 5, S. 483–99. <http://dx.doi.org/10.1007/s00401-007-0200-2>. – DOI 10.1007/s00401-007-0200-2
- [436] UNWIN, R ; GRIFFITHS, J ; WHETTON, A: A sensitive mass spectrometric method for hypothesis-driven detection of peptide post-translational modifications: multiple reaction monitoring-initiated detection and sequencing (MIDAS). In: *Nat Protoc* 4 (2009), Nr. 6, 870–7. <http://dx.doi.org/10.1038/nprot.2009.57>. – DOI 10.1038/nprot.2009.57
- [437] VANIER, M ; NEUVILLE, P ; MICHALIK, L ; LAUNAY, J: Expression of specific tau exons in normal and tumoral pancreatic acinar cells. In: *J Cell Sci* 111 (Pt 10) (1998), May, 1419–32. <http://www.ncbi.nlm.nih.gov/pubmed/9570759>
- [438] VENABLE, John D. ; DONG, Meng-Qiu ; WOHLSCHEGEL, James ; DILLIN, Andrew ; YATES, John R.: Automated approach for quantitative analysis of complex peptide mixtures from tandem mass spectra. In: *Nat Methods* 1 (2004), Oct, Nr. 1, S. 39–45. <http://dx.doi.org/10.1038/nmeth705>. – DOI 10.1038/nmeth705

- [439] VENNE, A ; KOLLIPARA, L ; ZAHEDI, R: The next level of complexity: crosstalk of posttranslational modifications. In: *PROTEOMICS* 14 (2014), Mar, Nr. 4-5, 513–24. <http://dx.doi.org/10.1002/pmic.201300344>. – DOI 10.1002/pmic.201300344
- [440] VERNY, M ; DUYNCKAERTS, C ; AGID, Y ; HAUW, J: The significance of cortical pathology in progressive supranuclear palsy. Clinico-pathological data in 10 cases. In: *Brain* 119 (Pt 4) (1996), Aug, 1123–36. <http://www.ncbi.nlm.nih.gov/pubmed/8813277>
- [441] VILLEMAGNE, Victor L. ; FODERO-TAVOLETTI, Michelle T. ; MASTERS, Colin L. ; ROWE, Christopher C.: Tau imaging: early progress and future directions. In: *The Lancet Neurology* 14 (2015), Jan, Nr. 1, S. 114–124. [http://dx.doi.org/10.1016/S1474-4422\(14\)70252-2](http://dx.doi.org/10.1016/S1474-4422(14)70252-2). – DOI 10.1016/S1474-4422(14)70252-2
- [442] VINCENT, I ; ROSADO, M ; DAVIES, P: Mitotic mechanisms in Alzheimer's disease? In: *J Cell Biol* 132 (1996), Feb, Nr. 3, S. 413–25
- [443] WADIA, Pettarusp M. ; LANG, Anthony E.: The many faces of corticobasal degeneration. In: *Parkinsonism Relat Disord* 13 Suppl 3 (2007), Jan, S336–40. [http://dx.doi.org/10.1016/S1353-8020\(08\)70027-0](http://dx.doi.org/10.1016/S1353-8020(08)70027-0). – DOI 10.1016/S1353-8020(08)70027-0
- [444] WAGSHAL, Dana ; SANKARANARAYANAN, Sethu ; GUSS, Valerie ; HALL, Tracey ; BERISHA, Flora ; LOBACH, Iryna ; KARYDAS, Anna ; VOLTARELLI, Lisa ; SCHERLING, Carole ; HEUER, Hilary ; TARTAGLIA, Maria ; MILLER, Zachary ; COPPOLA, Giovanni ; AHLJANIAN, Michael ; SOARES, Holly ; KRAMER, Joel ; RABINOVICI, Gil ; ROSEN, Howard ; MILLER, Bruce ; MEREDITH, Jere ; BOXER, Adam: Divergent CSF αN alterations in two common tauopathies: Alzheimer's disease and progressive supranuclear palsy. In: *Journal of neurology, neurosurgery, and psychiatry* 86 (2015), Mar, Nr. 3, 244–50. <http://dx.doi.org/10.1136/jnnp-2014-308004>. – DOI 10.1136/jnnp-2014-308004
- [445] WAKABAYASHI, Koichi ; TAKAHASHI, Hitoshi: Pathological heterogeneity in progressive supranuclear palsy and corticobasal degeneration. In: *Neuropathology* 24 (2004), Mar, Nr. 1, S. 79–86
- [446] WALKER, L ; LEVINE, H: The cerebral proteopathies. In: *Neurobiol Aging* 21 (2000), Jul, Nr. 4, 559–61. <http://www.ncbi.nlm.nih.gov/pubmed/10924770>
- [447] WALKER, L ; LEVINE, H: The cerebral proteopathies: neurodegenerative disorders of protein conformation and assembly. In: *Mol Neurobiol* 21 (2000), Feb, Nr. 1-2, 83–95. <http://dx.doi.org/10.1385/MN:21:1-2:083>. – DOI 10.1385/MN:21:1-2:083
- [448] WALKER, Lary C. ; DIAMOND, Marc I. ; DUFF, Karen E. ; HYMAN, Bradley T.: Mechanisms of protein seeding in neurodegenerative diseases. In: *JAMA Neurol* 70 (2013), Mar, Nr. 3, S. 304–10. <http://dx.doi.org/10.1001/jamaneurol.2013.1453>. – DOI 10.1001/jamaneurol.2013.1453
- [449] WANG, F ; SONG, C ; CHENG, K ; JIANG, X ; YE, M ; ZOU, H: Perspectives of comprehensive phosphoproteome analysis using shotgun strategy. In: *Anal Chem* 83 (2011), Nov, Nr. 21, 8078–85. <http://dx.doi.org/10.1021/ac201833j>. – DOI 10.1021/ac201833j
- [450] WANG, J ; GRUNDKE-IQBAL, I ; IQBAL, K: Glycosylation of microtubule-associated protein tau: an abnormal posttranslational modification in Alzheimer's disease. In: *Nature Medicine* 2 (1996), Aug, Nr. 8, 871–5. http://www.ncbi.nlm.nih.gov/entrez/query.fcgi?db=pubmed&cmd=Retrieve&dopt=AbstractPlus&list_uids=8705855
- [451] WANG, Jian-Zhi ; XIA, Yi-Yuan ; GRUNDKE-IQBAL, Inge ; IQBAL, Khalid: Abnormal hyperphosphorylation of tau: sites, regulation, and molecular mechanism of neurofibrillary degeneration. In: *J Alzheimers Dis* 33 Suppl 1 (2013), Jan, S. S123–39. <http://dx.doi.org/10.3233/JAD-2012-129031>. – DOI 10.3233/JAD-2012-129031
- [452] WANG, Yipeng ; MANDELKOW, Eckhard: Tau in physiology and pathology. In: *Nat Rev Neurosci* 17 (2016), Jan, Nr. 1, 22–35. <http://dx.doi.org/10.1038/nrn.2015.1>. – DOI 10.1038/nrn.2015.1
- [453] WANT, E ; CRAVATT, B ; SIUZDAK, G: The expanding role of mass spectrometry in metabolite profiling and characterization. In: *Chembiochem* 6 (2005), Nov, Nr. 11, 1941–51. <http://dx.doi.org/10.1002/cbic.200500151>. – DOI 10.1002/cbic.200500151

- [454] WASINGER, Valerie C. ; ZENG, Ming ; YAU, Yunki: Current status and advances in quantitative proteomic mass spectrometry. In: *Int J Proteomics* 2013 (2013), Jan, S. 180605. <http://dx.doi.org/10.1155/2013/180605>. – DOI 10.1155/2013/180605
- [455] WATANABE, Atsushi ; HONG, Won-Kyoung ; DOHMAE, Naoshi ; TAKIO, Koji ; MORISHIMA-KAWASHIMA, Maho ; IHARA, Yasuo: Molecular aging of tau: disulfide-independent aggregation and non-enzymatic degradation in vitro and in vivo. In: *J Neurochem* 90 (2004), Sep, Nr. 6, 1302–11. <http://dx.doi.org/10.1111/j.1471-4159.2004.02611.x>. – DOI 10.1111/j.1471-4159.2004.02611.x
- [456] WEGMANN, S ; MEDALSY, I. D. ; MANDELKOW, E ; MULLER, D. J.: The fuzzy coat of pathological human Tau fibrils is a two-layered polyelectrolyte brush. In: *Proceedings of the National Academy of Sciences* 110 (2013), Jan, Nr. 4, S. E313–E321. <http://dx.doi.org/10.1073/pnas.1212100110>. – DOI 10.1073/pnas.1212100110
- [457] WHITWELL, Jennifer L. ; XU, Jia ; MANDREKAR, Jay ; GUNTER, Jeffrey L. ; JACK, Clifford R. ; JOSEPHS, Keith A.: Imaging measures predict progression in progressive supranuclear palsy. In: *Mov Disord* 27 (2012), Dec, Nr. 14, 1801–4. <http://dx.doi.org/10.1002/mds.24970>. – DOI 10.1002/mds.24970
- [458] WILHELMSSEN, K C. ; LYNCH, T ; PAVLOU, E ; HIGGINS, M ; NYGAARD, T G.: Localization of disinhibition-dementia-parkinsonism-amyotrophy complex to 17q21-22. In: *Am J Hum Genet* 55 (1994), Dec, Nr. 6, S. 1159–65
- [459] WILLE, H ; DREWES, G ; BIERNAT, J ; MANDELKOW, E M. ; MANDELKOW, E: Alzheimer-like paired helical filaments and antiparallel dimers formed from microtubule-associated protein tau in vitro. In: *J Cell Biol* 118 (1992), Aug, Nr. 3, S. 573–84
- [460] WILLIAMS, D ; HOLTON, J ; STRAND, C ; PITTMAN, A ; SILVA, R de ; LEES, A ; REVESZ, T: Pathological tau burden and distribution distinguishes progressive supranuclear palsy-parkinsonism from Richardson's syndrome. In: *Brain* 130 (2007), Jun, Nr. Pt 6, 1566–76. <http://dx.doi.org/10.1093/brain/awm104>. – DOI 10.1093/brain/awm104
- [461] WILLIAMS, D. R.: Tauopathies: classification and clinical update on neurodegenerative diseases associated with microtubule-associated protein tau. In: *Intern Med J* 36 (2006), Oct, Nr. 10, S. 652–660. <http://dx.doi.org/10.1111/j.1445-5994.2006.01153.x>. – DOI 10.1111/j.1445-5994.2006.01153.x
- [462] WILLIAMS, D W. ; TYRER, M ; SHEPHERD, D: Tau and tau reporters disrupt central projections of sensory neurons in *Drosophila*. In: *J Comp Neurol* 428 (2000), Dec, Nr. 4, S. 630–40
- [463] WILLIAMS, David R. ; HOLTON, Janice L. ; STRAND, Catherine ; PITTMAN, Alan ; SILVA, Rohan de ; LEES, Andrew J. ; REVESZ, Tamas: Pathological tau burden and distribution distinguishes progressive supranuclear palsy-parkinsonism from Richardson's syndrome. In: *Brain* 130 (2007), Jun, Nr. Pt 6, S. 1566–76. <http://dx.doi.org/10.1093/brain/awm104>. – DOI 10.1093/brain/awm104
- [464] WILLIAMS, David R. ; LEES, Andrew J.: Progressive supranuclear palsy: clinicopathological concepts and diagnostic challenges. In: *The Lancet Neurology* 8 (2009), Mar, Nr. 3, S. 270–9. [http://dx.doi.org/10.1016/S1474-4422\(09\)70042-0](http://dx.doi.org/10.1016/S1474-4422(09)70042-0). – DOI 10.1016/S1474-4422(09)70042-0
- [465] WISCHIK, C ; STAFF, R: Challenges in the conduct of disease-modifying trials in AD: practical experience from a phase 2 trial of Tau-aggregation inhibitor therapy. In: *J Nutr Health Aging* 13 (2009), Apr, Nr. 4, S. 367–9
- [466] WISCHIK, C M. ; NOVAK, M ; EDWARDS, P C. ; KLUG, A ; TICHELAAR, W ; CROWTHER, R A.: Structural characterization of the core of the paired helical filament of Alzheimer disease. In: *Proc Natl Acad Sci USA* 85 (1988), Jul, Nr. 13, S. 4884–8
- [467] WISNIEWSKI, J ; ZOUGMAN, A ; NAGARAJ, N ; MANN, M: Universal sample preparation method for proteome analysis. In: *Nat Methods* 6 (2009), May, Nr. 5, 359–62. <http://dx.doi.org/10.1038/nmeth.1322>. – DOI 10.1038/nmeth.1322
- [468] WITTMANN, C W. ; WSZOLEK, M F. ; SHULMAN, J M. ; SALVATERRA, P M. ; LEWIS, J ; HUTTON, M ; FEANY, M B.: Tauopathy in *Drosophila*: neurodegeneration without neurofibrillary tangles. In: *Science* 293 (2001), Jul, Nr. 5530, S. 711–4. <http://dx.doi.org/10.1126/science.1062382>. – DOI 10.1126/science.1062382

- [469] WOLF-YADLIN, Alejandro ; HAUTANIEMI, Sampsa ; LAUFFENBURGER, Douglas A. ; WHITE, Forest M.: Multiple reaction monitoring for robust quantitative proteomic analysis of cellular signaling networks. In: *Proc Natl Acad Sci USA* 104 (2007), Apr, Nr. 14, S. 5860–5. <http://dx.doi.org/10.1073/pnas.0608638104>. – DOI 10.1073/pnas.0608638104
- [470] WRAY, Selina ; SAXTON, Malcolm ; ANDERTON, Brian H. ; HANGER, Diane P.: Direct analysis of tau from PSP brain identifies new phosphorylation sites and a major fragment of N-terminally cleaved tau containing four microtubule-binding repeats. In: *J Neurochem* 105 (2008), Feb, Nr. 6, S. 2343–2352. <http://dx.doi.org/10.1111/j.1471-4159.2008.05321.x>. – DOI 10.1111/j.1471-4159.2008.05321.x
- [471] WU, Guoxin ; SANKARANARAYANAN, Sethu ; WONG, Jacky ; TUGUSHEVA, Katherine ; MICHENER, Maria S. ; SHI, Xiaoping ; COOK, Jacquelynn J. ; SIMON, Adam J. ; SAVAGE, Mary J.: Characterization of plasma beta-secretase (BACE1) activity and soluble amyloid precursor proteins as potential biomarkers for Alzheimer's disease. In: *J Neurosci Res* 90 (2012), Dec, Nr. 12, 2247–58. <http://dx.doi.org/10.1002/jnr.23122>. – DOI 10.1002/jnr.23122
- [472] WU, Jiang ; WARREN, Peter ; SHAKEY, Quazi ; SOUSA, Eric ; HILL, Andrew ; RYAN, Terence E. ; HE, Tao: Integrating titania enrichment, iTRAQ labeling, and Orbitrap CID-HCD for global identification and quantitative analysis of phosphopeptides. In: *Proteomics* 10 (2010), Jun, Nr. 11, S. 2224–34. <http://dx.doi.org/10.1002/pmic.200900788>. – DOI 10.1002/pmic.200900788
- [473] YAMAMOTO, T ; HIRANO, A: A comparative study of modified Bielschowsky, Bodian and thioflavin S stains on Alzheimer's neurofibrillary tangles. In: *Neuropathol Appl Neurobiol* 12 (1986), Jan, Nr. 1, 3–9. http://www.ncbi.nlm.nih.gov/pubmed?Db=pubmed&Cmd=Retrieve&list_uids=2422580&dopt=abstractplus
- [474] YAMAZAKI, M ; NAKANO, I ; IMAZU, O ; TERASHI, A: Paired helical filaments and straight tubules in astrocytes: an electron microscopic study in dementia of the Alzheimer type. In: *Acta Neuropathol* 90 (1995), Jan, Nr. 1, S. 31–6
- [475] YAN, S D. ; YAN, S F. ; CHEN, X ; FU, J ; CHEN, M ; KUPPUSAMY, P ; SMITH, M A. ; PERRY, G ; GODMAN, G C. ; NAWROTH, P: Non-enzymatically glycosylated tau in Alzheimer's disease induces neuronal oxidant stress resulting in cytokine gene expression and release of amyloid beta-peptide. In: *Nat Med* 1 (1995), Jul, Nr. 7, S. 693–9
- [476] YOSHIDA, H ; IHARA, Y: Tau in paired helical filaments is functionally distinct from fetal tau: assembly incompetence of paired helical filament-tau. In: *J Neurochem* 61 (1993), Sep, Nr. 3, 1183–6. http://www.ncbi.nlm.nih.gov/pubmed?Db=pubmed&Cmd=Retrieve&list_uids=8360683&dopt=abstractplus
- [477] YOSHIDA, Mari: Cellular tau pathology and immunohistochemical study of tau isoforms in sporadic tauopathies. In: *Neuropathology* 26 (2006), Oct, Nr. 5, S. 457–70
- [478] YOSHIDA, Mari: Astrocytic inclusions in progressive supranuclear palsy and corticobasal degeneration. In: *Neuropathology* 34 (2014), Dec, Nr. 6, S. 555–70. <http://dx.doi.org/10.1111/neup.12143>. – DOI 10.1111/neup.12143
- [479] YOSHIYAMA, Y ; LEE, V. M. Y. ; TROJANOWSKI, J. Q.: Therapeutic strategies for tau mediated neurodegeneration. In: *Journal of Neurology, Neurosurgery & Psychiatry* 84 (2013), Jul, Nr. 7, S. 784–795. <http://dx.doi.org/10.1136/jnnp-2012-303144>. – DOI 10.1136/jnnp-2012-303144
- [480] YOSHIYAMA, Yasumasa ; HIGUCHI, Makoto ; ZHANG, Bin ; HUANG, Shu-Ming ; IWATA, Nobuhisa ; SAIDO, Takaomi C. ; MAEDA, Jun ; SUHARA, Tetsuya ; TROJANOWSKI, John Q. ; LEE, Virginia M-Y: Synapse loss and microglial activation precede tangles in a P301S tauopathy mouse model. In: *Neuron* 53 (2007), Feb, Nr. 3, S. 337–51. <http://dx.doi.org/10.1016/j.neuron.2007.01.010>. – DOI 10.1016/j.neuron.2007.01.010
- [481] YOST, R A. ; ENKE, C G.: Triple quadrupole mass spectrometry for direct mixture analysis and structure elucidation. In: *Anal Chem* 51 (1979), Oct, Nr. 12, S. 1251–64. <http://dx.doi.org/10.1021/ac50048a002>. – DOI 10.1021/ac50048a002
- [482] YOST, R L. ; ENKE, CG: Selected Ion Fragmentation with a Tandem Quadrupole Mass Spectrometer. In: *Journal of the American Chemical Society* 100 (1978), Nr. 7, S. 2274–5

- [483] YU, Y ; RUN, X ; LIANG, Z ; LI, Y ; LIU, F ; LIU, Y ; IQBAL, K ; GRUNDKE-IQBAL, I ; GONG, C: Developmental regulation of tau phosphorylation, tau kinases, and tau phosphatases. In: *J Neurochem* 108 (2009), Mar, Nr. 6, 1480–94. <http://dx.doi.org/10.1111/j.1471-4159.2009.05882.x>. – DOI 10.1111/j.1471-4159.2009.05882.x
- [484] YUZWA, S ; MACAULEY, M ; HEINONEN, J ; SHAN, X ; DENNIS, R ; HE, Y ; WHITWORTH, G ; STUBBS, K ; MCEACHERN, E ; DAVIES, G ; VOCADLO, D: A potent mechanism-inspired O-GlcNAcase inhibitor that blocks phosphorylation of tau in vivo. In: *Nature chemical biology* 4 (2008), Aug, Nr. 8, 483–90. <http://dx.doi.org/10.1038/nchembio.96>. – DOI 10.1038/nchembio.96
- [485] ZHANG, Bin ; CARROLL, Jenna ; TROJANOWSKI, John Q. ; YAO, Yuemang ; IBA, Michiyo ; POTUZAK, Justin S. ; HOGAN, Anne-Marie L. ; XIE, Sharon X. ; BALLATORE, Carlo ; SMITH, Amos B. ; LEE, Virginia M-Y ; BRUNDEN, Kurt R.: The microtubule-stabilizing agent, epothilone D, reduces axonal dysfunction, neurotoxicity, cognitive deficits, and Alzheimer-like pathology in an interventional study with aged tau transgenic mice. In: *J Neurosci* 32 (2012), Mar, Nr. 11, S. 3601–11. <http://dx.doi.org/10.1523/JNEUROSCI.4922-11.2012>. – DOI 10.1523/JNEUROSCI.4922-11.2012
- [486] ZHANG, Haixia ; LIU, Qinfeng ; ZIMMERMAN, Lisa J. ; HAM, Amy-Joan L. ; SLEBOS, Robbert J C. ; RAHMAN, Jamshedur ; KIKUCHI, Takefume ; MASSION, Pierre P. ; CARBONE, David P. ; BILLHEIMER, Dean ; LIEBLER, Daniel C.: Methods for peptide and protein quantitation by liquid chromatography-multiple reaction monitoring mass spectrometry. In: *Mol Cell Proteomics* 10 (2011), Jun, Nr. 6, S. M110.006593. <http://dx.doi.org/10.1074/mcp.M110.006593>. – DOI 10.1074/mcp.M110.006593
- [487] ZHANG, Wei ; ARTEAGA, Janna ; CASHION, Daniel K. ; CHEN, Gang ; GANGADHARMATH, Umesh ; GOMEZ, Luis F. ; KASI, Dhanalakshmi ; LAM, Chung ; LIANG, Qianwa ; LIU, Changhui ; MOCHARLA, Vani P. ; MU, Fanrong ; SINHA, Anjana ; SZARDENINGS, A K. ; WANG, Eric ; WALSH, Joseph C. ; XIA, Chunfang ; YU, Chul ; ZHAO, Tieming ; KOLB, Hartmuth C.: A highly selective and specific PET tracer for imaging of tau pathologies. In: *J Alzheimers Dis* 31 (2012), Jan, Nr. 3, S. 601–12. <http://dx.doi.org/10.3233/JAD-2012-120712>. – DOI 10.3233/JAD-2012-120712
- [488] ZHANG, Yong J. ; XU, Ya F. ; CHEN, Xiao Q. ; WANG, Xiao C. ; WANG, Jian-Zhi: Nitration and oligomerization of tau induced by peroxydinitrite inhibit its microtubule-binding activity. In: *FEBS Letters* 579 (2005), Apr, Nr. 11, S. 2421–7. <http://dx.doi.org/10.1016/j.febslet.2005.03.041>. – DOI 10.1016/j.febslet.2005.03.041
- [489] ZHENG-FISCHHÖFER, Q ; BIERNAT, J ; MANDELKOW, E M. ; ILLENBERGER, S ; GODEMANN, R ; MANDELKOW, E: Sequential phosphorylation of Tau by glycogen synthase kinase-3beta and protein kinase A at Thr212 and Ser214 generates the Alzheimer-specific epitope of antibody AT100 and requires a paired-helical-filament-like conformation. In: *Eur J Biochem* 252 (1998), Mar, Nr. 3, S. 542–52
- [490] ZHU, Wenhong ; SMITH, Jeffrey W. ; HUANG, Chun-Ming: Mass spectrometry-based label-free quantitative proteomics. In: *J Biomed Biotechnol* 2010 (2010), Jan, S. 840518. <http://dx.doi.org/10.1155/2010/840518>. – DOI 10.1155/2010/840518

Appendix

Table A1: Transition list of FLEXITau (see next page) Table with optimized tau transitions for a typical tryptic digest (first table) and LysC digest (second table). RTs are for a 30 min gradient. For details, see section 2.3.
RT, retention time; DP, declustering potential; CE, collision energy

Q1 m/z	Q3 m/z	RT (min)	Transition ID	DP (volts)
451.583	573.298	10.6	hTAU_4R2N.AKTDHGAEIVYK.+3y10+2.extraheavy_D5K8R10	63.5
444.57	566.785	10.6	hTAU_4R2N.AKTDHGAEIVYK.+3y10+2.light	63.5
451.583	641.352	10.6	hTAU_4R2N.AKTDHGAEIVYK.+3y11+2.extraheavy_D5K8R10	63.5
444.57	630.833	10.6	hTAU_4R2N.AKTDHGAEIVYK.+3y11+2.light	63.5
451.583	318.19	10.6	hTAU_4R2N.AKTDHGAEIVYK.+3y2.extraheavy_D5K8R10	63.5
444.57	310.176	10.6	hTAU_4R2N.AKTDHGAEIVYK.+3y2.light	63.5
451.583	787.444	10.6	hTAU_4R2N.AKTDHGAEIVYK.+3y7.extraheavy_D5K8R10	63.5
444.57	779.43	10.6	hTAU_4R2N.AKTDHGAEIVYK.+3y7.light	63.5
451.583	462.755	10.6	hTAU_4R2N.AKTDHGAEIVYK.+3y8+2.extraheavy_D5K8R10	63.5
444.57	458.748	10.6	hTAU_4R2N.AKTDHGAEIVYK.+3y8+2.light	63.5
501.766	507.799	11.1	hTAU_4R2N.C[PPa]GSLGNIHKKPGGGQVEVK.+4y10+2.extraheavy_D5K8R10	67.4
497.759	499.785	11.1	hTAU_4R2N.C[PPa]GSLGNIHKKPGGGQVEVK.+4y10+2.light	67.4
501.766	576.329	11.1	hTAU_4R2N.C[PPa]GSLGNIHKKPGGGQVEVK.+4y11+2.extraheavy_D5K8R10	67.4
497.759	568.315	11.1	hTAU_4R2N.C[PPa]GSLGNIHKKPGGGQVEVK.+4y11+2.light	67.4
501.766	786.932	11.1	hTAU_4R2N.C[PPa]GSLGNIHKKPGGGQVEVK.+4y15+2.extraheavy_D5K8R10	67.4
497.759	778.918	11.1	hTAU_4R2N.C[PPa]GSLGNIHKKPGGGQVEVK.+4y15+2.light	67.4
501.766	562.652	11.1	hTAU_4R2N.C[PPa]GSLGNIHKKPGGGQVEVK.+4y16+3.extraheavy_D5K8R10	67.4
497.759	557.309	11.1	hTAU_4R2N.C[PPa]GSLGNIHKKPGGGQVEVK.+4y16+3.light	67.4
501.766	591.663	11.1	hTAU_4R2N.C[PPa]GSLGNIHKKPGGGQVEVK.+4y17+3.extraheavy_D5K8R10	67.4
497.759	586.32	11.1	hTAU_4R2N.C[PPa]GSLGNIHKKPGGGQVEVK.+4y17+3.light	67.4
501.766	878.482	11.1	hTAU_4R2N.C[PPa]GSLGNIHKKPGGGQVEVK.+4y9.extraheavy_D5K8R10	67.4
497.759	870.468	11.1	hTAU_4R2N.C[PPa]GSLGNIHKKPGGGQVEVK.+4y9.light	67.4
737.323	718.838	12	hTAU_4R2N.DQGGYTM[Oxij]HQDQEGDTDAGLK.+3y13+2.extraheavy_D5K8R10	84.2
727.971	707.316	12	hTAU_4R2N.DQGGYTM[Oxij]HQDQEGDTDAGLK.+3y13+2.light	84.2
737.323	617.355	12	hTAU_4R2N.DQGGYTM[Oxij]HQDQEGDTDAGLK.+3y6.extraheavy_D5K8R10	84.2
727.971	604.33	12	hTAU_4R2N.DQGGYTM[Oxij]HQDQEGDTDAGLK.+3y6.light	84.2
737.323	794.414	12	hTAU_4R2N.DQGGYTM[Oxij]HQDQEGDTDAGLK.+3y8.extraheavy_D5K8R10	84.2
727.971	776.378	12	hTAU_4R2N.DQGGYTM[Oxij]HQDQEGDTDAGLK.+3y8.light	84.2
737.323	923.456	12	hTAU_4R2N.DQGGYTM[Oxij]HQDQEGDTDAGLK.+3y9.extraheavy_D5K8R10	84.2
727.971	905.421	12	hTAU_4R2N.DQGGYTM[Oxij]HQDQEGDTDAGLK.+3y9.light	84.2
731.992	1171.552	13	hTAU_4R2N.DQGGYTMHQDQEGDTDAGLK.+3y11.extraheavy_D5K8R10	83.8
722.64	1148.507	13	hTAU_4R2N.DQGGYTMHQDQEGDTDAGLK.+3y11.light	83.8
731.992	973.436	13	hTAU_4R2N.DQGGYTMHQDQEGDTDAGLK.+3y18+2.extraheavy_D5K8R10	83.8
722.64	961.913	13	hTAU_4R2N.DQGGYTMHQDQEGDTDAGLK.+3y18+2.light	83.8
731.992	396.27	13	hTAU_4R2N.DQGGYTMHQDQEGDTDAGLK.+3y4.extraheavy_D5K8R10	83.8
722.64	388.255	13	hTAU_4R2N.DQGGYTMHQDQEGDTDAGLK.+3y4.light	83.8
731.992	794.414	13	hTAU_4R2N.DQGGYTMHQDQEGDTDAGLK.+3y8.extraheavy_D5K8R10	83.8
722.64	776.378	13	hTAU_4R2N.DQGGYTMHQDQEGDTDAGLK.+3y8.light	83.8
803.694	1033.473	15.2	hTAU_4R2N.ESPLQPTPTEDGSEEPGSETSDAK.+3y10.extraheavy_D5K8R10	89.3
797.682	1020.448	15.2	hTAU_4R2N.ESPLQPTPTEDGSEEPGSETSDAK.+3y10.light	89.3
803.694	534.281	15.2	hTAU_4R2N.ESPLQPTPTEDGSEEPGSETSDAK.+3y5.extraheavy_D5K8R10	89.3
797.682	521.257	15.2	hTAU_4R2N.ESPLQPTPTEDGSEEPGSETSDAK.+3y5.light	89.3
803.694	750.356	15.2	hTAU_4R2N.ESPLQPTPTEDGSEEPGSETSDAK.+3y7.extraheavy_D5K8R10	89.3
797.682	737.331	15.2	hTAU_4R2N.ESPLQPTPTEDGSEEPGSETSDAK.+3y7.light	89.3

803.694	904.43	15.2	hTAU_4R2N.ESPLQPTPTEDGSEEPGSETSDAK.+3y9.extraheavy_D5K8R10	89.3
797.682	891.405	15.2	hTAU_4R2N.ESPLQPTPTEDGSEEPGSETSDAK.+3y9.light	89.3
803.694	452.719	15.2	hTAU_4R2N.ESPLQPTPTEDGSEEPGSETSDAK.+3y9+2.extraheavy_D5K8R10	89.3
797.682	446.206	15.2	hTAU_4R2N.ESPLQPTPTEDGSEEPGSETSDAK.+3y9+2.light	89.3
367.208	437.26	7	hTAU_4R2N.GAAPPQK.+2y4.extraheavy_D5K8R10	57.6
363.201	429.246	7	hTAU_4R2N.GAAPPQK.+2y4.light	57.6
367.208	534.313	7	hTAU_4R2N.GAAPPQK.+2y5.extraheavy_D5K8R10	57.6
363.201	526.298	7	hTAU_4R2N.GAAPPQK.+2y5.light	57.6
367.208	267.66	7	hTAU_4R2N.GAAPPQK.+2y5+2.extraheavy_D5K8R10	57.6
363.201	263.653	7	hTAU_4R2N.GAAPPQK.+2y5+2.light	57.6
367.208	605.35	7	hTAU_4R2N.GAAPPQK.+2y6.extraheavy_D5K8R10	57.6
363.201	597.336	7	hTAU_4R2N.GAAPPQK.+2y6.light	57.6
367.208	676.387	7	hTAU_4R2N.GAAPPQK.+2y7.extraheavy_D5K8R10	57.6
363.201	668.373	7	hTAU_4R2N.GAAPPQK.+2y7.light	57.6
382.223	323.217	9	hTAU_4R2N.GQANATRIPAK.+3y3.extraheavy_D5K8R10	58.5
376.216	315.203	9	hTAU_4R2N.GQANATRIPAK.+3y3.light	58.5
382.223	703.458	9	hTAU_4R2N.GQANATRIPAK.+3y6.extraheavy_D5K8R10	58.5
376.216	685.436	9	hTAU_4R2N.GQANATRIPAK.+3y6.light	58.5
382.223	774.495	9	hTAU_4R2N.GQANATRIPAK.+3y7.extraheavy_D5K8R10	58.5
376.216	756.473	9	hTAU_4R2N.GQANATRIPAK.+3y7.light	58.5
382.223	387.751	9	hTAU_4R2N.GQANATRIPAK.+3y7+2.extraheavy_D5K8R10	58.5
376.216	378.74	9	hTAU_4R2N.GQANATRIPAK.+3y7+2.light	58.5
382.223	444.773	9	hTAU_4R2N.GQANATRIPAK.+3y8+2.extraheavy_D5K8R10	58.5
376.216	435.761	9	hTAU_4R2N.GQANATRIPAK.+3y8+2.light	58.5
382.223	480.291	9	hTAU_4R2N.GQANATRIPAK.+3y9+2.extraheavy_D5K8R10	58.5
376.216	471.28	9	hTAU_4R2N.GQANATRIPAK.+3y9+2.light	58.5
1094.89	1003.535	28	hTAU_4R2N.HLSNVSSTGSIDM[Oxi]VDSPQLATLADEVASLAK.+3y10.extraheavy_D5K8R10	110.4
1087.21	990.51	28	hTAU_4R2N.HLSNVSSTGSIDM[Oxi]VDSPQLATLADEVASLAK.+3y10.light	110.4
1094.89	1116.619	28	hTAU_4R2N.HLSNVSSTGSIDM[Oxi]VDSPQLATLADEVASLAK.+3y11.extraheavy_D5K8R10	110.4
1087.21	1103.594	28	hTAU_4R2N.HLSNVSSTGSIDM[Oxi]VDSPQLATLADEVASLAK.+3y11.light	110.4
1094.89	1217.667	28	hTAU_4R2N.HLSNVSSTGSIDM[Oxi]VDSPQLATLADEVASLAK.+3y12.extraheavy_D5K8R10	110.4
1087.21	1204.642	28	hTAU_4R2N.HLSNVSSTGSIDM[Oxi]VDSPQLATLADEVASLAK.+3y12.light	110.4
1094.89	497.317	28	hTAU_4R2N.HLSNVSSTGSIDM[Oxi]VDSPQLATLADEVASLAK.+3y5.extraheavy_D5K8R10	110.4
1087.21	489.303	28	hTAU_4R2N.HLSNVSSTGSIDM[Oxi]VDSPQLATLADEVASLAK.+3y5.light	110.4
1094.89	584.349	28	hTAU_4R2N.HLSNVSSTGSIDM[Oxi]VDSPQLATLADEVASLAK.+3y6.extraheavy_D5K8R10	110.4
1087.21	576.335	28	hTAU_4R2N.HLSNVSSTGSIDM[Oxi]VDSPQLATLADEVASLAK.+3y6.light	110.4
1094.89	932.498	28	hTAU_4R2N.HLSNVSSTGSIDM[Oxi]VDSPQLATLADEVASLAK.+3y9.extraheavy_D5K8R10	110.4
1087.21	919.473	28	hTAU_4R2N.HLSNVSSTGSIDM[Oxi]VDSPQLATLADEVASLAK.+3y9.light	110.4
817.418	1003.535	30	hTAU_4R2N.HLSNVSSTGSIDMVDSPQLATLADEVASLAK.+4y10.extraheavy_D5K8R10	90.3
811.657	990.51	30	hTAU_4R2N.HLSNVSSTGSIDMVDSPQLATLADEVASLAK.+4y10.light	90.3
817.418	1217.667	30	hTAU_4R2N.HLSNVSSTGSIDMVDSPQLATLADEVASLAK.+4y12.extraheavy_D5K8R10	90.3
811.657	1204.642	30	hTAU_4R2N.HLSNVSSTGSIDMVDSPQLATLADEVASLAK.+4y12.light	90.3
817.418	584.349	30	hTAU_4R2N.HLSNVSSTGSIDMVDSPQLATLADEVASLAK.+4y6.extraheavy_D5K8R10	90.3
811.657	576.335	30	hTAU_4R2N.HLSNVSSTGSIDMVDSPQLATLADEVASLAK.+4y6.light	90.3
817.418	932.498	30	hTAU_4R2N.HLSNVSSTGSIDMVDSPQLATLADEVASLAK.+4y9.extraheavy_D5K8R10	90.3
811.657	919.473	30	hTAU_4R2N.HLSNVSSTGSIDMVDSPQLATLADEVASLAK.+4y9.light	90.3

501.038	591.867	18.6	hTAU_4R2N.HVPGGGSVQIVYKPVDSLK.+4y10+2.extraheavy_D5K8R10	67.3
495.778	581.348	18.6	hTAU_4R2N.HVPGGGSVQIVYKPVDSLK.+4y10+2.light	67.3
501.038	655.896	18.6	hTAU_4R2N.HVPGGGSVQIVYKPVDSLK.+4y11+2.extraheavy_D5K8R10	67.3
495.778	645.377	18.6	hTAU_4R2N.HVPGGGSVQIVYKPVDSLK.+4y11+2.light	67.3
501.038	355.243	18.6	hTAU_4R2N.HVPGGGSVQIVYKPVDSLK.+4y3.extraheavy_D5K8R10	67.3
495.778	347.229	18.6	hTAU_4R2N.HVPGGGSVQIVYKPVDSLK.+4y3.light	67.3
501.038	671.402	18.6	hTAU_4R2N.HVPGGGSVQIVYKPVDSLK.+4y6.extraheavy_D5K8R10	67.3
495.778	658.377	18.6	hTAU_4R2N.HVPGGGSVQIVYKPVDSLK.+4y6.light	67.3
501.038	535.325	18.6	hTAU_4R2N.HVPGGGSVQIVYKPVDSLK.+4y9+2.extraheavy_D5K8R10	67.3
495.778	524.805	18.6	hTAU_4R2N.HVPGGGSVQIVYKPVDSLK.+4y9+2.light	67.3
531.288	611.317	17.4	hTAU_4R2N.IGSLDNITHVPGGGNK.+3y12+2.extraheavy_D5K8R10	69.5
526.946	604.805	17.4	hTAU_4R2N.IGSLDNITHVPGGGNK.+3y12+2.light	69.5
531.288	711.375	17.4	hTAU_4R2N.IGSLDNITHVPGGGNK.+3y14+2.extraheavy_D5K8R10	69.5
526.946	704.863	17.4	hTAU_4R2N.IGSLDNITHVPGGGNK.+3y14+2.light	69.5
531.288	739.886	17.4	hTAU_4R2N.IGSLDNITHVPGGGNK.+3y15+2.extraheavy_D5K8R10	69.5
526.946	733.373	17.4	hTAU_4R2N.IGSLDNITHVPGGGNK.+3y15+2.light	69.5
531.288	537.287	17.4	hTAU_4R2N.IGSLDNITHVPGGGNK.+3y6.extraheavy_D5K8R10	69.5
526.946	529.273	17.4	hTAU_4R2N.IGSLDNITHVPGGGNK.+3y6.light	69.5
531.288	874.462	17.4	hTAU_4R2N.IGSLDNITHVPGGGNK.+3y9.extraheavy_D5K8R10	69.5
526.946	866.448	17.4	hTAU_4R2N.IGSLDNITHVPGGGNK.+3y9.light	69.5
576.657	679.371	15.7	hTAU_4R2N.IGSLDNITHVPGGGNKK.+3y13+2.extraheavy_D5K8R10	72.6
569.644	668.852	15.7	hTAU_4R2N.IGSLDNITHVPGGGNKK.+3y13+2.light	72.6
576.657	779.43	15.7	hTAU_4R2N.IGSLDNITHVPGGGNKK.+3y15+2.extraheavy_D5K8R10	72.6
569.644	768.91	15.7	hTAU_4R2N.IGSLDNITHVPGGGNKK.+3y15+2.light	72.6
576.657	807.94	15.7	hTAU_4R2N.IGSLDNITHVPGGGNKK.+3y16+2.extraheavy_D5K8R10	72.6
569.644	797.421	15.7	hTAU_4R2N.IGSLDNITHVPGGGNKK.+3y16+2.light	72.6
576.657	673.396	15.7	hTAU_4R2N.IGSLDNITHVPGGGNKK.+3y7.extraheavy_D5K8R10	72.6
569.644	657.368	15.7	hTAU_4R2N.IGSLDNITHVPGGGNKK.+3y7.light	72.6
576.657	337.202	15.7	hTAU_4R2N.IGSLDNITHVPGGGNKK.+3y7+2.extraheavy_D5K8R10	72.6
569.644	329.188	15.7	hTAU_4R2N.IGSLDNITHVPGGGNKK.+3y7+2.light	72.6
435.245	382.254	10.5	hTAU_4R2N.IGSTENLK.+2y3.extraheavy_D5K8R10	62.6
431.237	374.24	10.5	hTAU_4R2N.IGSTENLK.+2y3.light	62.6
435.245	511.297	10.5	hTAU_4R2N.IGSTENLK.+2y4.extraheavy_D5K8R10	62.6
431.237	503.282	10.5	hTAU_4R2N.IGSTENLK.+2y4.light	62.6
435.245	612.344	10.5	hTAU_4R2N.IGSTENLK.+2y5.extraheavy_D5K8R10	62.6
431.237	604.33	10.5	hTAU_4R2N.IGSTENLK.+2y5.light	62.6
435.245	699.376	10.5	hTAU_4R2N.IGSTENLK.+2y6.extraheavy_D5K8R10	62.6
431.237	691.362	10.5	hTAU_4R2N.IGSTENLK.+2y6.light	62.6
435.245	756.398	10.5	hTAU_4R2N.IGSTENLK.+2y7.extraheavy_D5K8R10	62.6
431.237	748.384	10.5	hTAU_4R2N.IGSTENLK.+2y7.light	62.6
587.271	396.27	10.8	hTAU_4R2N.KDQGGYTM[Oxi]HQDQEGDTDAGLK.+4y4.extraheavy_D5K8R10	73.3
578.254	388.255	10.8	hTAU_4R2N.KDQGGYTM[Oxi]HQDQEGDTDAGLK.+4y4.light	73.3
587.271	516.307	10.8	hTAU_4R2N.KDQGGYTM[Oxi]HQDQEGDTDAGLK.+4y5.extraheavy_D5K8R10	73.3
578.254	503.282	10.8	hTAU_4R2N.KDQGGYTM[Oxi]HQDQEGDTDAGLK.+4y5.light	73.3
587.271	617.355	10.8	hTAU_4R2N.KDQGGYTM[Oxi]HQDQEGDTDAGLK.+4y6.extraheavy_D5K8R10	73.3
578.254	604.33	10.8	hTAU_4R2N.KDQGGYTM[Oxi]HQDQEGDTDAGLK.+4y6.light	73.3

587.271	794.414	10.8	hTAU_4R2N.KDQGGYTM[Oxi]HQDQEGDTDAGLK.+4y8.extraheavy_D5K8R10	73.3
578.254	776.378	10.8	hTAU_4R2N.KDQGGYTM[Oxi]HQDQEGDTDAGLK.+4y8.light	73.3
583.273	396.27	12.2	hTAU_4R2N.KDQGGYTMHQDQEGDTDAGLK.+4y4.extraheavy_D5K8R10	73
574.255	388.255	12.2	hTAU_4R2N.KDQGGYTMHQDQEGDTDAGLK.+4y4.light	73
583.273	516.307	12.2	hTAU_4R2N.KDQGGYTMHQDQEGDTDAGLK.+4y5.extraheavy_D5K8R10	73
574.255	503.282	12.2	hTAU_4R2N.KDQGGYTMHQDQEGDTDAGLK.+4y5.light	73
583.273	617.355	12.2	hTAU_4R2N.KDQGGYTMHQDQEGDTDAGLK.+4y6.extraheavy_D5K8R10	73
574.255	604.33	12.2	hTAU_4R2N.KDQGGYTMHQDQEGDTDAGLK.+4y6.light	73
583.273	794.414	12.2	hTAU_4R2N.KDQGGYTMHQDQEGDTDAGLK.+4y8.extraheavy_D5K8R10	73
574.255	776.378	12.2	hTAU_4R2N.KDQGGYTMHQDQEGDTDAGLK.+4y8.light	73
384.897	370.218	13.3	hTAU_4R2N.KLDLSNVQSK.+3y3.extraheavy_D5K8R10	58.7
377.884	362.203	13.3	hTAU_4R2N.KLDLSNVQSK.+3y3.light	58.7
384.897	469.286	13.3	hTAU_4R2N.KLDLSNVQSK.+3y4.extraheavy_D5K8R10	58.7
377.884	461.272	13.3	hTAU_4R2N.KLDLSNVQSK.+3y4.light	58.7
384.897	583.329	13.3	hTAU_4R2N.KLDLSNVQSK.+3y5.extraheavy_D5K8R10	58.7
377.884	575.315	13.3	hTAU_4R2N.KLDLSNVQSK.+3y5.light	58.7
384.897	670.361	13.3	hTAU_4R2N.KLDLSNVQSK.+3y6.extraheavy_D5K8R10	58.7
377.884	662.347	13.3	hTAU_4R2N.KLDLSNVQSK.+3y6.light	58.7
508.787	370.218	15	hTAU_4R2N.LDLSNVQSK.+2y3.extraheavy_D5K8R10	67.7
502.275	362.203	15	hTAU_4R2N.LDLSNVQSK.+2y3.light	67.7
508.787	583.329	15	hTAU_4R2N.LDLSNVQSK.+2y5.extraheavy_D5K8R10	67.7
502.275	575.315	15	hTAU_4R2N.LDLSNVQSK.+2y5.light	67.7
508.787	670.361	15	hTAU_4R2N.LDLSNVQSK.+2y6.extraheavy_D5K8R10	67.7
502.275	662.347	15	hTAU_4R2N.LDLSNVQSK.+2y6.light	67.7
508.787	783.445	15	hTAU_4R2N.LDLSNVQSK.+2y7.extraheavy_D5K8R10	67.7
502.275	775.431	15	hTAU_4R2N.LDLSNVQSK.+2y7.light	67.7
508.787	903.482	15	hTAU_4R2N.LDLSNVQSK.+2y8.extraheavy_D5K8R10	67.7
502.275	890.458	15	hTAU_4R2N.LDLSNVQSK.+2y8.light	67.7
669.873	1097.595	18	hTAU_4R2N.LQTAPVPM[Oxi]PDLK.+2y10.extraheavy_D5K8R10	79.5
663.36	1084.571	18	hTAU_4R2N.LQTAPVPM[Oxi]PDLK.+2y10.light	79.5
669.873	485.301	18	hTAU_4R2N.LQTAPVPM[Oxi]PDLK.+2y4.extraheavy_D5K8R10	79.5
663.36	472.277	18	hTAU_4R2N.LQTAPVPM[Oxi]PDLK.+2y4.light	79.5
669.873	729.389	18	hTAU_4R2N.LQTAPVPM[Oxi]PDLK.+2y6.extraheavy_D5K8R10	79.5
663.36	716.365	18	hTAU_4R2N.LQTAPVPM[Oxi]PDLK.+2y6.light	79.5
669.873	996.548	18	hTAU_4R2N.LQTAPVPM[Oxi]PDLK.+2y9.extraheavy_D5K8R10	79.5
663.36	983.523	18	hTAU_4R2N.LQTAPVPM[Oxi]PDLK.+2y9.light	79.5
661.875	1081.6	21.1	hTAU_4R2N.LQTAPVPM[Oxi]PDLK.+2y10.extraheavy_D5K8R10	78.9
655.363	1068.576	21.1	hTAU_4R2N.LQTAPVPM[Oxi]PDLK.+2y10.light	78.9
661.875	713.394	21.1	hTAU_4R2N.LQTAPVPM[Oxi]PDLK.+2y6.extraheavy_D5K8R10	78.9
655.363	700.37	21.1	hTAU_4R2N.LQTAPVPM[Oxi]PDLK.+2y6.light	78.9
661.875	909.516	21.1	hTAU_4R2N.LQTAPVPM[Oxi]PDLK.+2y8.extraheavy_D5K8R10	78.9
655.363	896.491	21.1	hTAU_4R2N.LQTAPVPM[Oxi]PDLK.+2y8.light	78.9
742.68	1060.57	16.4	hTAU_4R2N.QEFEVM[Oxi]EDHAGTYGLGDRK.+3y10.extraheavy_D5K8R10	84.6
733.332	1037.537	16.4	hTAU_4R2N.QEFEVM[Oxi]EDHAGTYGLGDRK.+3y10.light	84.6
742.68	797.376	16.4	hTAU_4R2N.QEFEVM[Oxi]EDHAGTYGLGDRK.+3y14+2.extraheavy_D5K8R10	84.6
733.332	783.354	16.4	hTAU_4R2N.QEFEVM[Oxi]EDHAGTYGLGDRK.+3y14+2.light	84.6

742.68	321.236	16.4	hTAU_4R2N.QEFEVM[Oxi]EDHAGTYGLGDRK.+3y2.extraheavy_D5K8R10	84.6
733.332	303.214	16.4	hTAU_4R2N.QEFEVM[Oxi]EDHAGTYGLGDRK.+3y2.light	84.6
742.68	668.401	16.4	hTAU_4R2N.QEFEVM[Oxi]EDHAGTYGLGDRK.+3y6.extraheavy_D5K8R10	84.6
733.332	645.368	16.4	hTAU_4R2N.QEFEVM[Oxi]EDHAGTYGLGDRK.+3y6.light	84.6
742.68	989.533	16.4	hTAU_4R2N.QEFEVM[Oxi]EDHAGTYGLGDRK.+3y9.extraheavy_D5K8R10	84.6
733.332	966.5	16.4	hTAU_4R2N.QEFEVM[Oxi]EDHAGTYGLGDRK.+3y9.light	84.6
553.263	789.378	18.2	hTAU_4R2N.QEFEVMEDHAGTYGLGDRK.+4y14+2.extraheavy_D5K8R10	70.9
546.252	775.357	18.2	hTAU_4R2N.QEFEVMEDHAGTYGLGDRK.+4y14+2.light	70.9
553.263	526.588	18.2	hTAU_4R2N.QEFEVMEDHAGTYGLGDRK.+4y14+3.extraheavy_D5K8R10	70.9
546.252	517.24	18.2	hTAU_4R2N.QEFEVMEDHAGTYGLGDRK.+4y14+3.light	70.9
553.263	559.611	18.2	hTAU_4R2N.QEFEVMEDHAGTYGLGDRK.+4y15+3.extraheavy_D5K8R10	70.9
546.252	550.263	18.2	hTAU_4R2N.QEFEVMEDHAGTYGLGDRK.+4y15+3.light	70.9
553.263	611.379	18.2	hTAU_4R2N.QEFEVMEDHAGTYGLGDRK.+4y5.extraheavy_D5K8R10	70.9
546.252	588.346	18.2	hTAU_4R2N.QEFEVMEDHAGTYGLGDRK.+4y5.light	70.9
444.254	302.195	12.5	hTAU_4R2N.SEKLDKF.+2y2.extraheavy_D5K8R10	62.7
433.735	294.181	12.5	hTAU_4R2N.SEKLDKF.+2y2.light	62.7
444.254	422.233	12.5	hTAU_4R2N.SEKLDKF.+2y3.extraheavy_D5K8R10	62.7
433.735	409.208	12.5	hTAU_4R2N.SEKLDKF.+2y3.light	62.7
444.254	535.317	12.5	hTAU_4R2N.SEKLDKF.+2y4.extraheavy_D5K8R10	62.7
433.735	522.292	12.5	hTAU_4R2N.SEKLDKF.+2y4.light	62.7
444.254	671.426	12.5	hTAU_4R2N.SEKLDKF.+2y5.extraheavy_D5K8R10	62.7
433.735	650.387	12.5	hTAU_4R2N.SEKLDKF.+2y5.light	62.7
444.254	336.217	12.5	hTAU_4R2N.SEKLDKF.+2y5+2.extraheavy_D5K8R10	62.7
433.735	325.697	12.5	hTAU_4R2N.SEKLDKF.+2y5+2.light	62.7
444.254	400.738	12.5	hTAU_4R2N.SEKLDKF.+2y6+2.extraheavy_D5K8R10	62.7
433.735	390.219	12.5	hTAU_4R2N.SEKLDKF.+2y6+2.light	62.7
423.741	745.432	14.5	hTAU_4R2N.SRTPSLPTPPTREP.+4y6.extraheavy_D5K8R10	61.5
416.734	727.41	14.5	hTAU_4R2N.SRTPSLPTPPTREP.+4y6.light	61.5
423.741	373.22	14.5	hTAU_4R2N.SRTPSLPTPPTREP.+4y6+2.extraheavy_D5K8R10	61.5
416.734	364.208	14.5	hTAU_4R2N.SRTPSLPTPPTREP.+4y6+2.light	61.5
423.741	842.485	14.5	hTAU_4R2N.SRTPSLPTPPTREP.+4y7.extraheavy_D5K8R10	61.5
416.734	824.462	14.5	hTAU_4R2N.SRTPSLPTPPTREP.+4y7.light	61.5
423.741	421.746	14.5	hTAU_4R2N.SRTPSLPTPPTREP.+4y7+2.extraheavy_D5K8R10	61.5
416.734	412.735	14.5	hTAU_4R2N.SRTPSLPTPPTREP.+4y7+2.light	61.5
987.001	995.545	19.7	hTAU_4R2N.STPTAEDVTAPLVDEGAPGK.+2y10.extraheavy_D5K8R10	102.4
977.984	982.52	19.7	hTAU_4R2N.STPTAEDVTAPLVDEGAPGK.+2y10.light	102.4
987.001	1066.582	19.7	hTAU_4R2N.STPTAEDVTAPLVDEGAPGK.+2y11.extraheavy_D5K8R10	102.4
977.984	1053.557	19.7	hTAU_4R2N.STPTAEDVTAPLVDEGAPGK.+2y11.light	102.4
987.001	1167.63	19.7	hTAU_4R2N.STPTAEDVTAPLVDEGAPGK.+2y12.extraheavy_D5K8R10	102.4
977.984	1154.605	19.7	hTAU_4R2N.STPTAEDVTAPLVDEGAPGK.+2y12.light	102.4
987.001	892.962	19.7	hTAU_4R2N.STPTAEDVTAPLVDEGAPGK.+2y18+2.extraheavy_D5K8R10	102.4
977.984	883.944	19.7	hTAU_4R2N.STPTAEDVTAPLVDEGAPGK.+2y18+2.light	102.4
987.001	309.201	19.7	hTAU_4R2N.STPTAEDVTAPLVDEGAPGK.+2y3.extraheavy_D5K8R10	102.4
977.984	301.187	19.7	hTAU_4R2N.STPTAEDVTAPLVDEGAPGK.+2y3.light	102.4
382.534	417.259	11.9	hTAU_4R2N.TDHGAEIVYK.+3y3.extraheavy_D5K8R10	58.7
378.193	409.245	11.9	hTAU_4R2N.TDHGAEIVYK.+3y3.light	58.7

382.534	209.133	11.9	hTAU_4R2N.TDHGAEIVYK.+3y3+2.extraheavy_D5K8R10	58.7
378.193	205.126	11.9	hTAU_4R2N.TDHGAEIVYK.+3y3+2.light	58.7
382.534	530.343	11.9	hTAU_4R2N.TDHGAEIVYK.+3y4.extraheavy_D5K8R10	58.7
378.193	522.329	11.9	hTAU_4R2N.TDHGAEIVYK.+3y4.light	58.7
382.534	308.839	11.9	hTAU_4R2N.TDHGAEIVYK.+3y8+3.extraheavy_D5K8R10	58.7
378.193	306.168	11.9	hTAU_4R2N.TDHGAEIVYK.+3y8+3.light	58.7
382.534	522.774	11.9	hTAU_4R2N.TDHGAEIVYK.+3y9+2.extraheavy_D5K8R10	58.7
378.193	516.261	11.9	hTAU_4R2N.TDHGAEIVYK.+3y9+2.light	58.7
309.689	323.217	7	hTAU_4R2N.TPPAPK.+2y3.extraheavy_D5K8R10	53.4
305.682	315.203	7	hTAU_4R2N.TPPAPK.+2y3.light	53.4
309.689	420.27	7	hTAU_4R2N.TPPAPK.+2y4.extraheavy_D5K8R10	53.4
305.682	412.255	7	hTAU_4R2N.TPPAPK.+2y4.light	53.4
309.689	210.638	7	hTAU_4R2N.TPPAPK.+2y4+2.extraheavy_D5K8R10	53.4
305.682	206.631	7	hTAU_4R2N.TPPAPK.+2y4+2.light	53.4
309.689	517.322	7	hTAU_4R2N.TPPAPK.+2y5.extraheavy_D5K8R10	53.4
305.682	509.308	7	hTAU_4R2N.TPPAPK.+2y5.light	53.4
502.761	349.233	7	hTAU_4R2N.TPPSSGEPPK.+2y3.extraheavy_D5K8R10	67.5
498.753	341.218	7	hTAU_4R2N.TPPSSGEPPK.+2y3.light	67.5
502.761	709.361	7	hTAU_4R2N.TPPSSGEPPK.+2y7.extraheavy_D5K8R10	67.5
498.753	701.346	7	hTAU_4R2N.TPPSSGEPPK.+2y7.light	67.5
502.761	806.413	7	hTAU_4R2N.TPPSSGEPPK.+2y8.extraheavy_D5K8R10	67.5
498.753	798.399	7	hTAU_4R2N.TPPSSGEPPK.+2y8.light	67.5
502.761	403.71	7	hTAU_4R2N.TPPSSGEPPK.+2y8+2.extraheavy_D5K8R10	67.5
498.753	399.703	7	hTAU_4R2N.TPPSSGEPPK.+2y8+2.light	67.5
502.761	452.237	7	hTAU_4R2N.TPPSSGEPPK.+2y9+2.extraheavy_D5K8R10	67.5
498.753	448.23	7	hTAU_4R2N.TPPSSGEPPK.+2y9+2.light	67.5
480.272	620.854	15.6	hTAU_4R2N.TPSLPTPPTREPK.+3y11+2.extraheavy_D5K8R10	65.7
474.265	611.843	15.6	hTAU_4R2N.TPSLPTPPTREPK.+3y11+2.light	65.7
480.272	446.59	15.6	hTAU_4R2N.TPSLPTPPTREPK.+3y12+3.extraheavy_D5K8R10	65.7
474.265	440.582	15.6	hTAU_4R2N.TPSLPTPPTREPK.+3y12+3.light	65.7
480.272	842.485	15.6	hTAU_4R2N.TPSLPTPPTREPK.+3y7.extraheavy_D5K8R10	65.7
474.265	824.462	15.6	hTAU_4R2N.TPSLPTPPTREPK.+3y7.light	65.7
480.272	421.746	15.6	hTAU_4R2N.TPSLPTPPTREPK.+3y7+2.extraheavy_D5K8R10	65.7
474.265	412.735	15.6	hTAU_4R2N.TPSLPTPPTREPK.+3y7+2.light	65.7
480.272	520.796	15.6	hTAU_4R2N.TPSLPTPPTREPK.+3y9+2.extraheavy_D5K8R10	65.7
474.265	511.785	15.6	hTAU_4R2N.TPSLPTPPTREPK.+3y9+2.light	65.7
361.736	269.17	11.9	hTAU_4R2N.VQIINK.+2y2.extraheavy_D5K8R10	57.2
357.729	261.156	11.9	hTAU_4R2N.VQIINK.+2y2.light	57.2
361.736	382.254	11.9	hTAU_4R2N.VQIINK.+2y3.extraheavy_D5K8R10	57.2
357.729	374.24	11.9	hTAU_4R2N.VQIINK.+2y3.light	57.2
361.736	495.338	11.9	hTAU_4R2N.VQIINK.+2y4.extraheavy_D5K8R10	57.2
357.729	487.324	11.9	hTAU_4R2N.VQIINK.+2y4.light	57.2
361.736	623.397	11.9	hTAU_4R2N.VQIINK.+2y5.extraheavy_D5K8R10	57.2
357.729	615.382	11.9	hTAU_4R2N.VQIINK.+2y5.light	57.2
361.736	312.202	11.9	hTAU_4R2N.VQIINK.+2y5+2.extraheavy_D5K8R10	57.2
357.729	308.195	11.9	hTAU_4R2N.VQIINK.+2y5+2.light	57.2

644.823	1016.526	iRTpeptides.AGGSSEPVTGLADK.+2y10.light	78.1
644.823	604.33	iRTpeptides.AGGSSEPVTGLADK.+2y6.light	78.1
644.823	800.451	iRTpeptides.AGGSSEPVTGLADK.+2y8.light	78.1
726.836	584.269	iRTpeptides.DAVTPADFSEWSK.+2y10+2.light	84.1
726.836	1066.484	iRTpeptides.DAVTPADFSEWSK.+2y9.light	84.1
726.836	533.746	iRTpeptides.DAVTPADFSEWSK.+2y9+2.light	84.1
776.93	1051.557	iRTpeptides.FLLQFGAQGSPLFK.+2y10.light	87.8
776.93	504.318	iRTpeptides.FLLQFGAQGSPLFK.+2y4.light	87.8
776.93	904.489	iRTpeptides.FLLQFGAQGSPLFK.+2y9.light	87.8
699.338	605.341	iRTpeptides.GDLDAASYAPVR.+2y5.light	82.1
699.338	855.436	iRTpeptides.GDLDAASYAPVR.+2y7.light	82.1
699.338	926.473	iRTpeptides.GDLDAASYAPVR.+2y8.light	82.1
636.869	626.398	iRTpeptides.GTFIIDPAAIVR.+2y6.light	77.5
636.869	741.425	iRTpeptides.GTFIIDPAAIVR.+2y7.light	77.5
636.869	854.509	iRTpeptides.GTFIIDPAAIVR.+2y8.light	77.5
487.257	503.294	iRTpeptides.LGGNETQVR.+2y4.light	66.6
487.257	803.401	iRTpeptides.LGGNETQVR.+2y7.light	66.6
487.257	860.422	iRTpeptides.LGGNETQVR.+2y8.light	66.6
622.854	598.367	iRTpeptides.TGFIDPGGVIR.+2y6.light	76.5
622.854	713.394	iRTpeptides.TGFIDPGGVIR.+2y7.light	76.5
622.854	826.478	iRTpeptides.TGFIDPGGVIR.+2y8.light	76.5
669.838	841.384	iRTpeptides.TPVISGGPYER.+2y7.light	79.9
669.838	928.416	iRTpeptides.TPVISGGPYER.+2y8.light	79.9
669.838	1041.5	iRTpeptides.TPVISGGPYER.+2y9.light	79.9
683.854	855.4	iRTpeptides.TPVITGAPYER.+2y7.light	81
683.854	956.447	iRTpeptides.TPVITGAPYER.+2y8.light	81
683.854	1069.531	iRTpeptides.TPVITGAPYER.+2y9.light	81
683.828	663.294	iRTpeptides.VEATFGVDESANK.+2y6.light	81
683.828	819.384	iRTpeptides.VEATFGVDESANK.+2y8.light	81
683.828	966.453	iRTpeptides.VEATFGVDESANK.+2y9.light	81
547.298	633.32	iRTpeptides.YILAGVESNK.+2y6.light	71
547.298	704.357	iRTpeptides.YILAGVESNK.+2y7.light	71
547.298	817.441	iRTpeptides.YILAGVESNK.+2y8.light	71

Q1 m/z	Q3 m/z	RT (min)	Transition ID	DP (volts)	CE (volts)
451.583	573.298	10.6	hTAU_4R2N.AKTDHGAEIVYK.+3y10+2.extraheavy_D5K8R10	63.5	21.8
444.57	566.785	10.6	hTAU_4R2N.AKTDHGAEIVYK.+3y10+2.light	63.5	21.8
451.583	641.352	10.6	hTAU_4R2N.AKTDHGAEIVYK.+3y11+2.extraheavy_D5K8R10	63.5	21.8
444.57	630.833	10.6	hTAU_4R2N.AKTDHGAEIVYK.+3y11+2.light	63.5	21.8
451.583	318.19	10.6	hTAU_4R2N.AKTDHGAEIVYK.+3y2.extraheavy_D5K8R10	63.5	21.8
444.57	310.176	10.6	hTAU_4R2N.AKTDHGAEIVYK.+3y2.light	63.5	21.8
451.583	787.444	10.6	hTAU_4R2N.AKTDHGAEIVYK.+3y7.extraheavy_D5K8R10	63.5	21.8
444.57	779.43	10.6	hTAU_4R2N.AKTDHGAEIVYK.+3y7.light	63.5	21.8
451.583	462.755	10.6	hTAU_4R2N.AKTDHGAEIVYK.+3y8+2.extraheavy_D5K8R10	63.5	21.8
444.57	458.748	10.6	hTAU_4R2N.AKTDHGAEIVYK.+3y8+2.light	63.5	21.8
501.766	507.799	11.1	hTAU_4R2N.C[PPa]GSLGNIHHKPGGGQVEVK.+4y10+2.extraheavy_D5K8R10	67.4	24.7
497.759	499.785	11.1	hTAU_4R2N.C[PPa]GSLGNIHHKPGGGQVEVK.+4y10+2.light	67.4	24.7
501.766	576.329	11.1	hTAU_4R2N.C[PPa]GSLGNIHHKPGGGQVEVK.+4y11+2.extraheavy_D5K8R10	67.4	24.7
497.759	568.315	11.1	hTAU_4R2N.C[PPa]GSLGNIHHKPGGGQVEVK.+4y11+2.light	67.4	24.7
501.766	786.932	11.1	hTAU_4R2N.C[PPa]GSLGNIHHKPGGGQVEVK.+4y15+2.extraheavy_D5K8R10	67.4	24.7
497.759	778.918	11.1	hTAU_4R2N.C[PPa]GSLGNIHHKPGGGQVEVK.+4y15+2.light	67.4	24.7
501.766	562.652	11.1	hTAU_4R2N.C[PPa]GSLGNIHHKPGGGQVEVK.+4y16+3.extraheavy_D5K8R10	67.4	24.7
497.759	557.309	11.1	hTAU_4R2N.C[PPa]GSLGNIHHKPGGGQVEVK.+4y16+3.light	67.4	24.7
501.766	591.663	11.1	hTAU_4R2N.C[PPa]GSLGNIHHKPGGGQVEVK.+4y17+3.extraheavy_D5K8R10	67.4	24.7
497.759	586.32	11.1	hTAU_4R2N.C[PPa]GSLGNIHHKPGGGQVEVK.+4y17+3.light	67.4	24.7
501.766	878.482	11.1	hTAU_4R2N.C[PPa]GSLGNIHHKPGGGQVEVK.+4y9.extraheavy_D5K8R10	67.4	24.7
497.759	870.468	11.1	hTAU_4R2N.C[PPa]GSLGNIHHKPGGGQVEVK.+4y9.light	67.4	24.7
737.323	718.838	12	hTAU_4R2N.DQGGYTM[Oxi]HQDQEGDTDAGLK.+3y13+2.extraheavy_D5K8R10	84.2	37.2
727.971	707.316	12	hTAU_4R2N.DQGGYTM[Oxi]HQDQEGDTDAGLK.+3y13+2.light	84.2	37.2
737.323	617.355	12	hTAU_4R2N.DQGGYTM[Oxi]HQDQEGDTDAGLK.+3y6.extraheavy_D5K8R10	84.2	37.2
727.971	604.33	12	hTAU_4R2N.DQGGYTM[Oxi]HQDQEGDTDAGLK.+3y6.light	84.2	37.2
737.323	794.414	12	hTAU_4R2N.DQGGYTM[Oxi]HQDQEGDTDAGLK.+3y8.extraheavy_D5K8R10	84.2	37.2
727.971	776.378	12	hTAU_4R2N.DQGGYTM[Oxi]HQDQEGDTDAGLK.+3y8.light	84.2	37.2
737.323	923.456	12	hTAU_4R2N.DQGGYTM[Oxi]HQDQEGDTDAGLK.+3y9.extraheavy_D5K8R10	84.2	37.2
727.971	905.421	12	hTAU_4R2N.DQGGYTM[Oxi]HQDQEGDTDAGLK.+3y9.light	84.2	37.2
731.992	1171.552	13	hTAU_4R2N.DQGGYTMHQDQEGDTDAGLK.+3y11.extraheavy_D5K8R10	83.8	36.9
722.64	1148.507	13	hTAU_4R2N.DQGGYTMHQDQEGDTDAGLK.+3y11.light	83.8	36.9
731.992	973.436	13	hTAU_4R2N.DQGGYTMHQDQEGDTDAGLK.+3y18+2.extraheavy_D5K8R10	83.8	36.9
722.64	961.913	13	hTAU_4R2N.DQGGYTMHQDQEGDTDAGLK.+3y18+2.light	83.8	36.9
731.992	396.27	13	hTAU_4R2N.DQGGYTMHQDQEGDTDAGLK.+3y4.extraheavy_D5K8R10	83.8	36.9
722.64	388.255	13	hTAU_4R2N.DQGGYTMHQDQEGDTDAGLK.+3y4.light	83.8	36.9
731.992	794.414	13	hTAU_4R2N.DQGGYTMHQDQEGDTDAGLK.+3y8.extraheavy_D5K8R10	83.8	36.9
722.64	776.378	13	hTAU_4R2N.DQGGYTMHQDQEGDTDAGLK.+3y8.light	83.8	36.9
803.694	1033.473	15.2	hTAU_4R2N.ESPLQPTPTEDGSEEPGSETSDAK.+3y10.extraheavy_D5K8R10	89.3	41
797.682	1020.448	15.2	hTAU_4R2N.ESPLQPTPTEDGSEEPGSETSDAK.+3y10.light	89.3	41
803.694	534.281	15.2	hTAU_4R2N.ESPLQPTPTEDGSEEPGSETSDAK.+3y5.extraheavy_D5K8R10	89.3	41
797.682	521.257	15.2	hTAU_4R2N.ESPLQPTPTEDGSEEPGSETSDAK.+3y5.light	89.3	41
803.694	750.356	15.2	hTAU_4R2N.ESPLQPTPTEDGSEEPGSETSDAK.+3y7.extraheavy_D5K8R10	89.3	41
797.682	737.331	15.2	hTAU_4R2N.ESPLQPTPTEDGSEEPGSETSDAK.+3y7.light	89.3	41

803.694	904.43	15.2	hTAU_4R2N.ESPLQTPTEGSEEPGSETSDAK.+3y9.extraheavy_D5K8R10	89.3	41
797.682	891.405	15.2	hTAU_4R2N.ESPLQTPTEGSEEPGSETSDAK.+3y9.light	89.3	41
803.694	452.719	15.2	hTAU_4R2N.ESPLQTPTEGSEEPGSETSDAK.+3y9+2.extraheavy_D5K8R10	89.3	41
797.682	446.206	15.2	hTAU_4R2N.ESPLQTPTEGSEEPGSETSDAK.+3y9+2.light	89.3	41
382.223	323.217	9	hTAU_4R2N.GQANATRIPAK.+3y3.extraheavy_D5K8R10	58.5	18.1
376.216	315.203	9	hTAU_4R2N.GQANATRIPAK.+3y3.light	58.5	18.1
382.223	703.458	9	hTAU_4R2N.GQANATRIPAK.+3y6.extraheavy_D5K8R10	58.5	18.1
376.216	685.436	9	hTAU_4R2N.GQANATRIPAK.+3y6.light	58.5	18.1
382.223	774.495	9	hTAU_4R2N.GQANATRIPAK.+3y7.extraheavy_D5K8R10	58.5	18.1
376.216	756.473	9	hTAU_4R2N.GQANATRIPAK.+3y7.light	58.5	18.1
382.223	387.751	9	hTAU_4R2N.GQANATRIPAK.+3y7+2.extraheavy_D5K8R10	58.5	18.1
376.216	378.74	9	hTAU_4R2N.GQANATRIPAK.+3y7+2.light	58.5	18.1
382.223	444.773	9	hTAU_4R2N.GQANATRIPAK.+3y8+2.extraheavy_D5K8R10	58.5	18.1
376.216	435.761	9	hTAU_4R2N.GQANATRIPAK.+3y8+2.light	58.5	18.1
382.223	480.291	9	hTAU_4R2N.GQANATRIPAK.+3y9+2.extraheavy_D5K8R10	58.5	18.1
376.216	471.28	9	hTAU_4R2N.GQANATRIPAK.+3y9+2.light	58.5	18.1
501.038	591.867	18.6	hTAU_4R2N.HVPGGGSVQIVYKPVDSLK.+4y10+2.extraheavy_D5K8R10	67.3	24.6
495.778	581.348	18.6	hTAU_4R2N.HVPGGGSVQIVYKPVDSLK.+4y10+2.light	67.3	24.6
501.038	655.896	18.6	hTAU_4R2N.HVPGGGSVQIVYKPVDSLK.+4y11+2.extraheavy_D5K8R10	67.3	24.6
495.778	645.377	18.6	hTAU_4R2N.HVPGGGSVQIVYKPVDSLK.+4y11+2.light	67.3	24.6
501.038	355.243	18.6	hTAU_4R2N.HVPGGGSVQIVYKPVDSLK.+4y3.extraheavy_D5K8R10	67.3	24.6
495.778	347.229	18.6	hTAU_4R2N.HVPGGGSVQIVYKPVDSLK.+4y3.light	67.3	24.6
501.038	671.402	18.6	hTAU_4R2N.HVPGGGSVQIVYKPVDSLK.+4y6.extraheavy_D5K8R10	67.3	24.6
495.778	658.377	18.6	hTAU_4R2N.HVPGGGSVQIVYKPVDSLK.+4y6.light	67.3	24.6
501.038	535.325	18.6	hTAU_4R2N.HVPGGGSVQIVYKPVDSLK.+4y9+2.extraheavy_D5K8R10	67.3	24.6
495.778	524.805	18.6	hTAU_4R2N.HVPGGGSVQIVYKPVDSLK.+4y9+2.light	67.3	24.6
427.918	498.789	11	hTAU_4R2N.IATPRGAAPPGQK.+3y10+2.extraheavy_D5K8R10	61.9	20.5
421.91	489.778	11	hTAU_4R2N.IATPRGAAPPGQK.+3y10+2.light	61.9	20.5
427.918	549.313	11	hTAU_4R2N.IATPRGAAPPGQK.+3y11+2.extraheavy_D5K8R10	61.9	20.5
421.91	540.301	11	hTAU_4R2N.IATPRGAAPPGQK.+3y11+2.light	61.9	20.5
427.918	584.831	11	hTAU_4R2N.IATPRGAAPPGQK.+3y12+2.extraheavy_D5K8R10	61.9	20.5
421.91	575.82	11	hTAU_4R2N.IATPRGAAPPGQK.+3y12+2.light	61.9	20.5
427.918	437.26	11	hTAU_4R2N.IATPRGAAPPGQK.+3y4.extraheavy_D5K8R10	61.9	20.5
421.91	429.246	11	hTAU_4R2N.IATPRGAAPPGQK.+3y4.light	61.9	20.5
427.918	534.313	11	hTAU_4R2N.IATPRGAAPPGQK.+3y5.extraheavy_D5K8R10	61.9	20.5
421.91	526.298	11	hTAU_4R2N.IATPRGAAPPGQK.+3y5.light	61.9	20.5
531.288	611.317	17.4	hTAU_4R2N.IGSLDNITHVPGGGNK.+3y12+2.extraheavy_D5K8R10	69.5	26.3
526.946	604.805	17.4	hTAU_4R2N.IGSLDNITHVPGGGNK.+3y12+2.light	69.5	26.3
531.288	711.375	17.4	hTAU_4R2N.IGSLDNITHVPGGGNK.+3y14+2.extraheavy_D5K8R10	69.5	26.3
526.946	704.863	17.4	hTAU_4R2N.IGSLDNITHVPGGGNK.+3y14+2.light	69.5	26.3
531.288	739.886	17.4	hTAU_4R2N.IGSLDNITHVPGGGNK.+3y15+2.extraheavy_D5K8R10	69.5	26.3
526.946	733.373	17.4	hTAU_4R2N.IGSLDNITHVPGGGNK.+3y15+2.light	69.5	26.3
531.288	537.287	17.4	hTAU_4R2N.IGSLDNITHVPGGGNK.+3y6.extraheavy_D5K8R10	69.5	26.3
526.946	529.273	17.4	hTAU_4R2N.IGSLDNITHVPGGGNK.+3y6.light	69.5	26.3
531.288	874.462	17.4	hTAU_4R2N.IGSLDNITHVPGGGNK.+3y9.extraheavy_D5K8R10	69.5	26.3
526.946	866.448	17.4	hTAU_4R2N.IGSLDNITHVPGGGNK.+3y9.light	69.5	26.3

576.657	679.371	15.7	hTAU_4R2N.IGSLDNITHVPGGGNKK.+3y13+2.extraheavy_D5K8R10	72.6	28.6
569.644	668.852	15.7	hTAU_4R2N.IGSLDNITHVPGGGNKK.+3y13+2.light	72.6	28.6
576.657	779.43	15.7	hTAU_4R2N.IGSLDNITHVPGGGNKK.+3y15+2.extraheavy_D5K8R10	72.6	28.6
569.644	768.91	15.7	hTAU_4R2N.IGSLDNITHVPGGGNKK.+3y15+2.light	72.6	28.6
576.657	807.94	15.7	hTAU_4R2N.IGSLDNITHVPGGGNKK.+3y16+2.extraheavy_D5K8R10	72.6	28.6
569.644	797.421	15.7	hTAU_4R2N.IGSLDNITHVPGGGNKK.+3y16+2.light	72.6	28.6
576.657	673.396	15.7	hTAU_4R2N.IGSLDNITHVPGGGNKK.+3y7.extraheavy_D5K8R10	72.6	28.6
569.644	657.368	15.7	hTAU_4R2N.IGSLDNITHVPGGGNKK.+3y7.light	72.6	28.6
576.657	337.202	15.7	hTAU_4R2N.IGSLDNITHVPGGGNKK.+3y7+2.extraheavy_D5K8R10	72.6	28.6
569.644	329.188	15.7	hTAU_4R2N.IGSLDNITHVPGGGNKK.+3y7+2.light	72.6	28.6
435.245	382.254	10.5	hTAU_4R2N.IGSTENLK.+2y3.extraheavy_D5K8R10	62.6	24.4
431.237	374.24	10.5	hTAU_4R2N.IGSTENLK.+2y3.light	62.6	24.4
435.245	511.297	10.5	hTAU_4R2N.IGSTENLK.+2y4.extraheavy_D5K8R10	62.6	24.4
431.237	503.282	10.5	hTAU_4R2N.IGSTENLK.+2y4.light	62.6	24.4
435.245	612.344	10.5	hTAU_4R2N.IGSTENLK.+2y5.extraheavy_D5K8R10	62.6	24.4
431.237	604.33	10.5	hTAU_4R2N.IGSTENLK.+2y5.light	62.6	24.4
435.245	699.376	10.5	hTAU_4R2N.IGSTENLK.+2y6.extraheavy_D5K8R10	62.6	24.4
431.237	691.362	10.5	hTAU_4R2N.IGSTENLK.+2y6.light	62.6	24.4
435.245	756.398	10.5	hTAU_4R2N.IGSTENLK.+2y7.extraheavy_D5K8R10	62.6	24.4
431.237	748.384	10.5	hTAU_4R2N.IGSTENLK.+2y7.light	62.6	24.4
384.897	370.218	13.3	hTAU_4R2N.KLDLSNVQSK.+3y3.extraheavy_D5K8R10	58.7	18.1
377.884	362.203	13.3	hTAU_4R2N.KLDLSNVQSK.+3y3.light	58.7	18.1
384.897	469.286	13.3	hTAU_4R2N.KLDLSNVQSK.+3y4.extraheavy_D5K8R10	58.7	18.1
377.884	461.272	13.3	hTAU_4R2N.KLDLSNVQSK.+3y4.light	58.7	18.1
384.897	583.329	13.3	hTAU_4R2N.KLDLSNVQSK.+3y5.extraheavy_D5K8R10	58.7	18.1
377.884	575.315	13.3	hTAU_4R2N.KLDLSNVQSK.+3y5.light	58.7	18.1
384.897	670.361	13.3	hTAU_4R2N.KLDLSNVQSK.+3y6.extraheavy_D5K8R10	58.7	18.1
377.884	662.347	13.3	hTAU_4R2N.KLDLSNVQSK.+3y6.light	58.7	18.1
508.787	370.218	15	hTAU_4R2N.LDLSNVQSK.+2y3.extraheavy_D5K8R10	67.7	26.9
502.275	362.203	15	hTAU_4R2N.LDLSNVQSK.+2y3.light	67.7	26.9
508.787	583.329	15	hTAU_4R2N.LDLSNVQSK.+2y5.extraheavy_D5K8R10	67.7	26.9
502.275	575.315	15	hTAU_4R2N.LDLSNVQSK.+2y5.light	67.7	26.9
508.787	670.361	15	hTAU_4R2N.LDLSNVQSK.+2y6.extraheavy_D5K8R10	67.7	26.9
502.275	662.347	15	hTAU_4R2N.LDLSNVQSK.+2y6.light	67.7	26.9
508.787	783.445	15	hTAU_4R2N.LDLSNVQSK.+2y7.extraheavy_D5K8R10	67.7	26.9
502.275	775.431	15	hTAU_4R2N.LDLSNVQSK.+2y7.light	67.7	26.9
508.787	903.482	15	hTAU_4R2N.LDLSNVQSK.+2y8.extraheavy_D5K8R10	67.7	26.9
502.275	890.458	15	hTAU_4R2N.LDLSNVQSK.+2y8.light	67.7	26.9
332.858	226.164	11	hTAU_4R2N.LTFRENAK.+3y2.extraheavy_D5K8R10	54.9	15.4
326.85	218.15	11	hTAU_4R2N.LTFRENAK.+3y2.light	54.9	15.4
332.858	635.359	11	hTAU_4R2N.LTFRENAK.+3y5.extraheavy_D5K8R10	54.9	15.4
326.85	617.337	11	hTAU_4R2N.LTFRENAK.+3y5.light	54.9	15.4
332.858	782.427	11	hTAU_4R2N.LTFRENAK.+3y6.extraheavy_D5K8R10	54.9	15.4
326.85	764.405	11	hTAU_4R2N.LTFRENAK.+3y6.light	54.9	15.4
332.858	391.717	11	hTAU_4R2N.LTFRENAK.+3y6+2.extraheavy_D5K8R10	54.9	15.4
326.85	382.706	11	hTAU_4R2N.LTFRENAK.+3y6+2.light	54.9	15.4

332.858	442.241	11	hTAU_4R2N.LTFRENAK.+3y7+2.extraheavy_D5K8R10	54.9	15.4
326.85	433.23	11	hTAU_4R2N.LTFRENAK.+3y7+2.light	54.9	15.4
697.31	1061.52	17.8	hTAU_4R2N.QEFEVM[Oxi]EDHAGTYGLGDR.+3y10.extraheavy_D5K8R10	81.5	35.2
690.634	1046.501	17.8	hTAU_4R2N.QEFEVM[Oxi]EDHAGTYGLGDR.+3y10.light	81.5	35.2
697.31	729.321	17.8	hTAU_4R2N.QEFEVM[Oxi]EDHAGTYGLGDR.+3y13+2.extraheavy_D5K8R10	81.5	35.2
690.634	719.307	17.8	hTAU_4R2N.QEFEVM[Oxi]EDHAGTYGLGDR.+3y13+2.light	81.5	35.2
697.31	853.424	17.8	hTAU_4R2N.QEFEVM[Oxi]EDHAGTYGLGDR.+3y8.extraheavy_D5K8R10	81.5	35.2
690.634	838.405	17.8	hTAU_4R2N.QEFEVM[Oxi]EDHAGTYGLGDR.+3y8.light	81.5	35.2
697.31	924.461	17.8	hTAU_4R2N.QEFEVM[Oxi]EDHAGTYGLGDR.+3y9.extraheavy_D5K8R10	81.5	35.2
690.634	909.442	17.8	hTAU_4R2N.QEFEVM[Oxi]EDHAGTYGLGDR.+3y9.light	81.5	35.2
742.68	1060.57	16.4	hTAU_4R2N.QEFEVM[Oxi]EDHAGTYGLGDRK.+3y10.extraheavy_D5K8R10	84.6	37.5
733.332	1037.537	16.4	hTAU_4R2N.QEFEVM[Oxi]EDHAGTYGLGDRK.+3y10.light	84.6	37.5
444.254	302.195	12.5	hTAU_4R2N.SEKLDFK.+2y2.extraheavy_D5K8R10	62.7	24.5
433.735	294.181	12.5	hTAU_4R2N.SEKLDFK.+2y2.light	62.7	24.5
444.254	422.233	12.5	hTAU_4R2N.SEKLDFK.+2y3.extraheavy_D5K8R10	62.7	24.5
433.735	409.208	12.5	hTAU_4R2N.SEKLDFK.+2y3.light	62.7	24.5
444.254	535.317	12.5	hTAU_4R2N.SEKLDFK.+2y4.extraheavy_D5K8R10	62.7	24.5
433.735	522.292	12.5	hTAU_4R2N.SEKLDFK.+2y4.light	62.7	24.5
444.254	671.426	12.5	hTAU_4R2N.SEKLDFK.+2y5.extraheavy_D5K8R10	62.7	24.5
433.735	650.387	12.5	hTAU_4R2N.SEKLDFK.+2y5.light	62.7	24.5
444.254	336.217	12.5	hTAU_4R2N.SEKLDFK.+2y5+2.extraheavy_D5K8R10	62.7	24.5
433.735	325.697	12.5	hTAU_4R2N.SEKLDFK.+2y5+2.light	62.7	24.5
444.254	400.738	12.5	hTAU_4R2N.SEKLDFK.+2y6+2.extraheavy_D5K8R10	62.7	24.5
433.735	390.219	12.5	hTAU_4R2N.SEKLDFK.+2y6+2.light	62.7	24.5
722.351	1227.62	19.5	hTAU_4R2N.SENLYFQGDISR.+2y10.extraheavy_D5K8R10	83.2	34.6
714.841	1212.601	19.5	hTAU_4R2N.SENLYFQGDISR.+2y10.light	83.2	34.6
722.351	272.159	19.5	hTAU_4R2N.SENLYFQGDISR.+2y2.extraheavy_D5K8R10	83.2	34.6
714.841	262.151	19.5	hTAU_4R2N.SENLYFQGDISR.+2y2.light	83.2	34.6
722.351	690.361	19.5	hTAU_4R2N.SENLYFQGDISR.+2y6.extraheavy_D5K8R10	83.2	34.6
714.841	675.342	19.5	hTAU_4R2N.SENLYFQGDISR.+2y6.light	83.2	34.6
722.351	837.429	19.5	hTAU_4R2N.SENLYFQGDISR.+2y7.extraheavy_D5K8R10	83.2	34.6
714.841	822.41	19.5	hTAU_4R2N.SENLYFQGDISR.+2y7.light	83.2	34.6
722.351	1113.577	19.5	hTAU_4R2N.SENLYFQGDISR.+2y9.extraheavy_D5K8R10	83.2	34.6
714.841	1098.558	19.5	hTAU_4R2N.SENLYFQGDISR.+2y9.light	83.2	34.6
702.325	922.462	11.4	hTAU_4R2N.SGYSSPGSPGTPGSR.+2y10.extraheavy_D5K8R10	82	34
697.321	912.453	11.4	hTAU_4R2N.SGYSSPGSPGTPGSR.+2y10.light	82	34
531.298	485.301	16	hTAU_4R2N.SRLQTAPVPM[Oxi]PDLK.+3y4.extraheavy_D5K8R10	69.3	26.1
523.62	472.277	16	hTAU_4R2N.SRLQTAPVPM[Oxi]PDLK.+3y4.light	69.3	26.1
531.298	729.389	16	hTAU_4R2N.SRLQTAPVPM[Oxi]PDLK.+3y6.extraheavy_D5K8R10	69.3	26.1
523.62	716.365	16	hTAU_4R2N.SRLQTAPVPM[Oxi]PDLK.+3y6.light	69.3	26.1
531.298	925.511	16	hTAU_4R2N.SRLQTAPVPM[Oxi]PDLK.+3y8.extraheavy_D5K8R10	69.3	26.1
523.62	912.486	16	hTAU_4R2N.SRLQTAPVPM[Oxi]PDLK.+3y8.light	69.3	26.1
525.966	485.301	19	hTAU_4R2N.SRLQTAPVPM[Oxi]PDLK.+3y4.extraheavy_D5K8R10	68.9	25.8
518.289	472.277	19	hTAU_4R2N.SRLQTAPVPM[Oxi]PDLK.+3y4.light	68.9	25.8
525.966	713.394	19	hTAU_4R2N.SRLQTAPVPM[Oxi]PDLK.+3y6.extraheavy_D5K8R10	68.9	25.8
518.289	700.37	19	hTAU_4R2N.SRLQTAPVPM[Oxi]PDLK.+3y6.light	68.9	25.8

525.966	357.201	19	hTAU_4R2N.SRLQTAPVMPDLK.+3y6+2.extraheavy_D5K8R10	68.9	25.8
518.289	350.689	19	hTAU_4R2N.SRLQTAPVMPDLK.+3y6+2.light	68.9	25.8
987.001	995.545	19.7	hTAU_4R2N.STPTAEDVTAPLVDEGAPGK.+2y10.extraheavy_D5K8R10	102.4	44.1
977.984	982.52	19.7	hTAU_4R2N.STPTAEDVTAPLVDEGAPGK.+2y10.light	102.4	44.1
987.001	1066.582	19.7	hTAU_4R2N.STPTAEDVTAPLVDEGAPGK.+2y11.extraheavy_D5K8R10	102.4	44.1
977.984	1053.557	19.7	hTAU_4R2N.STPTAEDVTAPLVDEGAPGK.+2y11.light	102.4	44.1
987.001	1167.63	19.7	hTAU_4R2N.STPTAEDVTAPLVDEGAPGK.+2y12.extraheavy_D5K8R10	102.4	44.1
977.984	1154.605	19.7	hTAU_4R2N.STPTAEDVTAPLVDEGAPGK.+2y12.light	102.4	44.1
987.001	892.962	19.7	hTAU_4R2N.STPTAEDVTAPLVDEGAPGK.+2y18+2.extraheavy_D5K8R10	102.4	44.1
977.984	883.944	19.7	hTAU_4R2N.STPTAEDVTAPLVDEGAPGK.+2y18+2.light	102.4	44.1
987.001	309.201	19.7	hTAU_4R2N.STPTAEDVTAPLVDEGAPGK.+2y3.extraheavy_D5K8R10	102.4	44.1
977.984	301.187	19.7	hTAU_4R2N.STPTAEDVTAPLVDEGAPGK.+2y3.light	102.4	44.1
382.534	417.259	11.9	hTAU_4R2N.TDHGAEIVYK.+3y3.extraheavy_D5K8R10	58.7	18.2
378.193	409.245	11.9	hTAU_4R2N.TDHGAEIVYK.+3y3.light	58.7	18.2
382.534	209.133	11.9	hTAU_4R2N.TDHGAEIVYK.+3y3+2.extraheavy_D5K8R10	58.7	18.2
378.193	205.126	11.9	hTAU_4R2N.TDHGAEIVYK.+3y3+2.light	58.7	18.2
382.534	530.343	11.9	hTAU_4R2N.TDHGAEIVYK.+3y4.extraheavy_D5K8R10	58.7	18.2
378.193	522.329	11.9	hTAU_4R2N.TDHGAEIVYK.+3y4.light	58.7	18.2
382.534	308.839	11.9	hTAU_4R2N.TDHGAEIVYK.+3y8+3.extraheavy_D5K8R10	58.7	18.2
378.193	306.168	11.9	hTAU_4R2N.TDHGAEIVYK.+3y8+3.light	58.7	18.2
382.534	522.774	11.9	hTAU_4R2N.TDHGAEIVYK.+3y9+2.extraheavy_D5K8R10	58.7	18.2
378.193	516.261	11.9	hTAU_4R2N.TDHGAEIVYK.+3y9+2.light	58.7	18.2
309.689	323.217	7	hTAU_4R2N.TPPAPK.+2y3.extraheavy_D5K8R10	53.4	19.9
305.682	315.203	7	hTAU_4R2N.TPPAPK.+2y3.light	53.4	19.9
309.689	420.27	7	hTAU_4R2N.TPPAPK.+2y4.extraheavy_D5K8R10	53.4	19.9
305.682	412.255	7	hTAU_4R2N.TPPAPK.+2y4.light	53.4	19.9
309.689	210.638	7	hTAU_4R2N.TPPAPK.+2y4+2.extraheavy_D5K8R10	53.4	19.9
305.682	206.631	7	hTAU_4R2N.TPPAPK.+2y4+2.light	53.4	19.9
309.689	517.322	7	hTAU_4R2N.TPPAPK.+2y5.extraheavy_D5K8R10	53.4	19.9
305.682	509.308	7	hTAU_4R2N.TPPAPK.+2y5.light	53.4	19.9
502.761	349.233	7	hTAU_4R2N.TPPSSGEPK.+2y3.extraheavy_D5K8R10	67.5	26.8
498.753	341.218	7	hTAU_4R2N.TPPSSGEPK.+2y3.light	67.5	26.8
502.761	709.361	7	hTAU_4R2N.TPPSSGEPK.+2y7.extraheavy_D5K8R10	67.5	26.8
498.753	701.346	7	hTAU_4R2N.TPPSSGEPK.+2y7.light	67.5	26.8
502.761	806.413	7	hTAU_4R2N.TPPSSGEPK.+2y8.extraheavy_D5K8R10	67.5	26.8
498.753	798.399	7	hTAU_4R2N.TPPSSGEPK.+2y8.light	67.5	26.8
502.761	403.71	7	hTAU_4R2N.TPPSSGEPK.+2y8+2.extraheavy_D5K8R10	67.5	26.8
498.753	399.703	7	hTAU_4R2N.TPPSSGEPK.+2y8+2.light	67.5	26.8
502.761	452.237	7	hTAU_4R2N.TPPSSGEPK.+2y9+2.extraheavy_D5K8R10	67.5	26.8
498.753	448.23	7	hTAU_4R2N.TPPSSGEPK.+2y9+2.light	67.5	26.8
478.91	618.81	7	hTAU_4R2N.TPPSSGEPKSGDR.+3y12+2.extraheavy_D5K8R10	65.5	23.2
471.232	607.294	7	hTAU_4R2N.TPPSSGEPKSGDR.+3y12+2.light	65.5	23.2
478.91	682.38	7	hTAU_4R2N.TPPSSGEPKSGDR.+3y6.extraheavy_D5K8R10	65.5	23.2
471.232	659.347	7	hTAU_4R2N.TPPSSGEPKSGDR.+3y6.light	65.5	23.2
478.91	779.433	7	hTAU_4R2N.TPPSSGEPKSGDR.+3y7.extraheavy_D5K8R10	65.5	23.2
471.232	756.4	7	hTAU_4R2N.TPPSSGEPKSGDR.+3y7.light	65.5	23.2

328.882	349.233	10.5	hTAU_4R2N.VAVVRTPPK.+3y3.extraheavy_D5K8R10	54.7	15.2
322.875	341.218	10.5	hTAU_4R2N.VAVVRTPPK.+3y3.light	54.7	15.2
328.882	616.39	10.5	hTAU_4R2N.VAVVRTPPK.+3y5.extraheavy_D5K8R10	54.7	15.2
322.875	598.367	10.5	hTAU_4R2N.VAVVRTPPK.+3y5.light	54.7	15.2
328.882	715.458	10.5	hTAU_4R2N.VAVVRTPPK.+3y6.extraheavy_D5K8R10	54.7	15.2
322.875	697.436	10.5	hTAU_4R2N.VAVVRTPPK.+3y6.light	54.7	15.2
328.882	407.767	10.5	hTAU_4R2N.VAVVRTPPK.+3y7+2.extraheavy_D5K8R10	54.7	15.2
322.875	398.756	10.5	hTAU_4R2N.VAVVRTPPK.+3y7+2.light	54.7	15.2
328.882	443.285	10.5	hTAU_4R2N.VAVVRTPPK.+3y8+2.extraheavy_D5K8R10	54.7	15.2
322.875	434.274	10.5	hTAU_4R2N.VAVVRTPPK.+3y8+2.light	54.7	15.2
361.736	269.17	11.9	hTAU_4R2N.VQIINK.+2y2.extraheavy_D5K8R10	57.2	21.7
357.729	261.156	11.9	hTAU_4R2N.VQIINK.+2y2.light	57.2	21.7
361.736	382.254	11.9	hTAU_4R2N.VQIINK.+2y3.extraheavy_D5K8R10	57.2	21.7
357.729	374.24	11.9	hTAU_4R2N.VQIINK.+2y3.light	57.2	21.7
361.736	495.338	11.9	hTAU_4R2N.VQIINK.+2y4.extraheavy_D5K8R10	57.2	21.7
357.729	487.324	11.9	hTAU_4R2N.VQIINK.+2y4.light	57.2	21.7
361.736	623.397	11.9	hTAU_4R2N.VQIINK.+2y5.extraheavy_D5K8R10	57.2	21.7
357.729	615.382	11.9	hTAU_4R2N.VQIINK.+2y5.light	57.2	21.7
361.736	312.202	11.9	hTAU_4R2N.VQIINK.+2y5+2.extraheavy_D5K8R10	57.2	21.7
357.729	308.195	11.9	hTAU_4R2N.VQIINK.+2y5+2.light	57.2	21.7
598.773	351.201	11	hTAU_4R2N_phospho.SPVVSGDTS[Pho]PR.+2y3-98.extraheavy_D5K8R10	74.2	30.1
596.268	351.201	11	hTAU_4R2N_phospho.SPVVSGDTS[Pho]PR.+2y3-98.heavy_R10	74.2	30.1
591.264	341.193	11	hTAU_4R2N_phospho.SPVVSGDTS[Pho]PR.+2y3-98.light	74.2	30.1
598.773	449.178	11	hTAU_4R2N_phospho.SPVVSGDTS[Pho]PR.+2y3.extraheavy_D5K8R10	74.2	30.1
596.268	449.178	11	hTAU_4R2N_phospho.SPVVSGDTS[Pho]PR.+2y3.heavy_R10	74.2	30.1
591.264	439.17	11	hTAU_4R2N_phospho.SPVVSGDTS[Pho]PR.+2y3.light	74.2	30.1
598.773	727.285	11	hTAU_4R2N_phospho.SPVVSGDTS[Pho]PR.+2y6.extraheavy_D5K8R10	74.2	30.1
596.268	722.274	11	hTAU_4R2N_phospho.SPVVSGDTS[Pho]PR.+2y6.heavy_R10	74.2	30.1
591.264	712.266	11	hTAU_4R2N_phospho.SPVVSGDTS[Pho]PR.+2y6.light	74.2	30.1
598.773	814.317	11	hTAU_4R2N_phospho.SPVVSGDTS[Pho]PR.+2y7.extraheavy_D5K8R10	74.2	30.1
596.268	809.306	11	hTAU_4R2N_phospho.SPVVSGDTS[Pho]PR.+2y7.heavy_R10	74.2	30.1
591.264	799.298	11	hTAU_4R2N_phospho.SPVVSGDTS[Pho]PR.+2y7.light	74.2	30.1
598.773	913.385	11	hTAU_4R2N_phospho.SPVVSGDTS[Pho]PR.+2y8.extraheavy_D5K8R10	74.2	30.1
596.268	908.375	11	hTAU_4R2N_phospho.SPVVSGDTS[Pho]PR.+2y8.heavy_R10	74.2	30.1
591.264	898.367	11	hTAU_4R2N_phospho.SPVVSGDTS[Pho]PR.+2y8.light	74.2	30.1
598.773	1012.454	11	hTAU_4R2N_phospho.SPVVSGDTS[Pho]PR.+2y9.extraheavy_D5K8R10	74.2	30.1
596.268	1007.443	11	hTAU_4R2N_phospho.SPVVSGDTS[Pho]PR.+2y9.heavy_R10	74.2	30.1
591.264	997.435	11	hTAU_4R2N_phospho.SPVVSGDTS[Pho]PR.+2y9.light	74.2	30.1
644.823	1016.526		iRTpeptides.AGGSSEPVTGLADK.+2y10.light	78.1	32.1
644.823	604.33		iRTpeptides.AGGSSEPVTGLADK.+2y6.light	78.1	32.1
644.823	800.451		iRTpeptides.AGGSSEPVTGLADK.+2y8.light	78.1	32.1
726.836	584.269		iRTpeptides.DAVTPADFSEWSK.+2y10+2.light	84.1	35
726.836	1066.484		iRTpeptides.DAVTPADFSEWSK.+2y9.light	84.1	35
726.836	533.746		iRTpeptides.DAVTPADFSEWSK.+2y9+2.light	84.1	35
776.93	1051.557		iRTpeptides.FLLQFGAQGSPLFK.+2y10.light	87.8	36.8
776.93	504.318		iRTpeptides.FLLQFGAQGSPLFK.+2y4.light	87.8	36.8

776.93	904.489	iRTpeptides.FLLQFGAQGSPLFK.+2y9.light	87.8	36.8
699.338	605.341	iRTpeptides.GDLDAASYYPVR.+2y5.light	82.1	34
699.338	855.436	iRTpeptides.GDLDAASYYPVR.+2y7.light	82.1	34
699.338	926.473	iRTpeptides.GDLDAASYYPVR.+2y8.light	82.1	34
636.869	626.398	iRTpeptides.GTFIIDPAAIVR.+2y6.light	77.5	31.8
636.869	741.425	iRTpeptides.GTFIIDPAAIVR.+2y7.light	77.5	31.8
636.869	854.509	iRTpeptides.GTFIIDPAAIVR.+2y8.light	77.5	31.8
487.257	503.294	iRTpeptides.LGGNETQVR.+2y4.light	66.6	26.4
487.257	803.401	iRTpeptides.LGGNETQVR.+2y7.light	66.6	26.4
487.257	860.422	iRTpeptides.LGGNETQVR.+2y8.light	66.6	26.4
622.854	598.367	iRTpeptides.TGFIDPGGVIR.+2y6.light	76.5	31.3
622.854	713.394	iRTpeptides.TGFIDPGGVIR.+2y7.light	76.5	31.3
622.854	826.478	iRTpeptides.TGFIDPGGVIR.+2y8.light	76.5	31.3
669.838	841.384	iRTpeptides.TPVISGGPYER.+2y7.light	79.9	33
669.838	928.416	iRTpeptides.TPVISGGPYER.+2y8.light	79.9	33
669.838	1041.5	iRTpeptides.TPVISGGPYER.+2y9.light	79.9	33
683.854	855.4	iRTpeptides.TPVITGAPYYER.+2y7.light	81	33.5
683.854	956.447	iRTpeptides.TPVITGAPYYER.+2y8.light	81	33.5
683.854	1069.531	iRTpeptides.TPVITGAPYYER.+2y9.light	81	33.5
683.828	663.294	iRTpeptides.VEATFGVDESANK.+2y6.light	81	33.5
683.828	819.384	iRTpeptides.VEATFGVDESANK.+2y8.light	81	33.5
683.828	966.453	iRTpeptides.VEATFGVDESANK.+2y9.light	81	33.5
547.298	633.32	iRTpeptides.YILAGVESNK.+2y6.light	71	28.6
547.298	704.357	iRTpeptides.YILAGVESNK.+2y7.light	71	28.6
547.298	817.441	iRTpeptides.YILAGVESNK.+2y8.light	71	28.6

List of publications

- [1] Zhang X, Hernandez I, Rei D, **Mair W**, Laha JK, Cornwell ME, Cuny GD, Tsai LH, Steen JA, Kosik KS. (2013) Diaminothiazoles Modify Tau Phosphorylation and Improve the Tauopathy in Mouse Models. *J Biol Chem.* PMC3724657
- [2] **Mair W**, Muntel J, Tepper K, Tang S, Biernat J, Seeley WW, Kosik KS, Seeley WW, Mandelkow E, Steen H, Steen JA. FLEXITau: Quantifying Post-translational Modifications of Tau Protein *in vitro* and in Human Disease; *Anal. Chem.* online published 15 February 2016
- [3] **Mair W***, Tang S*, Rotunno M, Muntel J, Kosik KS, Miller BL, Grinberg LT, Hedreen JC, Seeley WW, Steen H, Steen JA. Quantitative Profiling of Tau Peptides Identifies Diagnostic Signatures for Neurodegenerative Tauopathies; *manuscript in preparation*

Curriculum Vitae

Personal Data

Name Waltraud Mair
Phone +49 621 3247942
Address Karl-Ladenburgstr. 45, 68163 Mannheim
Date of birth 15th December, 1986
Place of birth Heidelberg, Germany
Citizenship German

Education

2011 – present *Doctoral candidate*, Chair of Proteomics and Bioanalytics
Technical University Munich (TUM), Germany
Thesis under the supervision of Prof. Dr. Bernhard Kuster
2008 – 2010 *MSc in Biology*, Systems Biology Major
Swiss Federal Institute of Technology Zurich (ETH Zurich), Switzerland
2005 – 2008 *BSc in Molecular Biotechnology*
Ruprecht-Karls University, Heidelberg, Germany

Work Experience

07/2011 – present Boston Children's Hospital / Harvard Medical School, Boston, US
Prof. Judith Steen, Department of Neurobiology
08/2010 – 03/2011 Butantan Institute, Sao Paulo, Brazil, *Internship*
Dr. Solange Serrano, Special Laboratory of Applied Toxinology
10/2009 – 04/2010 ETH Zurich, Switzerland, *Master thesis*
Prof. Ruedi Aebersold, supervision by Dr. Bernd Wollscheid
04/2008 – 06/2008 Deutsches Krebsforschungszentrum (DKFZ) Heidelberg, Germany
Bachelor thesis with Dr. Ursula Klingmüller
Institute of Systems Biology of Signal Transduction
03/2008 – 04/2008 Babraham Institute, Cambridge, UK, *Internship*
Dr. Martin Bootman, Institute of Molecular Signaling

Awards

2011 Willi Studer Prize for highest grades of the year
in the Master Program Biology, ETH Zurich